Max-Planck-Institut für Meteorologie

Max Planck Institute for Meteorology

MAX-PLANCK-GESELLSCHAFT

IMPRS

Indonesian Forest and Peat Fires: Emissions, Air Quality, and Human Health

Angelika Heil

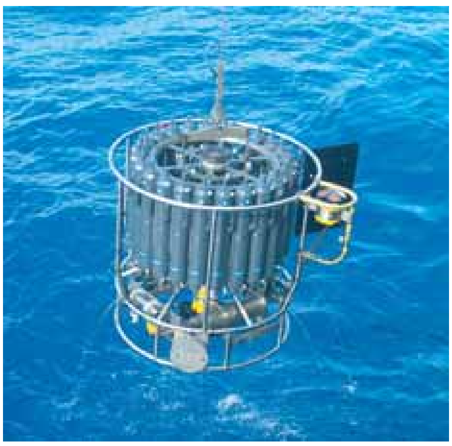

Berichte zur Erdsystemforschung

50
2007

Reports on Earth System Science

Hinweis

Die Berichte zur Erdsytemforschung werden vom Max-Planck-Institut für Meteorologie in Hamburg in unregelmäßiger Abfolge herausgegeben.

Sie enthalten wissenschaftliche und technische Beiträge, inklusive Dissertationen.

Die Beiträge geben nicht notwendigerweise die Auffassung des Instituts wieder.

Die "Berichte zur Erdsystemforschung" führen die vorherigen Reihen "Reports" und "Examensarbeiten" weiter.

Notice

The Reports on Earth System Science are published by the Max Planck Institute for Meteorology in Hamburg. They appear in irregular intervals.

They contain scientific and technical contributions, including Ph. D. theses.

The Reports do not necessarily reflect the opinion of the Institute.

The "Reports on Earth System Science" continue the former "Reports" and "Examensarbeiten" of the Max Planck Institute.

Anschrift / Address

Max-Planck-Institut für Meteorologie
Bundesstrasse 53
20146 Hamburg
Deutschland

Tel.: +49-(0)40-4 11 73-0
Fax: +49-(0)40-4 11 73-298
Web: www.mpimet.mpg.de

Layout:

Bettina Diallo, PR & Grafik

Titelfotos:
vorne:
Christian Klepp - Jochem Marotzke - Christian Klepp
hinten:
Clotilde Dubois - Christian Klepp - Katsumasa Tanaka

Berichte zur Erdsystemforschung 50/2007

Indonesian Forest and Peat Fires: Emissions, Air Quality, and Human Health

Dissertation zur Erlangung des Doktorgrades der Naturwissenschaften
im Departement Geowissenschaften der Universität Hamburg
vorgelegt von

Angelika Heil
aus Frankfurt/Main

Hamburg 2007

Reports on Earth System Science 50/2007

ISSN 1614-1199

Angelika Heil
Max-Planck-Institut für Meteorologie
Bundesstrasse 53
20146 Hamburg
Germany

Als Dissertation angenommen
vom Departement Geowissenschaften der Universität Hamburg

auf Grund der Gutachten von
Prof. Dr. Hartmut Graßl
und
Prof. Dr. Hand Graf

Hamburg, den 29. Oktober 2007
Prof. Dr. Kay-Christian Emeis
Leiter des Departements für Geowissenschaften

ISSN 1614-1199

Indonesian Forest and Peat Fires:
Emissions, Air Quality, and Human Health

Angelika Heil

Hamburg 2007

“ada asap ada api.”

(Indonesian language)

“Where there’s smoke, there’s fire.”

(direct English translation)

“There's a cause of everything.”

(translated meaning of the Indonesian proverb)

The cover page shows fires in Sumatra on June 25, 2005 with smoke plumes travelling towards Peninsular Malaysia. The image has been acquired by the Moderate-resolution Imaging Spectroradiometer (MODIS), available online at http://rapidfire.sci.gsfc.nasa.gov/gallery/2005176-0625/Indonesia2.A2005176.0650.250m.jpg (June 28 2005).

CONTENTS

Abstract

Fires, which are used as a tool to clear tropical forest and to convert peat areas for agricultural purposes, have been strongly increasing in Indonesia during the last decades. The emissions of these fires strongly influence the air quality in the entire Southeast Asian region. Furthermore, the concentration of climatic active trace species in the atmosphere is considerably changed by these emissions in particular years.

The aim of this study is to provide a long-term fire emission inventory for Indonesia that resolves the spatial and temporal variation of the emissions. Emissions from fires in surface vegetation and peat soil are calculated separately using various new satellite fire products and soil and vegetation maps. The results allow a first assessment of the relative contribution of peat fire emissions to the total fire emissions in Indonesia. The newly developed monthly emission inventory in 0.5 degree resolution covers the period from 1960 to 2006 and has been integrated into the global RETRO (REanalysis of the TROpospheric chemical composition over the past 40 years) emission inventory which is used in various atmospheric chemistry modeling studies.

The decrease in precipitation in Indonesia during El Niño years is strongly correlated with an increase in fire activity. In particular, large fractions of the normally moist peat areas of Kalimantan suffer from extreme drought and are thus very susceptible to fires. In the year 1997, 22% of the total burned area in Indonesia was covered by peat. Most of this area was located in Kalimantan and slightly less in Sumatra. The emissions from these peat fires are far beyond those produced by surface vegetation fires. The fire emissions of the year 1997 significantly contribute to the total amount of global emissions. The total carbon emissions of 1.1 GtC represent 17% of the global anthropogenic emissions. The CO and aerosol emissions account for around 30% of their global emissions from anthropogenic sources and fires.

The inventory is applied to estimate the effects of the 1997 Indonesian fires on the regional air quality and human health. This study focuses on the air pollution caused by particulate matter emissions which are of primary relevance for public health. The atmospheric transport and removal of fire aerosols is investigated using a regional atmospheric chemistry climate model (REMO) at 0.5° horizontal resolution. The model performance was evaluated in detail with station measurements. The surface concentrations predicted for the Southeast Asian region largely exceed the air pollution threshold in wide areas downwind to the fires. The predicted concentrations are used to estimate the number of premature mortality cases in adults attributable to the Indonesian fire emissions. The mortality rate increases by about 3%. The model study indicates that the particular meteorological conditions prevailing during El Niño events aggravate the public health impact of such an air pollution episode.

Zusammenfassung

Feuer, eingesetzt zur Rodung des Tropenwaldes und der landwirtschaftlichen Nutzbarmachung von Torfgebieten, haben in den letzten Jahrzehnten in Indonesien stark zugenommen. Die Emissionen, die durch diese Brände entstehen, beeinflussen zum einen erheblich die Luftqualität im südostasiatischen Raum, zum anderen können sie in manchen Jahren die globale Konzentration klimarelevanter Spurenstoffe in der Atmosphäre erheblich ändern.

Zielsetzung dieser Arbeit ist, ein räumlich und zeitlich aufgelöstes Feueremissionsinventar für Indonesien zu erstellen um damit Abschätzungen über die Auswirkung der Emissionen auf die regionale Luftqualität und die menschliche Gesundheit vorzunehmen. Feuer in Oberflächenvegetation und in Torfschichten werden bei der Berechnung der Emissionen separat parametrisiert. Dabei wurden verschiedene neuartige Feuersatellitenprodukte und Bodenkarten evaluiert und benutzt. Anhand der Ergebnisse wird eine erstmalige Abschätzung des Anteils von Torfbrandemission an den Gesamtemissionen in Indonesien vorgenommen. Es wird zudem aufgezeigt, in welchem Ausmaß die Variabilität der Feueraktivität durch Niederschlagsschwankungen im Zusammenhang mit dem Klimaphänomen El Niño beeinflußt wird. Das entwickelte, monatliche Emissionsinventar in 0.5° horizontaler Auflösung umfaßt den Zeitraum 1960 bis 2006 und findet als Bestandteil des globalen RETRO Emissionsinventars (REanalysis of the TROpospheric chemical composition over the past 40 years) Verwendung in Modellstudien der Atmosphärenchemie.

Es zeigt sich, daß die Niederschlagsmenge in Indonesien in El Niño Jahren stark abnimmt, während die Feueraktivität stark zunimmt. Insbesondere große Anteile der sonst feuchten Torfgebiete Kalimantans sind dann von extremer Trockenheit betroffen und somit feuergefährdet. 22% der verbrannten Fläche während des ungewöhnlich starken El Niños im Jahr 1997 war Torfgebiet, hauptsächlich in Kalimantan gefolgt von Sumatra. Die Emissionen, die aus den Torfbänden entstehen, überwiegen bei Weitem die Emissionen, die bei Feuern in Oberflächenvegetation entstehen. Die daraus resultierenden Emissionen des Jahres 1997 stellen einen erheblichen Anteil der globalen Gesamtemissionen dar (1.1 GtC oder 17% der anthropogenen Emissionen). Die CO- und Aerosolemissionen machen etwa 30% der globalen Gesamtemissionen einschließlich Feueremissionen aus.

Die Auswirkungen der indonesischen Feueremissionen auf die regionale Luftqualität werden am Beispiel der extremen Vegetationsbrandepisode während des El Niño Jahres 1997/98 analyziert, wobei der Schwerpunkt auf den für die menschliche Gesundheit relevanten Feinstaubemissionen (PM_{10}) liegt. Um zu untersuchen, welchen Einfluß meteorologische Faktoren auf den atmosphärischen Transport und Austrag der Rauchpartikel haben, wurden Modellstudien mit einem regionalen Atmosphären-Chemie-Modell (REMO) in 0.5° Auflösung durchgeführt, welches zuvor eingehend mit Stationsmessungen evaluiert wurde. Die für den südostasiatischen Raum modellierten Feinstaubkonzentrationen werden verwendet, um eine erste grobe Abschätzung der Gesundheitsfolgen vorzunehmen, die sich durch die feuerbedingte Luftbelastung in der betroffenen Bevölkerung ergeben. Es zeigt sich, daß die indonesischen Feueremissionen zu einer großflächigen Überschreitung der Luftgrenzwerte führt. Die Mortalität der erwachsenen Bevölkerung steigt dadurch um etwa 3%. Die besonderen meteorologischen Bedingungen, die während der El Niño Jahre vorherrschen, verstärken die durch die Brände verursachte Luftbelastung.

1 Introduction

1.1 Vegetation and Peat Fires and Their Emissions

The majority of vegetation and peat fires are man-made, natural fires (or ‘wildfires’, mainly from lightening) are estimated to account for only 10% of global biomass burning (Crutzen and Andreae 1990). The human-induced fires are generally linked to land conversion activities, as fire is a cheap and fast tool to remove the original vegetation and to prepare the land for different land use systems such as cropland, plantations, grazing areas or settlements (Suyanto et al. 2004). Anthropogenic fires also comprise deliberately set fires, which got out of control (Stott 2000). The emissions emanating from land conversion fires can therefore be considered as anthropogenic emissions.

The emissions from biomass burning represent a large perturbation to global atmospheric chemistry, especially in the tropics, where most biomass burning emissions are produced (Andreae and Merlet 2001, Crutzen and Lelivield 2001). Biomass burning is estimated to contribute 39 ±6% to the carbon monoxide (CO) globally emitted (Schultz et al. *submitted to Biogeochemical Cycles 2007*) and more than 20% to the nitric oxides (NO_x), non-methane hydrocarbons (NMHC) and methyl chloride (CH_3Cl) emissions (Andreae 1991). To the global emissions of elemental carbon (EC) and particulate organic carbon (POC), biomass burning contributes even 63 ±9% and 91 ±10%, respectively (Ito and Penner 2005). The emitted trace gases affect the oxidizing capacity of the atmosphere and lead to the photo-chemical production of ozone in the troposphere (Granier et al. 2000). In the stratosphere, the halogen compounds contribute to ozone depletion (Cicerone 1994). Aerosols emitted during biomass burning events may influence climate directly by reflecting solar radiation back into space. Furthermore, aerosols act as cloud condensation nuclei (CCN), and may thus affect climate indirectly by modifying cloud microphysics and sunlight reflectance (Kaufman and Nakajima 1993, Kaufman and Fraser 1997). Studies from regions affected by smoke plumes from biomass burning indicate that fire aerosols can cause a suppression of rainfall over large areas by reducing cloud droplet size (Rosenfeld 1999, Andreae et al. 2004, Langmann 2006, Graf et al. 2007).

Biomass burning is presently the principle source of air pollution in the tropics. While it principally produces the same trace species as burning of fossil fuels, it emits generally a higher amount of species relevant to air pollution, such as those leading to the production of ozone and photochemical smog (Crutzen and Lelieveld 2001). The smoke plumes emanating from the fires may be subject to long-range transport and can thereby affect air quality even more than thousand kilometres away from the fires (Crutzen and Andreae 1990, Bertschi and Jaffe 2005).

Van der Werf et al. (2006) and Schultz et al. (*submitted to Biogeochemical Cycles 2007*) estimate that roughly 2.5 ±0.4 Gt carbon (C) or 8.9 ±1.4 Gt carbon dioxide (CO_2) are currently emitted by biomass burning every year on a global scale[1]. Nevertheless, compared to the current carbon dioxide emissions from anthropogenic fossil fuel combustion of 26.4 ±1.1 Gt CO_2 (or 7.2 ±0.3 GtC) (95% confidence interval)[2] (IPCC 2007), biomass burning constitutes another significant, but smaller source of emission. Carbon dioxide is the most important anthropogenic greenhouse gas. It is nowadays considered as very likely that most of the observed increase in global average surface temperatures since the mid-20th century is due to the observed increase in anthropogenic greenhouse gas concentrations in the atmosphere (IPCC 2007).

[1] A gigaton (Gt) equals to 10^{15} grams. GtC denotes one gigaton carbon (C).

[2] The uncertainty in the result is generally measured in terms of standard deviation (1σ), here denoted as ±. If the uncertainty range (±) refers to the 95% confidence interval (95% CI), it is noted explicitely.

According to the estimate by Mouillot and Field (2005) and Schultz et al. (*submitted to Biogeochemical Cycles 2007),* global fire-related carbon emissions have increased by around 50% in the decadal mean since the 1960ies, mainly due to the drastic intensification of deforestation fires in the tropics. However, such longer-term emission estimates are affiliated with very high uncertainties. Before the mid-1990ies, burned area information required to estimate fire emissions is principally based either on fragmentary and inconsistent national to regional forestry statistics or on very assumptive model calculations. The establishment of continuous satellite-based remote sensing of fires at a global or regional scale which took place the mid-1990ies has drastically improved this situation, although various there are still various qualitative restriction associated with these products. Most widely used are the following active fire products derived from the following satellite-borne sensors: Along Track Scanning Radiometer (ATSR) available since mid-1996, Advanced Very High Resolution Radiometer (AVHRR) basically available since the year 1996, and MODIS (Moderate Resolution Imaging Spectroradiometer) available since in 2001 (Justice et al. 2003).

Also fire emission estimates based on remote sensing fire products are still affiliated with a high uncertainty (uncertainty range of at least ± 50%), mainly because of difficulties to accurately estimate the amounts of surface and subsurface biomass combusted per unit area (Andreae and Merlet 2001). Until recently, global and regional biomass burning emission inventories only included emissions from surface vegetation while omitting emissions from burning soil organic matter, in particular peat (Hao et al. 1990, Crutzen and Andreae 1990, van der Werf et al. 2003, Hoelzemann et al. 2004). Peat soils (widely also referred to as organic soils, histosols, peatlands or peat swamps) are characterized by a mighty layer (horizon) of partly decomposed organic material (generally at least 30 cm deep and more than 65% organic matter content) (Andriesse 1988). Globally, peatlands cover an area of about 400 million hectares (Mha)[3] (equivalent to 4 million km^2 or roughly 3% of the global land surface) and store approximately as much carbon as surface vegetation globally (around 460 GtC) (Gorham 1991, Immirzi et al. 1992, IPCC 2001). Recent studies have shown that in some ecosystems these emissions may equal or even exceed the emissions produced from burning surface vegetation, and that the occurrence of peat fires and the resultant emission production has been increasing in several regions of the world over the last decades due to human perturbations, mainly drainage, and climatic change (Poulter et al. 2006, Turetsky et al. 2006). For example, Kasischke et al. (2005) estimated that burning of soil organic matter, notably peat, contributed between 46% and 72% of all emissions from wildland fires in the boreal regions. Page et al. (2002) found that burning peat soil contributed between 79% and 84% of all carbon emitted (in total 0.5 – 2.6 GtC) during the 1997 Indonesian wildland fire event. Peat fires may, in some regions, largely control the total amount and the interannual variability of fire emissions. The omission of peat fires in global and regional fire emission inventories may therefore lead to biased or wrong results.

1.2 Spatiotemporal Fire Patterns and Climate Variability

Global fire activity is highly variable in space and in time. For each geographic location on earth, a typical fire season exists (Carmona-Moreno et al. 2005). The timing of the fire season is linked to the typical seasonal variation of the prevailing climate conditions in a given region, namely precipitation and temperature, which directly influence fuel moisture and ignitability of the vegetation (Chuvieco et al. 2004). For example, in northern hemispheric winter (DJF), global fire activity concentrates across Africa’s northern savanna belt, where particularly dry conditions prevail during that season (Cahoon et al. 1992). During northern hemispheric spring (MAM), in contrast, most fires occur between 3° to 17° N, namely in Central America and continental South Asia, as well as in southern Australia.

The fire seasonality is very stable with respect to climate variability in regions such as the African savannas, the high and medium latitudes in the Northern Hemisphere and the Far-East of China-

[3] 1 million hectares (1 Mha) corresponds to 10,000 km^2.

Russia. In these areas interannual variations in climate have little or no effect on fire seasonality. In contrast, other regions such as Indonesia, Southern Europe, Southern and East Africa, California, Australia, Southern East Asia and areas in Latin America, are much more sensitive to interannual climate variability and show considerable interannual variations in regional fire activity and hence regional to global emission production (Carmona-Moreno et al. 2005). Carmona-Moreno et al. (2005) demonstrate that the strong regional variability in the fire seasonality and overall fire activity is largely correlated with the El Niño Southern Oscillation (ENSO), an interannual climate anomaly that significantly alters precipitation regimes in several regions of the world. Notably in the northern hemisphere and in the tropics between 5° N to 5° S, fire activity is strongest during the El Niño periods. This connection is particularly pronounced in Indonesia where unusually large fire events occur during El Niño years.

Figure 1-1 illustrates the inter- and intraannual variability of global fire activity and of the contribution from different regions in Equatorial Asia (EQAS) to the global total during the period July 1996 to December 2006. EQAS is defined as the countries Indonesia, Malaysia, Brunei, Singapore, Papua New Guinea (Giglio et al. 2006). Fire activity is derived from thermal anomalies ("fire counts") observed by the satellite-borne Along Tracking Scanning Radiometer (ATSR). The ATSR sensor has a horizontal resolution of 1 x 1 km[4]. An ATSR fire count in Figure 1-1 denotes a 1 km^2 pixel, in which a nighttime temperature exceedance above 35° C (308 K) was observed (Algorithm 2). Active fire counts provide information on the spatiotemporal patterns of fire incidence, but not the fraction of the pixel area that actually burned (Mota et al. 2006). As a result, the observed fire activity cannot be directly translated into actual amount of area burned.

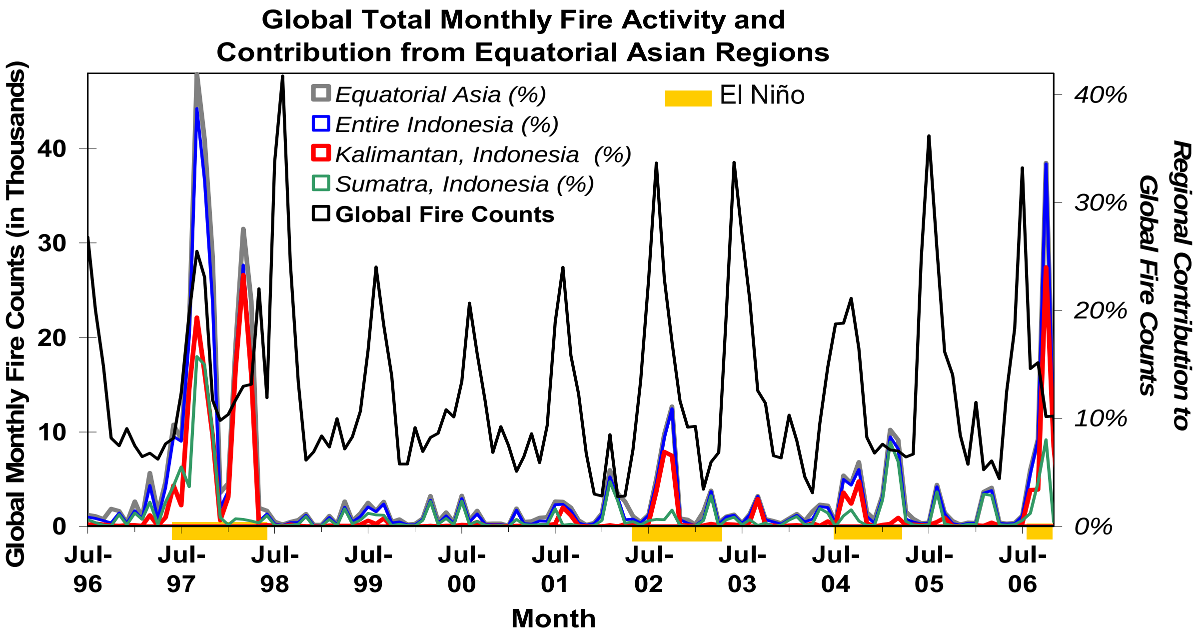

Figure 1-1: Global monthly total fire activity counts (left ordinate) and relative contribution from different Equatorial Asian (EQAS) regions (right ordinate). Fire activity is derived from the Along Track Scanning Radiometer (ATSR) Algorithm 2 nighttime data from the ATSR World Fire Atlas (Data Source: Web-Reference 1). The yellow bars along the abscissa indicate periods designated as warm phase (El Niño) according to (Data Source: Web-Reference 2), see also Chapter 2.2.

[4] Note that the revisit time of the ATSR at the equator is three days, meaning that many short duration fires are not observed (Mota et al. 2006). Vegetation type (biome) specific differences in fire persistence are likely to introduce a bias in favour of the detection of longer duration fires (e.g. forest fires), to the detriment of shorter duration fires such as savanna fires (Giglio et al. 2006).

Global fire activity fluctuates strongly from month to month, ranging from 3,123 to 47,709 fire counts (average 14,606 ±809, sample size n is 125). The maximum burning generally occurs during July to September. Periods of unusually high or low global burning occur likewise during El Niño and non-El Niño conditions, indicating that other factors besides ENSO control global fire activity. The interannual variability in global fire activity is much less pronounced than the intraannual fire activity. Yearly totals vary from 141,227 to 238,149 fire counts (by a factor of 1.7), whereas monthly fire activity may vary by a factor of 3.9 within a single year.

The contribution of the entire EQAS region to global monthly fire activity ranges from 0.04% to 41.9% (average 3.5 ±1.2%) while the contribution of Indonesia alone (having 70% of the EQAS land area) is 0.02% to 38.7% (average 3.1 ±1.1%). Most of the fires in EQAS thus occur in Indonesia (on average 77.5 ±3.1%). On average, 73 ±4.4% of all Indonesian fires occur on the islands of Sumatra and Borneo-Kalimantan (Indonesian part of the island Borneo), which contribute only 53% to Indonesia's land area. This illustrates that fire activity in the entire region of Equatorial Asia appears to be dominated by fires on the Indonesian islands Sumatra and Borneo-Kalimantan.

Figure 1-1 illustrates that unusually large burning in Indonesia occurs in periods categorized as El Niño (warm phase) (i.e. 1997/98, 2002, 2004/05 and 2006). During El Niño periods, the contribution of fires in Indonesia to global monthly fire activity is on average 8.5 ±3.4% (maximum 38.7%, n=35) and is statistically significantly[5] higher than in other periods (average 1.0 ±0.3%, maximum 7.2%, n=90). Since fire emissions are proportional to fire activity, it is evident that the fires in Indonesia, notably in Sumatra and Kalimantan, make up a relevant contribution to global fire emission production and thus global budget of atmospherically and climatically active trace species during some El Niño-related extreme fire events. During normal fire years, however, Indonesian fires are only of minor importance to global fire activity and thus global fire emissions.

1.3 Deforestation and Peat Reclamation Fires in Indonesia – Trends and Causes

Before modern humans (homo sapiens) started populating Indonesia around 50-60 kiloyears (ka) ago, the land mass of today's Indonesia (181 Mha excluding inland waters) was most probably to over 90% covered by tropical forest (FWI/GFW 2002). In forested areas with water saturated soils, where plant debris production was faster than the related plant debris decomposition, peat accumulation started from around 30 ka before present (Weiss et al. 2002, Page et al. 2004). Most peat deposits in Indonesia formed in surface depressions where rainfall water is logged. Because tree biomass is the predominant organic matter source for tropical peat, the peat material is predominantly composed of partly decomposed woody material ("woody peat"), in contrast to peat in the temperate regions, which is predominantly composed of moss-derived material such as Sphagnum. Since the tropical peat deposits in their natural state are generally forested, they are also called peat-swamp forests (PSF)) (Rieley et al. 1995, Weiss et al. 2002).

Around 17 – 27 Mha of peat soil (also referred to as organic soils, peatland or peat swamp) formed since then in Indonesia, corresponding to 9 – 14% of Indonesia's country area (Immirzi et al. 1992, Rieley et al. 1995). However, these estimates are very uncertain and strongly depend on the data source used (Figure 1-2). The depth of peat deposits range from 0.4 m to more than 16 m (Sorensen 1993, Hope et al. 2005). According to a recent estimate (Rieley and Page 2005) the Indonesian peat deposits store about 35 GtC. The estimate is based on an assumed peat area of 20 Mha and an average depth of 4 m. Because of the particularly favorable conditions for peat accumulation in Indonesia, the peat deposits contain about 3.5 times more carbon than Indonesia's aboveground vegetation (around 10 GtC in 1995) (FAO 2006). Furthermore, Indonesia has the highest country-related peat area and peat carbon stock, and also the highest peat coverage (fractional peat area per country area) within the tropics. Indonesian peatlands represent around 80%, 56% and 5% of the total peatland area in Equatorial Asia (EQAS), the tropics and the

[5] The significance was tested using t-test statistics with a significance level > 99.99%.

world, respectively. At the same time, they contribute around 87%, 66% and 8%, respectively, to the total peatland carbon stored in these regions (Andriesse 1988, Rieley and Page 2005). Compared to peat deposits in boreal regions, the tropical peat soils tend to be generally deeper and therefore may store more biomass and carbon per unit area (Stolbovoi 2002, Rieley and Page 2005).

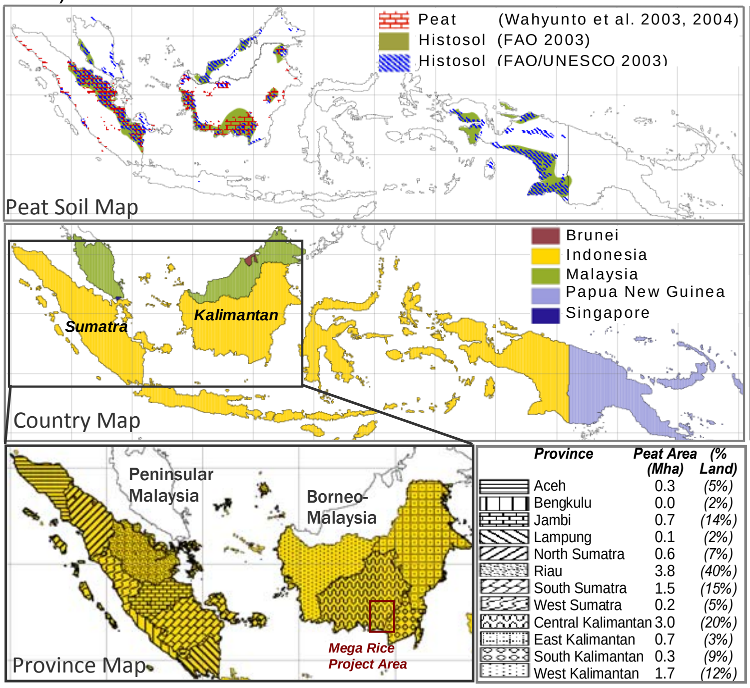

Province	Peat Area (Mha)	(% Land)
Aceh	0.3	(5%)
Bengkulu	0.0	(2%)
Jambi	0.7	(14%)
Lampung	0.1	(2%)
North Sumatra	0.6	(7%)
Riau	3.8	(40%)
South Sumatra	1.5	(15%)
West Sumatra	0.2	(5%)
Central Kalimantan	3.0	(20%)
East Kalimantan	0.7	(3%)
South Kalimantan	0.3	(9%)
West Kalimantan	1.7	(12%)

Country	Land Area	Histosol Area		Histosol Area		Peat Area	
Peat Soil Map Source		FAO/ UNESCO 2003		FAO 2003		Wahyunto et al. 2003,2004	
	Mha	Mha	(% Land)	Mha	(% Land)	Mha	(% Land)
Indonesia	190.4	20.3	(11%)	39.4	(21%)	-	-
Kalimantan	53.9	3.9	(7%)	11.8	(22%)	5.6	(10%)
Sumatra	47.4	7.2	(15%)	11.6	(24%)	6.5	(14%)
Irian Jaya	42.2	9.2	(22%)	15.9	(38%)	-	-
Malaysia	33.0	2.6	(8%)	3.7	(11%)	-	-
Sabah/Sarawak	19.8	1.9	(10%)	2.6	(13%)	-	-
Brunei	0.6	0.2	(28%)	0.2	(35%)	-	-
Pap.N.Guinea	46.3	0.0	(0%)	0.2	(1%)	-	-
Singapore	0.1	0.0	(0%)	0.0	(0%)	-	-
Total Area	**270.3**	**23.1**	(9%)	**43.5**	(16%)	-	-

Figure 1-2: Estimated peat distribution in the EQAS region based on different map sources. The Wahyunto et al. (2003, 2004) peat map for Sumatra and Kalimantan includes peaty soil and peat. This Peat Atlas has been established recently based on satellite imagery and field surveys. It also provides information on the maturity and physical and chemical characteristics of the peat including peat carbon storage. Despite the still limited amount of field data collection, it represents the best island-covering and consistent survey of peat deposits available for Indonesia (personal communication Aljosja Hooijer 2006). In the soil science terminology used by the FAO, peat soils are referred to as histosols. Histosols are defined as having an organic (histic) soil horizon of at least 40 cm. In this figure, the area assigned as histosol by the FAO (2003) and FAO/UNESCO (2003) soil maps is displayed. FAO (2003) and FAO/UNESCO (2003) use a different soil classification system. However, in the FAO (2003) map, which simplifies the distribution of soils types to a generalized pattern of major soil regions, the area classified as histosol may also contain associated gleysols.

Since the beginning of the 20th century, the population in Indonesia has been growing exponentially (BPS 2001). Linked to this, the demand for land that can be used for agriculture (e.g. rice) and agroforestry (e.g. palm oil, rubber) and the demand for wood resources (cooking fuel, timber products, plywood) has been increasing drastically (Inoue 1999, Sunderlin and Resosudarmo 1999). As a consequence, Indonesian forests have been increasingly deforested or logged (Holmes 2002), most notably since the 1960ies, when deforestation was further accelerated by the industrialization in the forest sector. The industrialization is characterized by an expansion of industrial logging and plantations (e.g. palm oil, rubber) using chainsaws for cutting and heavy machinery for extraction and transport (Inoue 1999). Mainly due to these causes, around 75 Mha or 45% of Indonesia's original forest cover has been cleared, most of which (≈ 52 Mha) since 1960 (Holmes 2002, FAO 2006).

Peat swamp forests were also affected by forest fragmentation (selective logging) and deforestation for agricultural purposes. However, before the 1980ies, deforestation activities in peat swamp forests for agricultural purposes normally only occurred when the peat layer was shallow (below around 0.6 m depth). The shallow peat soils can be transformed into fertile cropland after some shallow drainage (Andriesse 1988, Limin et al. 2000). Drainage is done by digging channels into the swampy land with the aim of lowering the water table and thereby rendering the soils cultivable for rice or other crops (Sumawijaya 2006). With increasing peat depth, however, the crop suitability is sharply decreasing, even after deep drainage (Limin et al. 2000).

Starting from 1980ies, the “drainage and reclamation” practice strongly expanded also into deep peat areas (Sorensen 1993). Agricultural scientists have broadly recommended this practice to the Southeast Asian governments since the 1960ies, as illustrated by the following advice given to the Malaysian government in 1957 in the Malayan Agricultural Journal:

“It would seem that the optimum method of developing these peat soils would be to take the potential padi[6] areas [….] and crop them with dryland crops with the ultimate view of getting rid of the peat and then growing padi. During the period of dryland cropping every effort should be made to hasten the disappearance of the peat. Thus deep drainage, burning the peat, and removing and burning the timber are all highly desirable.” (Coulter 1957)

In 1995, the Indonesian government initiated a gargantuan land reclamation program, the so-called program “Mega-Rice-Project” (MRP) covering 1.5 Mha of deep and so far largely undisturbed peat swamp forests in the Central Kalimantan (see Figure 1-3). The aim was to convert land into agricultural areas, especially rice fields. Between 1996 and 1998 more than 4000 km of deep drainage and irrigation channels were constructed in this area (Boehm and Siegert 2001), however, without properly considering the hydrological conditions (hydraulic gradient) while planning. The drained peat soil frequently got too dry and acid to render crop cultivation feasible; the project finally failed (Inoue 2000). According to Rieley et al. (1997), more than 20% of the peat swamp forests of Indonesia have been subject to conversion so far.

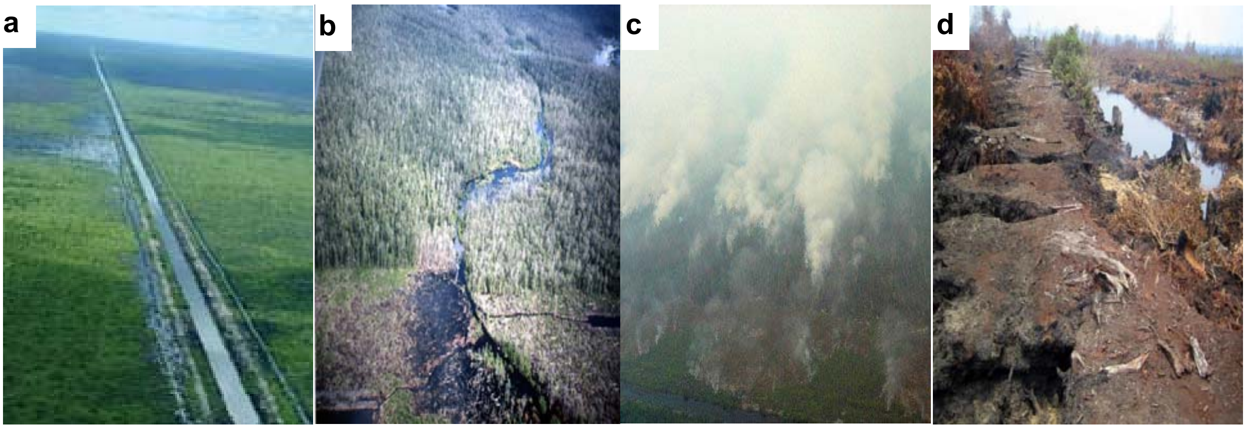

Figure 1-3: Photos from of the Mega-Rice Project (MRP) in Central Kalimantan showing forested, deforested, burning and burned peat swamp forests close a to drainage channel (Photos taken from (a) Aldhous 2004, (b,d) Web-Reference 3, and (c) Web-Reference 4).

Before the beginning of the large-scale deforestation and peat reclamation, fires in the natural tropical forests or undisturbed peat swamps were rare. Fires occurred only during periods of extreme drought, when normally moist fuels are drying out, become potentially flammable and thereby susceptible to fires (Takahashi et al. 2001, Cochrane 2003 and references therein). The extreme drought conditions are generally linked to El Niño conditions (Ropelewski and Halpert 1987, Aldrian and Susanto 2003).

In the undisturbed state, the closed canopy makes evergreen tropical forests remarkably resistant to drought. In peat swamp forests, a closed canopy also protects the underlying peat soil layers from drying. Partial opening or removal of the forest canopy decreases the ability of forests and the underlying peat deposits to maintain moisture. The induced changes in the microclimate and

[6] padi (Bahasa Indonesia) paddy

regional climate include a decrease in relative humidity and an increase in temperature and wind speeds (Taylor et al. 1999, Hoffmann et al. 2003). In addition, human disturbances to the forest related to deforestation and logging such as felling, cutting and debarking may render fuels in a tropical forest more flammable by reducing their size, volume and distribution (Stott 2000). All these changes are making the available biomass more vulnerable to fire. At the same time they alter the fire behavior towards higher fuel availability (fuel capable of sustained combustion) and higher fire severity (burned area per fire event, tree mortality) (Cochrane 2003).

The most important disturbance controlling fire susceptibility and fire severity of peat layers is drainage. Water tables above, at or just below the surface generally prevailing in intact peat swamps render the peat inflammable (Wösten et al. 2006). Under sustained dry conditions, however, the upper peat layer may occasionally gradually dry out and potentially ignite, especially when the aboveground vegetation cover has been removed (Usup et al. 2004, Wösten et al. 2006). A permanent lowering of the water table by drainage renders the entire peat horizon above the drainage water level susceptible to fire. Drainage drastically increases fuel availability and fire severity because peat soils generally provide both, high fuel density and continuity. Both factors promote sustained, vertically and laterally spreading peat fires (Usup et al. 2004). Once the peat fire is ignited, it can keep burning for months and can even persist heavy rainfalls. Fires in deep peat deposits frequently spread below the surface, progressing around 30 cm per day (Usup et al. 2004). Observations show that fires may cause a decrease in surface elevation of the affected peat area by 1 m within a single burning season (Wösten et al. 2006). Because of their sustained burning, peat fires may act as a long-lasting and hardly controllable potential ignition source for new surface fires (Goldammer and Seibert 1990).

The strong connection between accessibility and peat fire occurrence on the one hand and peat drainage and peat fire frequency on the other hand is apparent in Figure 1-4. The figure shows the number of active fires in each 1x1 km^2 pixel detected per year by the MODIS fire satellite in the Mega-Rice-Project (MRP) area in Central Kalimantan during 2001 to 2006. There is a clear clustering of fire activity close to rivers. Rivers facilitate humans the accessibility to these areas. Furthermore, there is a clear clustering of fire activity along the drainage canals established in deep peatlands within the framework of the Mega-Rice-Project. The pattern of fire occurrence derived from MODIS fire data coincide surprisingly well with the map of drainage canals published by Aldhous (2004). Peat fire activity generally occurs up to 3 km away from drainage canals or rivers. Peat areas which have not been subject to drainage or which are remote from rivers, are generally spared from fires. An example is the large area of deep peat deposits north of the MRP area. High frequency fires (> 10 fire counts per year) are scarce in non-peat areas. Non-peat fires generally occurred less than 5 times per year within the same pixel. Compared to this, high frequency fires are much more prevalent in peat areas, notably in direct vicinity to a drainage canal. Furthermore, fires in these areas frequently occurred in recurrently throughout 2001 to 2006. It illustrates that the strong lowering of the water table close to drainage canals brings about sufficiently dry conditions for persistent, recurrent peat fires. In contrast to surface vegetation, deep peat deposits provide sufficient biomass to sustain such fires.

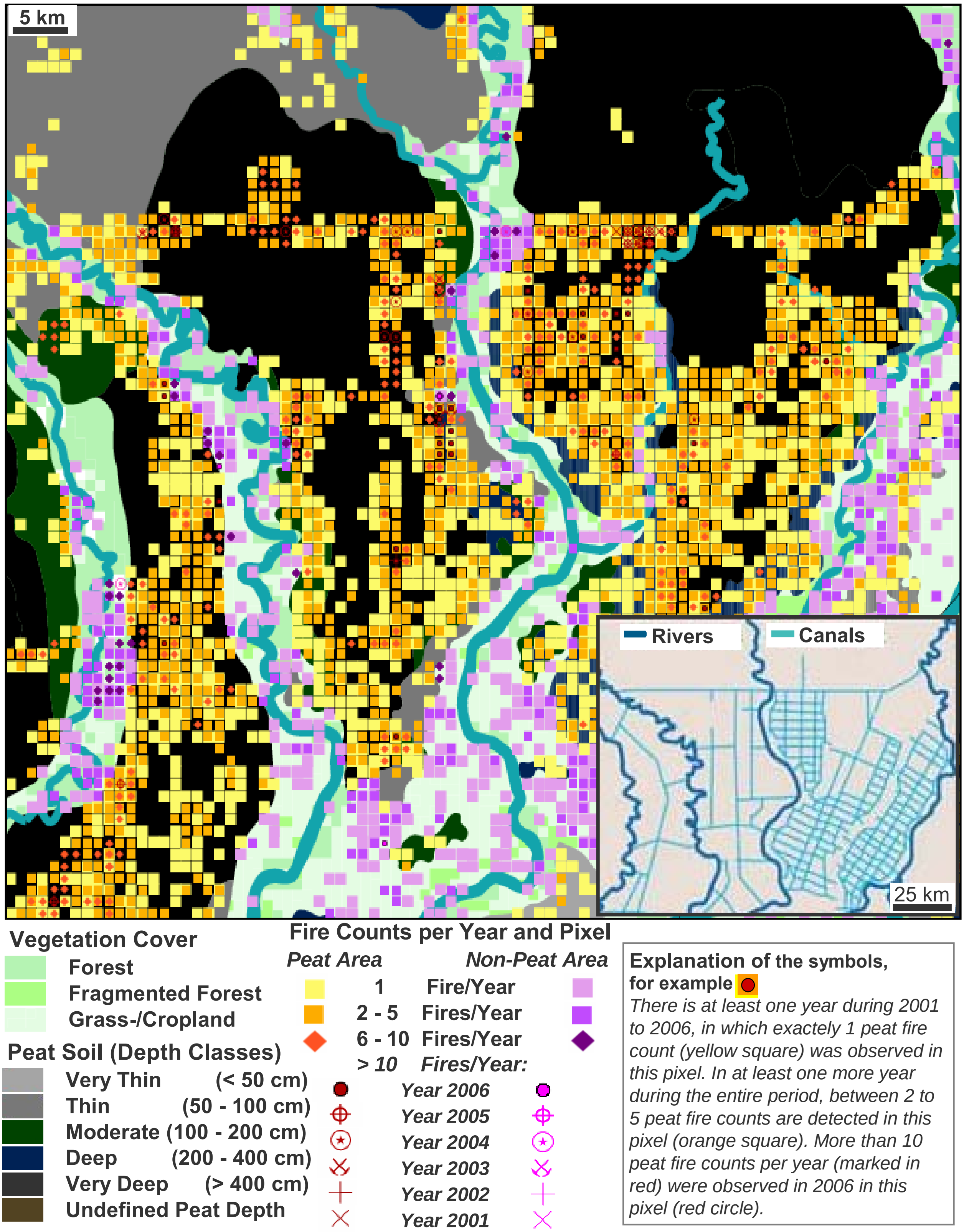

Figure 1-4: Number of fire counts per year in each 1x1 km pixel during the period 2001 to 2006 observed by the MODIS fire satellite in the 'Mega-Rice Project' area in Central Kalimantan (Heil et al. in preparation). The small map at the right bottom shows major rivers and the canal system established during 1996 to 1998 in order to drain the peat soil for agricultural conversion (Aldhous 2004). Fires are discriminated into peat and non-peat fires using the peat soil map established by Wahyunto et al. (2004) (see also Figure 1-2). Fire counts observed on peat soils are shown as yellowish to reddish symbols. A yellow (light orange) square symbols is assigned to a pixel if there is at least a single year during 2001 to 2006 in which MODIS observed exactly 1 peat fire count (2 to 5 peat fire counts) per year. An orange rhomb is assigned to a pixel if annual fire activity was between 6 to 10 fires in at least a single year. The "at least" points out that the multiple occurrence if the same symbol cannot be resolved in this figure. Pixels in which fire frequency was more than 10 fire per year are shown in red symbols. For each year, a different symbol is assigned. As a result, the multiple occurrences of years with such a high fire frequency fires is discernible in the figure (superimposed symbols). The same principle is used to display fire in non-peat areas, for which purple to pinkish symbols are used.

Figure 1-5 schematically illustrates the major feedbacks between human disturbances to a tropical peat swamp forest (deforestation, logging, and drainage), potential fire behavior (susceptibility, severity and fuel availability) and forest and peat fire occurrence. It also adumbrates the likely positive feedback loops between forest and peat fires and deforestation by inducing climatic changes. Altered drought frequency and intensity represents the most important climatic change related to this feedback process. Climate change comprises effects of increased greenhouse gas emissions, aerosol loading and land cover change on regional droughts (Cochrane 2003). Air pollution caused by fire emissions adversely affects human health. It also leads to visibility degradation, which may reduce the country's revenues out of the tourism and transportation sector. Both, the health and visibility effects of fire-related air pollution have thus a negative impact on the economic well-being of the countries and the population. Poverty, in turn, is an important driver in deforestation and deforestation fires.

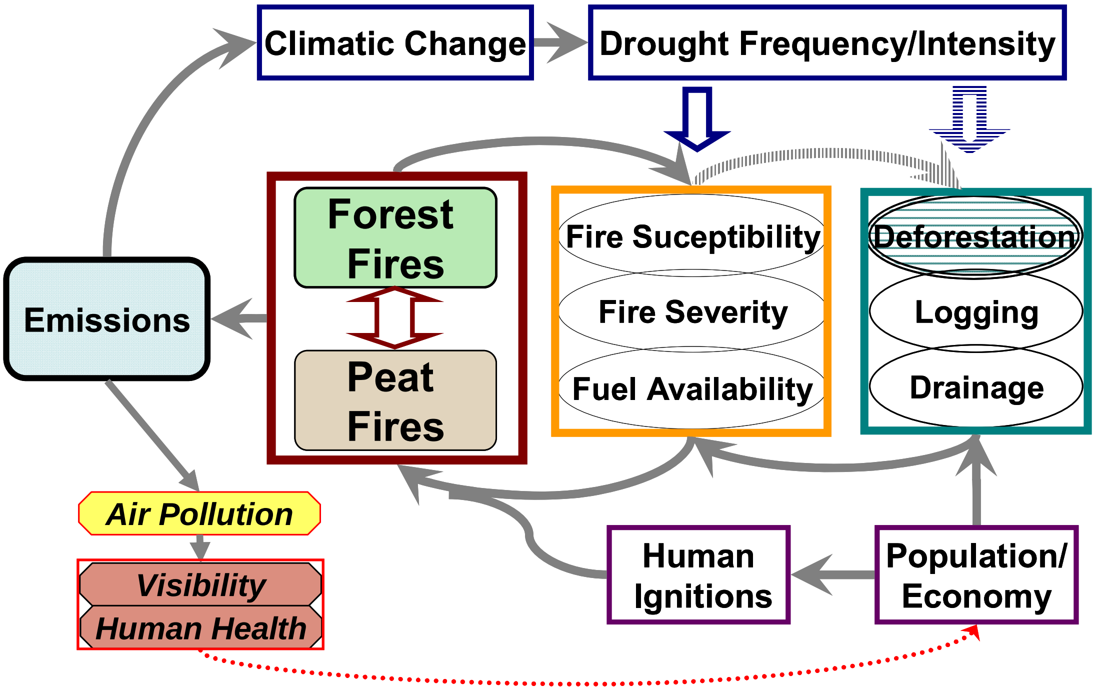

Figure 1-5: Feedbacks controlling fires, fire behavior and emissions and land cover change in a tropical peat swamp forests (partially adopted from Cochrane (2003)).

1.4 Fire-Related Air Pollution Events in Southeast Asia

In the three recent decades, widespread air pollution episodes from fires in Indonesia have been becoming more and more regular. Characteristically for these episodes is a strong and persistent impairment in horizontal visibility and strongly enhanced ambient air pollution levels, mainly caused by fire aerosols (particulate matter) (Heil and Goldammer 2001) (Figure 1-6). In addition, highly enhanced concentrations of ozone, carbon monoxide and other trace species can be observed throughout the troposphere (Fujiwara et al. 1999, Matsueda et al. 1999, 2002).

Figure 1-6: Photography of Kuala Lumpur's skyline in January 2005 during clear sky conditions (left) and during haze conditions in August 2005 (Photos taken from Web-Reference 5).

Since the 1960ies, at least 16 such events have been reported in which smoke from fires Indonesia covered not only regions within Indonesia, but also neighboring countries. Figure 1-7 illustrates the monthly development of horizontal visibility (25^{th} percentile of daily values) at two locations on Sumatra and two locations on Borneo. To indicate periods, where El Niño-related droughts have been occurring in Indonesia since 1960, the Ocean Niño Index (ONI) is displayed as well.

Figure 1-7 shows that all locations experienced short periods of abnormally reduced visibility, which generally coincide with positive ONI values (El Niño conditions). Since the 1990ies, periods of strongly reduced visibility have become more frequent. In the recent years, smoke-haze episodes occur almost annually. Since 1990, 11 smoke haze episodes have been reported, of which the episode in 1997/98 is frequently considered to be unprecedented in extent and intensity (Field et al. 2004).

Reports on smoke-haze and fire events prior 1990 are very anecdotal and fragmentary. When using visibility data as a proxy for fire-related smoke haze episodes, there are indications that there were likely smoke haze episodes prior to 1990 for which written reports are completely missing (e.g. 1961 and 1965). These episodes were, however, were less severe than those recorded in the recent decade. The number of studies on the impact of fire emissions on the tropospheric composition and ambient air quality has increased gradually since the 1990ies - mainly due to the progressive establishment of satellite and ground based monitoring systems. The increasing attention that has been paid to the more recent fire and smoke-haze events by the international media and organizations contributed to this development. Most studies so far focus on the extreme smoke-haze events of 1994 and 1997/98. They investigate the impacts of fire emissions on a) ambient air quality with focus on aerosol concentrations (Nichol 1997, Davies and Unam 1999, Heil and Goldammer 2001, Soleiman et al. 2003), b) aerosol chemical composition (Orlic et al. 1999, Igekama et al. 2001), and c) tropospheric concentrations of ozone, carbon monoxide, and carbon dioxide (e.g. Tsutsumi et al. 1999, Matsueda et al. 1999, Fujiwara et al. 1999, Kita et al. 2000). First numerical model studies to investigate the smoke-haze dispersion in the region were conducted by Koe et al. (2001), Roswinarti and Raman (2003) and Keywood et al.

(2003). They miss, however, a realistic prescription of the amount and composition of fire emissions.

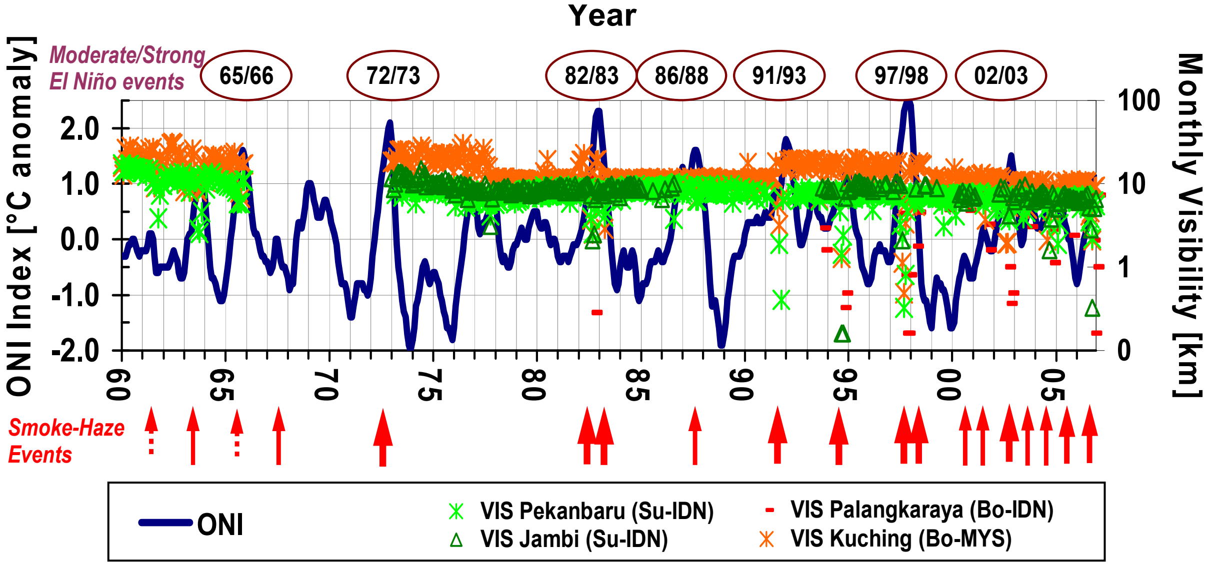

Figure 1-7: Development of the El Niño Southern Oscillation (represented by the monthly Ocean Niño Index (ONI)) as well as monthly visibility (VIS) at 2 locations on Borneo (Bo) and Sumatra (Su), respectively, from 1960 to 2006 (IDN=Indonesia, MYS=Malaysia). Visibility data are missing for 1967 to 1973. Reported smoke-haze events are marked with a red arrow. Dotted arrows indicate likely smoke-haze events for which written reports are missing. A detailed description of the smoke-haze events is given in Table 1-1.

All these studies constituted a fundamental first step towards the understanding of the characteristics and the relative importance of air pollution problems due to Indonesian fires. Due to the paucity of scientific data and studies, however, many aspects of this environmental problem are still not well understood and need further research.

Year	Reported Haze Episodes and Evidences of Corresponding Fire Events
1961	Written reports on haze are missing. There was most likely a haze episode over eastern parts of Sumatra and northern Borneo between JUL and NOV '61, as indicated by impaired visibility (Figure 1-7). *Written reports of fires are missing, but are likely, because of abnormally dry conditions prevailing in 1961 (Chokkalingam et al.2006).*
1963	Haze in Singapore (Taylor et al. 1999 and references therein (a.r.t.)). Visibility data show also haze in Sumatra. *Fires in Indonesia (Taylor et al. 1999 a.r.t.).*
1965	No written reports on haze. There was most likely a haze episode over eastern parts of Sumatra and Borneo between AUG and NOV '63, as indicated by impaired visibility (Figure 1-7). *Major fires in Indonesia (Taylor et al. 1999 a.r.t.).*
1967	Haze in Singapore (Taylor et al. 1999 a.r.t.). *No written reports on fires.*
1972	Severe haze over the eastern parts of Sumatra, Kalimantan, entire Malaysia and Singapore in between AUG and OCT '72 leading to disruptions in air traffic (Brookfield et al. 1995 a.r.t., Taylor et al. 1999 a.r.t). *Major fires in southeastern Sumatra and the southern part of Borneo (Taylor et al. 1999 a.r.t.).*
1982	Severe haze stretching over Indonesia to Borneo and to Peninsular Malaysia. From SEP to DEC '82. Daily mean particle concentrations (TSP) in Kuala Lumpur (Malaysia) generally ranged between 160 and 680 µg/m³ compared to a typical range between 50 and 80 µg/m³ (Aidid 1985). *Major fires occurred from SEP to DEC '82. Most of the fires occurred on Borneo, notably in East and West Kalimantan and Sarawak. Large fires also occurred in southeastern Sumatra (Taylor et al. 1999 a.r.t.). In total, roughly 1 Mha burned in the year 1982 (Goldammer and Seibert 1990 a.r.t., Zoumas et al. 2004).*
1983	Severe haze over entire Malaysia in APR '83 (Soleiman et al. 2003 a.r.t.) and SEP '83 (Radojevic et al. 2003 a.r.t.). *Major fires occurred from MAR to MAY '83. Most of the fires occurred on Borneo, notably in East Kalimantan, Sarawak and Sabah and Brunei. In total, around 5 Mha burned in 1982/83, of which around 4 Mha in 1983. Of the total burned area, an estimated 3.5 Mha burned in East Kalimantan only, of which 16% in peat swamp areas (Goldammer and Seibert 1990 a.r.t.).*
1987	Extensive haze in SEP '87 (Radojevic et al. 2003 a.r.t.). Haze in Sumatra (Wang et al. 2004). *Large fires in Indonesia exceeding the normal annual burning. According to official estimates, around in 0.05 Mha burned (Makarim et al. 1998).*
1991	Severe haze over entire Peninsular Malaysia and western Sarawak, notably in SEP and OCT '91. For greater Kuala Lumpur region, the haze episode was considered to be unprecedented in severity and persistence. In the latter, daily mean particle concentrations (TSP) generally ranged between 200 and 570 µg/m³ compared to a typical range between 50 and 80 µg/m³ (Soleiman et al. 2003 a.r.t.). Haze in Singapore during AUG to NOV '91 with weekly mean particle concentrations (TSP) ranging between 60 and 80 µg/m³ compared to a typical range between 40 and 50 µg/m³ (Chew et al. 1999). *Large fires in Indonesia (Sumatra and Kalimantan) that exceeded the normal annual burning. According to official estimates, around in 0.12 Mha burned (Makarim et al. 1998).*

Year	Reported Haze Episodes and Evidences of Corresponding Fire Events
1994	Severe haze over Indonesia, Malaysia, Brunei and Singapore during AUG to OCT '94. The maximum extent of the smoke-haze layer was at least 3 million km^2 (Nichol 1994). In Kuala Lumpur, TSP values during this period were 2-4 time higher than the long-term mean. The highest daily value measured was 464 $\mu g/m^3$ (Soleiman et al. 2003 a.r.t.). Severe haze during SEP and NOV '94 in Kalimantan and Sumatra derived from visibility data (Field et al. 2004). Severe haze also in Singapore during AUG and NOV '94 with weekly mean particle concentrations (PM_{10}) between 50 and 90 $\mu g/m^3$ compared to a typical range of 30 and 50 $\mu g/m^3$ (Chew et al. 1999). The maximum PM_{10} concentration in Singapore was 255 $\mu g/m^3$ (OCT '94) (Nichol 1997). During the entire period, strong enhancements in tropospheric ozone across the troposphere were observed across the Southeast Asian region (Fujiwara et al. 1999). *Large fires in the southern part of Sumatra and Kalimantan. Numbers given in literature on the estimated burned area highly contradictory. According to the Nature Conservation Service of the Republic of Indonesia (PHPA) statistics, in total 0.16 Mha burned (Makarim et al. 1998). In contrast, Dennis (1999) and Goldammer and Hoffmann (2001) provide numbers ranging from 0.41 Mha to 5.1 Mha*
1997	Severe haze over Sumatra and Borneo during AUG and NOV '97 with daily TSP levels generally between 150 and 4000 $\mu g/m^3$ compared to a normal background concentration of below 100 $\mu g/m^3$ TSP. Severe haze also affected Peninsular Malaysia and Singapore mainly during AUG and OCT '97, with daily TSP levels reaching between 100 and 500 $\mu g/m^3$ TSP (Heil and Goldammer 2001, see also Chapter 3). *Major fires in south-eastern Sumatra and the southern part of Borneo during JUL and NOV '97. While 0.3 Mha burned according to official estimates, most scientific estimates of the total burned area range between 4.6 to 13.6 Mha (see Chapter 3).*
1998	Severe haze over entire Borneo and Peninsular Malaysia during FEB and APR '98. In Brunei PM_{10} concentrations were generally between 50 and 650 $\mu g/m^3$, compared to a normal average of 50 $\mu g/m^3$ (Yadav et al. 1998). *Major fires in East Kalimantan during FEB to APR '98 burning a total area of around 5.2 Mha (Siegert and Hoffmann 2000) (see Figure 3-9 and Figure 3-8).*
2000	Haze in Singapore during MAR to JUL '00. Daily particle levels ($PM_{2.5}$) levels increased to 40 to 70 $\mu g/m^3$ compared to 10 to 40 $\mu g/m^3$ during non-haze episodes (Balasubramanian et al. 2003). *Fires in Sumatra burn around 0.2 to 0.4 Mha during this period (see Figure 3-8).*
2001	Haze over Sumatra, Singapore and parts of Peninsular Malaysia up to the southern Thailand in July 2001. Visibility was down to 500 m in several areas affected by the haze. In some areas, schools were closed and people were advised to wear protective masks when going outdoors (Web-Reference 6). *Fires in Sumatra in JUL burning around 0.08 to 0.1 Mha (see Figure 3-8).*
2002	Severe smoke-haze southern and western Kalimantan during AUG to NOV '02. In Palangkaraya, monthly mean PM_{10} concentration in SEP and OCT was 790 and 630 $\mu g/m^3$. Daily maxima of above 1300 $\mu g/m^3$ PM_{10} were frequently observed. In Pontianak, monthly mean PM_{10} concentration was around 300 $\mu g/m^3$ in JUL and AUG, with daily maxima reaching 850 $\mu g/m^3$. Also in northern Sumatra, severe smoke-haze conditions were observed during this period. In Medan, monthly PM_{10} concentration rose to above 450 $\mu g/m^3$. Typically, monthly mean PM_{10} concentrations are between 50 and 100 $\mu g/m^3$ (KLH 2003). Moderate haze in Singapore during AUG to OCT '02 with PM_{10} levels reaching 133 $\mu g/m^3$ (Web-Reference 7). *Major fires in Kalimantan burning 1.2 to 1.5 Mha during AUG to NOV'02 (see Figure 3-8).*
2003	Severe haze during MAY to AUG over central Sumatra, namely the province Riau in JUN '03. The smoke-haze also affected areas at the west coast of Peninsula Malaysia from Kuala Lumpur northwards for a few days in JUN and AUG'03 (see also Chapter 2.5). The smoke-haze also reached southern Thailand. In southern Thailand PM_{10} levels rose to about twice the normal background concentration on a few days in JUN and AUG '03 (i.e. between 90-110 $\mu g/m^3$ compared to a typical background concentration of between 30 to 50 $\mu g/m^3$ (Pentamwa 2006). Light haze occurred in Singapore in JUN' (Web-Reference 7). *Enhanced fire activity in Sumatra, notably in Riau, in JUN '03 burning in total around 0.1 to 0.3 Mha (see Figure 3-8).*
2004	Slight to moderate haze in the months of JUN to SEP '04 along the west coast of Peninsular Malaysia, mainly due to fires in Sumatra (DOE 2005). The smoke plumes also reached southern Thailand for a few days in JUN, JUL and AUG '04. Particle concentrations rose to twice the typical background concentration of about 30 to 50 $\mu g/m^3$ PM_{10} (Pentamwa 2006). Fires in Kalimantan caused haze in Sarawak (Borneo-Malaysia) (DOE 2005). In Palangkaraya, monthly mean PM_{10} concentration increased from 277 $\mu g/m^3$ in SEP '04 to 848 $\mu g/m^3$ in OCT '04 (KLH 2005). *Large fires in Sumatra JUN to SEP'04 burning in total around 0.2 to 0.7 Mha (see Figure 3-8). Large fires also in Kalimantan during AUG to OCT '04 burning in total around 0.4 to 0.5 Mha (see Figure 3-8).*
2005	Severe haze over Sumatra and Northern Peninsular Malaysia, no haze in Singapore during JUL to AUG'05. The Malaysian government declared the state of emergency in AUG '05 in two cities where the air pollution levels exceeded hazardous according to the Malaysian air quality classification. Schools in the capital Kuala Lumpur were closed and people have been advised to stay indoors and wear masks if they go outside (Web-Reference 5). The smoke plumes also reached southern Thailand for a few days in JUL and AUG '05. Particle concentrations rose to twice the typical background concentration of about 30 to 50 $\mu g/m^3$ PM_{10} (Pentamwa 2006). *Large fires in Sumatra during this JUL to AUG, burning in total around 0.2 to 0.5 Mha (see Figure 3-8).*
2006	Severe haze over Sumatra and Kalimantan during AUG to NOV '06 (UN-OCHA 2006). Haze affected the neighboring countries Singapore, Malaysia and Brunei, namely in OCT '06. In Malaysia, PM_{10} levels were between 150 and 300 $\mu g/m^3$ PM_{10} on several days in many locations (Web-Reference 8) while in Singapore PM_{10} levels reached 161 $\mu g/m^3$ (Web-Reference 7). *Large fires in Sumatra during AUG to OCT'06 burning in total around 0.6 to 1.1 Mha. Abnormally large fires in Kalimantan during this period, namely in OCT'06 in which around 0.8 to 1.6 Mha burned (see Figure 3-8).*

Table 1-1: Reported smoke-haze and fire events in Southeast Asia since 1960.

1.5 Atmospheric Aerosols, Air Quality and Health

Airborne particles are composed of solid and/or liquid material with a multi-modal size spectrum ranging from a few nanometers to around 100 µm diameter. Airborne particles are either directly released to the atmosphere from a source (primary particles, such as soot, dust) or formed in the atmosphere by gas-to-particle conversion of precursor gases (secondary particles, such as the oxidative formation of sulfate aerosols in the atmosphere from SO_2) (Seinfeld and Pandis 2006).

Particle size is one of the most important parameters in determining atmospheric behavior and impacts of particles. The total surface area and number of particles, chemical composition, atmospheric lifetime, emission sources, health impacts and visibility impairment, - all vary with particle size. Figure 1-8 shows an idealized schematic of principal modes, sources, and particle formation and removal mechanisms of atmospheric aerosols. Based on particle size and formation mechanism, airborne particles can be classified into two fundamental modes: the fine and coarse (C) mode. The cut-off of these two modes is at particle diameters of around 2.5 µm. The fine mode can be further subdivided into an ultrafine mode (U) and an accumulation mode (A), the cut-off of these two fine modes is at around 0.1 µm (USEPA 2004).

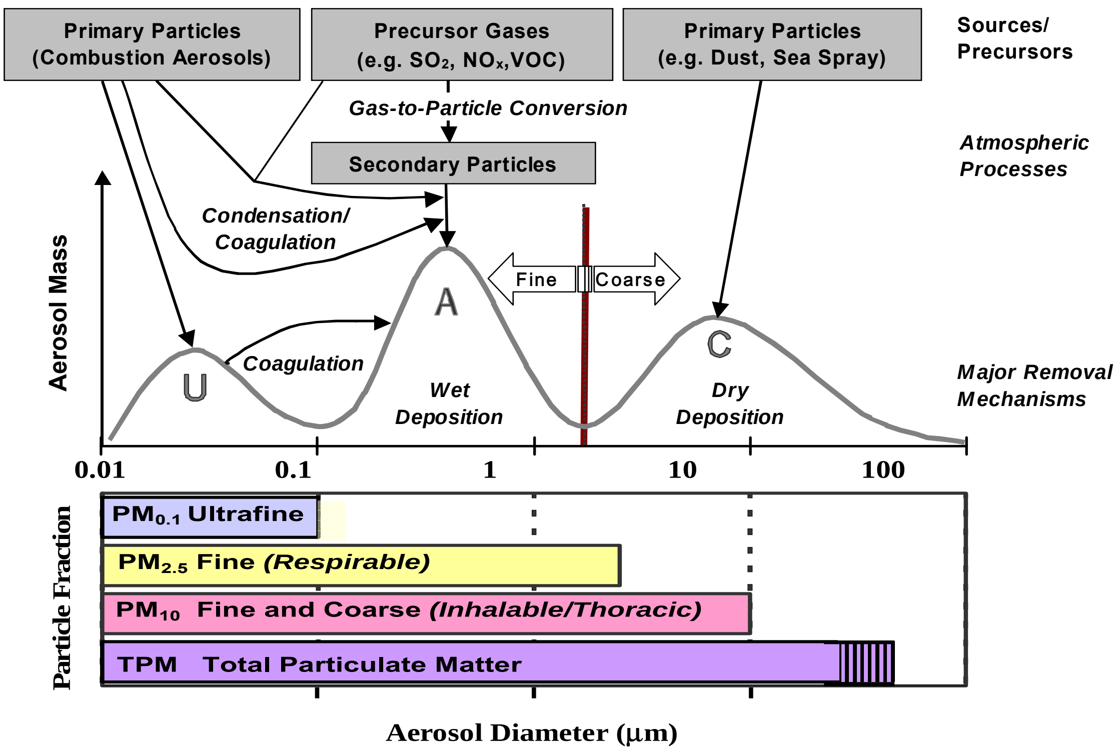

Figure 1-8: Idealized schematic of principal modes, sources, and formation and removal mechanisms of atmospheric aerosols. The abscissa shows the aerosol diameter while the ordinate the size-dependent aerosol mass (based on Seinfeld and Pandis 1998). U stands for ultrafine particle mode, A for accumulation mode and C for coarse mode particles. In ambient air quality monitoring, the following particulate matter (PM) size fractions are typically measured: TPM, PM_{10}, $PM_{2.5}$ and $PM_{0.1}$. Total Particulate Matter (TPM, frequently also referred to as Total Suspended Particles (TSP)) includes the entire size range of airborne particles, which may vary dependent on the environmental conditions. PM_{10} is the fraction of total airborne particles smaller than 10 µm diameter. This fraction can be inhaled through the larynx and that can penetrate into the thoracic region. These particles are therefore are also termed 'inhalable' or 'throracic'. $PM_{2.5}$, which is the particle fraction smaller than 2.5 µm diameter, can penetrate even deeper into the lungs, namely into the alveolar regions, where they are deposited for long periods. These particles are generally denoted as 'respirable'. Ultrafine particles (generally denoted as $PM_{0.1}$, i.e. particles smaller than 0.1 µm diameter) are likely to even pass through the lung into the bloodstream (Brunekreef and Holgate 2002). Note that the term 'coarse particle' is used commonly for both, the TPM and PM_{10}-fraction, respectively, minus the $PM_{2.5}$-fraction.

In general, fine mode particles originate mostly from combustion sources and include primary and secondary particles, whereas the coarse fraction is predominantly derived from natural sources (including windblown soil, sea spray) and mechanical processes (tire abrasion). Ultrafine particles rapidly coagulate and thereby transmute into the accumulation mode. Particles in this mode have, with up to weeks, the longest residence time in the atmosphere and can travel long distances (hundreds to thousands of kilometers). Their elimination out of the atmosphere is mainly due to wet deposition (rain-out, wash-out). Particles in the coarse mode are generally removed within hours up to a day by dry deposition (mainly sedimentation and impaction) (USEPA 2004).

Numerous recent epidemiological studies (e.g. Ostro 1993, Schwartz 1994, Dockery and Pope 1994, Pope 2000) have shown consistent, statistically-significant associations between increased exposure to daily aerosol loadings at levels typical of modern cities and morbidity and mortality – with no apparent threshold. Schwartz et al. (1996) suggested that increased daily mortality is specifically related to $PM_{2.5}$, and not to the coarse fraction of PM_{10} ($PM_{10-2.5}$). Fine particles may penetrate into the lower respiratory tract ('respirable fraction'), where they are retained for a long period whereas the larger particles are predominantly deposited in the upper respiratory system (DIN 1996). Acute morbidity outcomes resulting from the exposure to particulate air pollution include respiratory symptoms, cardiovascular diseases and decreased lung function. For instance, studies have observed increases in respiratory hospital admissions and emergency department visits by ~1% per 10 µg m^{-3} PM_{10} increment (Dockery and Pope 1994). In addition to the acute effects of particulate exposure, chronic respiratory diseases such as chronic bronchitis and permanently decreased lung function are likely to follow (Schwartz 1993). Generally, individuals with pre-existing respiratory or cardiac diseases, but also elderly people and children are most susceptible to adverse health outcomes (Schwartz 1994).

Responding to the epidemiological studies, the US Environmental Protection Agency (USEPA) revised the national air quality standards for particulate matter and included thresholds for $PM_{2.5}$. An air quality standard of 65 µg m^{-3} $PM_{2.5}$ as 24-hour average threshold and 15 µg m^{-3} as annual mean, respectively, was introduced in 1997. Meanwhile, the daily and annual mean PM_{10} standards remained unchanged at 150 µg m^{-3} and 50 µg m^{-3}, respectively. In December 2006, the daily standard has been revised to 35 µg m^{-3} $PM_{2.5}$ while revoking the annual mean PM_{10} standard (USEPA 1999, USEPA 2006a). According to the USEPA, the benefits of meeting the recently revised 24-hour $PM_{2.5}$ standards include an estimated reduction of 2,500 premature deaths in people with heart or lung disease, 1,630 hospital admissions for cardiovascular or respiratory symptoms, 97,000 cases of upper and lower respiratory symptoms, and 2 million days when people must restrict their activities because of particle pollution related symptoms (Web-Reference 9).

To make the status of local air quality and the related health risks easily understandable to the general public, the US Environmental Protection Agency (EPA) has developed the Air Quality Index (AQI, formerly Pollution Standard Index (PSI)) (USEPA 2006c). The AQI translates the concentration dependent health effects that have been found in various epidemiological studies into an index between 0 to 500 (Figure 1-9a). The AQI values are classified into five different air quality classifiers ranging from “Good” to “Hazardous”. The different slope of the AQI function for $PM_{2.5}$ compared to PM_{10} in Figure 1-9 reflects the higher relative health risks due to an incremental increase in the exposure to the finer particles compared to coarser particles. The difference is most pronounced at relatively low particle concentrations (below the ambient air quality standard for 65 µg m^{-3}).

So far, there is no sufficient evidence to conclude that particles emitted from forest or peat burning are significantly less or more damaging to health than those contained in urban aerosols (Hinwood and Rodriguez 2005, Naeher et al. 2007). Air quality reporting during fire-related haze-episodes using the AQI system, however, may lead to a strongly underestimated health risk if solely PM_{10} measurements are taken into account. This is the case for Southeast Asia where $PM_{2.5}$ air quality monitoring systems are not yet established. In Indonesia, air quality monitoring is even still based on TPM, only. Table 1-2 illustrates that the typical particle size distribution of ambient urban aerosols, for which the AQI system is primarily defined, is much less dominated by fine particles than air masses that are strongly influenced by fire emissions (Heil and Goldammer 2001). It is because vegetation and peat fire emissions almost exclusively consist of $PM_{2.5}$ while urban aerosols have a substantial coarse mode fraction.

For example, granted that the daily mean PM_{10} concentration in urban air is 60 µg m^{-3}. This concentration corresponds to an AQI of 54 (‘moderate’). Assuming a typical $PM_{2.5}/PM_{10}$ ratio for an urban aerosol of 54%, the $PM_{2.5}$ level in the air is 32 µg m^{-3} and the corresponding AQI is 84 (‘moderate’). In urban air that is strongly influenced by fire emissions, the $PM_{2.5}/PM_{10}$ ratio may increase to 80% (Table 1-2). A daily mean PM_{10} level of 60 µg m^{-3} then contains 48 µg m^{-3} $PM_{2.5}$. This concentration, in turn, translates into an AQI of 116, which is categorized as ‘unhealthy for sensitive groups’.

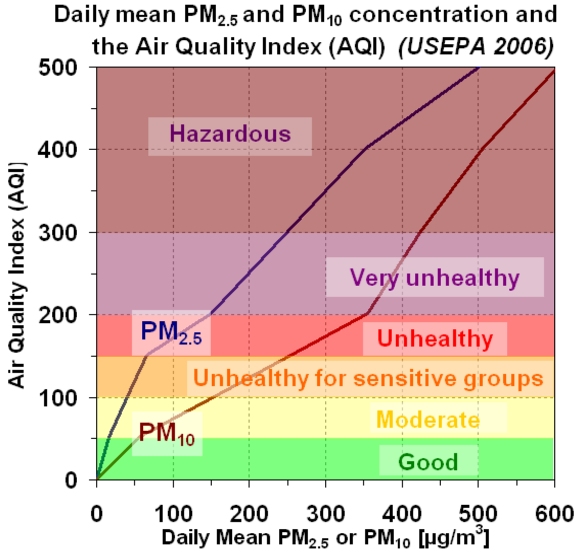

Table 1-2

Typical Particle Size Mass Ratios	PM_{10}/ TSP	$PM_{2.5}$/ TSP	$PM_{2.5}$/ PM_{10}
Road and Soil Dust (i)	52%	11%	20%
Diesel Truck Exhaust (i)	96%	92%	96%
Residential Wood Combustion (i)	96%	93%	97%
Urban Aerosol Mixture (background) (ii)	55%	33%	60%
Urban, Kuala Lumpur (no haze) (iii)	46%	-	-
Urban *during haze*, Kuala Lumpur (iii)	78%	-	-
Urban, Singapore (no haze) (iv)	-	-	54%
Urban *during haze*, Singapore (iv)	-	-	81%

Figure 1-9: (left) Relation between the daily Air Quality Index (AQI) and ambient $PM_{2.5}$ and PM_{10} concentration (USEPA 2006b).

Table 1-2: (right) Typical particle size distributions of directly emitted particles ((i) USEPA 2004) and aged urban aerosols which is or is not influenced by forest fire aerosols (“haze”) ((ii) Dockery and Pope 1994, (iii) Heil and Goldammer 2001, (iv) Tang and Orlic (unpublished)).

1.6 Objectives and Outline of this Thesis

The aim of this work is to quantify the emissions produced by Indonesian forest and peat fires during the last four decades and to assess the impact of fire aerosol emissions on air quality and human health. Further, the work aims at investigating the role of the climatic anomaly El Niño Southern Oscillation (ENSO) in influencing fire emission production and dispersion.

This chapter *(Chapter 1)* provides a general introduction into the causes and trends of Indonesian forest and peat fires and elaborates why these fires are of potential relevance for regional and global emission production and air pollution.

The objective of *Chapter 2* is to provide an answer to the question how strongly the climatic anomaly El Niño Southern Oscillation (ENSO) influences forest and peat fire activity in Indonesia. The study uses temporal and spatial statistical analyzes applied upon different fire satellite datasets combined with land cover and soil maps and ENSO indices.

Chapter 3 presents the results from a regional fire emission model that has been developed for Indonesia in order to quantify how much carbon and trace species were produced by fires in Indonesia between 1960 and 2006 and how these emissions contribute to total global emissions of these species. A particular focus of this chapter is to explore the relative importance of fires in peatlands to the overall emission production in Indonesia. A first application of the Indonesian fire emission inventory was in the framework of the RETRO project (REanalysis of the TROpospheric chemical composition over the past 40 years, 5^{th} EC framework programme). The results are part of the publication by Schultz et al. that has been *submitted* to *Global Biogeochemical Cycles.* The Indonesian fire emission inventory has been incorporated into the GEIA (Global Emission Inventory Activity) inventory and can therefore be used by a large science community for further studies.

Chapter 4 analyzes the influence of the abnormally severe fires in 1997 in Indonesia on regional air quality in Southeast Asia using daily air quality measurements for particulate matter from several stations in Indonesia, Malaysia and Singapore. Statistical analyzes are used to describe regional patterns in the temporal evolution and severity of fire-related air pollution and to ascertain the particular contribution of fire aerosols to the prevailing background air pollution levels. This chapter has been published in the journal *Regional Environmental Change* (Heil and Goldammer 2001).

As a tool to study the transport and removal processes of fire aerosols in the atmosphere, the regional climate and atmospheric chemistry model REMO is used in this work. The numerical model is also used as a tool to predict ambient concentrations of fire aerosols across the entire Southeast Asian regions, which – in contrast to measurements - are continuous in space and time.

Chapter 5 demonstrates the performance of the REMO model in predicting the physical state of the atmosphere. A precise prediction of atmospheric dynamics is a prerequisite for the reliable forecast of fire aerosol dispersion. The performance is tested by an extensive comparison of modeled parameters with observations. The model is then used to constrain the total amount of emissions produced by the 1997 Indonesian fires. This is done by a series of simulations with different fire emission scenarios (low to high) and by the subsequent comparison of modeled particle concentrations with measurements. This chapter has been published in the journal *Atmospheric Chemistry and Physics* (Langmann and Heil 2004).

Chapter 6 uses a experimental model set-up that is similar to *Chapter 6.* The aim of this study is to investigate the sensitivity of fire aerosol dispersion to the differing meteorological conditions of an El Niño and a normal year. Furthermore, the respective contributions of each, surface vegetation and peat fires, to the regional air pollution episode of 1997 are studied. This chapter has been published in the journal *Mitigation and Adaptation Strategies for Global Change* (Heil et al. 2007).

Chapter 7 uses modeled concentrations of fire-related ambient particle levels to provide a rough estimate of the number of cases of premature mortality in adults attributable to the 1997 extreme smoke-haze event.

The final chapter of this dissertation (*Chapter 8*) summarizes the main findings together with a conclusion that includes an outlook on essential future research requirements.

2 Linkage between El Niño Southern Oscillation (ENSO) and Indonesian Fires

2.1 Introduction

Nowadays, there is strong evidence that the interannual variability of fire activity in Indonesia is influenced by year-to-year variations in the ocean-atmosphere circulation associated with the El Niño Southern Oscillation (ENSO) phenomenon (Hope et al. 2005, Fuller and Murphy 2006). The ENSO phenomenon strongly alters rainfall regime in Indonesia and the entire so-called Maritime Continent (Ramage 1971, Ropelwski and Halpert 1987, Hamada et al. 2003, Aldrian 2003, Chang et al. 2004), which in turn, influence the fuel moisture and ignitability of the vegetation (Chochrane 2003, s.a. section 1.3). The evidence of the fire-ENSO linkage is supported by a series of paleoclimatic studies (Hope et al. 2005, Thevenon et al. 2004), the reanalysis of climatic and fire data of recent decades (Carmona-Moreno et al. 2005, Fuller and Murphy 2006) and mechanistic explanations of the phenomenon.

This chapter investigates the influence of ENSO on precipitation, drought-related fire activity and fire-related air quality in Indonesia.

2.2 Indonesian Rainfall Variability and ENSO

The intra-annual variability in Indonesian rainfall is characterized by two monsoonal seasons, the "wet monsoon" from around October/November until March/April, when wet winds blow over the archipelago from the northeast, and the "dry monsoon" from around May until September/October, when the dry southeasterly wind blows from Australia (Ramage 1971). Figure 2-1 displays the intra- and interannual variability of monthly accumulated precipitation rate in various regions of Equatorial Asia (EQAS) based on TRMM (Tropical Rainfall Mission Measurement) 3B43-V6 rainfall data which are available since January 1998. The TRMM 3B43-V6 product represent a "best-estimate" of monthly accumulated precipitation rate at a 0.25° horizontal resolution. It bases on the combination of 3-hourly microwave and infrared sensor estimates from the TRMM satellite that are merged with daily rain gauge data (Web-Reference 10).

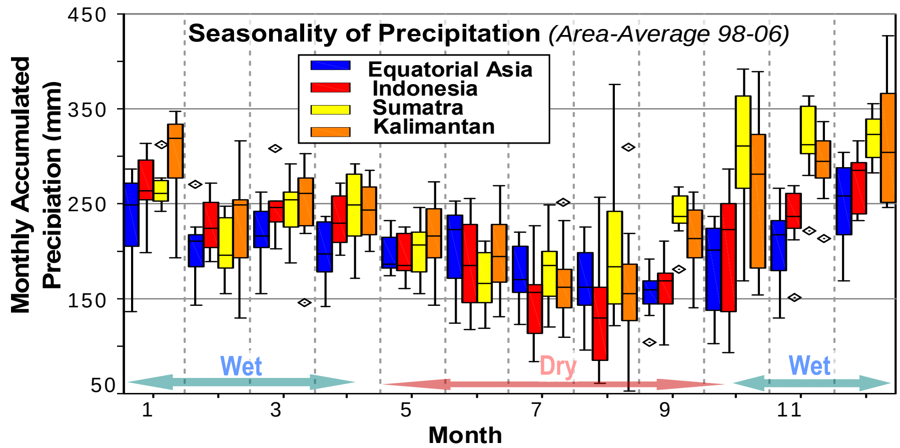

Figure 2-1: Boxplots[7] of monthly accumulated precipitation rate derived from TRMM (Tropical Rainfall Mission Measurement) 3B-43 satellite data product for Equatorial Asia, Indonesia, Sumatra and Kalimantan for the period January 1998 to December 2006 (Data Source of TRMM data: Web-Reference 11).

[7] The lower and upper edge of the box represents the 25th and 75th percentile value, respectively. The box thus covers 50% of all values of the sample, its length is a measure of the sample variability. The line across the box displays the median (50th percentile value or median). The whiskers extend from the smallest to the largest value that inside a "reasonable" distance from the end of the box. Values are

The advantage of the satellite-based TRMM data is that they have a complete spatial and temporal coverage while the network of rainfall monitoring station in EQAS is coarsely meshed. Several studies (e.g. Chang et al. 2005, Li and Fu 2005, Huffman et al. 2007) have shown that the TRMM data represent the annual cycle of rainfall in tropical EQAS very well, notably over land, and that there is no consistent bias in the TRMM data in this region towards too much or too little rainfall when compared to ground-based measurements.

During the wet season, Indonesia as whole experiences on average 245 mm rainfall per month while it is 165 mm per month during the dry season. The Indonesian islands Sumatra and Kalimantan-Borneo experience on average 30 mm per month more rainfall throughout the years than the country's average. This difference is most pronounced during August to December, i.e. from the end of the dry season to the first half of the wet season, when rainfall is on average 20 to 40% higher in Sumatra and Kalimantan. While around 10% more rainfall falls over Indonesia compared to the average rainfall of the entire Equatorial Asian (EQAS) region during the wet season, conditions are comparatively drier during the dry season (around 10% less rainfall than in EQAS during June to August).

As indicated by the length of the boxplots in Figure 2-1, there is also a pronounced intraannual variability in monthly precipitation rate, which is most pronounced during the second half of the year. This year-to-year variability in Indonesian rainfall is largely related to the effects of the El Niño Southern Oscillation (ENSO) (Philander 1989, Hendon 2003).

The ENSO phenomenon refers to the cyclic variations in oceanic and atmospheric quantities across the equatorial Pacific Ocean, such as sea surface temperatures, convective rainfall, surface air pressure, and atmospheric circulation (McPhaden et al. 2006). The ENSO cycle exhibits two extremes:

a) El Niño refers to the period of warming of sea-surface temperatures across the east-central equatorial Pacific. It represents the "warm phase" of the ENSO cycle. During a "warm phase", warm surface waters which are normally concentrated over the western equatorial Pacific region an eastward shift eastwards. This shift induces a displacement of the centre of tropical convective activity towards the central and eastern equatorial Pacific regions. As a consequence, the western equatorial Pacific regions including Indonesia experience a period of abnormally reduced rainfall.

b) La Niña refers to the periodic cooling of sea-surface temperatures across the east-central equatorial Pacific. It represents the "cold phase" of the ENSO cycle. During this phase, the Pacific warm pool and tropical convective rainfall are confined to the extreme western part of the equatorial Pacific basin. As a consequence, Indonesia experiences a period of abnormally enhanced rainfall.

The sea surface temperature (SST) anomalies in the tropical Pacific are used to calculate indices, which characterize the phase and strength of the ENSO cycle. The Oceanic Niño Index (ONI), for example, is calculated from the running 3-month mean SST anomaly for the region 5°N – 5°S and 120°W - 170°W) ("Niño 3.4 region"). A warm event ("El Niño") prevails if the 3-month mean SST exceeds a 0.5°C anomaly threshold at least 5 times in succession (Web-Reference 12). An event is categorized as weak if the SST anomaly ranges between 0.5° - 1.0° C, moderate for the range 1.0° - 1.5°C and strong for SST anomalies ≥ 1.5°C. Figure 2-2 shows the development of the 3-month average SST anomaly based on the ONI index from January 1960 to March 2007.

There is considerable variability in the ENSO cycle from decade to decade. Since the 1980ies, there has been a very active ENSO cycle with warm episodes prevailing. Since 1960, there have been in total 17 warm events, 7 of which were moderate to strong El Niño episodes (1965/66, 1972/73, 1982/83, 1987/88, 1992/93, 1997/98, and 2002/03). The El Niño episodes of 1982/83

considered to be beyond this distance, if they are beyond one and a half box lengths from either end of the box distribution (so-called "outliers" shown as squares. If the values exceed even three box lengths, there are categorised as extreme values (shown as stars).

and 1997/98 were even the strongest of the century (McPhaden 1999). During the same period, there have been in total 13 cold phases, 6 of which were moderate to strong La Niña episodes (1970/71, 1973/74, 19751984/85, 1988/89, 1995/96). The El Niño and La Niña episodes last on average 10 ±4 months. They often begin to form during June-August, reach peak strength during December-April, and then decay during May-July of the next year.

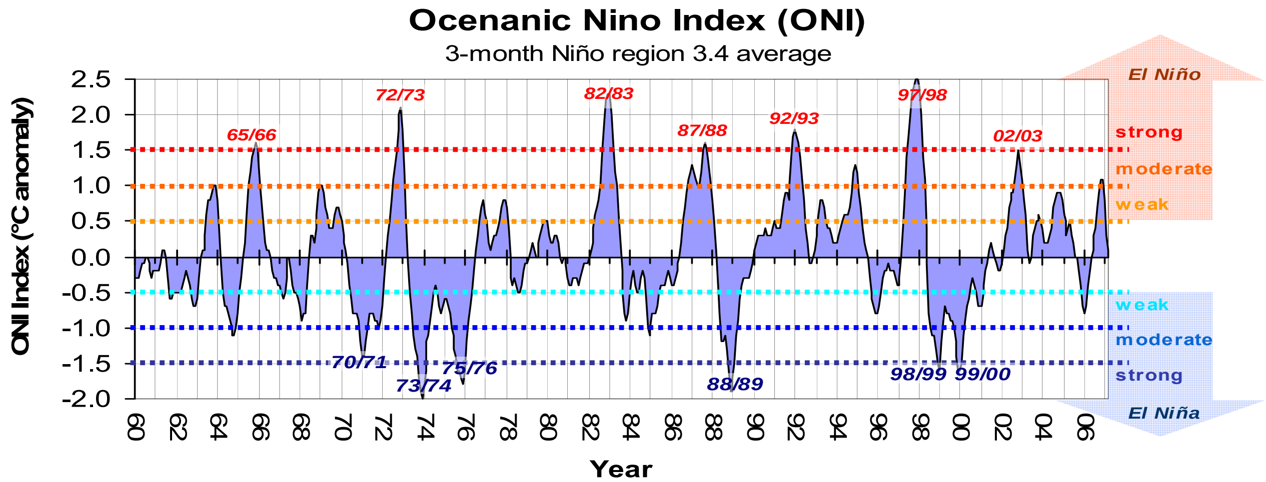

Figure 2-2: Development of the Oceanic Niño Index (ONI) from January 1960 to March 2007. Anomalies refer to the 1971-2000 base period. Marked are years with moderate to strong El Niño and La Niña conditions (Data Source: Web-Reference 12).

The fluctuations in ocean temperatures during El Niño and La Niña are accompanied by even larger-scale fluctuations in air pressure known as the Southern Oscillation, which is used to derive the Southern Oscillation Index (SOI). The SOI is calculated from the differences in air pressure anomaly between Tahiti and Darwin, Australia. Reverse to the ONI, the SOI is negative during El Niño episodes, with abnormally high air pressure over Indonesia and the western tropical Pacific and abnormally low air pressure over the eastern tropical Pacific (Hendon 2003). The reverse situation prevails during La Niña episodes.

There are various other indices used as an indicator for the sign and strength of ENSO. They all differ in the climatological parameters (ocean and/or atmospheric quantities) used to calculate the index and to which area they refer to (Gergis and Fowler 2005). Some of them, like the Multivariate El Niño Index (MEI), are based on a combination of both, observed anomalies in oceanic and atmospheric variables over the tropical Pacific, thereby better reflecting the nature of the coupled ocean-atmosphere system (Web-Reference 13). Because of the missing consensus on a standard index and on a standard anomaly threshold for the classification of an El Niño or La Niña event, large discrepancies exist in literature on whether a certain month or a certain year is categorized as "normal", "El Niño" or "La Niña", respectively (Gergis and Fowler 2005). In late 2003, the Ocean Niño Index (ONI) has been introduced by NOAA as a standard for the identification of weak to strong "El Niño" and "La Niña" events, which becomes increasingly adopted in climatic research. There are some advantages of using sea surface temperature (SST) to calculate the index over using atmospheric quantities (e.g. air pressure), among others, because atmospheric quantities are strongly influenced by chaotic weather fluctuations and because measurements of ENSO using SST are done over the entire tropical Pacific and will be much less susceptible to local changes than, for example, the SOI which is derived from only two measurements (Haylock 2002).

Accordingly, the monthly SOI time series exhibits a much higher variability than the oceanic index ONI or the combined index MEI. The linear correlation between the monthly SOI (period 1960 to 2006) with ONI or MEI is rather weak (coefficient of determination R^2=0.54 and 0.56) [8], while

[8] By default, the Pearson correlation coefficient is used for the calculation of R^2 in normally distristributed data. Normal distribution of the data is tested using the Kolmogorov-Smirnow D test. If the data do not follow a normal distribution, the Spearman's rho, a non-parametric

correlation between ONI and MEI yields an R^2 of 0.84. However, if smoothed by a running mean over several months, the SOI shows a largely coherent temporal pattern to the ONI and the MEI. For example, when the July to December means (1960-2005) of these three indices are linearly correlated, 85 to 91% of the observed variance can be explained by the regression model (i.e. R^2 of 0.85-0.91). The values are statistically significant at the 99%-Confidence Level (CI_{99}).

Various studies have found that there is a good and statistically significant correlation between rainfall variations in Indonesia and various El Niño indices. The indices can therefore be used as a predictor for Indonesian rainfall anomaly. While the SOI was the most commonly used index for such studies in the past (e.g. Braak 1919, Berlage 1927, Schell 1947, Hamada et al. 2002), several recent studies used SST-based indices, such as the ONI, notably for the so-called Niño3 region (5°N – 5°S and 90°W - 150°W) (Aldrian and Susanto 2003, Hendon 2003, Chang et al. 2004, Aldrian et al. 2007).

For example, Aldrian et al. (2007) examined the spatial patterns of the correlation between rainfall and Niño3 SST during the study period from 1961 to 1993 based on rain gauge data for a) the dry season (May to September) and b) the wet season (November to March). Except for the northwest region of Indonesia, he found that rainfall during the dry season has a statistically significant correlation with Niño3 SST, and the correlation is more sensitive to El Niño than La Niña events. Rainfall in Indonesia during the wet season tends to be largely uncorrelated with SST and spatially incoherent (Hendon 2003).

For the same study period, Aldrian (2003) examined monthly rainfall anomalies of strong El Niño years (1965, 1969, 1972, 1982, 1987, and 1991) compared to normal years based on rain gauge data. The influence of El Niño is detected first over Indonesia in May with a sharp decrease of rainfall in southern islands (Figure 2-3). From June onward, the negative anomalies increase and extend from southeast Indonesia westward and northward. By August the anomaly covers almost the whole country except North Sumatra and North Kalimantan. Most of the regions experience a reduction of rainfall of at least 60%. The maximum reduction occurs in September. The influence of El Niño, which begins to decrease in October, leads to a statistically significant delay of the onset of the northern monsoonal rainy season (Hamada et al. 2002). In return, rainfall amounts in December tend to be higher during a strong El Niño year than during normal years (Aldrian 2003).

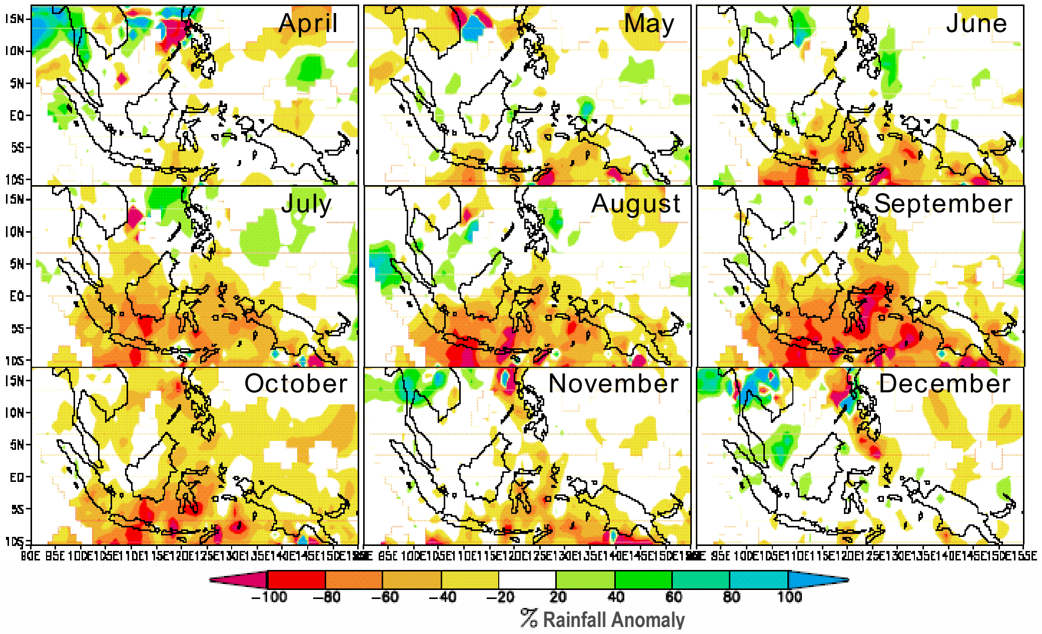

Figure 2-3: Monthly rainfall anomaly during strong El Niño years relative to normal years (1961 –1993) (Aldrian 2003).

version of the Pearson correlation coefficient is used for calculating R^2. It bases on the rank order instead of the actual value of the data in the sample (Schönwiese 2006).

Figure 2-4a) shows the development of monthly precipitation anomaly in entire Equatorial Asia as well as Indonesia, Sumatra and Kalimantan since January 1998, when regionally-consistent satellite-derived precipitation data for the region became available. Before this period, regional precipitation information is solely based on interpolated station measurement data, which, however, leads to poor results as many measurements are missing (Spessa et al. *in preparation*). Figure 2-4a) illustrates the reciprocal connection between the El Niño Southern Oscillation, reflected by the ONI, and precipitation rate in the region. During El Niño conditions, when the ONI is above 0.5, precipitation rate tends to be below average, while it is above average during La Niña conditions, when ONI is negative (below 0.5). In the first half of 1998, i.e. during the very strong El Niño of 1997/98, which prevailed from May 1997 to April 1998, suppression of rainfall rate is very pronounced in Kalimantan. The almost complete suppression of the northern monsoonal rainfalls in Kalimantan, notably Eastern Kalimantan, that would normally occur during November to April, is a typical feature occurring during very strong El Niño years (e.g. 1982/83 and 1997/98) (Hope et al. 2005). At the same time, rainfall in Sumatra is near to normal. Rainfall rate tends to be above normal during mid-1998 to mid-2001 when weak to moderate La Niña conditions preponderate. With the exception of October 2005 to April 2006, ONI values are positive in the subsequent years until the end of 2006, with weak to moderate El Niño conditions prevailing in May 2002 to March 2003, July 2004 to February 2005, and September 2006 to January 2007. During these periods, precipitation is generally below average.

Throughout 1998 to 2006, the monthly development of precipitation rate anomaly in Indonesia is highly linearly correlated to the development in entire EQAS (coefficient of determination R^2 of 0.62). However, the absolute values in precipitation anomaly tend to be distinctively higher in Indonesia. A linear regression model also shows that around 63% of the variation of monthly precipitation rate in Indonesia can be explained by the variation in precipitation rate anomaly in Borneo (and 56% by Sumatra). Monthly variation in precipitation rate anomaly in Sumatra is only moderately correlated to the one in Borneo (R^2 of 0.47), reflecting the spatial heterogeneity of precipitation variability across Indonesia. Monthly variations in the ONI explain only 18% and 11%, respectively, of the variations in monthly precipitation rate anomaly in Borneo and Sumatra, while it is 39% for entire Indonesia and 52% for entire equatorial Asia.

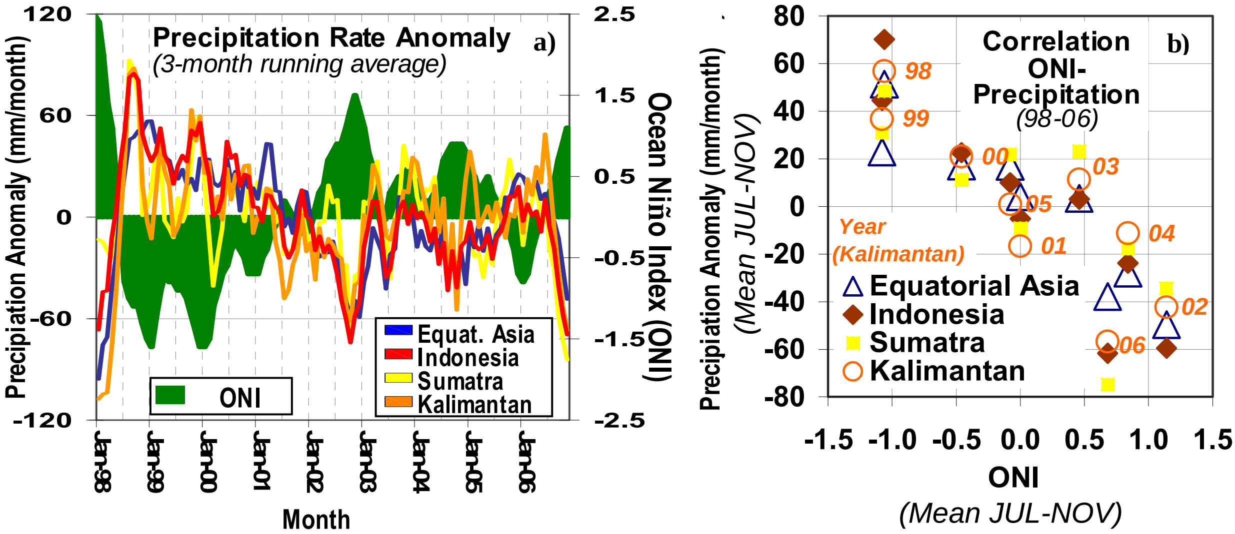

Figure 2-4: a) Development of monthly precipitation anomaly and of the Ocean Niño Index (ONI) during January 1998 to December 2006 in Equatorial Asia, Indonesia, Sumatra and Kalimantan, derived from TRMM data (Data Source: see Figure 2-1). Precipitation anomaly was calculated from the deviation from the 'climatological' 1998-2006 monthly means. b) Scatterplot between TRMM precipitation rate anomaly and the Ocean Niño Index (ONI) based on July to November averages (Data Source of ONI data: Web-Reference 12).

The time series of the monthly precipitation rate anomaly exhibit a high variability due to a high stochastic component that is characteristic for weather fluctuations ("white noise"). In contrast, the ONI time series exhibits only little fluctuation from one month to the other reflecting that the ocean and its temperature is a very inertial system. In a statistical sense, this means that the ONI time series is highly autocorrelated and can therefore be represented as an autoregressive process of high order (von Storch and Zwiers 1998).

The low correlation found between monthly ONI and precipitation for Sumatra and Borneo reflect that, at a more localised scale, other factors than changes in the ocean temperature (ONI) predominantly influence the month-to-month fluctuations in precipitation. Such factors include local topography or local air-sea interactions (Aldrian 2003). This also partly explains, for example, the short period of distinctively reduced rainfall occurring in Sumatra in spring 2000 during moderate La Niña conditions, when rainfall rate is expected to be higher than normal.

When averaging over larger areas or several months, the influence of ENSO on longer-term rainfall anomaly becomes more apparent. The strong correlative association between the ONI and precipitation rate anomaly is shown in Figure 2-4b for the respective July to November (JASON) means. This averaging period was chosen as because it includes the months where a) according to the above mentioned studies, the influence of El Niño on precipitation tends to be strongest, b) the monthly precipitation rate of TRMM data exhibits the largest interannual variability (results not shown), and c) generally most drought-related vegetation fires occur. Finally, the averaging creates non-autocorrelated time series which are required for classical testing of statistical significance (von Storch and Zwiers 1998).

Linear correlation of JASON-averaged ONI and precipitation yields a coefficient of determination (R^2) of 0.86 for Indonesia, 0.74 for Kalimantan and 0.58 for Sumatra. The results are statistically significant at the $CI_{99\%}$-level ($CI_{95\%}$-level for Sumatra, n=9). Similarly large or even larger R^2 values are found when other ENSO indices such as the MEI (R^2=0.65-0.84) and the SOI (R^2=0.73-0.92) are used instead of the ONI. In agreement with the results found for the ONI, the strength of association between precipitation anomaly and both, MEI and SOI index, is highest for entire Indonesia and lowest for Sumatra. For equatorial Asia, the strength of association between precipitation and all ENSO indices is always around 10-20% lower than for Indonesia.

2.3 Interannual Variability in Indonesian Rainfall and Indonesian Fires

Figure 2-5 illustrates the intraannual variability of the spatial distribution of TRMM-precipitation rate and ATSR fire activity across Equatorial Asia (EQAS) during the traditional land clearing fire season from July to November (JASON). The fire data cover the years 1997 to 2006. The TRMM precipitation observations start in 1998 only, thereby missing the strong El Niño year of 1997. Fire activity is shown separately for surface and peat fires, because a) the rainfall-dependency of fires in surface vegetation and peat soils is expected to differ and b) because peat fires are much more relevant in terms of fire emission production and air quality degradation (Section 1.3). The discrimination between surface and belowground peat soil fires has been done based on whether a fire count has been recorded on a non-peat soil area ("surface fires") or an area with known peat deposits ("peat fires"). The latter information comes from the data provided by Wahyunto et al. (2003, 2004) and FAO (2003) (Figure 1-2). Using this approach, however, fires in peat areas that only burn the surface vegetation above the peat deposit are wrongly classified as peat fires. This peat fire classification therefore represents an upper bound estimate of actual peat fires as it may also include surface fires.

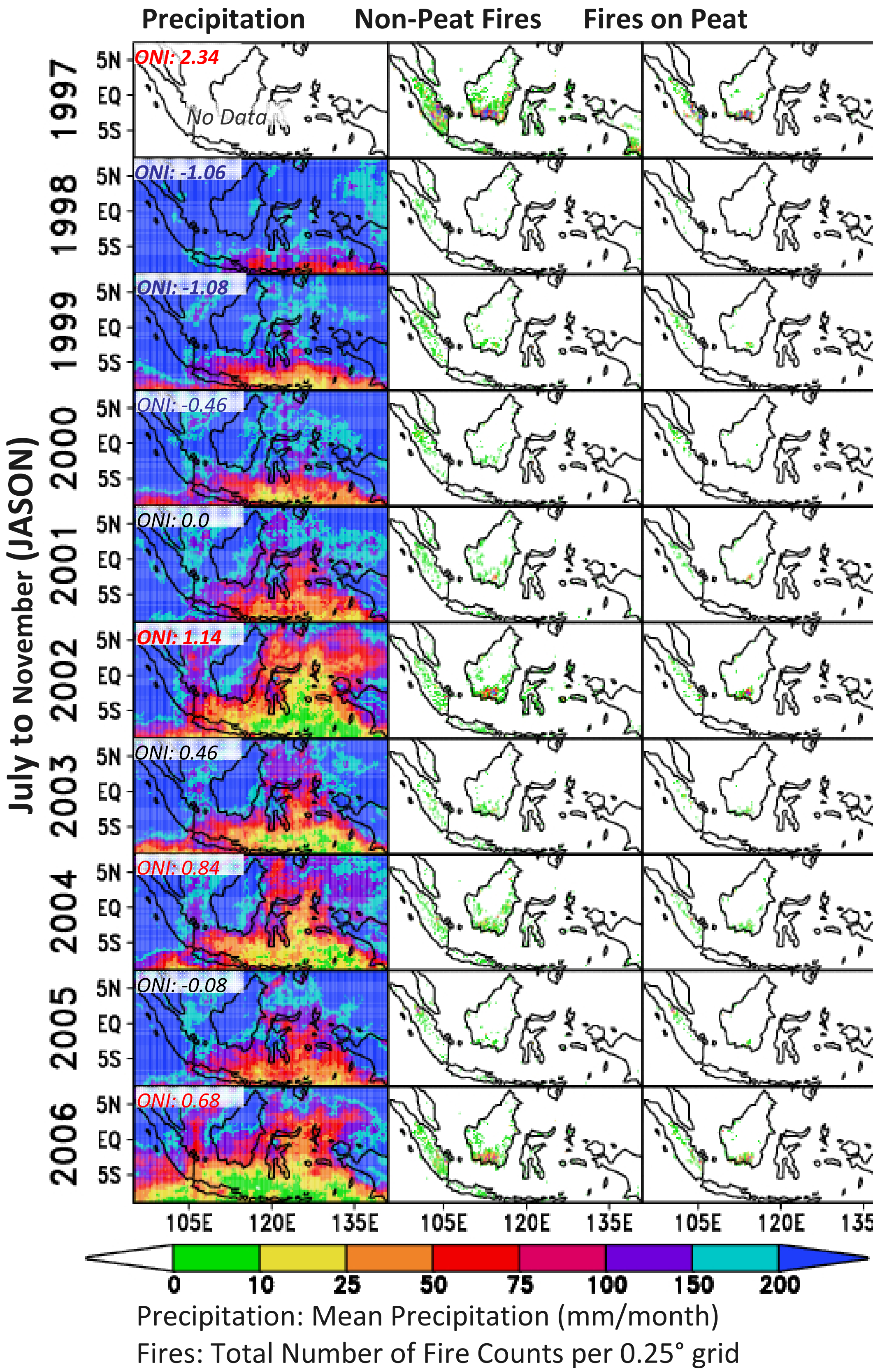

Figure 2-5: Left panel: Mean July to November (JASON) precipitation rate (in mm/month) in Equatorial Asia (excluding Papua New Guinea) during 1998 to 2006 based on TRMM data (Data Source: see Figure 2-1) and corresponding mean Ocean Niño Index (ONI). El Niño (La Niña) events are marked in red (blue), and moderate to strong events in bold. Middle and right panel: Total number of ATSR fire counts detected during JASON on areas with no peat soil cover ("surface fires") and peat soil areas ("peat fires"), respectively (Data Source of ATSR data: Web-Reference 14).

In El Niño years (i.e. 2002, 2004, 2006), drought conditions (<100 mm/month) during JASON expand north-westward with the southern monsoonal winds from Australia to far beyond the equator (Figure 2-5 left column). The drought conditions do not only affect entire Java, Nusa Tenggara and Sulawesi, but also the southeastern parts of Kalimantan and Sumatra. During normal ENSO conditions (2000, 2001, 2003, 2005), the northward expansion of dry conditions is suppressed. Drought conditions prevail only over Java and the Nusa Tenggara islands, while precipitation rate over the more northern islands (e.g. Kalimantan, Sumatra, Irian Jaya) generally experience 100 to 300 mm rainfall per month. During La Niña years (1998, 1999), the northward expansion of the dry conditions is even more suppressed. Except for the eastern parts of Java and Nusa Tenggara, almost the entire country of Indonesia experiences wet to very wet conditions (> 200 mm per month). Contrary to Indonesia, JASON precipitation rate in Malaysia and the other countries of EQAS is much less affected by interannual variations and remains above 200 mm per month throughout 1998 to 2006.

Most of the total surface fire activity in EQAS throughout 1997 to 2006 occur in Kalimantan south of the equator and in entire Sumatra except its very north (Figure 2-5 middle column). Fire activity during JASON shows a strong interannual variability which largely follows the variations in precipitation rate associated with the ENSO (Figure 2-5 left column). During La Niña and normal ENSO conditions, fire density is generally low (less than 10 active fires per 0.25° x 0.25° grid cell during JASON). Fire activity is almost exclusively confined to Sumatra and Kalimantan, whereas the area coverage is larger in Sumatra than in Kalimantan. Except for the 2004, a pronounced increase in fire density and the spatial expansion of fire activity is apparent during El Niño years (1997, 2002, 2006). Vast areas of southern Central Kalimantan exhibit dense fire activity (50 to 100 fires per grid cell). During the strong El Niño year of 1997, fire density widely increases even to above 200 fires per grid cell. Clusters of high fire density also occur in some areas of South Sumatra. Fire activity also strongly affects Sulawesi, eastern Java and south-eastern Irian Jaya in some El Niño years. Malaysia and the other countries of EQAS exhibit only scattered fire activity throughout 1998 to 2006.

Peat fires in EQAS during JASON 1998 to 2006 almost exclusively occur in the peat deposits of southern Kalimantan and Sumatra , while the peat deposits in western Kalimantan, and Malaysia are generally spared (Figure 2-5 right column, for peat soil distribution please refer to Figure 1-2). Fires in the extensive peat areas of Irian Jaya only occur in 1997, and here only in the southeast. Peat fire activity exhibits a largely similar interannual variability pattern to surface fires. Fire density detected by the ATSR sensor in peat areas is generally low. Dense peat fire activity occurs during El Niño years of 1997, 2002 and 2006, but is widely confined to the Mega-Rice-Project area in Central Kalimantan (Figure 1-2), and some sporadic occurrences in peat deposits of Sumatra.

Figure 2-6 shows the correlation between the mean precipitation rate during a) JASON and b) January to March (JFM), respectively, and surface fire activity (left column) and peat fire activity (left column), respectively. Due ensure a minimum number of degrees of freedom for the statistical analysis, the correlation covers only those areas where fires have been recurrently burning for at least 5 years during 1998 and 2006. With a few exceptions, surface fire activity in Kalimantan during JASON is negatively correlated with the amount of precipitation falling during this season. This connection between decreases in rainfall and increases in surface fire activity is most prominent in the southwesternmost parts of Kalimantan, where a correlation coefficient R between -0.5 and -1 is found (medium to very high correlation). In Sumatra, surface fire activity during JASON appears to be largely uncorrelated to precipitation.

Recurrent peat fires in Kalimantan during JASON almost exclusively occur within the region of the Mega-Rice-Project (see also Figure 1-2). Without exception, fire activity in these areas is negatively correlated with the mean precipitation rate. The correlation is generally medium to high (R lower than -0.5) and statistically significant at the 95% or even 99% significance level. The connection between peat fires in Sumatra and rainfall during JASON is very inconsistent and generally not statistically significant.

The area covered by recurrent fires during JFM is much lower than during JASON and is largely confined to Sumatra, namely the province Riau. Peat fires prevail over surface fires during this season. The fires are predominantly negatively correlated, the correlation is mostly moderate to high (R lower than -0.5), but in most cases not statistically significant.

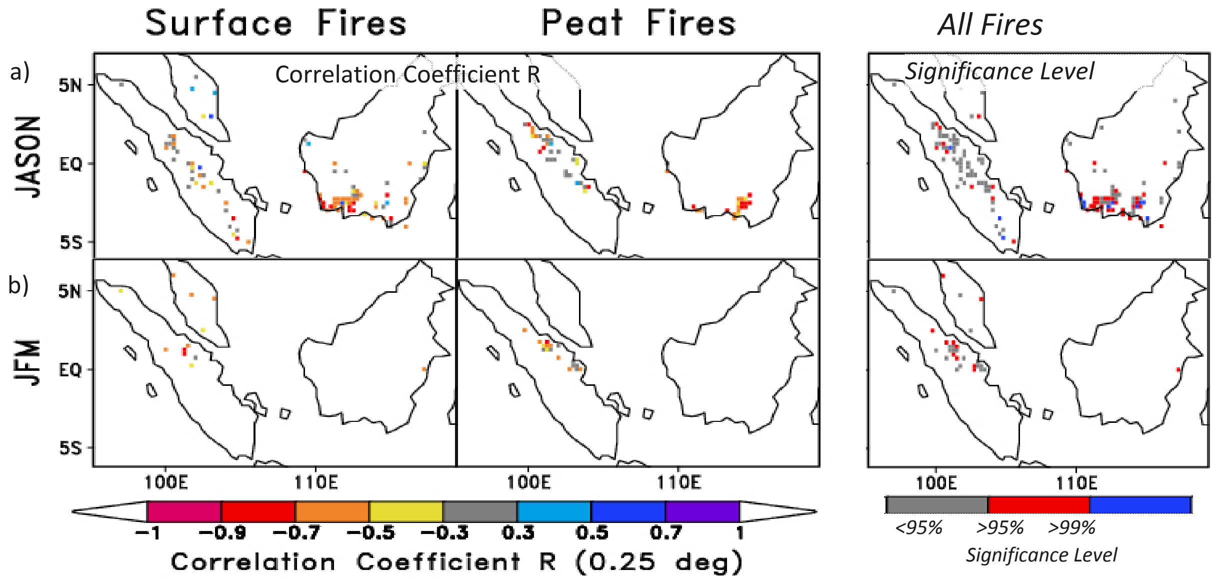

Figure 2-6: a) Correlation coefficient (R) calculated from linearly regressing mean monthly TRMM precipitation rate and total number of ATSR fire counts per 0.25° grid (July to November JASON) for the years 1998 to 2006 (Data Source: see Figure 2-5). For the statistical analysis, only those grid cells are included in which fires were detected for more than 5 years fires. The correlation coefficient is calculated for fires on non-peat soil cover ("surface fires") and peat soil areas ("peat fires") separately (left and middle panel, respectively). The right panel displays the statistical significance of the correlation coefficient (t-test statistics). b) Same as a) but for the period January to March (JFM).

The analysis of how monthly precipitation rate is distributed across peat and non-peat areas in Kalimantan and Sumatra reveals that Kalimantan's peat areas experience significantly more drought conditions during the main dry season (July to September) of El Niño years relative to the total area than non-peat areas (Figure 2-7). The difference is also apparent during normal ENSO conditions, but unapparent during La Niña conditions. During El Niño conditions, 62% of Kalimantan's peat area experience dry conditions (< 100 mm rainfall per month), 48% severe drought (< 50 mm per month) and 15% extreme drought (< 20 mm per month). Compared to this, only 44%, 25% and 5% of Kalimantan's non-peat area, respectively, experiences drought to extreme drought conditions. The relative occurrence of extreme dry (dry) conditions is thus around 2.7 (1.4) time larger in Kalimantan's peat areas compared to the non-peat areas. The difference in rainfall distribution gradually equalizes towards higher precipitation classes.

In contrast to El Niño conditions, the occurrence of extreme to severe drought conditions (< 40 mm per month) is negligible during neutral ENSO conditions in both, peat and non-peat areas. Very dry conditions prevail over 16% of Kalimantan's peat, but only 6% of the non-peat areas. The relative occurrence of dry conditions in Kalimantan's peat and non-peat areas is much lower during neutral ENSO conditions in Kalimantan's peat area (42% versus 62% in El Niño years), and notably the non-peat areas (18% versus 44%). Similar to the situation found for El Niño conditions, dry conditions in peat and non-peat area are relatively more frequent – the ratio is even larger than during El Niño conditions (ratio of 2.3 versus 1.4). Finally, during La Niña years, almost the entire peat and non-peat areas of Kalimantan (> 95% for) experience abundant rainfall (> 100 mm per month).

Dry conditions in Sumatra during July to September occur in less than 10% of the land area only during La Niña and neutral conditions, and are almost equally distributed among peat and non-peat areas. Contrary to the situation in Kalimantan, drought conditions in Sumatra are relatively less frequent peat than in non-peat areas during El Niño conditions.

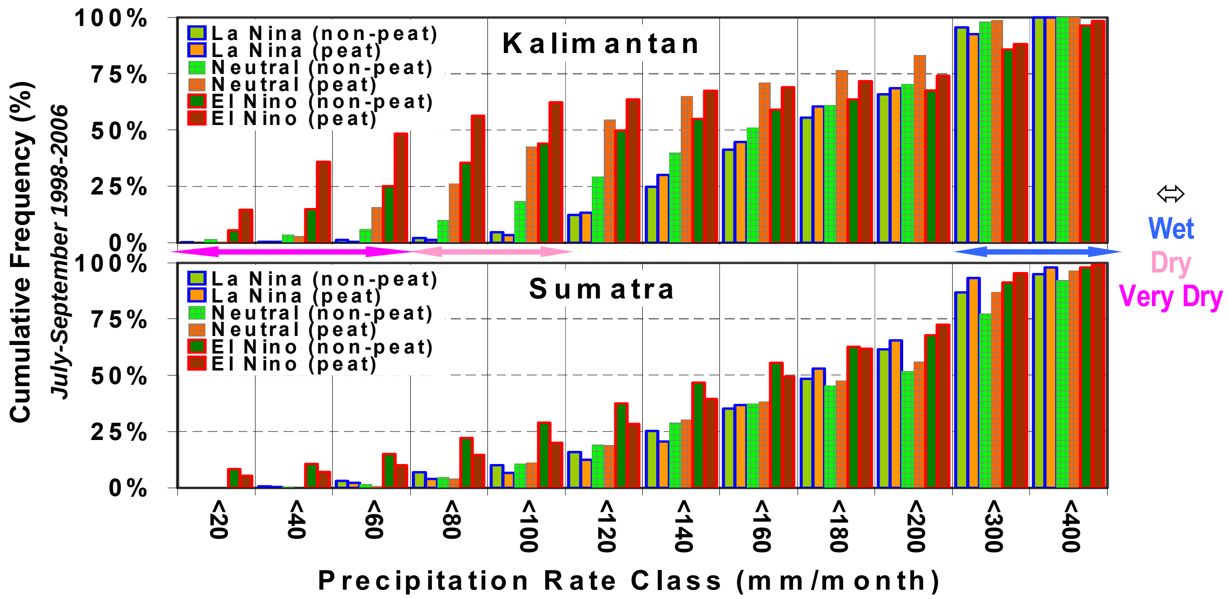

Figure 2-7: a) Distribution of monthly precipitation rate classes during July to September dependent on the soil type (non-peat versus peat areas), the ENSO condition (La Niña, Neutral and El Niño years), and the region (Kalimantan and Sumatra) based on TRMM data from 1998 to 2006 (Data Source: see Figure 2-5).

In summary, the accumulated amount of precipitation falling over Indonesia throughout the traditional land clearing fire season from July to November is strongly connected to the state of the El Niño Southern Oscillation (ENSO) with abnormally dry (wet) conditions prevailing during El Niño (La Niña). The connection is more pronounced for Kalimantan than for Sumatra. The length of the relatively dry season in the second half of the year in the Indonesia, combined with the frequency and the amount of precipitation falling by intermittent rains, strongly determines fuel moisture and thus fuel ignitability during this period.

The connection between the amount of rainfall during JASON and fire activity is most pronounced in Kalimantan. The weaker correlation found for Sumatra indicate that other factors than precipitation predominantly determine fire activity. As a conclusion, ENSO conditions clearly influence fire risk in Indonesia: the risk of abnormally large and sustained fires is expected to increase with intensifying El Niño conditions while abnormally low fire activity is expected during La Niña conditions. ENSO indices can therefore be used as a reasonable proxy of fire activity.

2.4 Variability in Indonesian Fire Activity

Fire activity in Indonesia exhibits strong intraannual and interannual variability. Figure 2-8 provides an overview of the development of monthly fire activity in Indonesia and other regions of Equatorial Asia (EQAS) during July 1996 and November 2006 based on ATSR active fire count data (Algorithm 2, see also Section 1.2). The left panel of Figure 2-8 shows the total fire activity observed while the right panel shows the fire activity observed exclusively on peat soils. The differentiation between peat fires and non-peat fires was done at 0.01 degree resolution (~1.16 km at the equator) using information on the distribution on peat soils given in Wahyunto et al. (2003, 2004) and FAO/UNESCO (2003) (Figure 1-2). As discussed on section 2.2, the assignment may lead to an over-prediction of the actual number of peat fires since some fires occurring on peat soils may have only affected the surface vegetation above the peat.

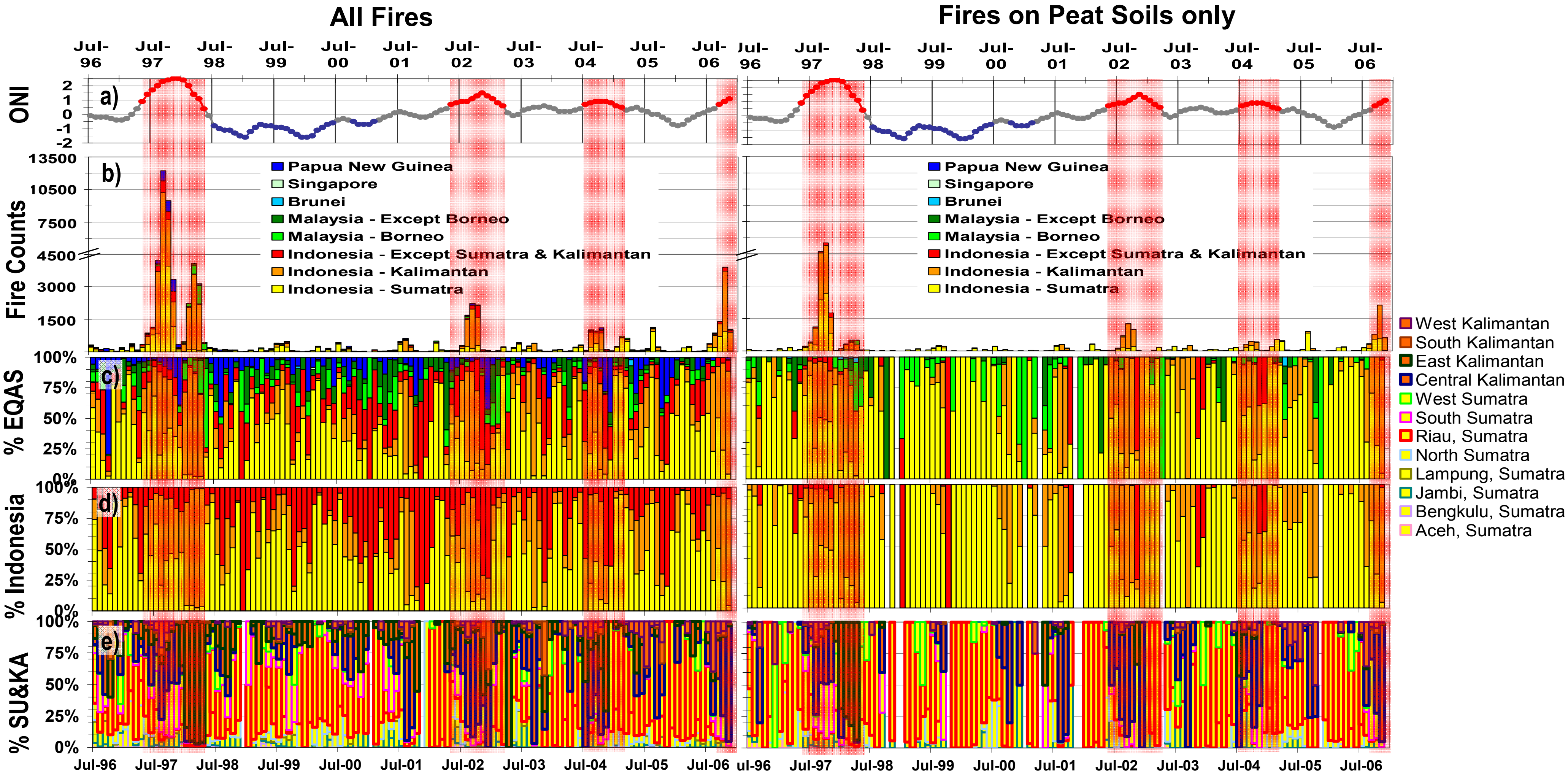

Figure 2-8: a) Temporal development of the monthly Ocean Niño Index (ONI). b) Temporal development of monthly ATSR02 fire counts in different regions of equatorial Asia (EQAS) (left: total fires, right: fires on peat soil only). c) Relative contribution of different regions of EQAS to total monthly number of fire counts observed in all EQAS countries. d) Relative contribution of fire counts observed in Sumatra and Kalimantan to the total number of fire counts observed in entire Indonesia. e) Relative contribution of fire counts observed in the different provinces of Sumatra(SU) and Kalimantan(KA) to the total number of fire counts observed in Sumatra and Kalimantan.

Figure 2-8 illustrates the strong interannual and intraannual variability of fire activity in EQAS. On a monthly basis, the highest number of fires detected in the entire region 12,219 in September 1997, compared to a minimum 5 active fires observed per month in detected January 2001.

The majority all fires recorded in EQAS throughout July 1996 to December 2006 (in total 75,022 ATSR fire counts) occur in Indonesia (89%). The remaining ~11% are equally distributed among Malaysia and Papua New Guinea.[9] 91% of all Indonesian fires (in total 66,791 fire counts) occur in Sumatra and Kalimantan, with fires in Kalimantan being 49% more numerous than in Sumatra (36,232 versus 24,334 fire counts).

Fires in non-peat areas make up 59% of all fires recorded in EQAS during 1996 to 2006 (in total 44,034 non-peat fire counts compared to 30,988 peat fire counts). When regarding the major sub-regions of EQAS, fires in non-peat areas dominate overall fire activity in Irian Jaya, Malaysia, Kalimantan-Indonesia and the so-called ‘rest of Indonesia (rINO)’ (Indonesia except Kalimantan and Sumatra). Surface fires contribute 100%, 73%, 88% and 61%, respectively, to the overall fire activity observed in these regions. The reverse situation prevails in Sumatra, where fires in peat areas dominate overall fire activity (62% of all fires).

Figure 2-9 summarizes the contribution of various regions to the total number of fires recorded on non-peat and peat areas in EQAS during July 1996 to December 2006. Fires in non-peat areas of EQAS are clearly dominated by Kalimantan (51% of all non-peat fires in EQAS). Together with 21% from Sumatra and 12% from rINO, entire Indonesia contributes 86% to all non-peat fires in EQAS. The remaining 9% and 7% come from Papua New Guinea and Malaysia, respectively. Most fires occurring in Kalimantan (84%) are distributed almost equally among the two provinces East and Central Kalimantan. In Sumatra, most fires occur in the province South-Sumatra (46% of all non-peat fires), followed by Riau (27%) and Jambi (12%).

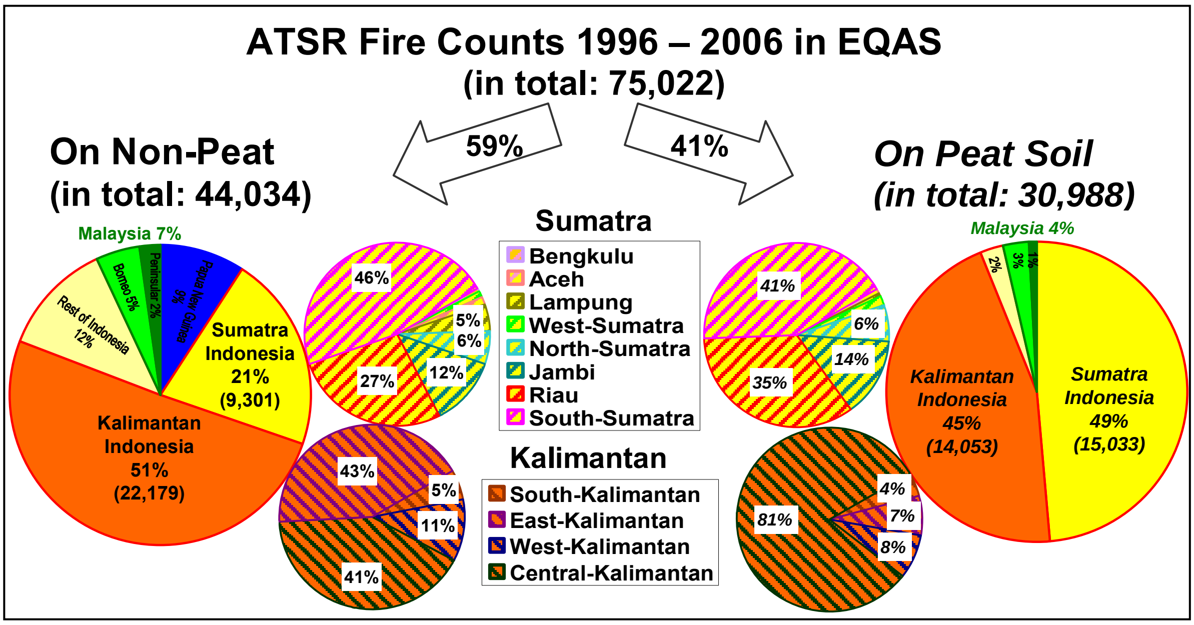

Figure 2-9: Regional distribution of ATSR fire counts observed during July 1996 to December 2006 on non-peat soil areas (left) and peat soil areas (right). For Kalimantan and Sumatra, the distribution of fire counts among the various provinces is shown in separate circle diagrams.

Fires in peat areas of EQAS are dominated by Sumatra (49% of all peat fires), closely followed by Kalimantan (45%), while rINO contributes only 2%. The remaining 4% occur in Malaysia. 90% of all fires in peat soils in Sumatra occur in the following three provinces: South-Sumatra (41% of all

[9] The contribution of fires in Brunei and Singapore are negligible (in total 0.1%).

peat fires in Sumatra), followed by Riau (35%) and Jambi (14%), while in Kalimantan the vast majority of peat fires (81%) occur in only one province, which is Central-Kalimantan.

Due to the relatively short time series of fire data available combined with a high interannual variability of annual fire activity, there is no clear, statistically significant trend in annual fire activity during 1996 to 2006. However, there is a clear positive trend in the relative contribution of peat fires to total fire activity in Indonesia, Sumatra and Kalimantan, respectively. The trend is highest and statistically most significant in Sumatra: the relative contribution of peat fires increased on average 4% per year from 39% in 1996 to 79% in 2006. The linear regression equation explains 72% of the observed variance and is statistically very significant. In Kalimantan, the trend is also positive, but lower (3% per year) and statistically non-significant. The calculated trend for entire Indonesia is 3.6%.

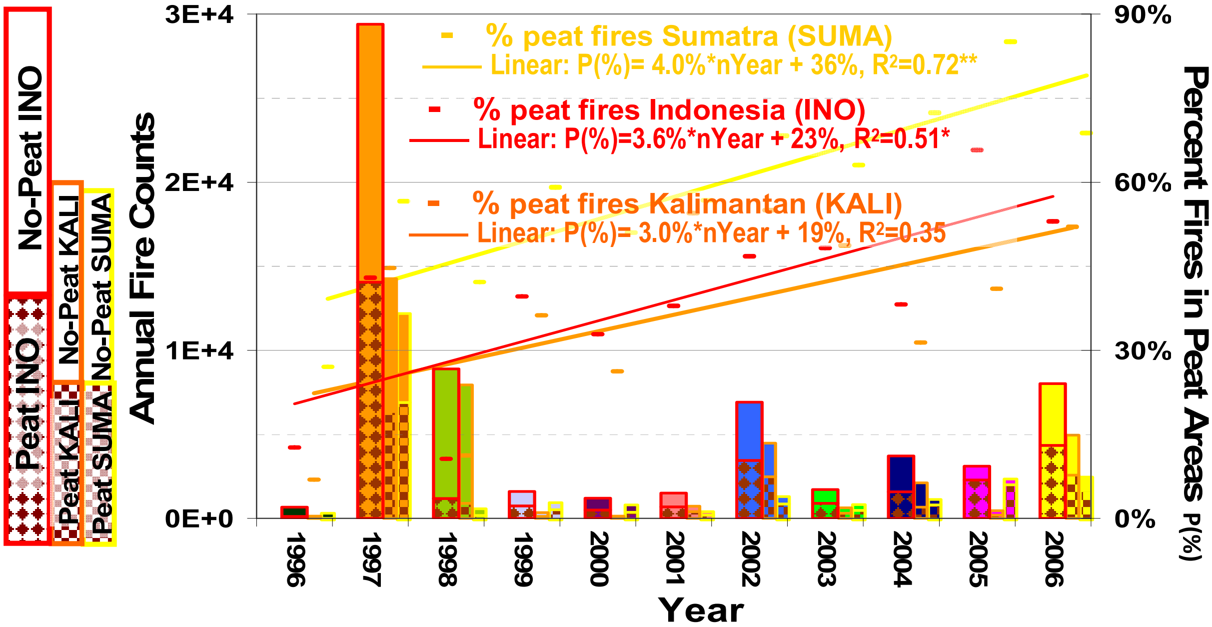

*Figure 2-10: Annual total number of ATSR fire counts in Indonesia, Kalimantan and Sumatra during 1996 to 2006 (left ordinate). The markers display the annual relative contribution of fires in peat soil areas to the total number of fire counts observed in these regions while the line displays the linear regression of these values (right ordinate). nyear denotes the number of years starting in 1996. The coefficient of determination (R^2) calculated from the linear regression is marked with a star, if the correlation is statistically significant (based on F-statistics). * marks if the result is significant ($0.01 \leq p < 0.05$), ** if the result is very significant ($0.001 \leq p < 0.01$), and *** if the result is highly significant ($p < 0.001$).*

The fire activity in Indonesia shows a clear seasonal pattern. The main fire season occurs during July to September (median above 100 fire counts per months), i.e. during the typical dry season in Indonesia (Figure 2-11a). A second, minor and more variable peak occurs in March, which is, however, less apparent for peat fires. Fires in northern hemispheric spring most frequently occur in Sumatra, where a relatively dry season occurs during this period (Figure 2-1). Fire activity in October, i.e. at the normal end of the dry season, shows strong year-to year variability (length of the boxplot-box). Very little burning (median below 50 fire counts per month) occurs in December, January and April of each year, which are generally wet months.

The contribution of peat fires to total fire activity in Indonesia changes throughout the season. Its seasonal cycle is weakly, but statistically significantly correlated to the seasonal cycle of overall fire activity (Figure 2-11a). The contribution of peat burning to total fire activity tends to be lower when overall fire activity exhibits a seasonal minima (e.g. April and November/December). The contribution generally increases when there is a seasonal enhancement in fire activity (February/March and July-September). It indicates that ignitability of peat fires increases over-proportionally with intensifying drought conditions. Accordingly, the intensification and prolongation of drought conditions during El Niño periods leads to a pronounced increase of the contribution of peat fires to the total fire activity during the late fire season (September and October) (Figure 2-11b). Reversely, the relative contribution of peat fires during La Niña conditions is lower than during normal years.

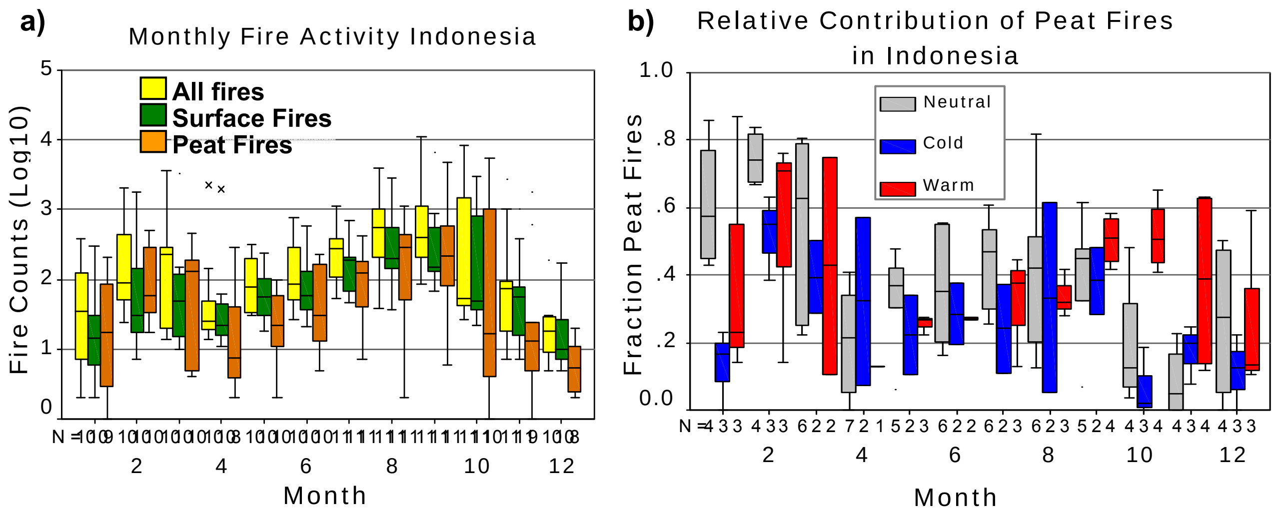

Figure 2-11: a) Seasonal cycle of fire activity (Log10 transformed data) observed in Indonesia by ATSR02 for all fires, fires on non-peat areas and fires on peat areas. b) Seasonal cycle of the contribution of peat fires in Indonesia dependent on the state of the ENSO (Cold= La Niña, Warm=El Niño).

2.5 Linkage between ENSO and Indonesian Fire Activity

Fire activity in various regions of EQAS has a clear connection to the ENSO index. This connection has been analyzed by various authors (Tapper 2002, Hoffmann et al. 2003, Fuller and Murphy 2006), however, on a rather qualitative level. In this study, a regression analysis has been conducted using fire data from 1996 to 2006 to explore this connection in more detail.

Figure 2-12 shows the results of the regression of the total number of JASON ATSR fire counts and the average October-March ONI index for the period 1996 to 2006. For the regression analysis, an exponential regression model is used as it provides the best fit. Total fire activity generally exhibits a high to very high correlation with the ENSO index values (Figure 2-12 a). The highest correlation is found for Kalimantan, where 81% of the observed variance can be explained by the regression. The very high correlation is statistically significant. The correlation is much weaker for Sumatra (R^2=0.49), but still statistically significant. The stronger ENSO-fire relationship found for Kalimantan compared to Sumatra can be explained with the stronger correlation of precipitation with the ENSO index in Kalimantan (see Figure 2-3b). For fires on peat soils, the correlation is lower, but still statistically significant (Figure 2-12 a). A similar tendency can be observed for peat fires only (Figure 2-12 b).

The results show that the ENSO index can be used as a proxy of fire activity for Indonesia. The connection between ENSO conditions is most pronounced for fire activity in Kalimantan.

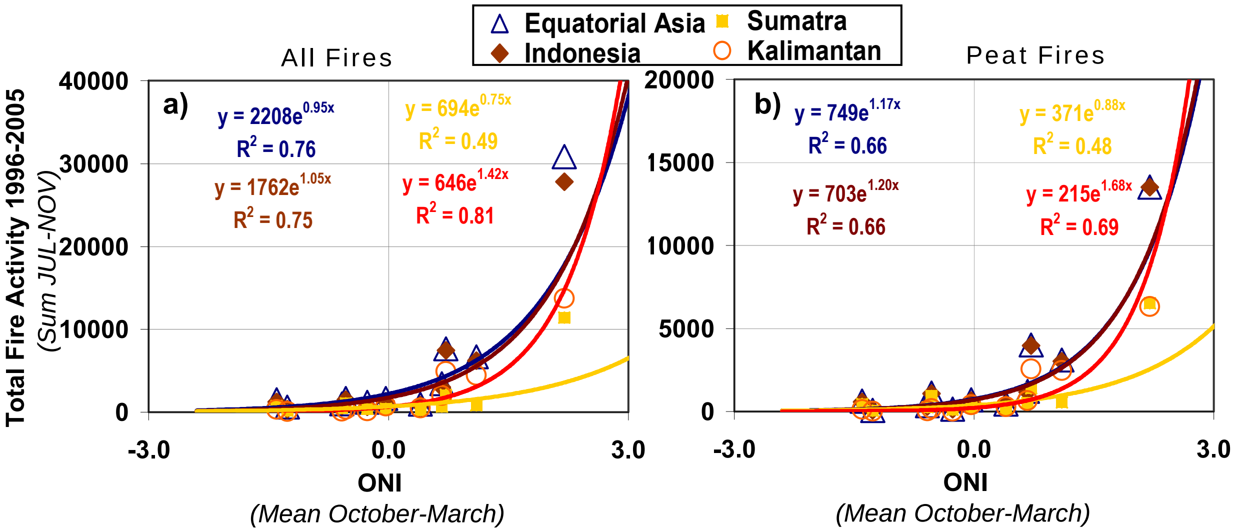

Figure 2-12: Scatterplot of fire activity during July to November in EQAS, Indonesia, Sumatra and Kalimantan, respectively, and the October to March mean Ocean Niño Index (ONI) a) total fire activity and b) fires on peat soil only. The equation of the exponential regression analysis is shown in each figure.

2.6 Conclusion

Patterns and trends in fire activity in various regions of EQAS have been analyzed for the period 1996 to 2006. The analysis distinguished between fires occurring in peat and non-peat areas. The study explored the interrelation between fires, ENSO and rainfall patterns.

Most of the fires in EQAS during this period occurred in Indonesia (88% of all fires), first of all in Kalimantan (48%) and followed by Sumatra (32%). Most of the fires in Kalimantan were surface fires (61%) while most fires in Sumatra were peat fires (62%).

The analysis demonstrates that rainfall and fire activity are statistically correlated to the ENSO phenomenon. During El Niño conditions, rainfall is suppressed and fire activity is increased while the reverse situation is observed during La Niña conditions. The strongest correlation occurs in the region of Kalimantan, and there notably in peat areas. Consequently, the ENSO-related fire susceptibility is higher in peat areas of Kalimantan compared to Sumatra. As a further consequence, the amount of emissions from peat fires are directly related to the ENSO in Kalimantan, allowing to relatively accurately predict these emissions from ENSO indices.

3 Indonesian Fire Emission Inventory for 1960 to 2006

This chapter contains contributions to the following publication (as second author): Schultz MG, Heil A, Hoelzemann JJ, Spessa A, Thonicke K, Goldammer JG, Held AC, Pereira JM, and van het Bolscher M (submitted 2007) Global Emissions from Wildland Fires from 1960 to 2000. Accepted by Global Biogeochemical Cycles.

3.1 Introduction

A new inventory of monthly emissions from Indonesian fires has been established for the period 1960 to 2000 as a contribution to the RETRO project ("REanalysis of the TROpospheric chemical composition over the past 41 years"). RETRO is a global modeling study to investigate the trends and variability of tropospheric ozone and other air pollutants over the past decades. The study includes the compilation of global monthly emission inventories for biomass burning and anthropogenic emissions at a 0.5 degree horizontal resolution (Schultz et al. *submitted 2007*). The Indonesian fire emission inventory established here has been incorporated into the global RETRO biomass burning inventory, which has been made available to the global earth science community through the GEIA Internet Portal (Global Emission Inventory Activity, available online at http://www.geiacenter.org).

Recently, the inventory has been continued up to the year 2006, which allows an intercomparison with other inventories available only for recent years. Furthermore, an uncertainty assessment of the calculated emissions has been added.

The Indonesian emission inventory represents the first attempt to explicitly include not only emissions from burning above-ground vegetation, but also from burning peat soils. It is also the first inventory to cover such a long time period. It therefore allows a comprehensive assessment of the relative importance of Indonesian fire emissions for the global budget of atmospherically and climatically active trace species.

3.2 Methodology

3.2.1 RETRO Emission Inventory (1960 to 2006)

Principally, the development of a biomass burning inventory comprises the following main steps (Seiler and Crutzen 1980):

1) Compiling spatially resolved burned area data for different fuel types (different surface vegetation types and organic soil material),
2) Establishing spatially resolved information on the distribution of different fuel types,
3) Assigning fuel loads (amount of combustible material per area) and combustion characteristics to each fuel type, and
4) Calculating the amount of biomass burned per fuel type and area and applying fuel-type specific emission factors to each unit mass of biomass burned.

A description of the main parameterization and the data source used to establish the long-term Indonesian emission inventory is given in Heil et al. (2007) (Section 6.2.2). Heil et al. (2007) calculated the emissions produced by burning of surface vegetation and peat deposits during the extreme fire episode of July 1997 to June 1998 in Indonesia. Using basically the same approach, the RETRO emission inventory has been extended recently until the end of the year 2006.

The Indonesian fire emission estimate within the framework of the RETRO project ("RETRO estimate") has been calculated using a first guess approach aiming at providing an intermediate estimate of fire emissions. This implies that the burned area, the extent of the peat soil cover and the parameterization of the biomass load, the burning efficiency and the emission factors was based on average values from literature.

The burned area was estimated for peat soil and following three surface vegetation fuel classes: 1) tropical forest (undisturbed to partly disturbed), 2) perennial plantations and fragmented forest, and 3) agricultural land, savannah, and grassland. The calculation of burned area is based on active fire count data obtained from the satellite-borne Along-Track Scanning Radiometer (ATSR). A fuel-type specific burned area was attributed to each fire count. The attribution (scaling) factors were obtained from fitting aggregated fire count data to detailed burned area statistics available for the 1997/98 episode (Tacconi et al. 2003) and by considering that the ratio of burned area per fire count decreases with increasing percentage tree cover (van der Werf et al. 2003).

Emissions of the years 1996 to 2006, for which ATSR data are available, were calculated using the approach described in Heil et al. (2007). For the period prior to the availability of satellite fire data, i.e. for the period 1960 to 1995, burned area was estimated by extrapolation based on the assumption that variations in fire activity in Indonesia can be described by the variations in the state of the El Niño Southern Oscillation (ENSO), as reflected by the Multivariate El Niño Index (MEI). The MEI is calculated using a combination of atmospheric and ocean parameters (Wolter and Timlin 1998). The assumption is supported by the high correlation (R^2 of 0.93) found between the total annual number of ATSR fire counts (July to June) observed during July 1996 to June 2003 and the corresponding mean October to March MEI (Figure 3-2a). This approach is circumstantiated by a recent, more detailed analysis on the connection between El Niño conditions, rainfall, and drought-related fire activity in Indonesia, which is based on a longer time series (Chapter 2).

Because of the pronounced dependency of the seasonal and spatial distribution of Indonesian fires on the state of the Southern Oscillation, we developed four different monthly July to June templates from the 1996-2003 ATSR time series, reflecting 1) neutral ENSO, 2) La Niña, 3) weak El Niño, and 4) strong El Niño conditions. The classification of a given year into these ENSO categories was made according to the analysis by Null (2004) (Table 3-1). This composite approach provides a relatively realistic treatment of the extreme temporal and spatial variability of fire activity observed in Indonesia.

Classification	Year (July-June)
El Niño years 1960-2003 (in total 11 years)	57/58, 65/66, 72/73 (strong), 77/78, 82/83 (strong), 87/88, 91/92 (strong), 92/93, 94/95, 97/98 (strong), 02/03
La Niña years 1960-2003 (in total 12 years)	50/51, 55/56 (strong), 56/57, 64/65, 70/71, 71/72, 73/74 (strong), 74/75, 75/76 (strong), 88/89 (strong), 98/99, 00/01

Table 3-1: El Niño, Normal and La Niña years during 1960 and 2003 (classified according to Null (2004))

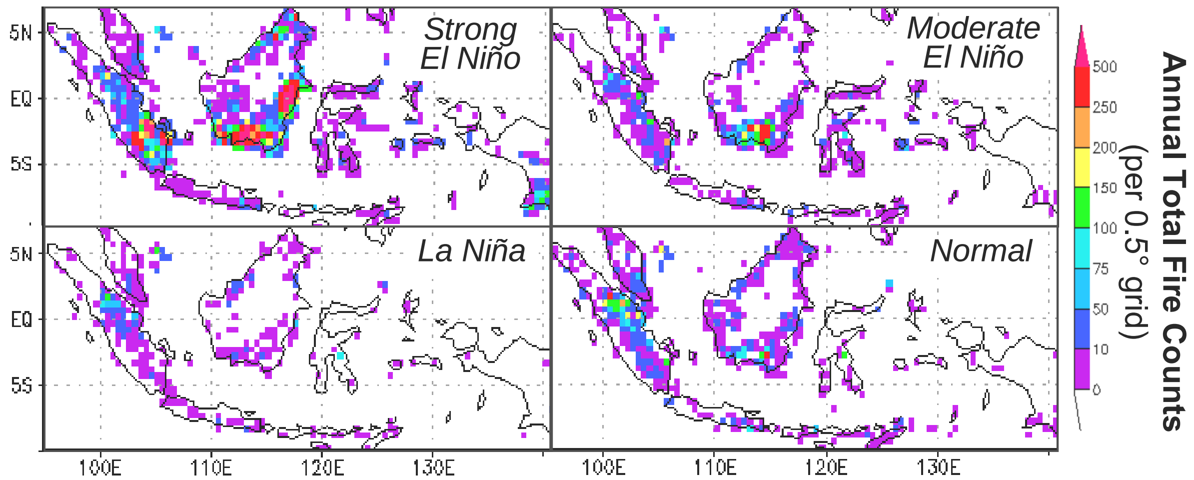

Figure 3-1: Templates of fire activity for different ENSO conditions derived from ATSR fire count data from 1996 to 2003. The total number of fire counts per 0.5 degree grid cell per template year (July –June) is shown.

Over the past decades, land use activities in Indonesia leading to deforestation and forest fragmentation have been increasing drastically. According Holmes (2002), forest cover in Indonesia increasingly disappeared since the 1960ies. The total forest cover decreased from around 116 Mha in the beginning of 1900 to 94 Mha in 1960, and 57 Mha in the year 2000 (Figure 3-2b). As a result, the deforestation rate increased from as low as 0.2 Mha in 1900 to 0.5 Mha/year in 1960 to 2.0 in the year 2000. Most of the deforestation occurring in Indonesia (around 80%) took place in Sumatra and Kalimantan. Deforestation and fire activity are linked twofold: Fire, on the one hand, causes deforestation. Deforestation and forest fragmentation, on the other hand, increases fire vulnerability and severity in tropical forests (Cochrane et al. 1999).

In order to account for the effects of the increasing land conversion activities on fire frequency in the extrapolation to 1960, the complete time series of fire activity prior to 1996 was linearly scaled to the interpolated deforestation trend given in Holmes (2002). The latter has been calculated by the following polynomial fitting function:

$$\text{Relative Forest Loss Rate (\%)} = 0.22+0.014 * n_{year} + 1.8 * 10^{-4} * n_{year}^{2} \quad (R^2=0.99)$$

(relative to the year 2000) *(n_{year} is the number of years since 1960)*

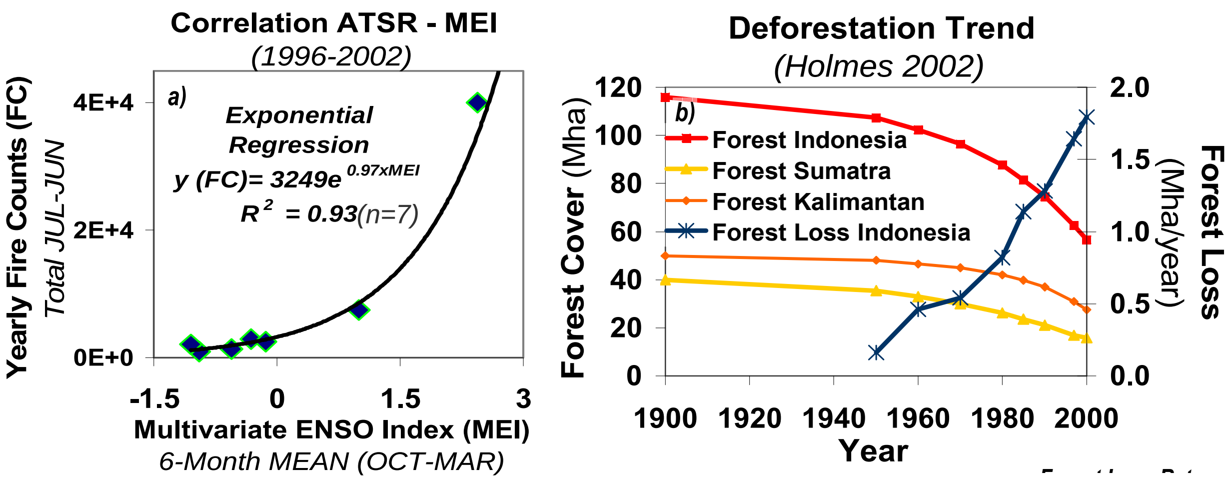

Figure 3-2: a) Correlation of the total annual number of ATSR fire counts observed in Indonesia during 1996 to 2002 and the Multivariate ENSO Index (MEI) and b) forest cover loss in Indonesia since 1900 based on Holmes (2002).

3.2.2 Uncertainty Assessment

Large uncertainties are associated with the current bottom-up approach of estimating emission from biomass burning, primarily due to the difficulty to accurately estimate areas burned and the amount of fuel per area actually combusted. The uncertainty in the assumptions of these parameters is still large and can be more than ± 50% (Robinson 1989, Liousse et al. 2004). The uncertainty in the emission factors of various trace species has been significantly reduced to about 20 – 30% over the last decade (Andreae and Merlet 2001) but can still be up to 30 – 40% and more for many less characterized fuel types and trace species (Reid et al. 2005). The uncertainty in estimating fire emissions from Indonesia is particularly high when compared to regions with no or only minor peat burning (e.g. South and Central America, Africa), because not only surface vegetation but also peat fire emissions have to be ascertained.

Estimating emissions from peat fires in Indonesia is especially difficult because

i) information on the spatial distribution, extent and depth of peat soils in Indonesia is very uncertain (Rieley et al. 1995),

ii) satellite-based monitoring of fires combined with ground-based validation is generally only very little developed in Indonesia and derived estimates of the burned area are uncertain. This applies notably to the burned area by peat fires, because they are more difficult to detect than surface fires (Siegert et al. 2004),

iii) the combustion and emission characteristics of tropical fuels in general and tropical peat in particular have only been rarely studied compared to extratropical fuels and are still largely undetermined (Andreae and Merlet 2001, Christian et al. 2003).

Fuel-type specific fire emissions are calculated from the multiplicative combination of the following four parameters: 1) the burned area, 2) the amount of biomass available for burning (biomass load), 3) the fraction of biomass actually combusted by the fire (burning efficiency), and 4) the amount of species x emitted per unit mass combusted (emission factor) (Figure 3-3). The values reported in the literature for the parameters 2-4 are summarized in Table 3-2.

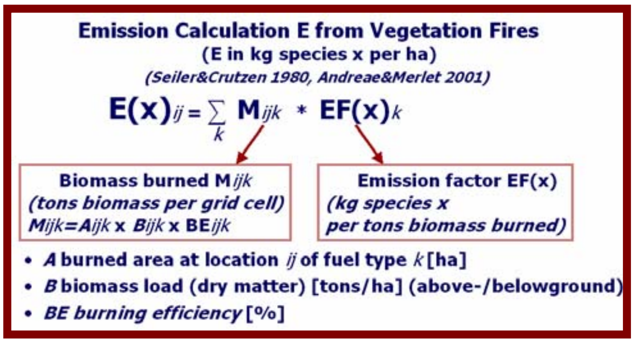

Figure 3-3: Formula used to calculate emissions from vegetation and peat fires.

The reported values of each of these parameters of the biomass burning emission equation exhibit a large uncertainty range. When imprecisely known terms are combined multiplicatively, the uncertainty quickly explodes to very high levels (because the relative errors are additive), which strongly decreases the confidence in the precision of the final emission estimate (Robinson 1989).

Figure 3-4 (a-d) illustrates the large range of over which reported values of biomass density scatter within each fuel class used in this study. For example, reported biomass density values for vegetation contained in the fuel class "grassland, cropland and savannah" range from 1 tons/ha to 200 tons/ha, i.e. span about 2 orders of magnitude. It reflects the high heterogeneity in vegetation types and resultant biomass density in this highly aggregated fuel class. The width of the range of values reported for the other fuel classes used in this study is still generally around one order of magnitude and is comparatively smaller because they contain a more homogenous vegetation cover. The biomass density of peat soil may range from 336 tons/ha to 44,704 tons/ha. It is primarily a function of the depth of the peat soil, which may range from 0.4 m to 16 m in Indonesia. Secondarily, it is controlled by the peat bulk density, which may vary by about a factor of 3 (84 kg/m^3 to 279 kg/m^3) (Table 3-2).

Only few measurements exist of the burning efficiency of fires in different surface vegetation types. The values maximally vary by a factor of 2 to 3 (Table 3-2). For fires in peat soils, the burning efficiency is generally expressed in terms of peat depth burned, which can be determined from the lowering of the top soil layer height after burning. Figure 3-4 (e) illustrates the wide range of the peat depth burned observed during a fire season in Indonesia, which spans from 0.04 m to 2 m. The actual water table level in the peat soil primarily determines the actual peat depth burnt during a particular fire event at a given location. This information is unavailable for peat areas of Indonesia. As a consequence, the peat fire emission estimation has to rely upon empirical data of the typical peat depth burned in Indonesia during a fire event (Table 3-2).

The emission factors of the surface vegetation type are more precisely determined by a large number of measurements. For tropical forest, the emission factors vary less than a factor of two except for a few species (Table 3-2). There is generally a large spread between the minima and maxima emission factors measured for the fuel class agriculture/grassland and savanna for the different species (factor of 2 to 9), most likely due to the large heterogeneity of the fuel types included into this class. However, the spread between the 25 percentile and 75 percentile value is below a factor of two. In contrast, the emission factors for Indonesian peat that have been determined so far are based upon the measurements of a single peat sample (Christian et al. 2003). As a consequence, the variability of the emission factors dependent on the peat type measured, the measurement technique and other influencing factors is still unkown.

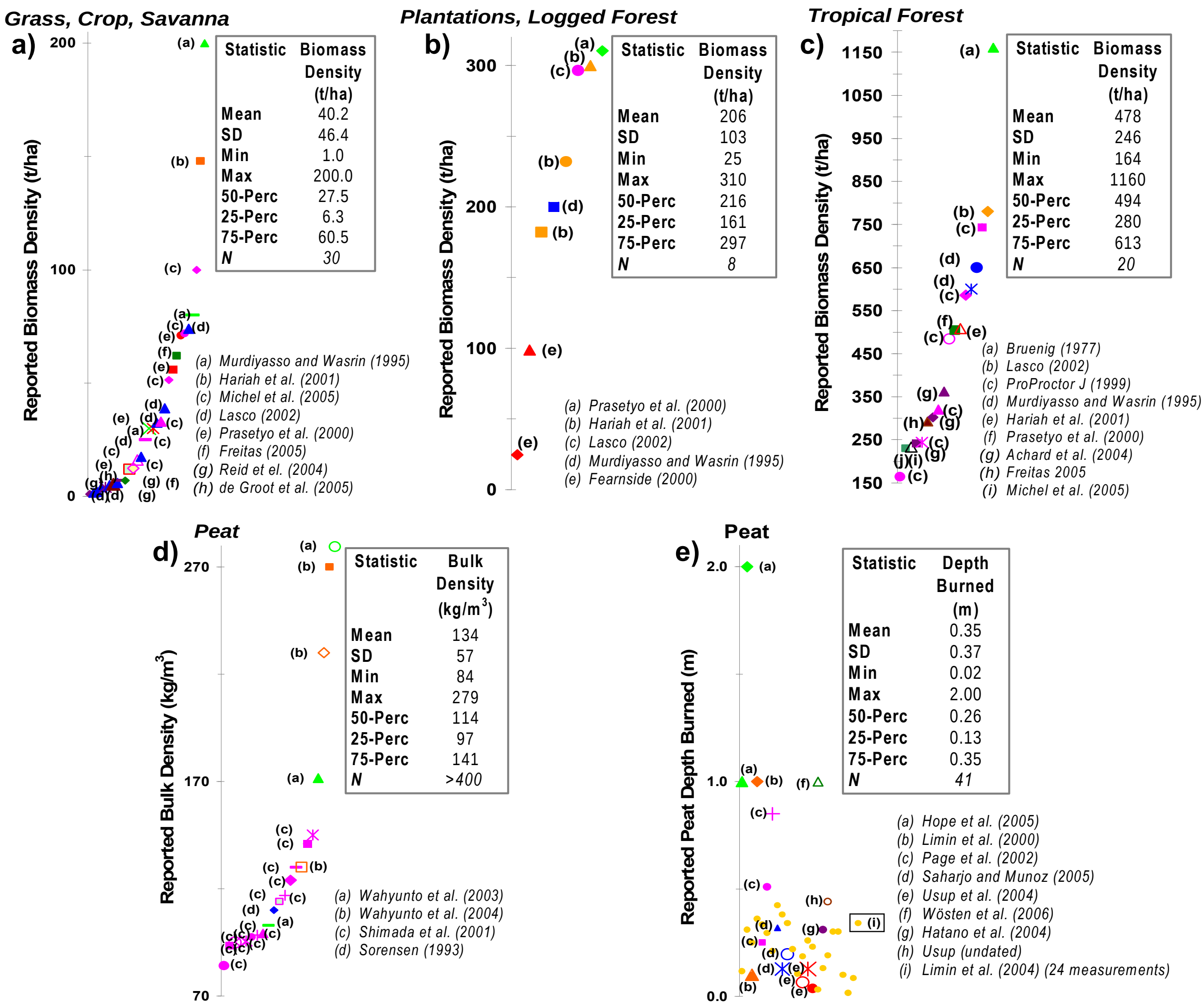

Figure 3-4: (a-c) Scatterplots of values for biomass density reported In literature for the for three surface vegetation classes used in this study. (d,e) Scatterplots of bulk density values reported for Indonesian peat and of the peat depth burned during a fire event, respectively.

To quantify the overall uncertainty range of the estimated emission density per unit area burned for each fuel type, a lower and upper bound estimate, respectively, has been calculated by using 25% and 75 percentile estimates of each of the parameters in the emission estimation equation (Table 3-2). In addition, a central estimate has been calculated using median values. The 25 and 75 percentiles have been chosen because they cover the range of values that are most likely to be representative for fires in entire Indonesia. It has to be noted that, because of missing data, the uncertainty assessment for peat soil burning ignores the uncertainty resulting from possible variations in the emission factors. The lower and upper bound of the estimated emission density per unit area differ by a factor of two to four in all fuel types and species shown in Table 3-2 except for the fuel class agriculture, grassland and savanna where the bounds vary by a factor of 17 to 36.

The estimated emission density per unit area burned the intermediate first-guess approach used in the RETRO inventory ranges between the 50 percentile and 75 percentile estimates for the fuel types agriculture, grassland and savanna and plantations and fragmented forest. For forest and peat soil, however, the emission density assumed in the RETRO inventory is generally 30 to 40 % higher than the 75 percentile estimate (Table 3-2). This is because the literature value of the burning efficiency and the peat depth burned, respectively, chosen when establishing the RETRO inventory is higher than most of the values provided in literature that have been published since then. The peat depth burned in the RETRO inventory refers to the average peat depth of 0.5 m burned during 1997 in Central Kalimantan as measured by Page et al. (2002). The latter represents the first detailed study on the depth of burning published by then. More recent studies (e.g. Limin et al. 2004, Saharjo and Munoz 2005) indicate that the peat depth burned during a fire event is on average lower than this value (0.35 for both, mean and 75 percentile value) (Figure 3-4).

To illustrate the strong differences and uncertainties in the calculated emission densities, the emission density per unit area for two different species emitted (CO_2 and PM_{10}) as a function of the fuel type and the statistical descriptors used is compared in Figure 3-5.

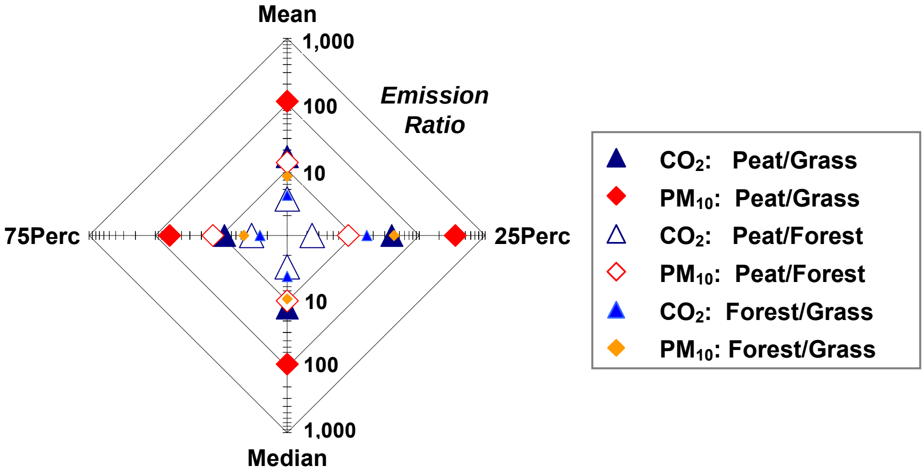

Figure 3-5: Radar diagram showing the ratio of the amount of CO_2 or PM_{10} emissions produced per unit area by i) peat or forest fires, respectively, compared to the amount produced by ii) grassland (including agriculture and savanna) or tropical forest fires, respectively. The ratio is calculated separately from four different emission estimate scenarios by multiplying 1) the arithmetic means, 2) the 50 percentile values (median), 3) the 25 percentile values, and the 75 percentile values, respectively, of the values reported for each of the terms required to calculate emissions (see Table 3-2).

If arithmetic mean parameters are used to calculate emission density, the amount of CO_2 emitted per unit area is 4.1 times higher for fires in forest compared to fires in grassland and 3.6 times higher for peat fires compared to forest fires, respectively. The resultant ratio of the emission density of peat fires to grassland fires is 15.9. The fuel-type dependent relative differences in emission density are much higher for PM_{10} than for CO_2. The ratio of the PM_{10} emission densities is 7.9 for forest fires compared to grassland fires and 3.6 for peat fires compared to forest fires. The resultant ratio of 110 for peat fires compared to grassland fires is 6.9 times higher than the corresponding ratio for CO_2. The PM_{10} emission ratio increases relative to CO_2 from grassland (1.9) over forest (3.6) to peat soil (6.9) because smoldering combustion increasingly dominates flaming combustion in the latter two fuel types. Smoldering combustion, in turn, releases relatively more products of incomplete combustion such as carbon monoxide (CO), methane and particulate matter (dominated by organic carbon) than flaming combustion (Ward 1990).

This higher difference implies that the accuracy of calculated PM_{10} emissions (and other products of incomplete combustion) is more sensitive to a proper classification of fuel types than of estimated CO_2 emissions. The accuracy of the estimated PM_{10} emissions is therefore strongly dependent on the quality of the vegetation and peat cover data. A detailed uncertainty assessment of fire emission estimates would hence require ensemble calculations using various vegetation cover (e.g. MODIS vegetation cover (Hansen et al. 2000), global land cover database for the year 2000 (GLC2000) (Bartholome and Belward 2005)) and peat soil datasets (e.g. Wahyanto et al. 2003, 2004) which has been neglected in this study. Furthermore, the effects of vegetation-dependent differences in the detecting of fires by various satellite-based fire monitoring systems would need to be quantified.

The Loveland et al. (2000) vegetation cover which is based on AVHRR data acquired during 1992/93 was used in this study as a first approximation of a vegetation cover that is representative for the situation prior to the extreme fires of 1997/98. The data underestimate fragmented forest cover while overestimating the undisturbed forest cover (FAO 2000). As a result, the fire emission inventory at hand most likely underestimates emissions from fragmented forest and/or agroforestry plantations and overestimates emissions from undisturbed forest. Furthermore, a static vegetation cover has been assumed in this study, which is primarily representative for the year 1992/93. Land cover change which has been occurring since this reference year – i.e. the decrease of undisturbed forest cover in favor of fragmented forest/plantations and grassland, agriculture and savannah is not taken into account in the emission calculation. Likewise, the relative increase in the abundance of undisturbed forest compared to the other two land cover classes prior to the reference year is ignored. This effect will enhance the overestimation (underestimation) of the relative contribution of forest fire (fragmented forest/plantation) emissions due to the AVHRR sensor in the inventory calculation in the years following 1992/93, while it may partly lead to a compensation of the effects of the AVHRR-related bias in the years prior to this reference year.

Also the peat soil cover was assumed to be constant during the inventory period. The calculated total peat depth burned during the entire period is far below the actual depth of the peat deposits present in the areas affected by the fires. In the RETRO calculations, for example, the peat depth burned during the entire inventory period is below 0.4 m in most areas. This is less than the minimum thickness of the peat layer in the peat areas, which were included into the study. Maximally 2.4 m of peat burned during the entire inventory period due to repetitive fires (Figure 3-9). Areas of deep peat burning (> 0.6 m) occurred in the provinces of Central Kalimantan (mainly in the Megarice Project Area), South Sumatra and Riau (Sumatra), where peat deposits are deeper than 4 m (Wahyunto et al. 2003, 2004). Repetitive peat burning would therefore have led to a reduction of the peat depth, but not to a reduction of the area distribution of peat soils. As a result, no distinct bias in the calculation of peat fire emissions is expected from the assumed static distribution of peat soil areas. However, in order to compensate for the overestimation of the total area of peat soils by the FAO (2003) map used in this study, the maximum fraction of peat soil distribution within each 0.5° grid (corresponding to roughly 2,500 km^2) was restricted to 50% (Heil et al. 2007, see Section 6.2.2.1). As a result, it is likely that the emissions from peat burning are underestimated in grid cell areas with complete peat soil coverage (e.g. Megarice Project Area) while there might be an overestimation of the total area in which peat fire emissions actually occur.

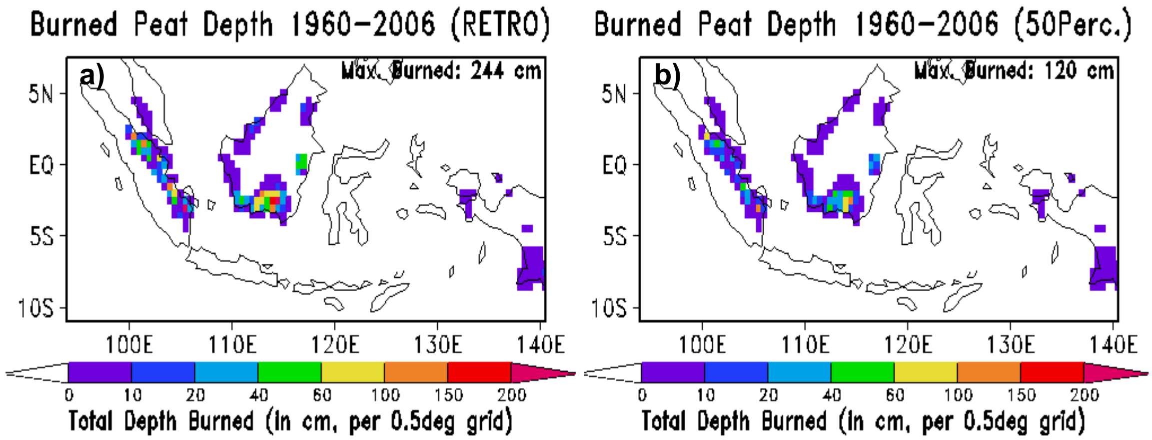

Figure 3-6: Calculated total peat depth burned per 0.5° grid during 1960 to 2006 a) RETRO emission inventory assuming 0.5 m of peat depth burned per fire pixel and b) estimate based on a assumed peat depth burned per fire pixel of 0.26 m (using 50 percentile values).

Lastly, Figure 3-5 reflects the distinct differences in calculated emission density ratios for a single species that result from the wide range of literature values for the corresponding biomass load, burning efficiency and emission factors, notably in case of the aggregated fuel class grassland (including agriculture and savanna). The PM_{10} emission density ratio of peat fires to grassland fires ranges from 351 to 60 (i.e. varies by a factor of 6.9), respectively, if the calculation is based on 25 percentile and 75 percentile values.

3.3 Estimated Burned Area in Indonesia during 1960 to 2006

We estimate that a total area of 47.9 Mha burned in Indonesia over the 47-year period from 1960 to 2006, corresponding to a long-term mean burning rate of about 1.0 Mha per year. Kalimantan contributed most (47.5% or 22.7 Mha) to the burned area in Indonesia, followed by Sumatra (43.9% or 21.0 Mha). The remaining islands of Indonesia contributed only 8.9% to the total burned area. (Table 3-3). During the entire period, fires in Indonesia strongly dominate (94.1% on average) the burning occurring in the entire Equatorial Asian (EQAS) region, which also includes Malaysia, Papua New Guinea and Brunei (Figure 3-7).

Of the total burned area in Indonesia during 1960 to 2006, 43% was covered by grassland, agriculture and savanna, 20% by fragmented forest and 37% by forest. In 24% of the area affected by surface vegetation fires, the underlying peat soil burned as well. This corresponds to 10.5 Mha of peat soil burned in Indonesia during the entire period. When calculating the accumulated totals of burned area over the inventory period, however, areas affected by repetitive burning during several months or years will be counted several times. This is most likely to occur in peat areas due to the comparably higher amount of fuel available for repetitive burning than in surface vegetation. It is noteworthy that peat burning in the EQAS region during the entire inventory period was almost exclusively confined to Indonesia (98.2% of the total peat area burned). Of the total peat area burned in Indonesia, 51% occurred in Kalimantan and 39% in Sumatra, while the remaining 10% occurred in Irian Jaya.

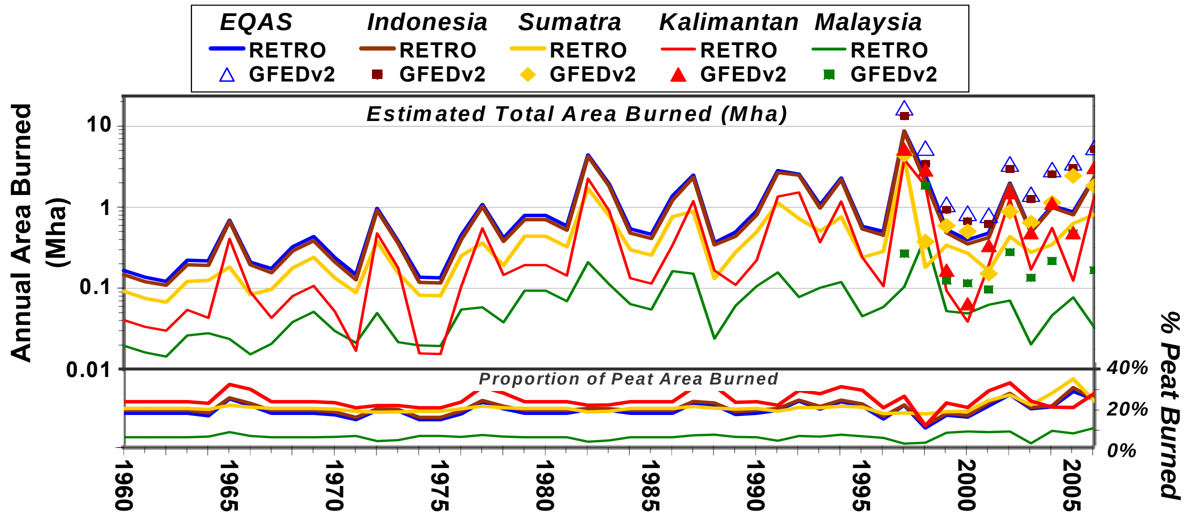

Figure 3-7: RETRO estimates of the annual burned area in entire Indonesia, Sumatra, Kalimantan, Malaysia and entire Equatorial Asia (EQAS) during the period 1960 to 2006 (left ordinate). For the period 1997 to 2006, the annual burned areas of the GFEDv2 inventory are displayed for comparison. The relative contribution of fires in peat areas to the total annual burned area in the RETRO inventory is shown on the right ordinate.

Vegetation Type	Agriculture, Grassland, Savannah									Plantations, Fragmented Forest								
Parameter	RETRO	Mean	SD	MIN	MAX	50Perc	25Perc	75Perc	N	RETRO	Mean	SD	MIN	MAX	50Perc	25Perc	75Perc	N
Biomass Density (tons/ha)	**40**	**40**	46	**1**	**200**	**28**	**6**	**61**	30	**200**	**206**	103	**25**	**310**	**216**	**161**	**297**	8
Burning Efficiency (%)	**93**	**75**	24	**35**	**100**	**85**	**55**	**90**	11	**54**	**38**	23	**22**	**54**	**38**	**30**	**46**	2
Carbon Content (%)	**50**									**50**								
Carbon Consumption (tons/ha)	**19**	**15**		**0.2**	**100**	**12**	**2**	**27**		**54**	**39**		**3**	**83**	**41**	**24**	**68**	
Emission Factors (EFx) in g species x emitted per kg dry fuel consumed by a fire:																		
Species x	RETRO/Mean		SD	MIN	MAX	50Perc	25Perc	75Perc	N	RETRO/Mean		SD	MIN	MAX	50Perc	25Perc	75Perc	N
Carbon Dioxide (CO_2)	**1,664**		78	**1,532**	**1,783**	**1,675**	**1,599**	**1,706**	12	Emission Factors of Tropical Forest Used								
Carbon Monoxide (CO)	**62.6**		16	**24.5**	**91.4**	**63.7**	**55**	**71.5**	29									
Methane (CH_4)	**2.2**		0.8	**0.6**	**5**	**2.2**	**1.9**	**2.5**	29									
Nonmethane Hydrocarb.(NMHC)	**3.4**		1	**2.2**	**5.6**	**3.4**	**2.9**	**3.6**	10									
Nitrogen Oxide (NO_x as NO)	**2.4**		1	**1.1**	**3.7**	**2.1**	**1.6**	**3.3**	8									
Total Particulate Matter (TPM)	**8.5**		3	**6.3**	**15**	**7.3**	**6.5**	**9.6**	8									
Particulate Matter <10µm (PM10)	**5.4**		1.7	**3.4**	**8.4**	**5.2**	**3.9**	**5.6**	(a)									
Particulate Matter <2.5µm (PM2.5)	**4.9**		1.5	**3.1**	**7.7**	**4.8**	**3.6**	**5.2**	9									
Organic Carbon (OC)	**3.2**		1.3	**1.6**	**5.8**	**3.2**	**2.6**	**3.4**	7									
Black Carbon (BC)	**0.5**		0.2	**0.2**	**0.7**	**0.5**	**0.4**	**0.6**	10									
Area-related Emission Density (EDx) in kg of species x emitted per ha burned:																		
Species x	**RETRO**	**Mean**				**50Perc**	**25Perc**	**75Perc**		**RETRO**	**Mean**				**50Perc**	**25Perc**	**75Perc**	
CO_2	627	498				392	55	929		1,790	1,289				1,364	764	2,321	
CO	23.6	18.7				14.9	1.9	38.9		67.4	48.5				51.9	26.3	97.3	
CH_4	0.85	0.67				0.51	0.06	1.36		2.42	1.74				1.8	0.9	3.4	
NMHC	1.29	1.03				0.79	0.1	1.98		3.69	2.65				2.8	1.4	5	
NO_X	0.89	0.7				0.48	0.05	1.8		2.53	1.82				1.7	0.8	4.5	
TPM	3.21	2.55				1.69	0.22	5.21		9.15	6.59				5.9	3.1	13	
PM_{10}	**2.02**	**1.61**				**1.22**	**0.13**	**3.06**		**5.77**	**4.16**				**4.2**	**1.9**	**7.6**	
$PM_{2.5}$	1.86	1.48				1.12	0.12	2.81		5.31	3.83				3.9	1.7	7	
OC	1.21	0.96				0.74	0.09	1.85		3.46	2.49				2.6	1.2	4.6	
BC	0.17	0.14				0.11	0.01	0.32		0.5	0.36				0.4	0.2	0.8	

Vegetation Type	Tropical Forest									Peat Soil								
Parameter	RETRO	Mean	SD	MIN	MAX	50Perc	25Perc	75Perc	N	RETRO	Mean	SD	MIN	MAX	50Perc	25Perc	75Perc	N
Biomass Density (tons/ha)	**504**	**478**	246	**164**	**1,160**	**494**	**280**	**613**	**20**	**2,938**	**5,511**		**336**	**44,704**	**4,560**	**1,948**	**11,280**	
Peat Depth (m)										***2.3***	**4.1**	**(b)**	**0.4**	**16**	**4**	**2**	**8**	17
Bulk Density (kg/m^3)										***128***	**134**	**57**	**84**	**279**	**114**	**97**	**141**	>400
Peat Depth Burned (m)										**0.5**	**0.35**	**0.4**	**0.02**	**2**	**0.26**	**0.13**	**0.35**	41
Burning Efficiency (%) (c)	**39**	**27**	13	**20**	**50**	**20**	**20**	**25**	5	***22.2***	***8.4***	***(c)***	***3.8***	***12.5***	***6.4***	***6.4***	***4.3***	
Carbon Content (%)	**50**									**54**	**52**	**8.4**	**30.8**	**60.3**	**56**	**50**	**57**	>400
Carbon Consumption (tons/ha)	**98**	**65**		**16**	**290**	**49**	**28**	**77**		**355**	**240**		**4**	**3,370**	**161**	**63**	**276**	
Emission Factors (EFx) in g species x emitted per kg dry fuel consumed by a fire:																		
Species x	RETRO/Mean		SD	MIN	MAX	50Perc	25Perc	75Perc	N	RETRO/Mean		SD	MIN	MAX	50Perc	25Perc	75Perc	N
CO_2	**1,580**		90	**1,439**	**1,664**	**1,580**	**1,565**	**1,652**	5	**1,703**			Not determined					1
CO	**103.2**		19	**85.5**	**135**	**94.5**	**91**	**116.6**	9	**210.3**								1
CH_4	**6.8**		2	**4.8**	**9.3**	**6**	**5.1**	**9**	8	**20.8**								1
NMHC	**8.1**		3	**5.9**	**12.5**	**7.1**	**6.5**	**8.7**	4	**41.7**								1
NO_X	**1.9**		0.8	**0.7**	**2.7**	**2**	**1.6**	**2.3**	5	**1**								1
TPM	**8.5**		2.9	**6.5**	**10.5**	**8.5**	**7.5**	**9.5**	2	**52.5**								(a)
PM_{10}	**9.8**		1.6	**8.2**	**11.4**	**10**	**9.1**	**10.7**	(a)	**38**		4						4
$PM_{2.5}$	**9.1**		1.5	**7.5**	**10.5**	**9.2**	**8.4**	**9.8**	3	**35.5**								(a)
OC	**5.2**		1.5	**3.6**	**6.1**	**6.1**	**4.8**	**6.1**	3	**6**								1
BC	**0.7**		0.3	**0.3**	**1**	**0.6**	**0.5**	**1**	5	**0.04**								1
Area-related Emission Density (EDx) in kg of species x emitted per ha burned:																		
Species x	**RETRO**	**Mean**				**50Perc**	**25Perc**	**75Perc**		**RETRO**	**Mean**				**50Perc**	**25Perc**	**75Perc**	
CO_2	**3,090**	**2,040**				**1,645**	**886**	**2,396**		**11,095**	**7,921**				**4,951**	**2,116**	**8,284**	
CO	201.8	133.2				133.5	53	139.3		1370	978.1				611.3	261.3	1,023	
CH_4	13.2	8.7				9.2	3.4	7.8		135.5	96.7				60.5	25.8	101.2	
NMHC	15.9	10.5				12.4	4	10		271.6	193.9				121.2	51.8	202.8	
NO_X	3.6	2.4				2.7	1.1	2.4		6.5	4.7				2.9	1.2	4.9	
TPM	16.6	11				10.4	4.8	11.5		342.4	244.4				152.8	65.3	255.6	
PM_{10}	**19.2**	**12.7**				**11.2**	**5.6**	**13.9**		**247.6**	**176.7**				**110.5**	**47.2**	**184.9**	
$PM_{2.5}$	17.7	11.7				10.3	5.2	12.8		231.3	165.1				103.2	44.1	172.7	
OC	10.2	6.8				6	3.4	7.4		39.2	28				17.5	7.5	29.3	
BC	1.29	0.85				0.98	0.33	0.78		0.26	0.19				0.12	0.05	0.19	

(a) For all surface vegetation types, PM_{10} was derived from $PM_{2.5}$ using a $PM_{10}/PM_{2.5}$ ratio of 0.92 given in Peterson and Ward (1993). For peat, TPM and $PM_{2.5}$ was derived from PM_{10} using a corresponding ratio of 93% and 72%, respectively, given for smoldering fires in Peterson and Ward (1993). (b) Mean peat depth (best guess) for Indonesia given by Rieley and Page (2005). (c) Generally, the efficiency of combustion in peat fires is expressed as peat depth burned and not as burning efficiency. Nevertheless, the burning efficiency is calculated here for comparability with surface vegetation fires. The burning efficiency is calculated from the ratio of the burned peat depth to the assumed entire depth of the peat soil. Because both parameters are extracted from independent literature values, the calculated burning efficiency may not be representative.

Table 3-2: Summary statistics of values reported in the literature for the single terms required to calculate fire emissions. The statistics are presented separately for the four different fuel classes used in this study. Emission factors for 10 selected species are presented. For Indonesian peat burning, only a mean emission factor is available. The column entitled RETRO summarizes the values used for calculating Indonesian fire emissions within the framework of the RETRO study. The following abbreviations are used: SD= Standard deviation, N= number of reported values used for the statistical analysis, MIN= Minimum, MAX=Maximum, 50Perc = 50 percentile (median), 25Perc = 25 percentile, 75Perc = 75 percentile.

The estimated burned area in Indonesia per year increased from 0.25 Mha in the 1960ies to 2.1 Mha in the 1990ies. Following the ENSO-dependent approach used in this study to estimate burned area, years of abnormally large burning coincide with prevailing El Niño conditions (see Figure 2-2 and Figure 3-7). The year with the highest annual burned area during the 1960 to 2006 period was 1997 with an estimate 8.6 Mha burned, followed by 1982 (4.2 Mha). The extreme fires in both strong El Niño years contributed strongly to the increase in total burned area in Indonesia in the 1980ies and 1990ies (decadal total of 12.5 Mha and 21.3 Mha, respectively). On average 1.0 Mha burned in Indonesia per year during 2000 to 2006, with a maximum of 2.3 Mha per year during the weak El Niño of 2006. The average annual rate of 1.0 Mha is comparable to the one of 1980ies and 1990ies, if strong El Niño years occurring in these decades (e.g. 1982, 1991, 1997) (Table 3-1) are excluded.

Estimated burned area in this study is compared to a) burned area estimates for selected years from the remote sensing studies by Liew et al. (1998), Fuller and Fulk (2001) and Qadri (2001), b) official numbers on the annual burned area released by the Indonesian Ministry of Forestry (MoF), c) burned area from the yearly dataset of global burned area reconstructed by Mouillot and Field (2005) at a 1x1 degree resolution for the 1900-2000 period (http://www.cefe.cnrs.fr/fe/fichiers/deforestNC.zip), and d) monthly burned area estimates at 1x1 degree resolution from the "Global Fire Emissions Database version 2" (GFEDv2, http://ess1.ess.uci.edu/%7Ejranders/data/GFED2/) available for the time period January 1997 to December 2006 (van der Werf et a. 2006). In addition, the relative TOMS aerosol index measured over the Indonesian region (with background and volcanic contamination removed) (Duncan et al. 2003b) is used for comparison as a proxy for long-term interannual variations in burning.

Mouillot and Field (2005) estimated burned area in Indonesia based on a prescribed probabilistic year-to-year variability combined with qualitative historical reports of burning events and satellite-derived fire information for the year 1996 onwards.

Van der Werf et al. (2006) used ATSR, TRMM-VIRS (Visible and Infrared Spectrometer) and MODIS satellite fire data to derive burned areas for the GFEDv2 inventory. The CASA biogeochemical model was used to predict the spatiotemporal distribution and the corresponding fuel density of four major carbon pools: live leaf carbon, wood carbon of trees and shrubs, dead wood carbon, and soil organic carbon (including peat) up to a maximum soil depth of 30 cm. In assuming a type-specific fire behavior, calculation of burned area was done separately for each of these fuel types. The GFEDv2 inventory, however, contains only aggregated data on the total area burned area per 1x1 degree grid per month, and no information on the respective area contribution of the different fuel types.

The time series of estimated burned area in Indonesia for 1997 to 2006 in the GFEDv2 inventory shows a very coherent temporal development to the estimated area in the RETRO approach (Figure 3-7) (R^2=0.97). Also the monthly times series of both inventories for Sumatra, Kalimantan and entire Indonesia show a largely coherent pattern with a coefficient of determination (R^2) between 0.81 and 0.97 when a linear regression model is applied (Figure 3-8 a-c).

However, the GFEDv2 inventory yields on average 1.85 times more area burned in Indonesia (1997–2006 total of 34 Mha) than the RETRO inventory (18 Mha) (Table 3-3). The difference generally increases from 1997 to 2006. The increasing difference can be partly explained by the different fire datasets and scaling methods used in both inventories to derive burned area. The RETRO burned area calculations are based solely on ATSR fire count data, while GFEDv2 calculations use ATSR data for the period 1997-2000 which are combined with TRMM-VIRS data since the year 1998, while using MODIS data for the subsequent period (2000 to 2006). Because of the higher temporal resolution, the VIRS and MODIS sensor may detect relatively more fires than the ATSR sensor. Furthermore, the MODIS sensor is more sensitive to detect temperature anomalies induced by fires and will therefore detect more small or low-temperature fires than the other sensor (Giglio et al. 2006). As a result, the surface area in which burning is detected is larger. Furthermore, the sensitivity in detecting fires by each of the three sensors fires depends on the vegetation types. It is therefore expected that there are distinct biases in the relative area contribution of the different fuel-types to the total burned area in the GFEDv2 and the RETRO inventory. However, because the GFEDv2 database only contains total burned area, these differences cannot be quantified.

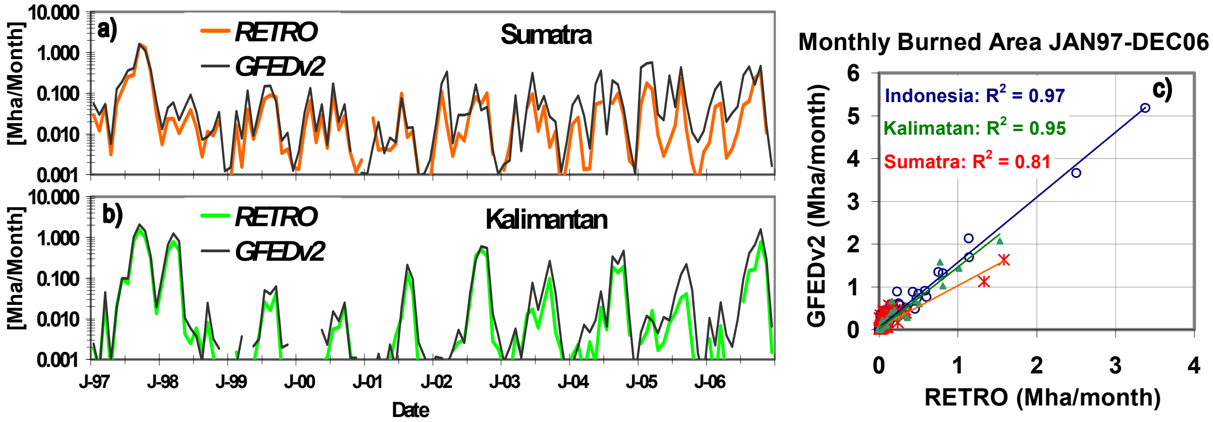

Figure 3-8: Comparison of monthly burned area in a) Sumatra and b) Kalimantan during January 1997 to December 2006 estimated for the RETRO inventory and the GFEDv2 inventory, respectively. c) Correlation of the time series of monthly area burned in Indonesia, Sumatra and Kalimantan, respectively, estimated by the RETRO and the GFEDv2 inventory.

The annual area burned estimated in the RETRO inventory fit well into the range of burned area estimates cited in various sources (Figure 3-9). However, for the years before the extreme fire event of 1997, only little information is available on the area burned and the available information has a low level of confidence. Even for the year 1997 and later, when satellite-based fire monitoring had been established, area burned values vary strongly dependent on the sources and the respective method used and are therefore difficult to compare.

When comparing estimates of total burned area during the 1997 Indonesian fires, the RETRO estimate of 8.6 Mha is in the intermediate range of values cited in literature (from as low as 4.5 Mha by Liew et al. (1998) to a maximum bound estimate of 13.2 Mha by Fuller and Fulk (2001))[10]. Most likely, the true value is slightly closer to the latter estimate. Consequently, the RETRO estimate is most probably on the lower bound of the intermediate range. The Mouillot and Field (2005) and the GFEDv2 database, respectively, yield 18 and 54% more burned area (10.2 and 13.3 Mha), respectively, than the RETRO estimate. For the total period 1960 to 2000, the annual burned area estimated by Mouillot and Field (2005) (171 Mha) is around 4 times higher than in the RETRO estimate and appears to be unrealistically high when compared to other area burned estimates (Figure 3-9) and the fact that this number is also 4 times higher than the total area that has been deforested in Indonesia during this period (Figure 3-2b). Furthermore, annual burned area in the Mouillot and Field (2005) data during the 1960 to 1970ies exhibit extreme peaks in 1966/1967 and 1974/75, which does neither corresponds to reported large fire or smoke-haze events nor the presence of El Niño related drought events. This is also reflected by the medium correlation of these data with the RETRO estimate (R^2=0.48).

The interannual variability of burned area in the RETRO estimate has a largely similar temporal pattern to that observed by the TOMS aerosol index (Duncan et al. 2003b) and results in a linear correlation of R^2=0.77 (N=21). In summary, the RETRO area burned estimate appears to realistically reproduce the area affected by fires in Indonesia and the interannual variability of the amount of burning.

[10] The RETRO estimate is 8% higher than the estimate in given in Chapter 5.3.3 (Heil et al. 2007) because it refers to the total area burned in Indonesia during January to December 2007 while the latter refers to the area burned during July to December 1997, only.

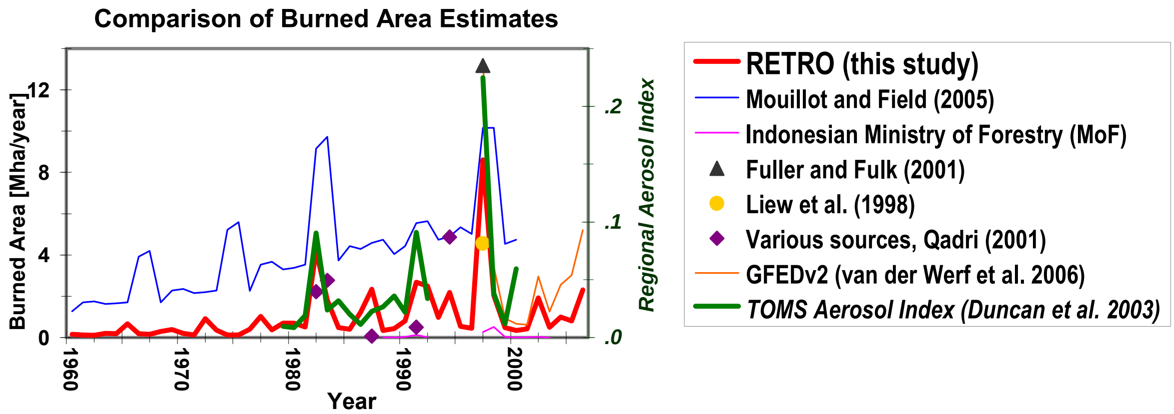

Figure 3-9: Comparison of estimated annual burned area in Indonesia during 1960 to 2006 (RETRO inventory) with various other burned area estimates.

3.4 Emissions from Indonesian Surface Vegetation and Peat Fires 1960 to 2006

3.4.1 Total Carbon Emissions

According to the RETRO emission inventory calculations, the Indonesian fires released an estimated 6.2 Gt of carbon (C) into the atmosphere during 1960 to 2006. 3.6 GtC or 59% were released from peat burning alone, which occurred on solely 24% of the total area burned (Table 3-3). Burning in Kalimantan contributed most (59%) to the carbon emitted, followed by Sumatra (39%). The remaining areas of EQAS emitted only 0.5 GtC during the same period, most of which (67%) from surface vegetation fires.

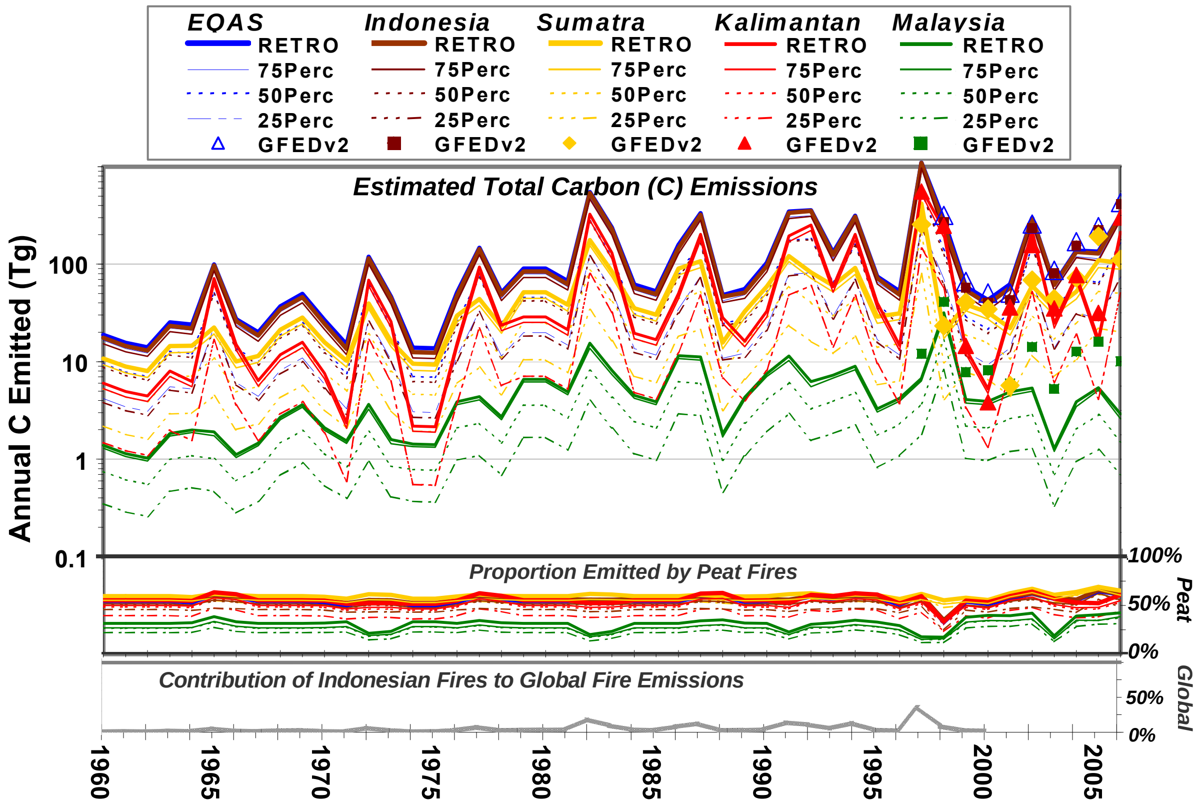

Figure 3-10: Estimated annual fire emissions of carbon (C) in entire Indonesia, Sumatra, Kalimantan, Malaysia and entire Equatorial Asia (EQAS) during the period 1960 to 2006 (left ordinate). For the period 1997 to 2006, the fire-related C-emissions in the GFEDv2 inventory are displayed for comparison. The relative contribution of fires in peat areas to the total annual C emitted by fires in the RETRO inventory is shown on the right ordinate. The contribution of C emitted by fires in Indonesia relative to the total annual C emitted by fires globally (RETRO estimates) is also shown.

RETROv1 Inventory		Annual Burned Area (Mha)								Annual C Emissions (Tg)							
		Indonesia			Sumatra		Kalimantan		EQAS	Indonesia			Sumatra		Kalimantan		EQAS
		Mean	MIN (Year)	MAX (Year)	Mean	% INO	Mean	% INO	Mean	Mean	MIN (Year)	MAX (Year)	Mean	% INO	Mean	% INO	Mean
Decade 1960-1969	All	**0.2**	0.11(1962)	0.67(1965)	**0.1**	51%	**0.1**	38%	**0.3**	**31.3**	13(1962)	97.4(1965)	**15.0**	48%	**15.0**	48%	**33.1**
	Peat	**0.1**	0.0	0.2	**0.0**	50%	**0.0**	49%	**0.1**	**18.1**	7.3	59.3	**9.0**	50%	**8.9**	49%	**18.7**
Decade 1970-1979	All	**0.4**	0.12(1975)	1.02(1977)	**0.2**	50%	**0.2**	40%	**0.5**	**54.5**	12.3(1975)	142.7(1977	**24.9**	46%	**27.0**	49%	**57.4**
	Peat	**0.1**	0	0	**0.0**	48%	**0.0**	50%	**0.1**	**31.0**	6	86	**14.9**	48%	**15.4**	50%	**31.9**
Decade 1980-1989	All	**1.2**	0.34(1988)	4.22(1982)	**0.6**	47%	**0.6**	44%	**1.3**	**158.1**	46.2(1988)	535(1982)	**66.3**	42%	**84.0**	53%	**165.3**
	Peat	**0.3**	0	1	**0.1**	45%	**0.1**	52%	**0.3**	**89.8**	27	299	**40.1**	45%	**46.7**	52%	**91.9**
Decade 1990-1999	All	**2.1**	0.45(1996)	8.61(1997)	**0.9**	41%	**1.1**	51%	**2.2**	**273.0**	48.4(1996)	1091(1997)	**95.1**	35%	**163.4**	60%	**282.2**
	Peat	**0.5**	0.1	1.9	**0.2**	37%	**0.3**	58%	**0.5**	**155.0**	25.5	657.6	**58.0**	37%	**90.5**	58%	**157.3**
2000-2006	All	**1.0**	0.35(2000)	2.31(2006)	**0.4**	40%	**0.5**	51%	**1.1**	**147.8**	39(2000)	322(2006)	**59.2**	40%	**84.4**	57%	**151.8**
	Peat	**0.3**	0.1	0.6	**0.1**	43%	**0.2**	57%	**0.3**	**90.0**	20.5	197.7	**38.5**	43%	**51.1**	57%	**91.5**
		RETROv1: Total Area Burned (Mha)								**RETROv1: Total C Emissions (Tg)**							
Total 1960-2006	All	**47.9**			**21.0**	44%	**22.7**	48%	**50.9**	**6204**			**2427**	39%	**3484**	56%	**6443**
	Peat	**10.51 (22% of total)**			**4.4**	39%	**5.8**	51%	**10.7**	**3569 (58% of total)**			**1490**	39%	**1973**	51%	**3639**
										Uncertainty Range (25% and 75% Percentile) Total C Emitted during the Inventory Period (Tg)							
Total 1960-2006	All									*25 Perc*	**1389**		**480**	35%	**845**	61%	**1450**
	Peat									*25 Perc*	**630 (45% of total)**		**263**	39%	**348**	51%	**642**
	All									*75 Perc*	**5415**		**2099**	39%	**3045**	56%	**5634**
	Peat									*75 Perc*	**2849 (53% of total)**		**1189**	39%	**1575**	51%	**2904**
		Comparison with GFEDv2 data								**Comparison with GFEDv2 data**							
		Mean	MIN (Year)	MAX (Year)	Mean	% INO	Mean	% INO	Mean	Mean	MIN (Year)	MAX (Year)	Mean	% INO	Mean	% INO	Mean
Total 1997-2006 all fuels	RETRO	**1.8**	0.35(2000)	8.61(1997)	**0.8**	41%	**1.0**	52%	**1.9**	**243.2**	39(2000)	1091(1997)	**89.1**	37%	**142.8**	59%	**250.2**
	25Perc									**54.7**	8.4(2000)	241(1997)	**17.4**	32%	**34.7**	64%	**56.4**
	75Perc									**212.1**	33.7(2000)	965(1997)	**77.1**	36%	**124.8**	59%	**218.5**
	GFEDv2	**3.4**	0.62(2001)	13.3(1997)	**1.3**	38%	**1.5**	45%	**4.2**	**253.5**	40.6(2000)	1011(1997)	**85.0**	34%	**145.9**	58%	**275.4**
GFED/RETRO		***1.85***	*1.78*	*1.55*	***1.72***		***1.61***		***2.16***	***1.04***	*1.04*	*0.93*	***0.95***		***1.02***		***1.10***
RETROv1 Inventory		Annual CO Emissions (Tg)								Annual TPM Emissions (Tg)							
		Indonesia			Sumatra		Kalimantan		EQAS	Indonesia			Sumatra		Kalimantan		EQAS
		Mean	MIN (Year)	MAX (Year)	Mean	% INO	Mean	% INO	Mean	Mean	MIN (Year)	MAX (Year)	Mean	% INO	Mean	% INO	Mean
Decade 1960-1969	All	**9.5**	3.9(1962)	30.4(1965)	**4.6**	48%	**4.7**	49%	**10.0**	**2.0**	0.8(1962)	6.4(1965)	**1.0**	49%	**1.0**	49%	**2.0**
	Peat	**7.0**	2.8	22.9	**3.5**	50%	**3.4**	49%	**7.2**	**1.7**	0.7	5.7	**0.9**	50%	**0.9**	49%	**1.8**
Decade 1970-1979	All	**16.5**	3.6(1975)	44.2(1977)	**7.6**	46%	**8.3**	50%	**17.2**	**3.4**	0.7(1975)	9.2(1977)	**1.6**	47%	**1.7**	50%	**3.5**
	Peat	**12.0**	2	33	**5.7**	48%	**5.9**	50%	**12.3**	**3.0**	1	8	**1.4**	48%	**1.5**	50%	**3.1**
Decade 1980-1989	All	**47.9**	14.2(1988)	161(1982)	**20.3**	42%	**25.6**	53%	**49.7**	**9.8**	3(1988)	32.8(1982)	**4.3**	44%	**5.1**	52%	**10.1**
	Peat	**34.7**	11	115	**15.5**	45%	**18.0**	52%	**35.5**	**8.7**	3	29	**3.9**	45%	**4.5**	52%	**8.9**
Decade 1990-1999	All	**82.8**	14.2(1996)	337(1997)	**29.1**	35%	**49.7**	60%	**85.0**	**17.0**	2.9(1996)	70.8(1997)	**6.2**	37%	**10.0**	59%	**17.3**
	Peat	**59.8**	9.9	253.7	**22.4**	37%	**34.9**	58%	**60.7**	**14.9**	2.5	63.4	**5.6**	37%	**8.7**	58%	**15.2**
2000-2006	All	**46.0**	11.4(2000)	101(2006)	**18.7**	41%	**26.4**	57%	**47.1**	**9.7**	2.3(2000)	21.2(2006)	**4.1**	42%	**5.5**	57%	**9.9**
	Peat	**34.7**	7.9	76.3	**14.9**	43%	**19.7**	57%	**35.3**	**8.7**	2.0	19.1	**3.7**	43%	**4.9**	57%	**8.8**
		RETROv1: Total CO Emissions (Tg)								**RETROv1: Total TPM Emissions (Tg)**							
Total 1960-2006	All	**1890**			**747**	40%	**1067**	56%	**1949**	**389**			**160**	41%	**216**	56%	**399**
	Peat	**1481 (78% of total)**			**575**	39%	**761**	51%	**1404**	**344 (88% of total)**			**26**	39%	**190**	51%	**351**
		Uncertainty Range (25% and 75% Percentile) Total CO Emitted during the Inventory Period (Tg)								**Uncertainty Range (25% and 75% Percentile) Total TPM Emitted during the Inventory Period (Tg)**							
Total 1960-2006	All	*25 Perc*	**398**		**147**	37%	**235**	59%	**412**	*25 Perc*	**77**		**31**	40%	**44**	57%	**79**
	Peat	*25 Perc*	**263 (71% of total)**		**110**	39%	**145**	51%	**268**	*25 Perc*	**71 (92% of total)**		**27**	39%	**36**	51%	**67**
	All	*75 Perc*	**1576**		**607**	39%	**902**	57%	**1631**	*75 Perc*	**306**		**125**	41%	**170**	56%	**314**
	Peat	*75 Perc*	**1028 (70% of total)**		**429**	39%	**568**	51%	**1048**	*75 Perc*	**276 (90% of total)**		**107**	39%	**142**	51%	**262**
		Comparison with GFEDv2 data								**Comparison with GFEDv2 data**							
		Mean	MIN (Year)	MAX (Year)	Mean	% INO	Mean	% INO	Mean	Mean	MIN (Year)	MAX (Year)	Mean	% INO	Mean	% INO	Mean
Total 1997-2006 all fuels	RETRO	**74.2**	11.4(2000)	337(1997)	**27.7**	37%	**43.5**	59%	**76.0**	**15.3**	2.3(2000)	71(1997)	**6.0**	39%	**8.7**	57%	**15.6**
	25Perc	**15.7**	2.4(2000)	71(1997)	**5.4**	35%	**9.6**	61%	**16.1**	**3.0**	0.4(2000)	14(1997)	**1.1**	38%	**1.8**	59%	**3.1**
	75Perc	**61.9**	9.5(2000)	282(1997)	**22.4**	36%	**36.8**	59%	**63.5**	**12.0**	1.8(2000)	56(1997)	**4.7**	39%	**6.9**	57%	**12.3**
	GFEDv2	**57.4**	9.2(2000)	229(1997)	**19.2**	33%	**33.1**	58%	**62.4**	**4.8**	0.8(2000)	19(1997)	**1.6**	34%	**2.8**	58%	**5.2**
GFED/RETRO		***0.77***	*0.80*	*0.68*	***0.70***		***0.76***		***0.82***	***0.31***	*0.33*	*0.27*	***0.27***		***0.32***		***0.33***

Table 3-3: Summary statistics of annual burned area (total area and peat area, respectively) and annual related fire emissions of carbon (C), carbon monoxide (CO) and total particulate matter (TPM) during 1960 to 2006 based on RETRO estimates. The decadal means and the totals over the entire inventory period are given. The estimated annual burned area (RETRO estimate) during 1997 to 2006 is compared with GFEDv2 estimates available for this period, only. In addition, the results of the emission calculations using 25 and 75 percentile values, respectively, are shown (see Section 3.2.2). (The following abbreviations are used: MIN= Minimum, MAX=Maximum, % INO= relative to the burned area in Indonesia (in percentage), 25Perc=25 percentile, 75Perc=75 percentile).

The ten-year totals of carbon emitted by Indonesian fires increases from 0.3 GtC in the 1960ies, 0.5 GtC in the 1970ies, 1.6 GtC in the 1980ies to 2.7 GtC in the 1990ies. During 2000 to 2006, 1.0 GtC has been emitted so far. Around 30 to 40% of the decadal totals are emitted during a single year with abnormally intensive burning, i.e. 1965 (0.10 GtC), 1972 (0.14 GtC), 1982 (0.54 GtC) and 1997 (1.1 GtC) (Figure 3-10). The latter contributes 35% to the total amount of carbon emitted globally by fires in this year (Schultz et al. *submitted*) and equals 17% of the global amount of carbon emitted by fossil fuel combustion per year in the 1990ies (6.3 GtC per year (IPCC 2001)).

Estimated monthly and annual total carbon emissions using the RETRO approach are in very good agreement with the corresponding GFEDv2 estimates concerning both, the total amount (Table 3-3) and the temporal variability (Figure 3-10 and Figure 3-11). In the GFEDv2 inventory, the amount of carbon emitted from fires in Indonesia averaged over the 1997 to 2006 period is 254 TgC per year compared to 243 Tg per year in the RETRO inventory, i.e. only 4% higher. The GFEDv2 estimate for the sub-regions Sumatra and Kalimantan agrees within 5% and 2%, respectively. However, the GFEDv2 inventory yields higher (lower) values for Sumatra (Kalimantan) compared to the RETRO inventory. A strong discrepancy between both inventories is observed for the estimated emissions from fires in the entire EQAS region except Sumatra and Kalimantan. Here, the GFEDv2 inventory yields 2.4 times higher carbon emissions compared to the RETRO inventory (45 versus 18 TgC per year). As a result, the estimated relative contribution of fires in these regions is 16% in the GFEDv2 inventory and only 7% in the RETRO inventory.

The very good agreement in the amount of carbon emitted by Indonesian fires in both inventories contrasts with the 1.85 times higher burned area estimated in the GFEDv2 inventory (see section 3.3 and Table 3-3). This implies that the GFEDv2 approach yields distinctively lower amounts of carbon emitted per unit area burned than the approach used in the RETRO inventory. For the area in EQAS affected by fires, the CASA model used in the GFED inventory calculates an average fuel load of 198 tons/ha, of which 132 tons/ha is associated to so-called litter fuel (including aboveground litter and peat) and 66 tons/ha to the so-called biomass fuel. Furthermore, the burning efficiency weighted by burned area and by fuel loads is 76% (44% for biomass fuel and 92% for litter fuel, respectively) (van der Werf et al. 2006). The corresponding values in RETRO inventory are: 862 tons/ha of which 618 tons/ha are attributed to peat and the remaining 244 tons/ha to surface vegetation fuels while the weighted burning efficiency for all fuels is 28% (45% for surface vegetation and 22% for peat). These numbers can be converted into an average carbon emission density for the entire burned area in EQAS, which is 79 tons C/ha in the GFEDv2 inventory and 124 tons C/ha in the RETRO inventory. The difference in the average carbon emission density is most pronounced for surface vegetation fuels. The GFEDv2 value (15 tons C/ha) is only 26% of the corresponding RETRO value (56 tons C/ha) and appears to be very low when compared to values generally given in literature (Table 3-2). The differences in the carbon emission density assumed for peat soil (“litter fuel”) is much lower in both inventories (61 tons C/ha by GFEDv2 compared to 74 tons C/ha by RETRO), mainly due to the compensating effects of the much higher burning efficiency and the much lower fuel load for peat soil (“litter fuel”) assumed in the GFEDv2. However, due to the different definition of the fuel types used in both inventories, they can only be compared by approximation.

The spatial pattern of the annual carbon emission densities calculated in both inventories for the years 1997 and 2006 is shown in Figure 3-11. The GFEDv2 yields a largely similar spatial pattern in carbon emission densities to the RETRO inventory, although the area with fire-related carbon emissions in GFEDv2 inventory is generally larger. In both, maximum carbon emission densities are distributed across areas with known peat deposits. However, especially in the year 1997, the area with values above 50 tons C/ha is smaller in the GFED inventory.

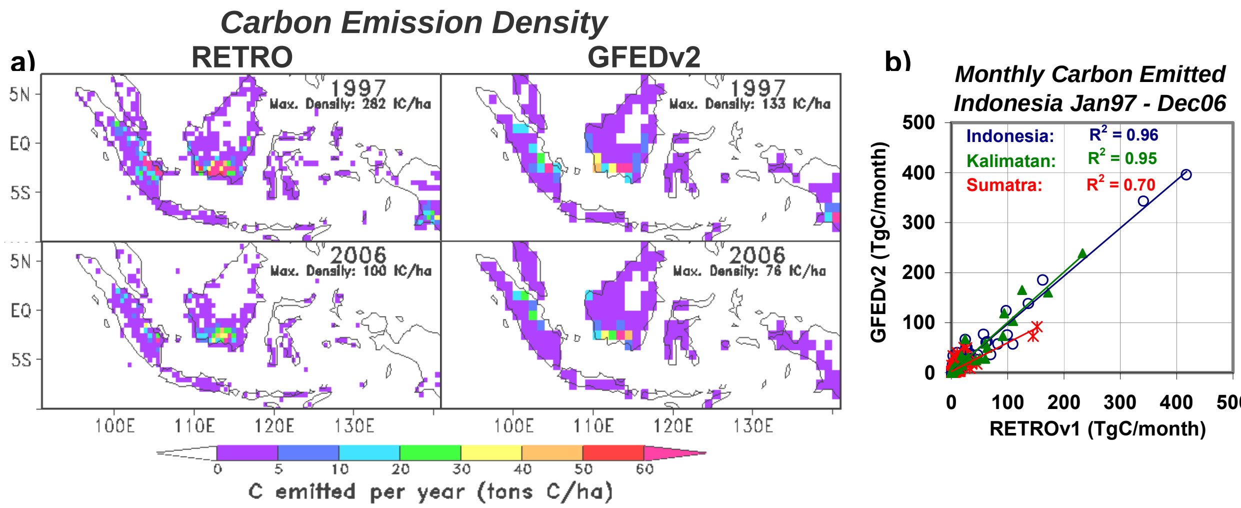

Figure 3-11: a) Fire-related carbon emission density calculated for the years 1997 and 2006 by the RETRO and the GFEDv2 inventory, respectively (in tons C/ha per year). The grid resolution of the RETRO inventory is 0.5x0.5 degree while it is 1x1 degree in the GFEDv2 inventory .b) relative contribution of C emitted by fires in Indonesia to the total annual C emitted by fires globally (RETRO estimates). b) Correlation of the time series of monthly total carbon emitted by fires in Indonesia, Sumatra and Kalimantan, respectively, estimated by the RETRO and the GFEDv2 inventory.

3.4.2 Total Carbon Monoxide (CO) Emissions

Fires in Indonesia during the period 1960 to 2006 released on average 40.2 Tg CO per year, 78% of which is attributable to peat burning only (RETRO estimate) (Table 3-3)). Similar to the carbon emissions, the decadal mean CO emissions per year increased by a factor of 8.7 from the 1960ies to the 1990ies (from 9.5 Tg to 82.8 CO per year). Furthermore, the relative proportion of the various subregions to the total amount of CO emitted in EQAS is largely similar.

To the global amount of CO emitted by fires during 1960 to 2000, fires in Indonesia are estimated to have contributed on average 9.5% (Figure 3-12). The global contribution of single years with abnormally intense burning increases throughout this period from 11% in 1965 to as much as 61% in 1997. The fires in 1997 emitted in total 337 Tg CO, which is 41% of the amount of CO emitted by fires during the entire 1990ies. When compared to the total amount of CO emitted globally by anthropogenic sources and fires, the burning in Indonesia accounts for 4.3% regarding the long-term average (1960 to 2000) and for up to 32% regarding the single year 1997.

Similar to the estimates of carbon released by the fires, the RETRO time-series of CO emissions (1997 to 2006) are largely correlated to the GFEDv2 estimates (Figure 3-12). The amount of CO emitted by fires in Indonesia, however, is 23% lower in the GFEDv2 estimate (57.4 Tg CO) than in the RETRO estimate (74.2 Tg CO) (Table 3-3) whereas the carbon emissions are 4% higher. The use of different emission factors for peat burning in both inventories likely explains most of this discrepancy. For peat fire emissions in the GFEDv2 inventory, van der Werf et al. (2006) used emission factors for tropical forests provided by Andreae and Merlet (2001) while tropical peat-specific emission factors are used in the RETRO inventory (Table 3-2). For CO, the factor used in the RETRO inventory (210 g CO emitted per kg dry fuel combusted) is twice the factor used in the GFEDv2 inventory (103 g CO per kg fuel). CO is a product of incomplete combustion, which dominates the emissions of the low-temperature fires in peat soils. By using emission factors for tropical forest burning, which is dominated by flaming combustion, the GFEDv2 inventory will underestimate the amount of emissions resulting from incomplete combustion while overestimating the amount of combustion products from high-temperature fires (e.g. NOx, black carbon (BC)) (Table 3-2).

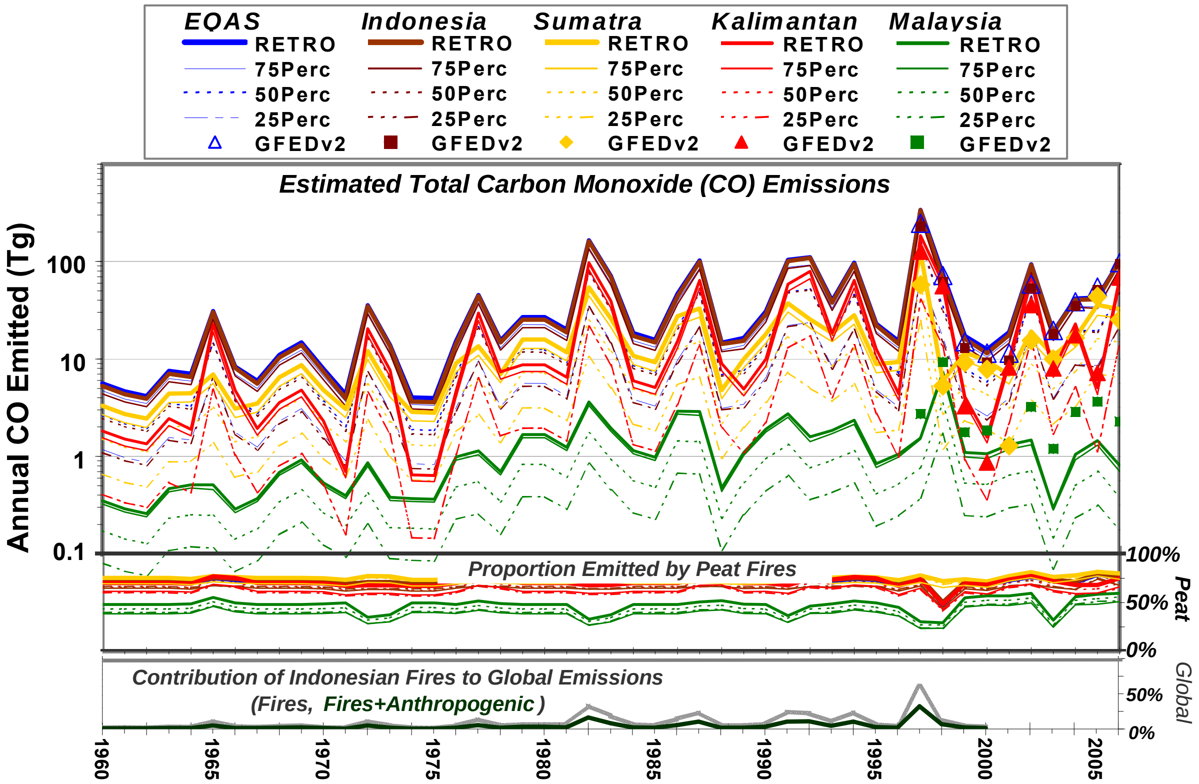

Figure 3-12: Estimated annual fire emissions of carbon monoxide (CO) in entire Indonesia, Sumatra, Kalimantan, Malaysia and entire Equatorial Asia (EQAS) during the period 1960 to 2006 (left ordinate). For the period 1997 to 2006, the fire-related CO-emissions in the GFEDv2 inventory are displayed for comparison. The relative contribution of fires in peat areas to the total annual CO emitted by fires in the RETRO inventory is shown on the right ordinate. The contribution of CO emitted by fires in Indonesia relative to the total annual CO emitted by fires globally (plus fires and all anthropogenic sources) (RETRO estimates) is also shown.

3.4.3 Total Particulate Matter (TPM) Emissions

Fires in Indonesia during the period 1960 to 2006 released on average 8.3 Tg TPM per year, 88% of which is attributable to peat burning only (RETRO estimate) (Table 3-3)). Throughout this period, the temporal trend and variability of TPM emissions is largely similar to the estimated C and CO emissions (Figure 3-10 and Figure 3-12) as is the relative contribution of the various subregions to fire emissions in entire EQAS (Table 3-3).

To the global amount of TPM emitted by fires during 1960 to 2000, fires in Indonesia are estimated to have contributed on average 15.6% (Figure 3-12). The global contribution of single years with abnormally intense burning increases throughout this period from 18% in 1965 to as much as 99% in 1997. The fires in 1997 emitted in total 71 Tg TPM, which is 28% of the estimated 250 Tg of aerosols emitted globally in the year 2000 by all anthropogenic sources and fires (IPCC 2001).

The TPM emissions released by fires in Indonesia during 1997 to 2006 in the RETRO estimate are distinctly higher than the fire-related TPM emissions in the GFEDv2 inventory. The annual GFEDv2 estimate is on average 4.8 Tg TPM during this period and only 31% of the 15 Tg TPM in the RETRO estimate. As explained in the previous section on CO emissions (Section 3.4.2), this is mainly due to the use of different TPM emission factors for peat burning in both inventories, which is 6.2 higher in the RETRO estimate compared to the GFEDv2 estimate (52.5 g TPM and 8.5 g TPM, respectively, per kg dry fuel consumed) (Table 3-2). The application of emissions factors determined for tropical forest on peat fires in the GFEDv2 inventory therefore leads to an even stronger underestimation of TPM emissions than of CO emissions (Table 3-3).

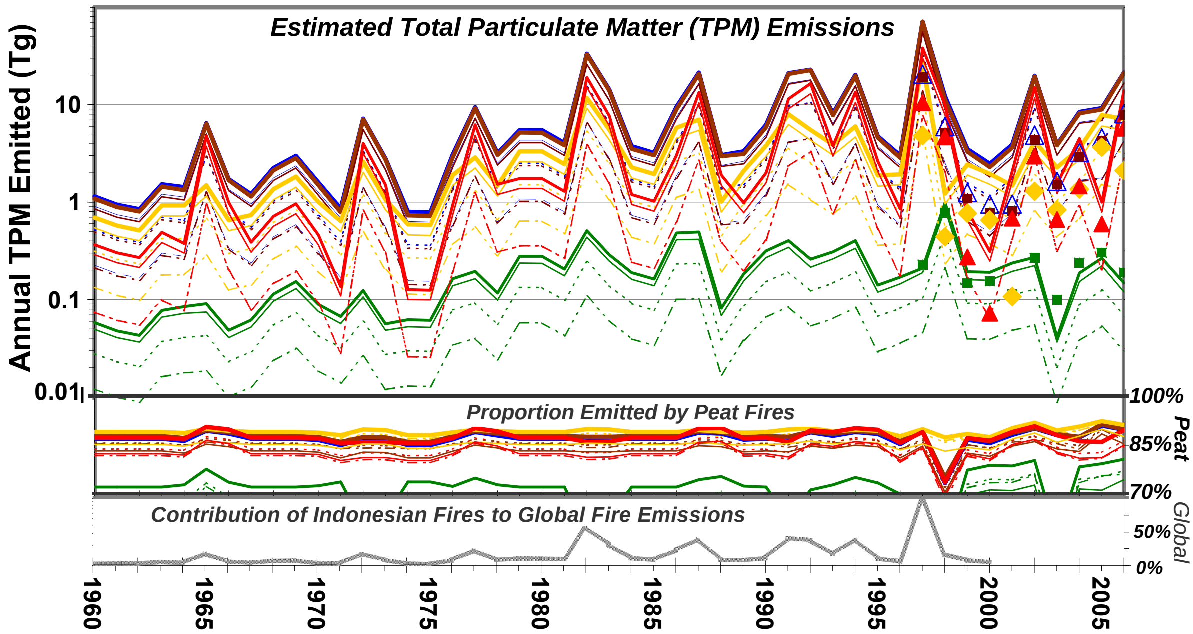

Figure 3-13: Estimated annual fire emissions of total particulate matter (TPM) in entire Indonesia, Sumatra, Kalimantan, Malaysia and entire Equatorial Asia (EQAS) during the period 1960 to 2006 (left ordinate). For the period 1997 to 2006, the fire-related TPM emissions in the GFEDv2 inventory are displayed for comparison. The relative contribution of fires in peat areas to the total annual TPM emitted by fires in the RETRO inventory is shown on the right ordinate. The contribution of TPM emitted by fires in Indonesia relative to the total annual TPM emitted by fires globally (RETRO estimates) is also shown.

3.5 Discussion and Conclusions

The comparison of the first-guess RETRO estimate with a more recent estimate using 75 percentile values of biomass density, burning efficiency and emission factors shows that the RETRO estimate yields 1.1, 1.2 and 1.3 times higher emissions for carbon, CO and TPM, respectively. The RETRO estimate is higher because it assumes a higher burning efficiency for tropical forest and a higher depth burned for peat soil than the 75 percentile value estimate. As a result, the assumed carbon consumption per area for both is 1.27 and 1.29 times higher, respectively. On the other hand, the carbon consumption per area assumed in the RETRO estimate for the two fuel classes agriculture, grassland and savanna, and plantations and fragmented forest is around 20 to 30% lower in the 75 percentile estimate, but still above a 50 percentile estimate (Table 3-2). Because of these partly compensating effects, the RETRO carbon emissions are relatively close to the 75 percentile estimate. Nevertheless, the estimated contribution of peat fires to the carbon emitted by all fires is 58% while it is 53% in the 75 percentile estimate (Table 3-3). This difference explains the higher deviation for CO and TPM emissions, because their difference in the emission factors between peat and surface fires is much higher than for carbon.

The probably slightly too low area burned assumed in the RETRO estimate (Figure 3-9) will balance the overprediction in the RETRO emissions. We therefore consider the RETRO emissions for Indonesia to be one of the most realistic currently available estimates. Regionally, we most probably overestimate (underestimate) the area of peat burning in Kalimantan (Sumatra) because the FAO (2003) map used on this study results in a 5% higher (11% lower) peat area in Kalimantan (Sumatra) than the probably more realistic, but only recently available peat map established by Wahyunto et al. (2003, 2004) (Figure 1-2 and Figure 2-9). [11]

This study indicates that the GFEDv2 inventory, which is nowadays widely used in atmospheric chemistry modeling studies (e.g. Dentener et al. 2006, van Noije et al. 2006) strongly underestimates the emissions resulting from incomplete combustion (e.g. CO, TPM, CH_4, NMHC), which is characteristic for smoldering peat fires. This is mainly because the emission factors used for peat burning in the GFEDv2 inventory were derived from the generally more flaming forest fires. The estimated TPM emissions in the GFEDv2 inventory for surface vegetation and peat fires in Indonesia are, for example, only 0.3 times the RETRO estimate and close to the 25 percentile value of our study, although a 1.9 times larger burned area was assumed (Table 3-3). The Indonesian fire emission inventory presented in this study used emission factors that were recently derived for peat burning. It is therefore a more realistic estimate of the total amounts of incompletely oxidized trace species emitted by peat fires in Indonesia and their relative contribution to the emissions produced by all fires.

Irrespective of differences between the GFEDv2 and the inventory established in this study in estimating the sum totals of area burned in Indonesia and related emissions, the temporal pattern estimated by both approaches is very similar. This provides further evidence that the new inventory established realistically represents the inter-and intraannual variability of burned area and related emissions in Indonesia.

The uncertainty of the estimate, however, is still large. The uncertainty range of the estimate of total fire emissions spans at least a factor of 4 due to imprecisely known biomass loads, burning efficiencies and emission factors alone.[12] Uncertainties in the burned area and the spatial distribution of vegetation cover and peat soil will further enhance the overall uncertainty range. Reconciling our inventory-based estimate with results from top-down inverse modeling (e.g. Roedenbeck et al. 2003) or regional smoke plume dispersion modeling studies (e.g. Langmann and Heil 2004, see Section 5) is a promising approach to constrain these uncertainties and should be addressed with priority.

[11] Note that only half of the area assigned as histosol in the FAO (2003) map was considered to be peat (see Heil et al. 2007, Section 6.2.2.1).
[12] Ratio between the 75 percentile emission estimate and the 25 percentile emission estimate in Table 3 3.

Our study demonstrates that fires in peat deposits predominate overall emission production by fires in Indonesia contributing an estimated 58%, 78% and 88% to the total amount of carbon (C), carbon monoxide (CO) and total particulate matter (TPM), respectively, released throughout 1960 to 2006. In contrast, the area contribution of peat fires to the total burned area is only 22%. The study highlights that emission inventories which omit or only partly consider peat fire emissions (e.g. Hao et al. 1990, Crutzen and Andreae 1990, van der Werf et al. 2003, Hoelzemann et al. 2004, van der Werf et al. 2006) tend to underestimate the total amount of emissions produced in areas with extensive peat burning, such as Indonesia. Furthermore, the omission of peat fires will lead to biases in the chemical composition of the emissions produced, as the relative contribution of incompletely oxidized species (e.g. CO, TPM, methane, aldehydes) is underestimated.

The interannual variability of fire activity in Indonesia and related emission production is large. Estimated annual carbon emissions by Indonesian fires in the 1990ies vary from 0.05 GtC per year in 1996 to 1.1 GtC per year in 1997, i.e. by a factor of around 22. Since 1960, fire emissions in Indonesia increased strongly due to deforestation and forest fragmentation activities. The ten-year total emitted in the 1990ies (2.7 GtC) is 9 times higher than in the 1960ies (0.3 GtC). Simultaneously, the relative contribution of Indonesian fires to the total amount of carbon and trace species emitted by fires globally increased significantly.

In years with abnormally large fire activity in Indonesia (e.g. 1997) Indonesia may contribute 35% to carbon emitted globally by fires, which equals around 17% of the global carbon emitted by fossil fuel combustion. The carbon monoxide emissions produced by fires in Indonesia may reach 41% of the global total emitted by fires and 32% of the global emissions produced by both, fires and anthropogenic sources. For selected trace species such as fire aerosols, the contribution of Indonesian fires to their global totals emitted by fires may even reach up to 100%. Fires in Indonesia may thus influence the interannual variability of the budget of climatically and atmospherically active trace species at a global scale.

4 Smoke-Haze Pollution: A Review of the 1997 Episode in South-East Asia

This chapter has been published as: Heil A and Goldammer JG (2001) Smoke haze pollution: A review of the 1997 episode in Southeast Asia. Regional Environmental Change 2:24-37.

Abstract

In the second half of 1997, large areas in Southeast Asia were severely affected by a smoke-haze pollution episode caused by the emissions of an estimated 45,600 km^2 of vegetation that burnt on the Indonesian islands Kalimantan and Sumatra. To document the impacts of these fires on air quality, data for total suspended particulate matter (TSP) and for particulate matter below or equal to 10 microns in diameter (PM_{10}) from selected sites in Indonesia, Malaysia and Singapore are analyzed in this paper. These data are supplemented by meteorological data, satellite images, and a summary of related research. TSP was above 2000 µg m^{-3} for several days in Indonesian locations close to the most extensive fire activity. In Malaysia and Singapore, ambient particle concentration increased to several times of their average September levels. Characteristically for emissions from vegetation burning, the additional atmospheric particle loading during the smoke-haze episode was predominantly due to an increase of the fraction below or equal to 2.5 microns in diameter ($PM_{2.5}$). Due to the dominance of respirable particles ($PM_{2.5}$) in the smoke-haze, air quality reporting based on TSP or PM_{10} may be inadequate to assess the health risk. Upgrading of $PM_{2.5}$ monitoring facilities is therefore needed. Reducing the probability of similar smoke-haze events in future would require appropriate fire use and smoke management strategies.

4.1 Introduction

In Southeast Asia, there is a regular (periodic) incidence of fire-related regional air pollution episodes. Since the 1970s nine such incidents have been reported (SMS 1995; WMO 1998; Goldammer 1999), the most recent of which (i.e. in 1994 and 1997-98) are frequently considered to be unprecedented in extent and intensity (SMS 1995; Nichol 1997; WHO 1998; UNEP 1999). Meanwhile, the term 'haze' or 'smoke-haze' in Southeast Asia has become associated with fire-related, large-scale air pollution. For instance, the regional and national Haze Action Plans for the Association of Southeast Asian Nations (ASEAN) aim to prevent and mitigate regional air pollution from large scale forest and land fires (CGIF 1998). However, the World Meteorological Organization (WMO 1992) defines haze as a suspension of extremely small, dry particles in the atmosphere and hence does not specify a specific source.

Most of the extensive smoke-haze events in Southeast Asia resulted from fires that occurred mainly in Sumatra and the Kalimantan region of Borneo island (Dennis 1998; Radojevic and Hassan 1999). They generally occurred when the Southeast Asian weather was strongly influenced by the El Niño Southern Oscillation (ENSO) event (WMO 1998). During ENSO years, the above normal atmospheric surface level pressure building up over the western Pacific region is coupled with a diminished upward motion. The ensuing reduction of convective activity results in abnormal drought throughout Southeast Asia generally reaching its peak between July and September in Indonesia (Philander 1990).

Throughout the tropical southern hemisphere, fires are set to clear vegetation during the relatively dry southern monsoon season from June to October (Olson et al. 1999). The burning activities generally cease by October/November when the gradually interspersing northern monsoon brings abundant rainfall. The prolonged drought during ENSO years increases the susceptibility of vegetation to fire enabling the clearing and conversion of more land (Goldammer et al. 1996; Goldammer and Price 1998). Under these conditions, fires are also more likely to become uncontrolled. For these reasons, the area burnt in Indonesia and the amount of emissions produced may greatly exceed the normal annual total.

The low-level, southern monsoon wind circulation prevailing during the main burning season produces a northward, cross-equatorial transport of fire emissions from Indonesia, particularly towards Singapore, Malaysia and Brunei. Subsidence generally characteristic of the southerly monsoon (Depperman 1941) increases atmospheric stability and favors the accumulation of fire products in the lower atmosphere. The ENSO-related anomalies tend to reinforce the meteorological conditions contributing to the development of persistent regional haze. Diminished ascending motion coupled with increased atmospheric stability and inversions causes fire emissions to be more efficiently trapped in the lower troposphere than during non-ENSO years (Chandra et al. 1998; Ziemke and Chandra 1999). Reduced rainfall prolongs atmospheric residence time of fire products as they are less abundantly scavenged by precipitation. Anomalous easterly surface winds during August to October in a canonical ENSO year over the Malay-Indonesia region (Rasmusson and Carpenter 1982) may enhance the westward transport of pyrogenic emissions from Kalimantan towards Peninsular Malaysia and Singapore. In summary, because of increased fire and reduced dispersion, the regional smoke-haze events in Southeast Asia generally occur during the southern monsoon period in ENSO years (SMS 1995).

Despite the existing in-depth knowledge on fire and its underlying causes in South East Asian ecosystems (Goldammer and Seibert 1990; Goldammer and Peñafiel 1990; Stott et al. 1990; Goldammer 1993; Goldammer et al. 1996), little literature and research exist on the implications of vegetation burning in this region on atmospheric chemistry and public health (Goldammer 1997; Goldammer et al. 1997; Nichol 1997, 1998; WHO 1998; Geophys Res Lett 1999; Balasubramanian et al. 1999; Fujiwara et al. 1999). This is mainly because the international fire-atmosphere science community has largely concentrated its research efforts on Africa and South America where regular wildland fire occurrence and land-use fire application created sufficient attention to set up focused research campaigns in the 1980-90s (J Geophys Res 1996; Lindesay et al. 1996; IGAC 1998; cf. also Hao and Liu 1994; Board et al. 1999), but also due to the scarcity of air quality and meteorological data as well as of health statistics, notably in Indonesia.

In this paper we document the impacts of the vegetation fires in Indonesia 1997 on air quality in Southeast Asia. Emphasis is given to the particulate emissions because they are by far the most important emission from a public health standpoint (Sharkey 1997). Data for particulate matter from selected sites in Indonesia, Malaysia and Singapore were obtained from the national routine air monitoring networks and are analyzed in this work.

4.2 Biomass Burning and Atmospheric Implications

Vegetation fires emit a wide spectrum of trace gases and aerosols (Andreae 1991; Yokelson et al. 1999a). Gaseous compounds released include carbon dioxide (CO_2), carbon monoxide (CO), oxides of nitrogen (NO_x), ammonia (NH_3), hydrogen (H_2), and a variety of hydrocarbons, e.g. methane (CH_4), formaldehyde, and methyl chloride. Secondarily, ozone (O_3) can be formed downwind from fires through photochemical reactions involving NO_x and other biomass burning products (Crutzen and Carmichael 1993). Particulate fire emissions are largely (~2/3) composed of carbonaceous material (organic carbon (OC) and elemental ("black") carbon (EC)) (Crutzen and Andreae 1990). Characteristically for combustion derived particles, the bulk of the particle mass emitted (40 to 95%) is in the fine size range (particulate matter ≤ 2.5 µm in diameter ($PM_{2.5}$)) (Ward 1990; Novakov et al. 1997).

The emission production and characteristics from vegetation fires strongly depend on the combustion stage (basically flaming and smoldering combustion), the combustion efficiency and the physico-chemical properties of vegetation burnt (Lobert and Warnatz 1993). Large diameter or densely packed necromass (such as logs, stumps, or peat) and large diameter live vegetation (trunks) are usually only partially consumed and mainly by smoldering combustion (Stocks and

Kaufman 1997; Yokelson et al. 1997), in contrast to the small-diameter, dry dead fuels (necromass) and low-density vegetation (such as grass and leaves). Characteristically for low-efficiency combustion processes, smoldering combustion emits larger amounts of incompletely oxidized compounds than flaming combustion per unit amount biomass consumed by a fire. These incompletely oxidized compounds include CO, methane (CH_4) and other hydrocarbons, NH_3 as well as fine particles (with high OC and low EC content) (Lobert and Warnatz 1993, Ward et al. 1996). Fine particulate emission factors range from ~3 g kg^{-1} fuel consumed in the flaming phase to ~12 g kg^{-1} for smoldering combustion (Einfield et al. 1991). The fuel loads of different vegetation types, in turn, range from 2 t ha^{-1} for low-productivity grasslands in Africa (Hoffa et al. 1999) to as much as 97.5 t ha^{-1} (dry matter) for dry peat of 1.5 m thickness (Supardi et al. 1993); depending on site conditions and degree of pre-fire forest utilization (logging) the total above-ground fuel loads in forest ecosystems may reach several hundreds of tons of dry organic matter per hectare.

The fate of the initial fire emissions depends strongly on both their composition and the regional state of the atmosphere. Once airborne, the particles begin to grow slightly in size as they age through condensation and coagulation. In addition, new fine particles are created by nucleation of gaseous fire emissions; such as the conversion of NO_x to nitrates (Jänicke 1993). Particles are removed from the atmosphere by gravitational settling, precipitation, and cloud scavenging. Because gravitational settling velocity increases with particle diameter, larger particles (particularly those with a diameter larger than 10 µm) are lost from the plume faster than smaller ones. Wet removal thus dominates the atmospheric lifetime of pyrogenic particles, which is therefore largely controlled by meteorology (Garstang et al. 1997). Ultimately, removal of trace gases from the atmosphere is mainly by oxidation processes (Crutzen and Carmichael 1993).

In the late 1970s it has been recognized first that tropical vegetation burning is a major global source of trace gases and aerosols with significant impacts on regional and global climate, atmospheric chemistry and hydrological cycles (Crutzen et al. 1979); this has been confirmed by numerous studies during the 1980-90s (Andreae 1998) which were synthesized in several review articles and monographs, e.g. by Crutzen and Andreae (1990); Goldammer and Crutzen (1993); and Levine (1996). Greenhouse gases released by the fires such as CO_2, CH_4 and ozone exert a permanent additional warming effect which conversely leads to changed climate-fire relationships in the tropics (Goldammer and Price 1998) and in other vegetation zones (Fosberg et al. 1996). Particulate emissions scatter and absorb incoming solar radiation both directly and indirectly through their role as cloud condensation nuclei, resulting in a global net cooling effect (Dickinson 1993; Charlson and Lelieveld 1994). Chemically active emissions may appreciably affect the oxidizing efficiency of the troposphere (Crutzen and Carmichael 1993) and stratospheric ozone chemistry (Andreae 1991; Manö and Andreae 1994). It is estimated that the gross CO_2 emission from biomass burning (i.e. 13,500 Tg CO_2 per year (1 teragram = 10^{12} g) contributes around 40% to the global anthropogenic annual gross release of carbon dioxide, while it accounts for roughly 43% and 23%, respectively, of CO and total particulate matter produced globally (Andreae et al. 1996).

4.3 Fire Development in Indonesia 1997 and Emission Production

Vegetation fires in Kalimantan and Sumatra started with the onset of the relatively dry season in May/June 1997 (UNDAC 1998; Fang and Huang 1998) and reached a maximum during September and October (Makarim et al. 1998). Many fires got out of control and affected the surrounding vegetation (logged forests, peat swamps and grassland) (Dennis 1998). Figure 4-1 shows the monthly distribution of fires on these islands in September and October as depicted as High-Temperature Events (HTEs or ‘fire pixels’) by the ATSR (Along-Track Scanning Radiometer) satellite instrument. It illustrates that the fire activity was mainly concentrated on the south-eastern parts of Sumatra and southern Kalimantan during these months. According to Stolle et al. (undated), a remarkably dense time spacing in the number of HTEs was recorded in the week from 12 to 18 October 1997 in Sumatra. In Kalimantan, a peak in fire activity was noticed in late

September (D. Fuller, pers. comm. 1999). By mid November, fire activity gradually subsided along with the onset of the monsoonal rain.

Using SPOT "quicklook" satellite images, Liew et al. (1998) estimated that an area of approximately 45,600 km^2 burnt from August to December 1997 in Kalimantan and Sumatra. The estimate of Liew et al. (1998) represents only a lower limit estimate since fires in other parts of Southeast Asia were not included. However, estimates of the area burnt vary significantly between different institutions (c.f. UNEP 1999).

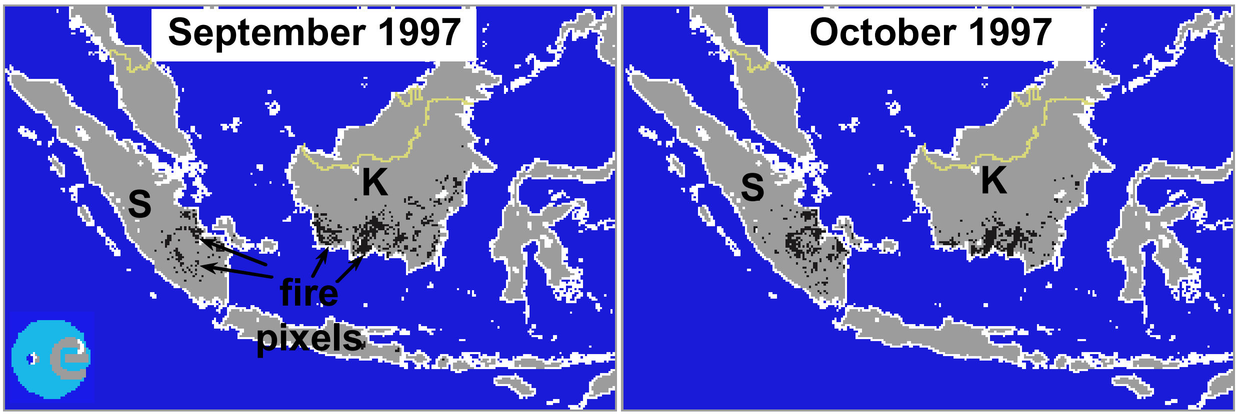

Figure 4-1: Monthly nighttime fire activity map of Kalimantan (K) and Sumatra (S) for September and October 1997 as depicted by the ATSR satellite instrument (adapted from Arino and Rosaz (1999)).

Levine (1999a, b) estimated the emission production resulting from the 1997 fires in Sumatra and Kalimantan. For his calculations, he used both the estimate of the area burnt and the estimate of the ecosystem burnt of Liew et al. (1998), which suggests that 20% of the area burnt consisted of peat swamp forests and the remainder of agricultural and plantation areas, forest and bushes. Levine assumed that the peat ignited everywhere and burned to a depth of one meter. As a result of this and other assumptions, fires in peat swamp forests accounted for the largest part of the total emission production with 89% for CO_2 and more than 93% for all other species. Levine proposes total emissions of 701.6 Tg CO_2, 76.5 Tg CO, 7.1 Tg O_3, 2.5 Tg CH_4, 3.1 Tg NH_3, 0.97 Tg $N(NO_x)$, and 16.2 Tg particulate matter and claims an uncertainty for these estimates of 50%. On the other hand, Nakajima et al. (1999) roughly estimated a total smoke aerosol production of 5.6 Tg for the entire burn, only, based on AVHRR-derived optical thickness distributions.

4.4 Development of the Smoke-Haze Layer and its Physicochemical Characteristics

Satellite images from September 1997 onwards reveal that the fire emissions formed a dense, widespread smoke-haze layer, merging together the plumes from many fires. Figure 4-2 shows examples of UV-absorbing aerosol index maps of the Southeast Asian region derived from the Total Ozone Mapping Spectrometer (TOMS) for (a) early and (b) late September 1997. Since the TOMS instrument measures the presence of aerosols in the whole atmospheric column with a height dependent sensitivity, the ground concentrations cannot be inferred without assumptions on the vertical profile of the aerosol layer (J.R. Herman pers. comm. 1999).

In early September (Figure 4-2a), the smoke-haze layer principally concentrated over the fire centers in southern Kalimantan and central Sumatra. On several days in late September (Figure 4-2b), the smoke-haze layer covered large parts of Kalimantan and Sumatra, Singapore and parts of Malaysia. Its northernmost extension reached as far as Thailand and the Philippines. After an intermediate decrease in early October, the smoke-haze layer increased again in the second half of October, but exhibited a stronger westward than northward component compared to September.

The smoke-haze layer gradually disappeared in the first half of November along with the onset of the rainy season. Based on AVHRR-optical thickness distribution, Nakajima et al. (1999) estimated that the smoke-haze layer covered an area of up to 10 million km^2, with a peak enhancement in October. Increased TOMS tropospheric column ozone spread between 75 – 110°E and 10°S – 8°N during that period (Chandra et al. 1998).

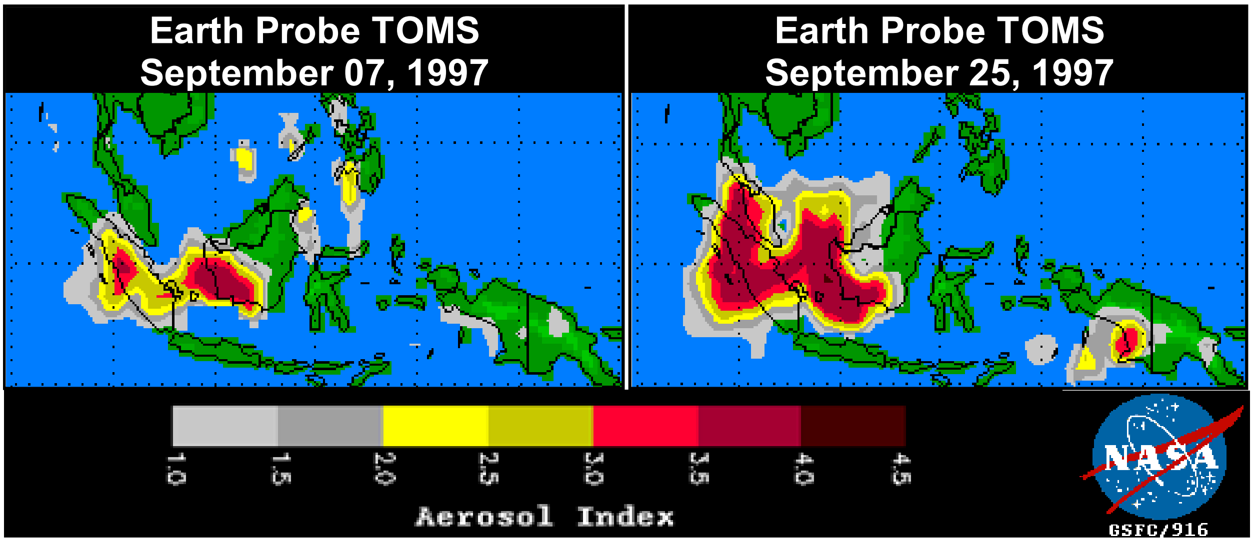

Figure 4-2: Total Ozone Mapping Spectrometer (TOMS) Aerosol Index Maps of Southeast Asia for (a) 7 September 1997 and (b) 25 September 1997. Map Source: Courtesy of Laboratory for Atmospheres, NASA/Goddard Space Flight Center, Greenbelt, MD 20771, USA.

Several aircraft and ground-based measurements confirmed increases of biomass burning products in the troposphere. Within the smoke-haze layer in the Southeast of Kalimantan, whose top was restrained below 4000 m, CO mixing ratios around two orders of magnitude higher than the background level and enhanced concentrations of NO_x, hydrogen (H_2), O_3 and aerosols were measured in late October (Tsutsumi et al. 1999; Sawa et al. 1999). Enhanced trace gas concentrations such as CO, CO_2, CH_4 and O_3 were observed throughout the troposphere from eastern Java to the South China Sea south of 10°N between September and November (Matsueda and Inoue 1999; Fujiwara et al. 1999). The appearance of anomalous increases of CO in the upper troposphere (8 – 13 km) over the entire western Pacific region up to 20°S during September to November 1997 indicates that air masses influenced by the Indonesian fires well reached to the upper troposphere and were possibly transported through the upper levels towards the southern subtropics (Matsueda et al. 1999; Fujiwara et al. 1999).

The optical properties of the aerosols found during the smoke-haze episode point to predominantly smoldering rather than flaming combustion sources (Gras et al. 1999; Nakajima et al. 1999; von Hoyningen-Huene et al. 1999). The small visible light absorption found indicates a very small elemental carbon content in the aerosols, which is characteristic for aerosols derived from smoldering combustion (Yokelson et al. 1997). In addition, the aerosols exhibited a strong hygroscopic growth in scattering comparable to that of peat smoke. These findings, with other observations (e.g. Narukawa et al. 1999), indicate that much of the emissions were produced by smoldering combustion, which points to a significant contribution of emissions from peat fires. The latter is also supported by the high concentration of sulfate aerosols observed during the smoke-haze episode which are attributed to the strong sulfur emission from peat fires (c.f. Gras et al. 1999; Balasubramanian et al. 1999). Furthermore, Legg and Laumonier (1999) stated that the source of probably 90% of the smoke-haze were seven clusters of fires along the edges of degraded peat-swamp forests in southern Sumatra and Kalimantan.

4.5 Impacts on Ambient Air Quality in Indonesia and its Neighboring Countries

The influence of the vegetation fires on ambient air quality in Southeast Asia was discernible by July 1997, peaked in September and decreased towards the beginning of the rainy season in November (DOE 1998; Fang et al. 1999). Similar to other smoke-haze episodes, the pollutant that consistently increased above national ambient air quality thresholds during the 1997 smoke-haze episode was particulate matter (DOE 1998; Emmanuel and Lim 1998; Phonboon 1998; WHO 1998; Radojevic and Hassan 1999). In Singapore, Malaysia and Thailand, gaseous compounds remained generally below the respective national air quality guidelines, although partially an increase of compounds such as CO, O_3 and SO_2 was observed (Brauer 1997; Emmanuel and Lim 1998; Phonboon 1998; DOE 1998; Davies and Unam 1999).

4.5.1 Air Quality Monitoring and Data Source

Indonesia does not yet have an integrated monitoring network which could provide real-time, region covering air quality information (Ferrari 1997; Kandun 1998). Only in some provinces, air pollution is monitored on behalf of the Meteorological and Geophysical Agency (BMG) and the Ministry of Health (MoH), but generally just discontinuously and solely TSP (total suspended particles including particles up to diameters of ~40 µm). As a surrogate, impairment of visibility was widely used as an indicator for ambient air quality during the smoke-haze episode. However, visibility is not only dependent on particle concentration, but also on the subjective perception of the observer, relative humidity and light conditions.

A more advanced air quality monitoring network is in place in Malaysia and Singapore. For reporting, Singapore adopted the pollutant standard index (PSI) used by the US Environmental Protection Agency (USEPA) until recently (c.f. USEPA 1994, 1999), while Malaysia employs an air pollutant index (API) based on similar principles (Radojevic 1998). The pollutant index includes sub-indices for particulate matter, O_3, CO, SO_2 and NO_2, which relate ambient pollutant concentrations to index values on a scale from 0 through 500. The upper bound index value of 500 is set at a level that represents an imminent and substantial endangerment to public health (significant harm level). During smoke-haze episodes, the PSI or API is invariably based on particulate matter concentrations, monitored as PM_{10} (particulate matter with an aerodynamic diameter $\leq$ 10 µm, 24-hour average), as these greatly exceed those of other pollutants (Radojevic and Hassan 1999). A pollutant index from 0 to 100 is described as 'good' to 'moderate' (corresponding to $PM_{10} \leq 150$ µg m^{-3}), an index value up to 200 as 'unhealthy' ($PM_{10} \leq 350$ µg m^{-3}), to 300 as 'very unhealthy' ($PM_{10} \leq 420$ µg m^{-3}), and an index from 301 to 500 as 'hazardous' (PM_{10} $\leq$ 600 µg m^{-3} (USEPA 1994). In Singapore and Malaysia, the national ambient air quality guidelines for PM_{10} (24-hour average) coincide with a PSI/API value of 100. In Indonesia, the national ambient air quality standard for particulate matter is 260 µg m^{-3} TSP (24-hour average) (DOE 1995; Ferrari 1997).

To document the impacts of the 1997 vegetation fires on ambient particle concentration in Southeast Asia, 24-hour average particle measurement data from selected stations in Indonesia, Malaysia and Singapore were compiled (Figure 4-3). TSP and PM_{10} records for Indonesia originate from the Ministry of Health (MoH) and from a special air quality monitoring campaign on behalf of the Environmental Impact Management Agency (BAPEDAL), respectively. TSP and PM_{10} records for Malaysia were obtained from the Malaysian Meteorological Services (MMS) collected at meteorological sites as a part of their routine air monitoring program. The recording is daily at Kuching and Petaling Jaya and every second day at the other locations. PM_{10} data for Singapore are converted from the daily PSI readings provided by the Ministry of Environment (MOE) Singapore which are derived from 12 ambient air monitoring stations throughout the island (Emmanuel and Lim 1998). Information on the range of uncertainty of the measurement results was not provided. However, according to Ferrari (1997), both Singapore and Malaysia use effective internationally accepted quality assurance procedures on data before reporting. Visibility records from the meteorological stations at the selected sites were provided by the respective meteorological services (BMG, MMS and Meteorological Services Singapore (MSS)). In Indonesia, visibility records were based on observations taking place at three hours intervals; in Malaysia and Singapore (Changi Airport Station), there were hourly records.

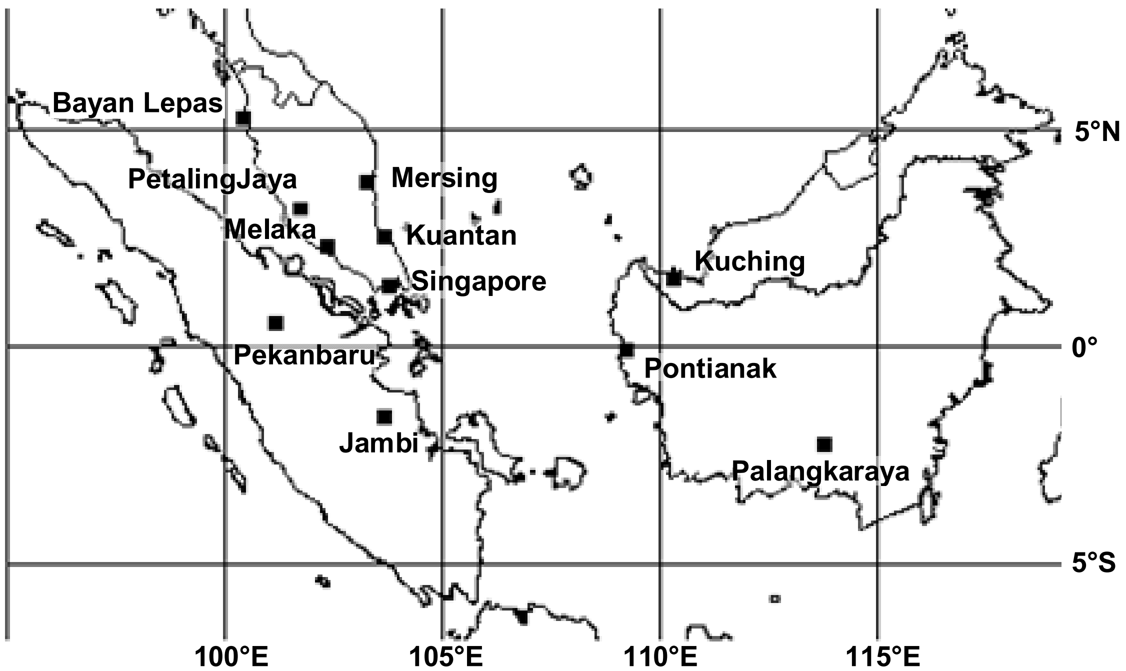

Figure 4-3: Map showing the locations mentioned in this paper.

4.5.2 Development of Ambient Particle Concentration

The development of ambient particle concentration as well as of daily mean horizontal visibility at selected sites in Indonesia, Malaysia and at Singapore during the second half of 1997 is displayed in Figure 4-4 and Figure 4-5. Scanty particle measurement data at hand for the four locations in Kalimantan and Sumatra (Figure 4-4) indicate that ambient particle concentration was above 2000 $\mu g\ m^{-3}$ TSP on several days in late September and October, with the highest concentrations (up to around 4000 $\mu g\ m^{-3}$ TSP) recorded at locations in the vicinity of the main fire activity (Palangkaraya and Jambi). Monthly mean horizontal visibility declined from above 5 km to around 1 km in Pontianak and Pekanbaru in July and to around 0.5 km in Palangkaraya and Jambi in September. Whereas at the first two locations, monthly mean visibility increased to 2.2 - 2.7 km in October, it remained below 1 km at Palangkaraya and Jambi until it sharply increased to above 6 km in mid-November. While particle measurement data are generally missing for the period before late September, impaired visibility suggests that ambient particle concentration had already exceeded background levels by late July/August.

In Kuching (Figure 4-4), north-western Borneo-Malaysia, ambient particle concentration rose gradually from background levels (around 60 µg m^{-3} TSP (DOE 1996)) in the first half of July to 290 µg m^{-3} TSP in the second half of August, reaching a peak value of 529 µg m^{-3} TSP on 24 August. Inversely, daily mean horizontal visibility declined from above 18 km to below 2 km during that period. After an intermediate decline in early September, TSP concentration rose sharply above 590 µg m^{-3} between 17 and 25 September. On 23 and 24 September, a peak concentration of 1030 µg m^{-3} TSP was recorded; the Ministry of Environment reported 930 µg m^{-3} PM_{10} on 24 September (Brauer 1997). Daily mean visibility during this peak episode was below 0.5 km, with hourly minima below 100 m. In the subsequent time until mid-November, TSP concentration fluctuated between 40 and 300 µg m^{-3} (mean of 100 µg m^{-3} TSP) and finally returned to rainy season background conditions from mid-November onwards.

Similar to the development in Kuching, particle concentration at all locations in Peninsular Malaysia exhibited a distinct rise during September, notably between 11 and 28 September (Figure 4-5). It was preceded by a gradual, but highly fluctuating increase from July till August. From October to mid-November, particle concentration decreased all over, though still exhibiting high fluctuations, and remained almost constant at approximate background levels in the subsequent period. The highest particle concentration in September was recorded at Melaka (TSP) and Petaling Jaya/Kuala Lumpur (PM_{10}), both at the southern west coast of Peninsular Malaysia approximately 400 – 800 km north of the main fire activity in Sumatra. Peak values ranged between 300 and 420 µg m^{-3} on several days, and monthly mean particle concentration in September between 210 and 240 µg m^{-3} TSP/PM_{10}, compared to 40 – 50 µg m^{-3} in December. At both locations, monthly visibility averaged 2.2 - 2.3 km in September, with daily minima below 0.4 km during the peak episode. In Petaling Jaya, a total of 22 days exceeded 150 µg m^{-3} PM_{10} ('unhealthy'), 4 days of which were in the 'very unhealthy' to 'hazardous' range (PM_{10} above 350 µg m^{-3}).

More distant from fires, at Bayan Lepas/Penang, around 270 km north-north-west of Kuala Lumpur, particle concentration exhibited a lower increase than in the south. Particle concentration averaged 125 µg m^{-3} TSP in September, compared to 50 µg m^{-3} TSP in December. Accordingly, the impairment of visibility in September (average 4.8 km) was less pronounced at Bayan Lepas. Kuantan, on the east coast of Peninsular Malaysia, exhibited a particle development similar to Petaling Jaya, but at a lower concentration range. Monthly mean particle concentration in September in Kuantan was 135 µg m^{-3} PM_{10} (maxima between 210 and 260 µg m^{-3} PM_{10}), compared to 20 µg m^{-3} in December.

Contrary to the development at all selected locations in Malaysia, particle concentration in Singapore was slightly higher in October (mean of 120 µg m^{-3} PM_{10}) than in September (110 µg m^{-3} PM_{10}). In September, it was also lower than in Petaling Jaya, Melaka or Kuantan, in spite of Singapore's close position to fires in Kalimantan and Sumatra. Consistently, horizontal visibility exhibited its low in October averaging 4.3 km at Changi Station and 2.6 km at Tengah Station in Singapore's west. On 12 days, particle concentration was between 151 and 226 µg m^{-3} PM_{10} ('unhealthy') in Singapore during the smoke-haze episode.

Figure 4-4 and Figure 4-5 show that day-to-day particle concentrations vary substantially in response to spatial and temporal changes of meteorological factors, such as wind conditions and intermediate rainfall, and of fire activity. However, throughout the fire episode, particularly between July and September, the southern Peninsular Malaysia locations Petaling Jaya, Melaka and Kuantan exhibited a largely coherent particle concentration development with correlation coefficients r above 0.7. This suggests that these locations were influenced by a similar wind and transmissions pattern. Such a correlation could not be found for Singapore, indicating that it was influenced by a special wind and transmission pattern.

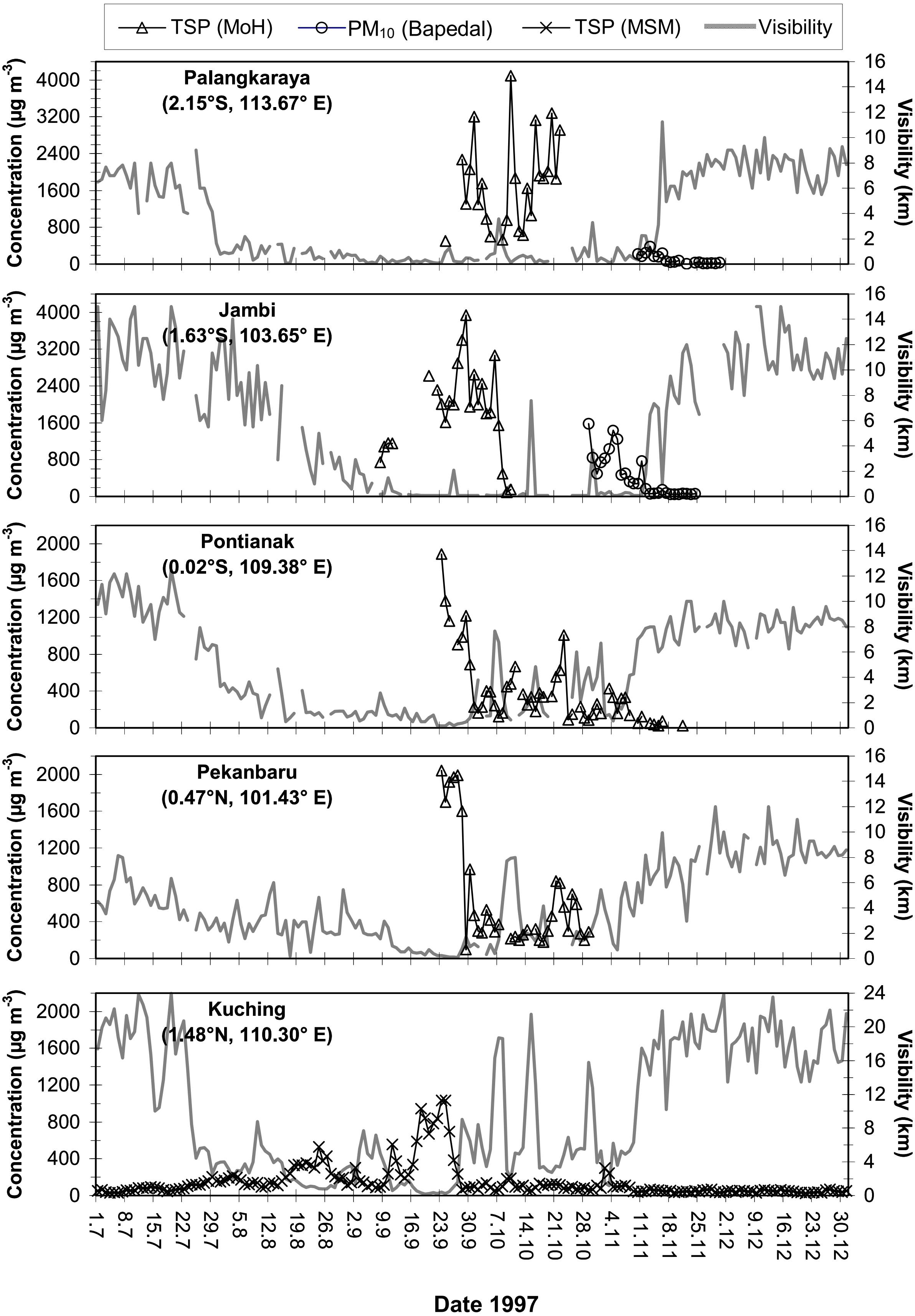

Figure 4-4: Development of ambient particle concentration (TSP and PM_{10}) and daily mean horizontal visibility at selected locations on Kalimantan and Sumatra as well as at Kuching, Borneo-Malaysia, during the second half of 1997. Data source: MoH, Bapedal, BMG, MMS.

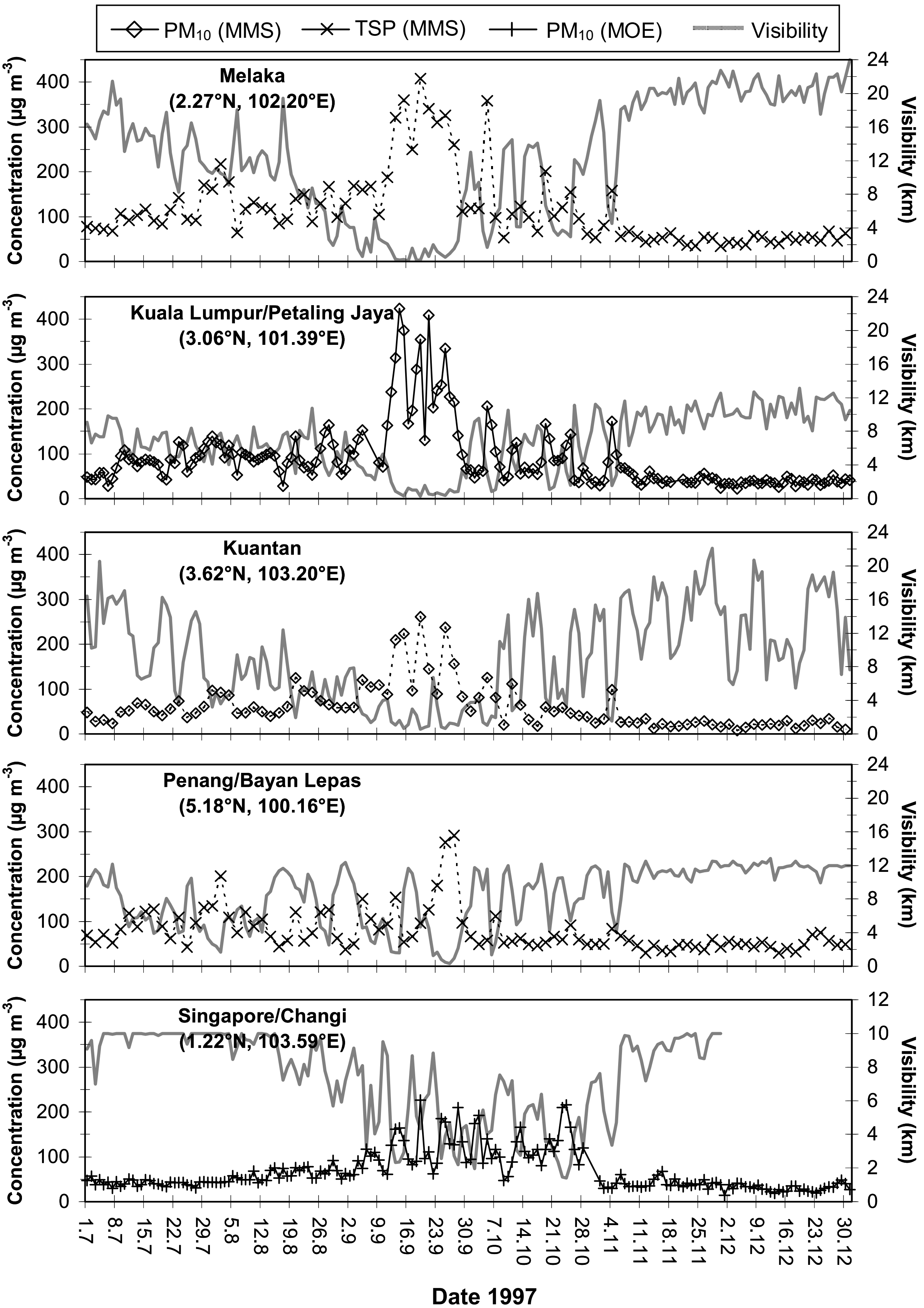

Figure 4-5: Development of ambient particle concentration (TSP and PM_{10}) and daily mean horizontal visibility at selected locations in Peninsular Malaysia as well as at Singapore during the second half of 1997. Dotted line if records every second day, only. Data source: MMS, MSS, MOE.

In September and October, monthly mean surface wind speed was below 1.6 m s^{-1} at all sites displayed in Figure 4-4 and Figure 4-5, except at Singapore Changi Station in September (3.2 m s^{-1}). These predominantly light surface wind conditions, characteristic for the transitional monsoonal period (Ramage 1971), provided unfavorable conditions for the dispersion of advected pyrogenic pollutants and of local vehicular or industrial emissions. The smoke-haze layer may also have contributed to the accumulation of pollutants near the surface by lowering radiative daytime warming of the surface and a decreasing convective mixing.

Though fire activity (by fire counts (Makarim et al. 1998)) and thus emission production was approximately similar in September and October, particle concentration at all locations in Malaysia was lower in October. This indicates a weakened cross-equatorial transport of pyrogenic emissions to Malaysia along with the retreating influence of the southerly monsoonal flow. According to von Hoyningen-Huene et al. (1999), the general weather situation in August and September was influenced by more frequent south-southeasterly winds compared to October, when a southeasterly flow was predominant. Back trajectory calculations made by the MMS indicate that in October southeasterly winds mainly transported pyrogenic emissions from fires in southern Kalimantan to Peninsular Malaysia, while south-southeasterly wind directions in August and September also transported stronger haze from fires at Sumatra to the Malaysian Peninsular (von Hoyningen-Huene et al. 1999). Considering the long distance from fires in Kalimantan to Peninsular Malaysia, increased dispersion and physicochemical removal processes of smoke plume constituents during transport may have contributed to lower ambient particle concentrations in October.

It appears that tropical cyclones in the South-China Sea generally enhancing the southerly monsoonal flow (Ramage 1971) contributed to an intermediate strengthening of the cross-equatorial transport of pyrogenic emissions during the smoke-haze episode (Phonboon 1998; Awang 1998). For instance, the simultaneous peak in particle concentration recorded at all locations in Malaysia and southern Thailand in late September as well as the final peak on 4 November (Figure 4-5) coincided with a developing tropical cyclone close to Vietnam. Such a connection between tropical cyclones and increased particle concentration was also observed during the 1994 smoke-haze event (SMS 1995).

4.5.3 Physicochemical Characteristics of the Smoke-Haze Particles

The particle size distribution of the 1997 smoke-haze, an important parameter with respect to health impacts, atmospheric residence time, and visibility impairment was poorly investigated. Simultaneous PM_{10} and TSP measurements at the MMS site in Petaling Jaya/Kuala Lumpur show a clear trend to higher PM_{10}/TSP ratios when PM_{10} concentration increased during the smoke-haze episode 1997. Table 1 shows that from July to mid-November ('haze episode'), the PM_{10} fraction contributed on average 66% to the TSP mass. At concentrations exceeding 150 µg m^{-3} PM_{10}, ('PM_{10} > 150'), the PM_{10}/TSP ratio ranged between 70 and 93% (mean 78%). During 'post-haze' conditions (mid-November to December), it was only 46%. The fraction TSP minus PM_{10} remained almost constant during and after the smoke-haze episode (48 versus 45 µg m^{-3}); apparently, the increase of TSP concentration was almost entirely attributed to the PM_{10} fraction.

Tang and Orlic (unpublished) monitored $PM_{2.5}$ and PM_{10} from January 1996 to December 1997 in Singapore. Before the smoke-haze episode, the $PM_{2.5}/PM_{10}$ ratio averaged 54% (mean $PM_{2.5}$ = 27 µg m^{-3}, PM_{10} = 50 µg m^{-3}), whereas the ratio increased to 81% during the smoke-haze episode (mean $PM_{2.5}$ = 89 µg m^{-3}, mean PM_{10} = 110 µg m^{-3}). In agreement, sky radiance measurements in Singapore and Kuala Lumpur showed that the volume size distribution of the smoke-haze aerosols tended to have a submicron peak around 0.25 µm (von Hoyningen-Huene et al. 1999; Nakajima et al. 1999). These size distribution measurements clearly indicate that higher TSP levels during the 1997 smoke-haze event were mainly attributed to the finer particle fraction ($PM_{2.5}$ and PM_{10}, respectively), resulting in higher PM_{10}/TSP and $PM_{2.5}/PM_{10}$ ratios than of the normal.

Inorganic and organic components of airborne particulate matter were analyzed in Singapore and Kuala Lumpur (Orlic et al. 1999; Fang et al. 1999; Narukawa et al. 1999). During the smoke-haze episode, an increase of typical tracer for biomass burning such as potassium (K) and vascular plant wax was observable, while typical vehicular or terrestrial fingerprint remained almost constant or decreased; apparently, related particle sources did not increase during the haze episode. Consequently, it was suggested that biomass burning made up a substantial contribution to the local aerosol loading.

Particle Concentration in µg m^{-3} Mean *(Range)*	Haze (1.7.-15.11.)		Post-haze (16.11.–31.12.)
	Total	PM_{10}>150	Total
PM_{10}	107 *(28-424)*	247 *(153-424)*	38 *(22-56)*
TSP	155 *(52-525)*	314 *(204-525)*	83 *(51-117)*
PM_{10}/TSP(%)	66 *(26-93)*	78 *(70-93)*	46 *(33-70)*

Table 4-1: PM_{10} and TSP during and after the smoke haze episode at Petaling Jaya 1997 (see text).

4.6 Impacts of the Smoke-Haze Event

The 1997 smoke-haze episode constituted an acute health risk to the public (WHO 1998) exposing almost 100 million people in five countries in Southeast Asia to increased air pollution (Phonboon 1998). An estimated 20 million suffered from respiratory problems in Indonesia alone (WHO 1998). The pollutant of major concern in respect to adverse health outcomes was particulate matter (WHO 1998), especially the fine particle fraction.

Numerous recent epidemiological studies (e.g. Ostro 1993; Schwartz 1994; Dockery and Pope 1994) have shown consistent, statistically-significant associations between increased daily aerosol loadings at levels typical of modern cities and morbidity and mortality – with no apparent threshold. They came to the conclusion that a 10 µg m^{-3} increase in PM_{10} is associated with a 1% increment in daily mortality. Schwartz et al. (1996) suggested that increased daily mortality is specifically related to $PM_{2.5}$, and not to the coarse fraction of PM_{10} ($PM_{10-2.5}$). Fine particles may penetrate into the lower respiratory tract ('respirable fraction'), where they are retained for a long period whereas the larger particles are predominantly deposited in the upper respiratory system (DIN 1996). Acute morbidity outcomes resulting from the exposure to particulate air pollution include respiratory symptoms, cardiovascular diseases and decreased lung function. For instance, studies have observed increases in respiratory hospital admissions and emergency department visits by ~1% per 10 µg m^{-3} PM_{10} increment (Dockery and Pope 1994). In addition to the acute effects of particulate exposure, chronic respiratory diseases such as chronic bronchitis and permanently decreased lung function are likely to follow (Schwartz 1993). Generally, individuals with pre-existing respiratory or cardiac diseases, but also elderly people and children are most susceptible to adverse health outcomes (Schwartz 1994). Responding to these epidemiological findings, the US Environmental Protection Agency revised the national air quality standards for particulate matter and included thresholds for $PM_{2.5}$ (e.g. 65 µg m^{-3} $PM_{2.5}$ as 24-hour average) (USEPA 1999).

While biomass burning particles were not specifically tested in the above (or other) epidemiological studies they could certainly have similar health impacts. Not surprisingly, an increase of adverse health outcomes was observed in all countries affected by the 1997 smoke-haze event (Brauer 1997; Kandun 1998; Emmanuel and Lim 1998; Awang et al. 1998; WHO 1998). The most frequent symptoms were asthma, upper respiratory tract illness as well as eye and skin irritations. In Kuching, outpatient visits increased two- to threefold during the main haze episode, and daily respiratory disease outpatient visits to Kuala Lumpur General Hospital rose from 250 to 800 (WHO

1998). In Singapore, hospital attendances for haze-related conditions rose by 30%; an increase in PM_{10} levels from 50 µg m^{-3} to 150 µg m^{-3} was associated with increases of 12% of upper respiratory tract illness, 19% of asthma, and 26% of rhinitis (Emmanuel and Lim 1998).

To alleviate the health impact, the governments recommended the public to remain indoors as much as possible, use air conditioning, wear respiratory masks and avoid physical exertion (WHO 1997). In Sarawak (Borneo), the Malaysian province most severely affected by pyrogenic emissions, the state of emergency was proclaimed on 19 September 1997 for 10 days, during which schools, public offices and factories were closed (DOE 1998). However, it is uncertain to what extent these measures can provide protection (WHO 1998; Brauer 1998). Moreover, large parts of the population can neither afford to refrain from outdoor work nor to purchase protective tools. Finally, some regional governments and populations may consider these health impacts to be minor in the context of widespread sub-optimal nutrition, starvation, malaria, cholera, dengue fever, typhoid fever, and other diseases.

Besides health impacts, impaired visibility seriously affected the economies of Indonesia, Singapore and Malaysia. Land, air and marine traffic was restricted, tourism revenues, industrial activity and fishing declined (EEPSEA/WWF 1998; Hassan et al. 1998). An airline crash in September in northern Sumatra caused 234 deaths and ship collisions in the Strait of Malacca killed dozens; both were partly attributed to impaired visibility (Simons 1998). A reduction of the downward solar flux due to smoke-haze layer (Herman et al. 1999; Ilyas et al. 1999; Nichol 1997) may also affect crop growth. For instance, Davies and Unam (1999) observed a 45-92% reduction of photosynthetically active radiation on hazy days in Kuching 1997.

EEPSEA/WWF (1998) roughly estimated the economic value of the damages caused by the 1997 fires and haze. They attributed 1 billion US$ to haze-related damages for Indonesia alone and for Malaysia and Singapore 0.4 billion US$. Including the fire related damages, the total damages amount 4.5 billion US$. However, due to insufficient data for Indonesia and parts of Malaysia, air pollution levels used for the assessment of the short-term health effects were derived from TOMS aerosol index maps, which do not necessarily reflect the real exposure during the smoke-haze.

4.7 Conclusions and Recommendations

The transboundary character of the 1997 smoke-haze event reveals that land and forest fires in Indonesia have an important international dimension in relation to severe air pollution. In Indonesia and parts of Malaysia, particulate air pollution reached levels considered as an imminent and substantial endangerment to public health (PSI $\geq$ 500). However, due the scarcity of air pollution data and health statistics, notably for Indonesia, an assessment of the exposure and adverse health outcomes resulting from the 1997 smoke-haze episode is limited. Nevertheless, there is every indication that the increased particle exposure during the smoke-haze also entailed premature deaths, in addition to the observed morbidity outcomes. Whereas the risk of long-term effects due to a single smoke-haze air pollution episode is even more difficult to detect than acute health outcomes, the repeated exposure of the South-East Asian population to smoke-haze merit attention (WHO 1998). Furthermore, these episodes add to the already existing air pollution emanating from other sources in this region, which, in turn, is expected to aggravate along with the continuing industrial development (Arndt et al. 1997; van Ardenne et al. 1999). For instance, already now, annual mean TSP and $PM_{2.5}$ in the city centre of Jakarta exceeds 400 µg m^{-3} and 50 µg m^{-3}, respectively (WHO/UNEP 1992; Gras and Cohen 1997). However, in regions in Brazil and Africa heavily influenced by biomass burning, $PM_{2.5}$ concentration may even reach ~5000 µg m^{-3} (R. Yokelson pers. comm.). Further epidemiological studies are required to assess the extent of the smoke-haze related health impacts. Recent update information are provided by the WHO "Guidelines for Vegetation Fire Events" including the background papers which are in the publication process at the time of writing this manuscript (Schwela et al. 1999; Goh et al. 1999)

The limited data available on the status of air quality in Indonesia and other countries affected by the smoke-haze demonstrate the need for a general upgrade of the national air quality monitoring facilities. This also applies for health statistics and the meteorological network. Enhanced co-ordination and networking among the smoke-haze affected countries, including a standardisation of measurement and reporting procedures, could improve the management of smoke-haze events and support decision making. Consistent region-covering air quality information and health statistics will not only provide the basis for an assessment of the health effect. The dissemination of real-time air quality information to the public may also contribute to increased transparency and environmental awareness in respect to fire related air pollution and air pollution in general.

Of particular concern in respect to adverse health impacts is the predominance of fine, respirable particles ($PM_{2.5}$) in the smoke-haze. Due to the resulting above-normal $PM_{2.5}/PM_{10}$ and PM_{10}/TSP ratio, ambient air quality reporting and standards based only on PM_{10} - and especially TSP - may be inadequate for smoke-haze episodes and may give a false sense of security. It would therefore be necessary to elaborate adequate PM_{10} and/or TSP standards for smoke-haze conditions; the best would be to measure and report $PM_{2.5}$ directly.

Even though most of the impacts of the 1997 fire and smoke-haze episode remain unknown, the observed ones call for an immediate revision of the current land conversion and fire use policies to prevent the reoccurrence of similar episodes. Ground-based and airborne investigations of the smoke-haze 1997 indicated that fires on peat swamp vegetation made a substantial contribution to the smoke-haze development, which, however, are estimated to have contributed only 20% to the total area burnt. Given this apparent particular relevance of peat swamp fires to the development of transboundary smoke-haze, emission reduction and control strategies will have to focus on the prevention of fires in this type of vegetation as a matter of priority. Controlling future smoke-haze events and air pollution will not only be crucial for public health, but also represents a beneficial factor for economic prosperity in future.

Acknowledgements

Sincere thanks are expressed for those agencies and persons, which supported the author's work in providing data and valuable inputs, in particular the Meteorological and Geophysical Agency (BMG), the Indonesian Ministry of Health, the WHO representative in Indonesia Dr. K. Bentley, the Malaysian Meteorological Services (MMS), here particularly Mr. Lim Sze Fook, and the Ministry of Environment and Meteorological Services in Singapore. This study was partly sponsored by the GTZ (German Technical Cooperation) projects "Integrated Forest Fire Management" (IFFM)" and "Strengthening the Management Capacities of the Indonesian Ministry of Forestry" (SMCP) and supported by the Max Planck Institute for Chemistry, Germany. Various activities of the BIOTROP-GCTE Global Change Impacts Centre for Southeast Asia (IC-SEA) related to transboundary pollution provided an important framework for this study and are hereby gratefully acknowledged. Finally, we thank Dr. Robert Yokelson (University of Montana, Missoula, U.S.A.), Dr. G.Helas, and Dr. M.O.Andreae (both Max Planck Institute for Chemistry, Biogeochemistry Department, Mainz, Germany) for their critical and helpful remarks.

5 Release and Dispersion of Vegetation and Peat Fire Emissions in the Atmosphere over Indonesia 1997/1998

This chapter has been published as: Langmann B and Heil A, Atmospheric Chemistry and Physics (2004), 4: 2,145-2,160.

Abstract

Smoke-haze episodes caused by vegetation and peat fires affect parts of Indonesia every year with significant impacts on human health and climate. Particularly fires in degenerated peat areas release huge amounts of trace gases, e.g. CO_2, CO and CH_4, and particles into the atmosphere, exceeding by far the emissions per unit area from fires in surface vegetation. However, only limited information is available about the current distribution of pristine and degenerated peat areas in Indonesia, their depth, drainage condition and modification by fire. Particularly during the strong El Niño event in 1997/1998 a huge uncertainty exists about the contribution of Indonesian peat fire emissions to the measured increase of atmospheric CO_2, as the published estimates of the peat area burned differ considerably. In this paper we study the contribution of peat fire emissions in Indonesia during the El Niño event 1997/1998. A regional three-dimensional atmosphere-chemistry model is applied over Indonesia using two emission estimates. These vegetation and peat fire emission inventories for Indonesia are set up in 0.5° resolution in weekly intervals and differ only in the size of the fire affected peat areas. We evaluate simulated rainfall and particle concentrations by comparison with observations to draw conclusions on the total carbon emissions released from the vegetation and peat fires in Indonesia in 1997/1998.

5.1 Introduction

Every year during the dry season, land clearing fires are set in Indonesia. Usually the burning activities cease in October/November with the beginning of the northern monsoon rains. The strong El Niño of 1997/1998, however, lead to severe drought conditions. Land-clearing fires became uncontrolled particularly on Kalimantan (Borneo) and Sumatra. Reduced convective activity during August until October 1997 favored wide-spread dispersion of the vegetation fire emissions causing several episodes of intense smoke-haze that affected also Malaysia and Singapore. Close to the vegetation fires at Palangkaraya on Kalimantan and Jambi on Sumatra up to 4,000 $\mu g/m^3$ total particulate matter was measured, exceeding the Indonesian national ambient air quality standard by a factor of 15 (Heil and Goldammer, 2001). Levine (1999) estimated the emissions released from the fires on Kalimantan and Sumatra islands between August and December 1997. Although this study assumed only 20% of the area burned to consist of peat areas, these regions contributed about 90% of the gaseous and particulate fire emissions. The reason is the huge storage of organic matter in the peat deposits that has accumulated over the last 5,000 to 10,000 years (Rieley et al. 1995). The majority of the estimated 170,000 to 270,000 km^2 of peat swamps in Indonesia is deeper than 1 m, frequently more than 15 m in depth (Rieley et al. 1997). Peat areas have become increasingly susceptible to fire in the past decades due to an intensification of their drainage for land conversion purposes. The amounts of gaseous, particularly CO_2, CO and CH_4 and particulate matter emissions released from peat fires in Indonesia are still rather uncertain, as well as the particle chemical composition (Langmann and Graf, 2003). Fires in peat areas may affect both the above-ground vegetation as well as the below-ground organic soil which can burn repeatedly at different depths. Peat fires are typically low temperature, smoldering fires which are difficult to detect from space. The determination of emissions released from peat fires is further complicated by the necessity to characterize additionally the soil and the depth of the soil burned. Generally, large uncertainties exist in the determination of the area burned during fire episodes. The uncertainties are reflected in the estimated areas of fire damaged peat lands during the strong El Niño event in 1997 in Indonesia which range from 14,500 to 68,047 km^2 (Page et al. 2002) resulting in a calculated range of 480 to 2,570 Mt of carbon released into the atmosphere. These emissions are equivalent to 13 - 40% of the mean annual global carbon emission from fossil fuels and represent a significant contribution and uncertainty to the largest annual increase of atmospheric CO_2 detected since record began in 1957 (IPCC, 2001). Recently, global climatological biomass burning emission inventories have been improved by means of satellite data to include an interannual variability (e.g. Duncan et al. 2003b). However, peat fires as a major source for gases and particles are not included in these inventories explicitly. In this paper we present a spatial-temporal resolved vegetation and peat fire emission estimate for Indonesia during 1997/1998. We applied the three-dimensional regional atmospheric-chemistry model REMO (REgional MOdel) introduced in section 5.2 over the region of Indonesia with two different peat fire emissions estimates described in section 5.3. The emission estimates and model results are evaluated by comparing the modeled atmospheric aerosol load with measurements (section 5.4). Section 5.5 draws conclusions on the total carbon emissions from the Indonesian fires in 1997/1998 and gives an outlook.

5.2 Model Description

The regional three-dimensional on-line atmosphere-chemistry model REMO (Langmann, 2000) determines at every model time step the physical and chemical state of the model atmosphere. The dynamical part of the model is based on the regional weather forecast model system EM/DM of the German Weather Service (Majewski, 1991). Beside the German Weather Service physical parameterizations, those of the global ECHAM-4 model (Roeckner et al. 1996) have been implemented in REMO (Jacob, 2001) and are used for the current study. The prognostic equations for surface pressure, temperature, specific humidity, cloud water, horizontal wind components and aerosol mass mixing ratios are written on an Arakawa-C-grid (Mesinger and Arakawa, 1976).

In the current model set-up, one prognostic species is included, representing the atmospheric aerosol without further differentiation according to the chemical composition and size distribution. Particle emissions are assumed to be released into the first model layer, because smoldering fires which are typical for fires in peat areas generally do not cause strong convective lifting. Although secondary aerosol formation may play an important role, it is not included in the present study. The particle transport is determined by horizontal and vertical advection according to the algorithm of Smolarkiewitz (1983), convective up- and downdraft by a modified scheme of Tiedtke (1989) and vertical diffusion after Mellor and Yamada (1974). Due to the elevated sulfur content of Indonesian vegetation and peat fire aerosols (Langmann and Graf, 2003) particle deposition is calculated as for sulfate. Dry deposition velocities are determined as described by Walcek et al. (1986) dependent on the friction velocities and stability of the lowest model layer. Wet deposition is computed according to Walcek and Taylor (1986) by integrating the product of the grid-averaged precipitation rate and the mean cloud water concentration, assuming 100% solubility of the particles as not only sulfate but also water soluble organic compounds contribute to the hygroscopicity of the particles (Balasubramanian et al. 2003, Narukawa et al. 1999, Okada et al. 2001).

For this study the REMO model was applied with 20 vertical layers of increasing thickness between the Earth's surface and the 10 hPa pressure level using terrain following hybrid pressure-sigma coordinates. The model domain covers Indonesia and Northern Australia (Figure 5-1) with a horizontal resolution of 0.5° and 101 grid points in longitude and 55 grid points in latitude with the lower left corner at 91° E and 19° S. A basic model time step of 5 min was chosen. REMO can be applied principally in two modes, the so-called "climate mode" or the "forecast mode". In the climate mode the model is initialized once and then run continuously until the end of the simulation period with an update of the meteorological analysis data every 6 h at the lateral model boundaries. Between these six hour intervals the analyzes are interpolated linearly in time. Meteorological analysis data are taken from European Center for Medium Range Weather Forecast with time varying fields of surface pressure, temperature, horizontal wind velocities and moisture. In the forecast mode the model is started at 0 UTC every day to compute a 30 h forecast and the analysis data are also updated every 6 h. The first six hours of the consecutive meteorological forecasts are neglected to account for a spin-up time. The total simulation period is composed of 24 h simulation segments with a discontinuity in the physical state of the atmosphere at 6 UTC. But, by starting the model again every day the internal model variability is suppressed and the model is forced to stay close to the observed weather situation. Particulate matter processes, however, are calculated continuously like in the climate mode. This is done by simulating meteorology only in the first six hours of each 30 h forecast. Then, combined particle matter and meteorology calculations continue for 24 h starting with the particulate matter information from the last time step of the previous forecast.

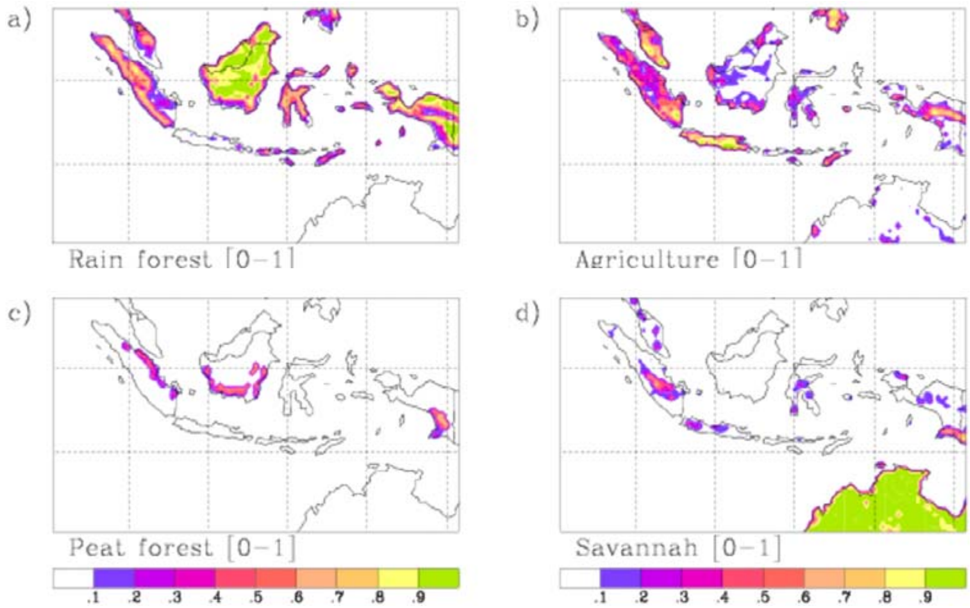

Figure 5-1: Distribution of the major vegetation classes as used in the REMO model domain in fraction (0–1) per model grid cell (0.5°×0.5°) for (a) rain forest, (b) agriculture, (c) peat forest and (d) savannah.

Previous studies and evaluation with the REMO atmosphere-chemistry model give confidence in the ability of the model to reproduce the physico-chemical state of the atmosphere. The model has been applied with various trace species modules to study for example summer smog episodes over Europe (e.g. Langmann et al. 2003), to determine the distribution and radiative forcing of sulfate aerosols over Europe (Langmann et al. 1998) and the Arctic region and to investigate CO_2 and ^{222}Rn fluxes and distributions over Euro-Siberia (Chevillard et al. 2002a, b). Recently, stable water isotope physics has been implemented in REMO.

5.3 Methodology

In this section we introduce our approach to derive the emissions of aerosols and trace gases from vegetation and peat fires in Indonesia during the period July 1997 to June 1998. We proceed in four steps: 1. set-up of vegetation maps, 2. collection of remotely sensed fire count data, 3. determination of area burned with spatial and temporal variability and 4. estimate of fire emissions.

5.3.1 Vegetation cover

In the first step we prescribed the distribution of four major vegetation classes: rain forest, agriculture, peat forest and savannah as fraction per model grid cell (Figure 5-1). This is based on a vegetation data set of Loveland et al. (2000) in 1×1 km^2 resolution derived with the AVHRR sensor during April 1992 and March 1993. We did not consider modifications of the vegetation cover between 1993 and 1997 due to the lack of data. Rain forests are found mainly on Borneo and Irian Jaya. Southern Sumatra, Java and the Peninsula of Malaysia represent the highest agricultural use while savannah is the main vegetation type only in Northern Australia. Peat forests are not defined in Loveland et al. (2000) and we supplemented this vegetation class using information from maps published by Nichol (1997) and Dierke Weltatlas (1980). Figure 1c shows peat forests mainly located near the coast of east Sumatra, Kalimantan and south-eastern Irian Jaya. The fraction of peat forest per grid cell in these areas was calculated assuming that it makes up 2/3 of the total forest cover.

5.3.2 Fire Counts from Remotely Sensed Data

We determined the temporal and spatial distribution of vegetation and peat fires in Indonesia by using fire counts from the ATSR sensor (Arino and Rosaz, 1999) on board the ESR-2 satellite in 1×1 km^2 resolution. A threshold of 312K (algorithm 1) or 308K (algorithm 2) is applied to the radiance of the 3.7 µm channel in order to detect fires. We used the ATSR pixels above the 312K threshold and incorporated them in weekly intervals into the REMO model grid. Figure 5-2 shows the number of ATSR fire counts per model grid cell from 1 July to 31 December 1997 and from January 1 to 30 June 1998, respectively. The areas with the highest fire count density were located in southern Kalimantan and south-eastern Sumatra in 1997 with more than 1,000 fire counts per grid cell and in 1998 in East–Kalimantan with more than 500 fire counts per grid cell. According to our estimates, peat forests make up 20 to 60% of the total vegetation cover in these regions (Figure 5-1c).

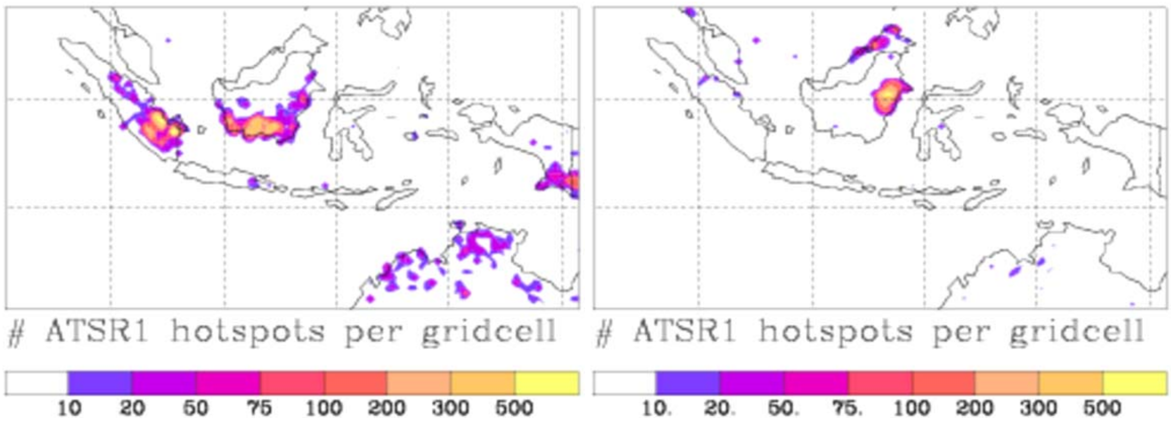

Figure 5-2: Distribution Number of ATSR fire counts per model grid cell over Indonesia (a) during the period from 1 July to 31 December 1997 and (b) from 1 January to 30 June 1998.

5.3.3 Area Burned

The ATSR fire count data over Indonesia were converted into area burned information, subdivided into the four vegetation classes utilised in this study, using the following empirical relationship:

$AB_i = MIN(FC/\alpha, 1/\beta) * A * V_i$ (1)

with

AB_i : area burned of vegetation class i per model grid cell and week (km^2),
FC : fire counts per model grid cell and week,
A : area per model grid cell (km^2),
V_i : fraction of vegetation class i per model grid cell,
α,β : empirical parameters.

The empirical parameter α=554 scales the area burned per week to less than the total area per grid cell. It is further assumed that not more than $1/\beta$ with =14 of a grid cell may burn during one week. A weekly interval is chosen to assure at least two overpasses of the ESR-2 satellite thereby smoothing the ATSR data. Both empirical parameters represent fitting constants that approximately adjust the ATSR fire counts for the model area north of 10°S (excluding Northern Australia) to the total area burned of 96,550 km^2 in Indonesia during 1997/1998 given by ADB/Bappenas (1999). This study compiles various assessments by Indonesian agencies and international organizations based either on satellite data, aerial surveillance or ground assessments for different regions and vegetation classes (Table 5-1, left column).

Area burned (km^2)	ADB (1999)	Standard case	High emission case
Total Indonesia	96,550	97,340	151,290
Kalimantan	65,000	56,940	96,060
Sumatra	17,550	29,080	40,300
Irian Jaya	9,000	8,260	11,870
Sulawesi+ Java	5,000	3,060	3,060
Rain forest	34,710[1)]	39,640	39,640
Agriculture	39,630[2)]	35,930	35,930
Peat forest	14,580	14,190	68,140
Savannah	7,630[3)]	7,590	7,590

[1)] sum of lowland forest and timber plantation
[2)] sum of agriculture and estate crops
[3)] dry scrub and grass

Table 5-1: Burned area estimates (km^2) for the Indonesian fire period 1997/1998. Left column: ADB/Bappenas (1999), middle column: standard estimate of this study, right column: high emission estimate of this study.

A comparison of the area burned estimate given by ADB/Bappenas (1999) and our "standard" estimate (Table 5-1, middle column) shows very similar values for the area burned per vegetation class but major differences for Kalimantan and Sumatra. With our approach we obtain a smaller area burned on Kalimantan and a greater one on Sumatra, revealing limitations to accurately estimate the area burned from satellite derived fire counts. First, the presence of clouds and haze (Siegert and Hoffmann, 2000) prevents a continuous and consistent detection of hot spots. Second, for the ATSR fire count product only night time observations are used which leads to an underestimation since fire activity generally peaks in the afternoon. Third, a fire pixel represents a defined area of 1 km^2. It indicates that a heat event is detected within this area, however, it tells nothing about the number, the size and the intensity of the fires and thus the area burned within this pixel (Malingreau, 1990). Fourth, the relatively low temperature and partly subsurface peat fires might be difficult to detect from space by commonly used temperature thresholds (Anderson, 2001). In addition to our standard estimate, a "high emission" estimate has been established where solely the area of the fire damaged peat forest during 1997/1998 has been increased by a factor of 4.8 compared to the standard estimate resulting in 68,140 km^2 (Table 5-1, right column). This number represents the upper estimate of fire damaged peat lands in Indonesia during 1997 given by Page et al. (2002). As a result the total area burned in Indonesia during 1997/1998 in the high emission case is 151,290 km^2. The area burned by sub-regions increases considerably on Kalimantan and Sumatra in the high emission case while it remains unchanged on Sulawesi and Java where peat forest is assumed to be negligible in our estimate (Figure 5-1c). The peat area burned per grid cell and week does not exceed 25% (~750 km^2) for the high emission estimate and 5% (~150 km^2) for the standard estimate during the whole simulation period from July 1997 to June 1998.

5.3.4 Fire Emissions

Particulate and gaseous emissions of the fires are determined based on the approach described by Levine (1999). Generally, the total mass of vegetation or peat consumed by burning (*M* in tons) is

$M = AB * B * E$ (2)

where *B* is the biomass load in tons/km^2 and *E* the burning efficiency. The total particulate matter emissions (*TPM_E* in tons) can then be determined by

$TPM\_E = M * EF(TPM)$ (3)

with *EF(TPM)* as emission factor for total particulate matter (TPM). Gaseous emissions of CO_2 (CO_2_E in tons of carbon) are calculated by considering the carbon content of the fuel (*C* as mass percentage of carbon) and the combustion efficiency *CE*:

$CO_2\_E = M * C * CE$ (4)

Emissions of other trace gases, notably CO or CH_4 are calculated by multiplying CO_2_E with a CO_2-normalised species emission ratio (ER). Table 5-2 summarizes the respective values of biomass load, burning efficiency, carbon content, combustion efficiency, emission factors and emission ratios for the different vegetation types used for our calculation. These values are fully taken from Levine (1999) and therefore we refer to that paper for more detailed information. At this point it has to be mentioned that we corrected for the further discussion in Equation 5 and Table 2 of the publication of Levine (1999) the unit for particulate matter emissions from “tons of carbon” to “tons”. The biomass load for peat deposits (Table 5-2) given by Levine (1999) is based on Supardi et al. (1993). It exceeds the one of rain forests by a factor of 10 because the sub-ground organic body (peat) is the major burning material and not the overlying vegetation. Together with the other factors used to calculate the emissions, the higher biomass load of peat deposits results in 43 and 85 times higher TPM emissions per unit area burned than rain forests and agriculture, respectively. This highlights the particular importance of peat fires as emission source.

	B [t/km^2]	E	C	CE	EF(TPM)	ER(CO)	ER(CH4)
Rain forest	10,000	0.2	0.45	0.90	0.020	0.0850	0.0032
Agriculture[1)]	5,000	0.2	0.45	0.90	0.020	0.0850	0.0032
Peat areas	97,500[2)]	0.5	0.5	0.77	0.035	0.1815	0.0104

[1)] agriculture and plantation areas
[2)] 1.5 m deep peat deposits

Table 5-2: Biomass load (B) in t/km^2 and dimensionless burning efficiency (E), carbon content (C), combustion efficiency (CE), emission factor (EF) and CO_2-normalised species emission ratios (ER) for rain forests, agricultural and peat areas in Indonesia based on Levine (1999). For savannah we use the same parameters as for agriculture.

Table 5-3 compares the estimate of Levine (1999) of the area burned on Sumatra and Kalimantan during August to December 1997 and the resulting particulate emissions with the results of our standard and high emission case for the same area and period. Compared to Levine (1999) we overestimate the area burned by 29% and the TPM emissions by 18% in the standard case. However, the relative contributions of the different vegetation classes is reproduced within 5% with our standard approach. In the high emission case, the area exceeds the one given by Levine (1999) by a factor of 2.2 and TPM emissions are 5.3 times higher. Levine (1999) gives an overall uncertainty of 50% for his emission calculations. The results of the standard estimate are within these uncertainty limits while the TPM emissions of our high emission estimate exceed the uncertainty range by far. Although fires in peat areas contribute only 18% to the total area burned in our standard emission case, they produce more than 90% of the TPM emissions. This applies also to the emissions of trace gases such as CO_2, CO and CH_4. In the high emission case, fires in peat areas make up even 52% of the total area burned and 98% of the TPM emissions. These numbers illustrate again the enormous emissions released from peat fires.

Area burned (km^2)	Total	Peat forest	Rain forest	Agriculture
Levine (1999)	45,600	9,120	13,680	22,800
Standard case	58,677	10,650	18,658	29,369
High emission case	99,147	51,120	18,658	29,369
TPM (Mt)	**Total**	**Peat forest**	**Rain forest**	**Agriculture**
Levine (1999)	16.568	15.561	0.547	0.460
Standard case	19.506	18.172	0.746	0.588
High emission case	88.559	87.225	0.746	0.588

Table 5-3: Area burned (km^2) and TPM emissions (Mt) from August to December 1997 in Sumatra and Kalimantan according to Levine (1999) and the standard and high emissions estimate of this study.

Figure 5-3 displays the temporal variability of TPM emissions from vegetation and peat fires over Indonesia during the whole period from July 1997 to June 1998 as determined for the standard and high emission case. High amounts of TPM were released into the atmosphere during two fire periods. TPM emissions during the second fire period in 1998 were by a factor of 4.7 lower than in 1997 because a considerably smaller area was burned in 1998 (26% of the total area burned in the standard case). Northern Australian emissions represent only 1.3% of the total emissions and were negligible compared to the Indonesian ones.

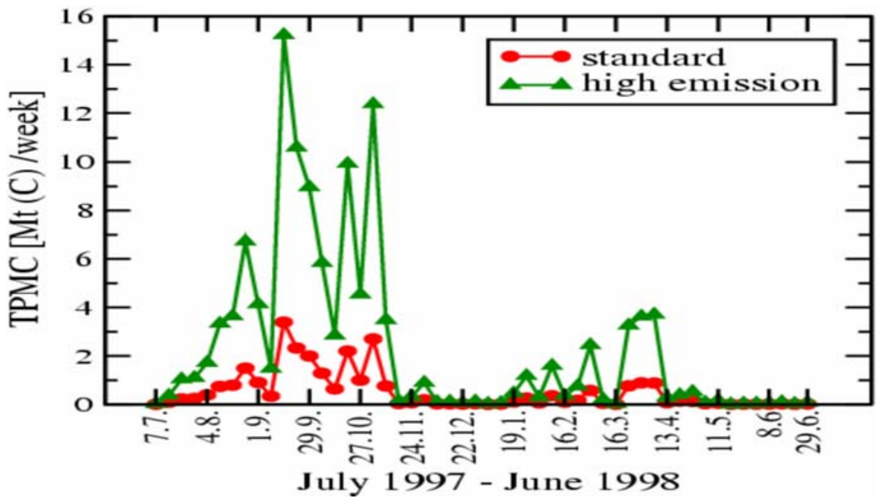

Figure 5-3: Temporal variability of total particulate matter (TPM) emissions from vegetation and peat fires in Indonesia and Northern Australia as determined for the standard and high emission case. The sum is 26.7 Mt/year for the standard estimate and 118.7 Mt/year for the high emission estimate, respectively.

Page et al. (2002) emphasized the relevance of peat areas for climate change as they act as a source of CO_2 when affected by fire. The authors estimated a release of 810 to 2,570 Mt of carbon to the atmosphere by burning forested peat areas in Indonesia in 1997. Page et al. (2002) classified their lower estimate of 480 Mt C as an underestimate. Duncan et al. (2003b) report emissions of about 700 Mt C for the 1997 Indonesian wildfires. In our standard estimate total carbon emitted from fires in Indonesia from July 1997 to June 1998 makes up 380 Mt C (6% of the mean annual global carbon emissions from fossil fuels), from which CO_2 represents about 83%, CO 14%, TPM-carbon 2% and CH_4 1%, respectively. In our high emission case 1,600 Mt C are released to the atmosphere. However, this estimate is still significantly lower than the upper estimate of Page et al. (2002) of 2,570 Mt C, even though the same extent of fire-damaged peat areas is considered. The differences can be explained as follows: Page et al. (2002) assume a peat bulk density of 0.1 g/m^3, an averaged peat depths burned of 0.51 m and a peat carbon content of 57% resulting in 29,070 $t(C)/km^2$ released by peat fires. Based on Levine (1999) only 24,375 $t(C)/km^2$ are released by peat fires, resulting from a lower peat bulk density of 0.065 g/m^3, a lower carbon content of 50%, but a higher effective peat depth burned of 0.75 m. Furthermore, Page et al. (2002) assume the peat areas to be covered by pristine peat swamp forests with a biomass carbon content of 25,000 $t(C)/km^2$ from which 50% is liberated by fire resulting in additional emissions of 400 Mt C in their upper estimate. However, mainly fragmented and logged over peat swamp forests are subject to fire. Therefore, we do not consider emissions from surface vegetation fires on peat areas in our emission estimates. In addition, it should be noted that the peat area burned estimate of Page et al. (2002) is based on a detailed investigation in a small, rather drained peat area in Central Kalimantan where 33% were affected by fire in 1997. This number was adopted to the peat areas all over Indonesia without any further modification, implying a general overestimation of the peat area burned.

5.4 Model Results and Discussion

The main goal of this study is to evaluate the two different emission estimates introduced in Section 5.3 by comparing the modeled spatial and temporal variability and intensity of smoke-haze from the 1997/1998 vegetation and peat fires in Indonesia with observations. The concentration and distribution of the particles depend on the emissions from the fires and also on meteorological factors including transport by advection, vertical redistribution by turbulent diffusion and convective clouds, chemical and microphysical modifications (not considered in the current study), and dry and wet deposition.

5.4.1 General Atmospheric Conditions in Indonesia

The tropical and wet conditions in Indonesia are characterized by uniformly high temperature, high humidity, relatively constant atmospheric pressure and weak wind velocities. The overall precipitation rate is highly variable in space and time in Indonesia (Aldrian, 2003) which represents the main centre of deep tropical convection on the Earth. Precipitation is therefore the quantity of greatest interest, particularly with respect to the removal of particles from the atmosphere by wet deposition, which is the dominant loss process.

Throughout the year Indonesia experiences a dry and a wet season induced by the two major flow patterns (Ramage, 1971). During the transitional months (September/October and April/May) the switching of the wind pattern results in relatively weak and variable winds. From about November to March low level trade winds blow in the northern hemisphere from the north-east towards the equator and continue into the southern hemisphere with a north-west component. This winter monsoon brings heavy rainfall to the Maritime Continent. The dry season from about June to September is characterized by the trade winds blowing from the south-east towards the equator in the southern hemisphere continuing in the northern hemisphere as south-west winds. During El Niño years, an additional suppression of precipitation occurs in Indonesia, which typically lasts for 13 months starting in March.

5.4.2 The 1997/1998 El Niño Period in Indonesia and Malaysia

5.4.2.1 Precipitation

In 1997/1998, during one of the most severe El Niño events of the 20th century (McPhaden, 1999), precipitation in Indonesia was significantly reduced. An averaged monthly rainfall deficit of 120–150 mm below normal was recorded in Indonesia (WMO, 1998), the annual rainfall deficit ranged from 1,000–1,500 mm (FAO/GIEWS, 1998). Compared to a long-term rainfall record of 48 years, the rainfall from June to November 1997 was below the 10th percentile in large parts of Indonesia (Kirono et al. 1999).

A compilation of rainfall measurement data over land is available from the Global Precipitation Climatology Centre (GPCC, http://www.dwd.de/en/FundE/Klima/KLIS/int/ GPCC) as area-averaged monthly mean data. GPCC data are interpolated from rain gauge measurements to a 1° × 1° geographical latitude-longitude grid over land. A combined dataset about rainfall over land and ocean is available from GPCP (Huffman et al. 1997). Over the ocean, GPCP data are based on infrared and microwave satellite observations, which are interpolated to a 2.5° grid. Due to the scarcity of rain gauge measurements for the Indonesian region, an uncertainty of more than 10% over land and 40% over the ocean is attributed to this data (http://www.mpimet.mpg. de/en/extra/wg/wg5/wg pr06.htm). Figure 5-4 illustrates the monthly total area averaged GPCC and GPCP rainfall and the corresponding REMO results for the climate and forecast mode from July 1997 to June 1998 for the whole area (ocean and land, Figure 5-4a) and over land only (Figure 5-4b). GPCC and GPCP data show dry conditions until November 1997 when the delayed northern monsoon rain started. The two maxima in rainfall during December 1997 and April 1998 are associated with the south- and northward movement of the Inter Tropical Convergence Zone. The REMO model reproduces the temporal development of measured rainfall data in detail, but yields principally higher precipitation rates. Overprediction by REMO is more pronounced in the climate mode than in the forecast mode as visible especially in Figure 5-4a. We obtain similar results when comparing the average of monthly total precipitation measured at seven Malaysian stations (Figure 5-4d) from July to December 1997 with the rainfall at the corresponding REMO grid points (Figure 5-4c).

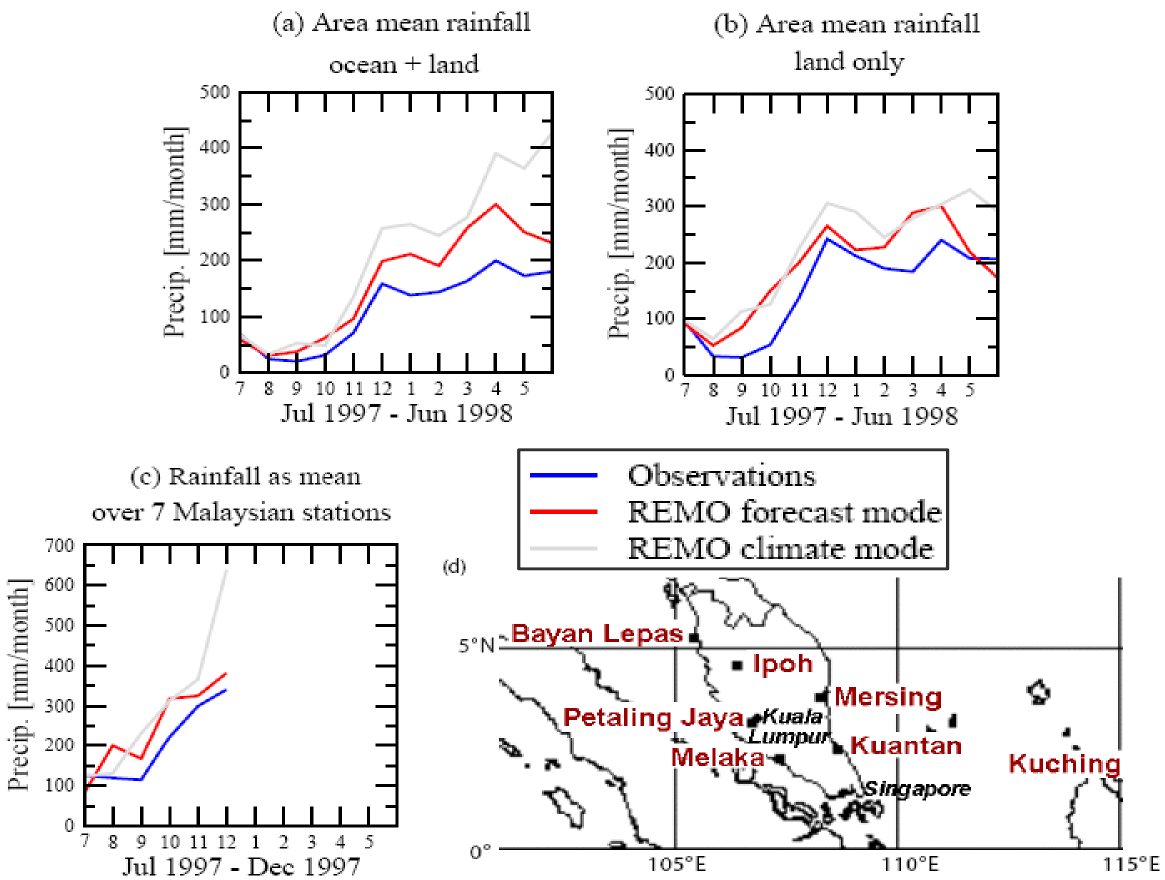

Figure 5-4: (a) and (b) Area mean of monthly total precipitation over Indonesia (96° - 136° E, 14°S – 3° N) from July 1997 to June 1998. Observations are taken from GPCC and GPCP. (c) Monthly total precipitation as mean over 7 Malaysian stations from July to December 1997. Observations are taken from the Malaysian Meteorological Service. REMO model results are shown for the climate and forecast mode simulation. (d) Location of the Malaysian stations.

Strongly differing results are obtained when comparing rainfall records from single Malaysian stations with REMO results (Figure 5-5). At Petaling Jaya/Kuala Lumpur (3.1°, 101.4°, 46m a.s.l.), observed monthly total precipitation exhibits a sharp increase from August reaching its maximum in November with 660 mm while rainfall modeled by REMO peaks in October with only around 300 mm (Figure 5-5a). Over a 6-month total, REMO underpredicts observed precipitation (observed 6-month total of 1,970 mm) by 820 mm in the forecast mode and 1030 mm in the climate mode. At Kuching (1.5°, 110.3°, 56m a.s.l.) REMO generally overpredicts the observed rainfall, most pronounced in the climate mode (Figure 5-5b). The 6-month total precipitation by REMO in the climate mode with 2,320 mm is 2.1 times higher than the observation (1,010 mm) while the REMO forecast mode is only 30% higher.

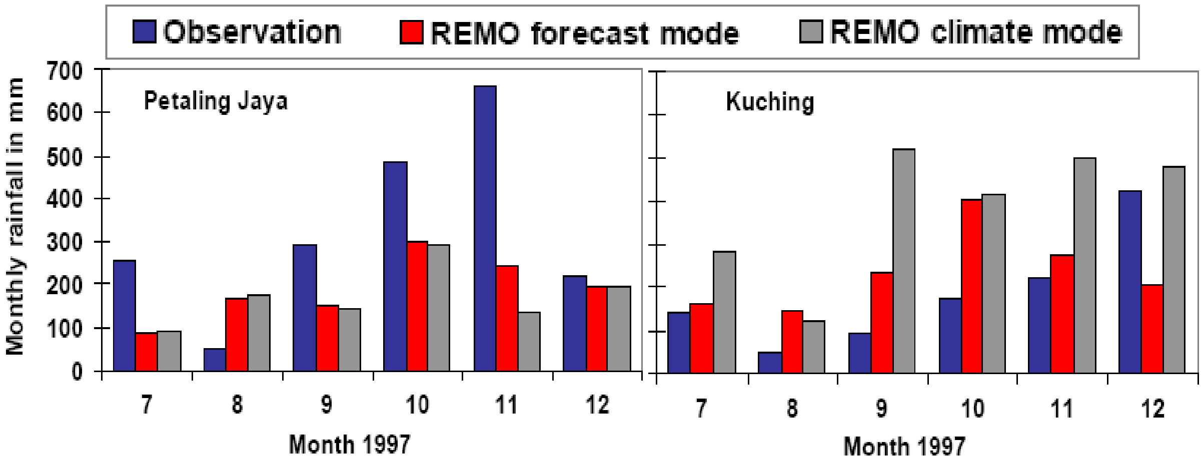

Figure 5-5: REMO monthly rainfall from forecast and climate mode simulations versus measurements at (a) Petaling Jaya (3.1° N, 101.4° E) and (b) Kuching (1.5° N, 110.3° E).

The observed and modeled rainfall in Indonesia and Malaysia (Figure 5-4 and Figure 5-5) exhibits strong variability in space and time. This highlights the difficulties of modeling convective clouds and precipitation with regional models such as REMO in this region of the world, where convective precipitation dominates over stratiform precipitation. It should be noted here, that model variables like wind speed and direction remain very similar in the forecast and climate mode simulations. As too much rainfall and associated wet deposition also influences the atmospheric particle burden, we focus in the following on the more realistic forecast mode simulation, unless noted otherwise. However, the spatial and temporal effectiveness of wet deposition might be affected by the physical discontinuity introduced once per day during the forecast mode simulation (Section 5.2). Additionally, the principal overprediction of precipitation in the whole area remains present in the forecast mode simulation, so that the modeled particle load of the atmosphere should be expected to present a lower boundary.

5.4.2.2 Wind Speed and Wind Direction

A comparison of observed and modeled monthly wind conditions at 925 hPa at Petaling Jaya and Kuching is shown in Figure 5-6 to illustrate the REMO model capabilities to determine particle transport by advection. The observations are based on 0 and 12 UTC sonde data obtained from the Malaysian Meteorological Services for the second half of 1997. Monthly wind speed is displayed as a box plot. The lower and upper edge of the box represents the 25th and 75th percentile value, respectively. The line across the box displays the median (50th percentile). Outliers are shown as squares, extreme values as stars. The wind roses in the upper band of Figure 5-6 display the monthly number frequency of wind direction in 10° sectors. At Petaling Jaya, observed median wind speed exhibits a minimum in October and November 1997 as typical for the inter-monsoon period. REMO model results show similar features, but principally higher wind speeds, particularly in December. The interquartile range (length of the box) modeled by REMO indicating the variability of the values is in good agreement with the observations, except in December when the model produces a higher variability than observed. Measured wind direction at Petaling Jaya shows a switching from southerly to northerly monsoon winds in December. In between, there is a typical transitional phase with variable wind directions in October and November. REMO simulations reproduce the switching of the wind direction but, in contrast to the observations, do not show a period with changing wind directions. Higher modeled wind speeds may contribute to this bias since wind direction tends to become less variable with increasing wind speeds (Mestayer et al. 2003). Observed monthly median wind speeds at Kuching (Figure 5-6b) are nearly constant from July to December 1997. On a 6-month summary, the observed and the REMO model mean wind speed are almost equal. A comparison of the observed interquartile range of monthly wind speed with REMO results also shows good agreement. In both the observations and the REMO simulations, southerly winds predominate in July and August, followed by a period of highly variable wind directions turning into more frequent northerly winds by December. In summary, REMO fairly well reproduces observed changes of wind conditions with time giving confidence in modeled particle advection.

5.4.2.3 Atmospheric Smoke-Haze Distribution

The spatial distribution of smoke-haze in Indonesia and Malaysia from July 1997 to June 1998 can be derived from the TOMS Aerosol Index (AI) data (Herman et al. 1997), shown in 1° resolution as monthly means in the left column of Figure 5-7. Positive TOMS AI values are derived from satellite measurements of UV absorbing aerosols in the entire vertical column of the atmosphere. Two periods of smoke-haze took place from August to November 1997 and from February to April 1998. During the first smoke-haze episode, TOMS AI exhibits maximum values over large parts of Sumatra and Kalimantan south of the equator, and southern Irian Jaya. The smoke-haze showed a strong west- and northward expansion from the main fire locations (Figure 5-2). In September and October 1997, the smoke-haze reached far into the Indian Ocean and partially covered Peninsular Malaysia. In these months, fire emissions were highest (Figure 5-3) while precipitation rates and associated wet deposition of smoke-haze particles was low (Figure 5-4). The second smoke-haze episode was restricted to Borneo only. TOMS AI maps in March and April 1998 show two separated smoke-haze plumes, one originating from fires in East Kalimantan and the other one mainly from fires in Borneo-Malaysia (eastern Sarawak and western Sabah) and Brunei. No substantial rainfall was recorded in East Kalimantan from January until April 1998, favoring the uncontrolled spread of fires in the region, whereas all the other provinces on Borneo had experienced normal to heavy rainfall (Siegert and Hoffmann, 2000). The right column of Figure 5-7 presents the monthly mean atmospheric column burden of total particulate matter as determined by the REMO model with the standard emission estimate. It should be emphasized at this point that Figure 5-7 displays only a qualitative comparison of the dimensionless TOMS AI with REMO calculated TPM column burden in mg/m^2 which however allows an evaluation of the simulated spatial and temporal variability of the smoke-haze distribution. The REMO model largely reproduces the spatial and temporal expansion and intensity of smoke-haze. A northward transport of smoke-haze dominates in the model results in August 1997, with an increasing westward motion until October 1997. Differences from TOMS AI occur in the modeled expansion and intensity of smoke-haze resulting from fires in Irian Jaya. A possible explanation for these disparities is that we may have underestimated the area of peat forests in south-eastern Irian Jaya. The REMO simulations also do not show a smoke-haze plume from fires in Borneo- Malaysia and Brunei in 1998 as visible in TOMS AI data, because we did not estimate any peat fires there. Ahmad- Zainal (2001), however, observed fires in Borneo-Malaysia in 1998 predominantly in peat forests.

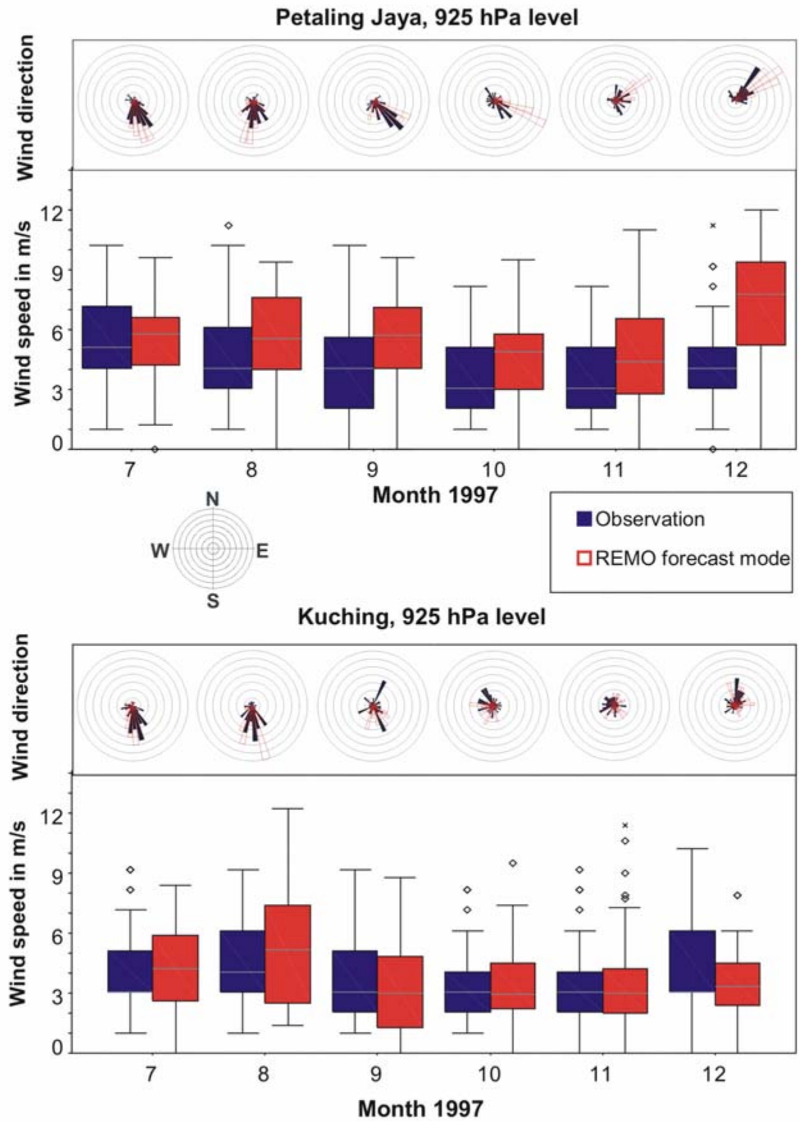

Figure 5-6: REMO wind speed and direction in 925 hPa versus measurements at (a) Petaling Jaya (3.1° N, 101.4° E) and (b) Kuching (1.5° N, 110.3° E).

5.4.2.4 Smoke-Haze Distribution in Surface Air

Monthly mean TPM concentration simulated for the first vertical model layer is shown in Figure 5-8 for the standard and high emission estimate. The spatial expansion of the simulated smoke-haze for the two emission estimates exhibits similar dispersion patterns, but the smoke-haze in the high emission case is more extensive pointing to longer atmospheric residence times of TPM in this case. As expected, modeled TPM concentrations are distinctly higher in the high emission case. In September 1997 maximum monthly TPM concentrations of 5,017 µg/m^3 and 23,814 µg/m^3 are determined in the standard and the high emission cases, respectively, for the first model layer. In our standard estimate we determine monthly mean TPM concentrations above 2,000 µg/m^3 from August until October only for 15 model grid cells in areas with high fire activity, while in the high emission case they are determined over roughly the entire region with recorded fire activity (159 model grid cells). In the high emission case, TPM concentrations downwind from the fires remain at high levels over long distances. In September 1997, monthly mean TPM concentrations between 1,000 and 2,000 µg/m^3 expand from the fire regions in southern Kalimantan into the South China Sea, including large areas of western Borneo. In the standard emission case, monthly mean TPM concentration in September are 300 to 1,000 µg/m^3 in the western parts of Borneo. For comparison, sparse measurements in Indonesia show ambient particle concentrations above 2,000 µg/m^3 TPM at several locations in Kalimantan and Sumatra during this time. Concentrations of up to around 4,000 µg/m^3 TPM are recorded in the vicinity to the main fire activity (Palangkaraya on Kalimantan and Jambi on Sumatra) (Heil and Goldammer, 2001). This comparison indicates that the high emission case overestimates observed TPM concentrations near the fires while the standard emission case approximately meets the range of observed concentrations in the vicinity of the fires.

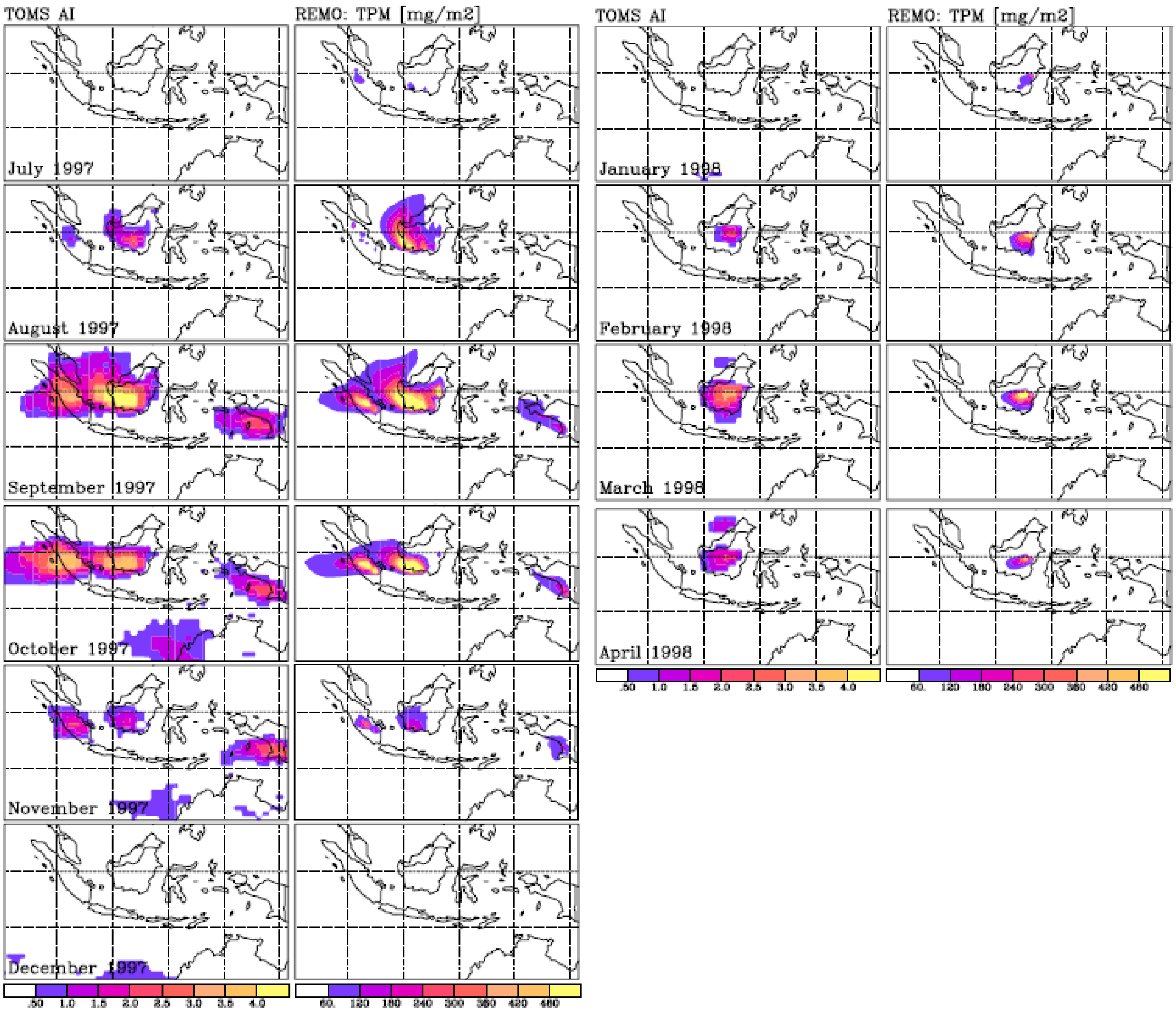

Figure 5-7: Qualitative comparison of TOMS Aerosol Index in 1° resolution (left column) with REMO calculated TPM column burden in mg/m^2 in 0.5° resolution (right column) as monthly means from July 1997 to April 1998. During May and June 1998 TOMS AI and REMO calculated TPM column burden do not exceed the lowest colour interval of 0.5 and 60mg/m^2, respectively. Model results with the standard emission estimate are shown.

5.4.2.5 Smoke-Haze at Malaysian Locations

To evaluate the modeled atmospheric TPM distribution downwind of the main fires in more detail, we quantitatively compare REMO simulation results with ambient particle measurements obtained from the Malaysian Meteorological Services for seven Malaysian sites for July to December 1997. Dependent on the station, particle measurements represent daily average concentrations of PM_{10} (Particulate Matter smaller than 10 µm in diameter) or TPM based on continuous (daily) or discontinuous (every second day) measurements. If we compare model results with PM_{10} measurements, we convert TPM concentrations derived from the model simulations into PM_{10} assuming a PM_{10}/TPM ratio of 80%. This ratio is based on emission factors given by Peterson and Ward (1993) for fuel combustion (large woody, litter and duff) in the smoldering stage.

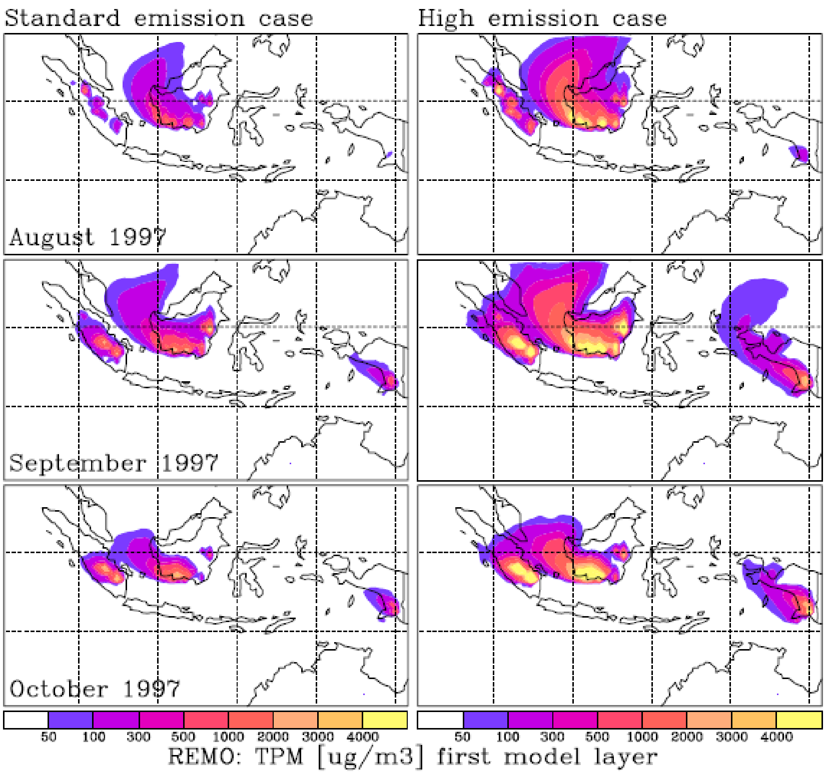

Figure 5-8: Monthly mean TPM concentrations in µg/m^3 in surface air during the main haze period from August to October 1997 as determined by REMO for the standard emission case (left column) and the high emission case (right column).

Figure 5-9 illustrates PM_{10} and TPM observations at Petaling Jaya on Peninsular Malaysia about 800 km downwind of the main fire regions and Kuching on Borneo-Malaysia, 400 km downwind of the fires, from July to December 1997 together with the corresponding REMO model results for the first model layer derived with the standard and high emission estimate. In early July 1997 and after mid-November, i.e. before and after the smoke-haze episode, background particle concentrations between 40 and 60 µg/m^3 are measured at both locations. This approximate particle background is missing in the REMO model results because we included solely primary particles released by vegetation and peat fires in our simulations, no other anthropogenic or natural particle sources and no secondary aerosol formation. PM_{10} measurements at Petaling Jaya show a gradual, but highly fluctuating increase during July and August, followed by a distinct rise in September with peak values around 400 µg/m^3 PM_{10}. Particle concentrations return to background levels in mid-November. The REMO model reproduces the temporal development of ambient particle concentration at Petaling Jaya with a linear correlation coefficient between observation and model output of R=0.66. When taking into account a constant background value of 50 µg/m^3, the peak values of particle concentrations in the high emission case are very similar to the measured concentrations, they exceed the measurements only during a few days. With the standard emission estimate peak concentration plus background concentrations reach 100 µg/m^3 in maximum at Petaling Jaya and thus clearly underestimate observed concentrations. Measured particle concentration at Kuching also peaked in September with maximum values around 1,000 µg/m^3 TPM. The REMO model reproduces the temporal variability of TPM concentrations observed at Kuching only moderately (R=0.44). At this location the high emission estimate overpredicts observed concentrations whereas the standard emission estimates shows better agreement with observations, although it underestimates the September peak values.

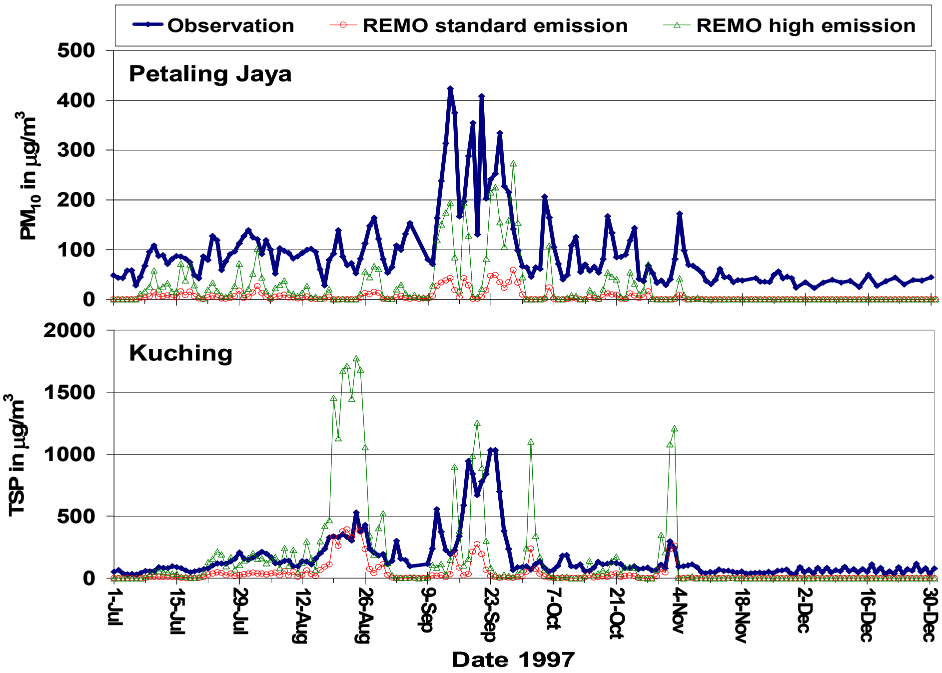

Figure 5-9: Daily mean ambient particle concentrations in µg/m³ at (a) Petaling Jaya on Peninsula Malaysia as PM_{10} and at (b) Kuching on Borneo-Malaysia as TPM. REMO model results derived with the standard and high emission estimate are compared with measurements.

Figure 5-10 illustrates the differences between observed TPM and PM_{10} concentrations and REMO model results for the standard emission estimate (Figure 5-10a) and the high emission estimate (Figure 5-10b) at the seven Malaysian locations from July to December 1997. Negative values represent model overprediction, positive values model underprediction. A bias of about 30–100 µg/m³ is visible outside the smoke-haze period due to the neglected particle background concentrations in the REMO model simulations. The highest deviations from observations occur at Kuching. High correlation ($R>0.73$) is found for particulate matter concentrations measured on Peninsular Malaysia at Ipoh, Petaling Jaya, Kuantan and Melaka throughout the fire episode (1 July to 15 November 1997), but no correlation is found for the post-haze period (16 November to 31 December 1997). This indicates that during the smoke-haze episode these locations are to a large degree influenced by the same air masses loaded with fire aerosols. REMO model results determined with the standard emission estimate differ from the observations on Peninsula Malaysia in maximum by +400 µg/m³ and −100 µg/m³. Model results calculated with the high emission estimate show an underprediction of 400 µg/m³ of the measurements on Peninsula Malaysia and a significant higher overprediction up to 600 µg/m³. The underpredicted values at the Malaysian stations show to a large degree a comparable pattern with both emission estimates, pointing to processes that affected atmospheric particle concentrations during long range transport in a similar way. Here uncertainties in the modeled precipitation especially over the South China Sea due to the forecast mode application, the convective cloud module or the prescribed sea surface temperature (SST) are revealed.

In summary, with the standard emission estimate particle concentrations in the vicinity of the fires can be reproduced well, but they are generally underestimated on Peninsula Malaysia. Using the high emission estimate, REMO model results clearly exceed observed particle concentrations close to the fires but at locations in Malaysia affected by long-range transport of fire emissions only a relatively small overestimation remains. It should be emphasized again, that principally a model underprediction of atmospheric particle concentrations is expected, because only primary emissions of particles released from the fires are considered, no secondary aerosol formation and no other anthropogenic or natural particle sources are included. Additionally, the overestimation of precipitation and related wet deposition tends to remove too much particles from the atmosphere in our model calculation. For these reasons, the model simulation using the high emission estimate is pointing to an overestimation of the vegetation and peat fire emissions and the assumed peat area burned in Indonesia in 1997/1998.

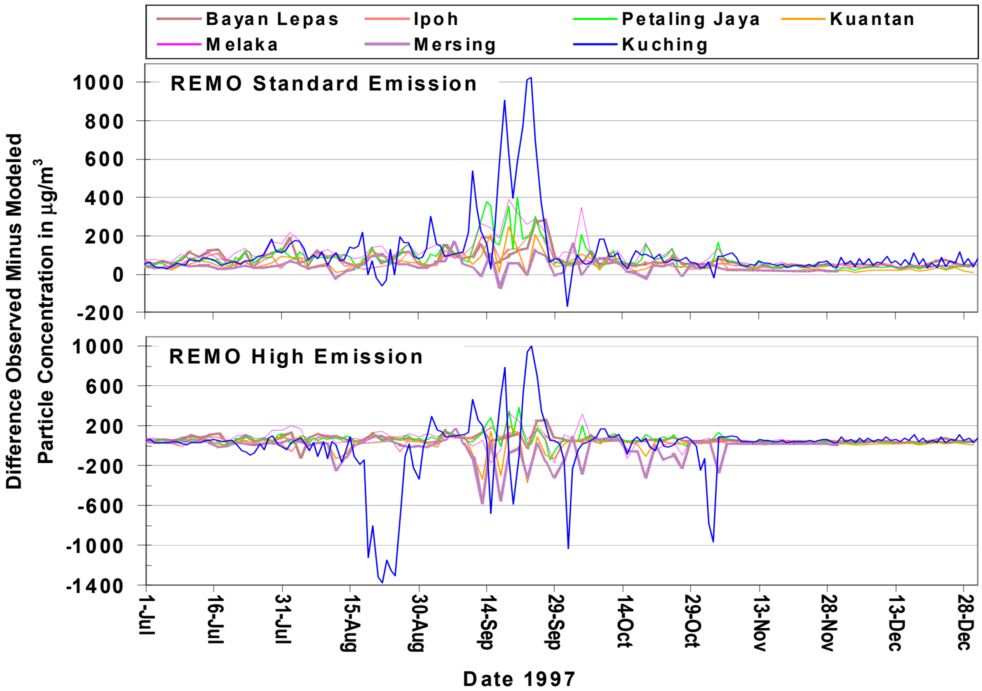

Figure 5-10: Difference between observed ambient particle concentrations (TPM Lepas, Ipoh, Melaka and Kuching and PM_{10} for Petaling Jaya, Kuantan and Mersing) and corresponding REMO model results for (a) the standard emission estimate and (b) the high emission estimate.

5.5 Conclusions and Outlook

Numerical model simulations of the severe smoke-haze periods in Indonesia during 1997/1998 have been carried out with the regional atmosphere-chemistry model REMO (Langmann, 2000). The model experiments focused on the dispersion of vegetation and peat fire emissions in the atmosphere using two emission inventories, which have been set up by modifying the size of the fire affected peat areas only. Although the model simulations are carried out with a number of simplifications and assumptions, conclusions on the total particulate and gaseous emissions released from the Indonesian fires in 1997/1998 can be drawn from comparison of modeled particle concentrations with available measurements. The high emission estimate with the total of 1600 Mt C (83% CO_2, 14% CO, 2% TPM-carbon and 1% CH_4) overestimates observed particle concentrations close to the fires. Downwind of the fires on Peninsula Malaysia the particle load is overestimated by the high emission estimate up to 600 µg/m^3 at several locations, a value that significantly exceeds ambient air quality standards. With the standard emission estimate (380 Mt C total emissions) observed particle concentrations in the vicinity of the main fires are much better reproduced, but downwind of the fires observed particle concentrations tend to be underpredicted. Here it has to be noted that a principal underprediction of modeled atmospheric particle concentrations is expected as outlined in the discussion in Section 5.4. Therefore, we conclude that a release of 1600 Mt C overestimates the vegetation and peat fire emissions in Indonesia in 1997/1998. We also conclude that the area of the fire affected peatlands which is based on Page et al. (2002) in the high emission case, is too large.

Burning peat areas in Indonesia have been a major source of gases and particles in recent smoke-haze events (Nichol, 1997, Levine, 1999, Page et al. 2002). Therefore, continuous monitoring of peat areas in Indonesia is necessary, particularly of the spatial distribution, depth and modification by fire. Such information helps to reduce the huge uncertainties in emission estimates of smoke haze particles, CO_2, CO, CH_4 and other trace gases for impact assessments of human health and climate change. Estimates of CO_2 emissions from burning peatlands in Indonesia in 1997 range from 13% to 40% (Page et al. 2002) of the mean global carbon emissions from fossil fuels. The reason for the measured large atmospheric CO_2 increase in 1997/1998 (IPCC, 2001), however, is still in discussion in the carbon cycle community. One possibility is also decreased photosynthesis of vegetation in the Amazon region due to decreased rainfall during the El Niño period (Scholze, 2003). Rödenbeck et al. (2003) and van der Werf et al. (2004) emphasized recently such anomalies in CO and CO_2 emissions from tropical South America during the El Niño event 1997/1998.

Repeated smoke-haze periods in Indonesia in recent years caused mainly by peat fires are a major threat to human health. Due to the lack of continuous countrywide measurements of air quality in Indonesia, numerical model simulations as presented here with the REMO model are an important tool to assess the sources, the amount and distribution of smoke-haze particles in the atmosphere over Indonesia and the possible impact on human health. Further developments are necessary to improve the quality of the simulation results. These include particularly the formation of secondary organic aerosols from low volatile organic compounds and the prediction of the chemical composition and size distribution of the smoke-haze particles.

Another key factor when modeling smoke-haze is the prediction of rainfall because wet deposition is the major removal process of smoke-haze particles from the atmosphere. As outlined by Aldrian (2003) and also in this paper, the REMO model tends to overestimate rainfall in Indonesia, especially over the ocean. During the winter monsoon season when the air masses approach from the Asian continent the model might overpredict precipitation because aerosol-cloud interactions in these polluted air masses are not taken into account. Locally, the influence of smoke-haze aerosols on clouds and precipitation could be important for a suppression of rainfall (Rosenfeld, 1999) and therefore a prolongation of the fires. Aldrian (2003) pointed to the importance of the local SST. With a coupled ocean-atmosphere model approach with variable SST, he was able to improve the determination of rainfall significantly. Another possibility to improve rainfall prediction is to take into account a fractional land-sea coverage in each grid cell according to Semmler et al. (2004) to represent the numerous small islands of Indonesia more realistically. As these islands act as heat engines for local convection in this most active convective region of the world, the effect is assumed be important. Neale and Slingo (2003) analyzed the performance of a global circulation model over Indonesia and showed that the non-representation of islands lead to an overall increase in precipitation. Moreover, the approach how to describe convective processes in the model has to be examined carefully.

Acknowledgements

The authors would like to thank E. Aldrian, S. Hagemann, J. H¨olzemann, A. Hoffmann, L. Kornblueh, M. Pfeffer and R. Podzun for support and valuable comments. The availability of data from ATRS, TOMS AI, GPCC and the Malaysian Meteorological Service is gratefully acknowledged. This work has been funded by the German Ministry for Education, Science, Research and Technology (BMBF) within the Focus Program AFO2000.

6 Indonesian Peat and Vegetation Fire Emissions: Study on Factors Influencing Large-Scale Smoke Haze Pollution Using a Regional Atmospheric Chemistry Model

This chapter has been published as: Heil A, Langmann B and Aldrian E (2007) Indonesian peat and vegetation fire emissions: Study on factors influencing large-scale smoke haze pollution using a regional atmospheric chemistry model. Mitigation and Adaptation Strategies for Global Change 12:113-133, doi: 10.1007/s11027-006-9045-6.

Abstract

Numerical modeling of fire-related smoke haze episodes in Southeast Asia is important for both prediction and assessment of atmospheric impacts, especially when observational data are fragmentary, as is the case in Indonesia. This work describes the atmospheric fate of smoke particles emitted during the 1997 Indonesian fires modeled with a regional atmospheric chemistry model. We established a new fire emission inventory and calculate that 55 teragram (Tg) of particulate matter and 1098 Tg of carbon were released during this fire episode. Our emission estimate is an intermediate value compared with other studies. Utilizing different scenarios, we demonstrate the variable atmospheric impacts of surface vegetation fires and peat soil fires separately and also investigate the sensitivity of smoke dispersion to the differing meteorological conditions of an El Niño and a normal year. When peat fires are included in the emission inventory, modeled ambient particle concentrations exceed the ambient air quality standard across transboundary scales. In a scenario including only surface vegetation fires, ambient air quality standards are exceeded only in areas close to the main fires. This scenario demonstrates the prominent role of fires in peat areas in causing regional air pollution episodes. In years with normal meteorological conditions, intermittent precipitation and associated wet deposition during the dry season are predicted to remove most of the particulate emissions close to the sources. Strongly reduced rainfall and generally stronger southeasterly winds during El Niño years provide favorable conditions for larger scale smoke haze pollution.

6.1 Introduction

Vegetation and peat fires in Indonesia are an important factor when dealing with transboundary air pollution in the Southeast Asian region. Particulate matter emitted by the fires is the dominant pollutant causing exceedances of ambient air quality thresholds on a regional scale (e.g., Heil and Goldammer 2001). In the El Niño year 1997, Indonesia experienced abnormal drought conditions, and the number of land clearing fires by far exceeded the normal annual dry season's burning. Land clearing fires mainly in southern Kalimantan, Sumatra, and Irian Jaya, which started with the onset of the relatively dry season in May/June 1997, progressively raged out of control in the following months and affected the surrounding vegetation. Kirono et al. (1999) noted that during the 1997 El Niño, virtually the entire country had rainfall below the 10^{th} percentile, with many locations receiving the lowest rainfall on record since 1950. These conditions contributed to a pronounced lowering of the water table in peat soils (Usup et al. 2000), making not only drained but also undrained peat soils susceptible to shallow peat fires (Zoltai et al. 1998).

The emissions released by the 1997 fires caused a regional air pollution episode with tremendous impacts on human health, visibility, and economy, and influenced regional to possibly global climates (ADB/BAPPENAS 1999, Rosenfeld 1999, Heil and Goldammer 2001, Page et al. 2002). Up to 300 million people across the Southeast Asian region were exposed to elevated particle levels during this episode. Up to five times the normal number of cases of respiratory diseases were observed in Malaysia in September alone (Awang et al. 2000). Severe transboundary smoke haze episodes have been recorded in earlier El Niño years as well. Particulate matter levels during the 1991 and 1994 smoke haze episodes in the Malaysian Klang Valley region, for example, were more than two times the ambient air quality standard for PM_{10} (particulate matter smaller than 10 µm diameter) (Soleiman et al. 2003). Even in 'normal' (non-El Niño) years, fires in Indonesia adversely affect particulate air quality in Indonesia and in neighboring countries. The atmospheric impacts of these smoke haze events are less severe, but they remain important for public health, as any increase in airborne particle levels enhances the risk of exposed populations to increased morbidity and mortality – even at concentrations below regulatory limits. A 10 µg/m^3 increase in daily PM_{10} levels, for example, has been found to increase daily mortality by around 0.5% and hospital admissions for respiratory diseases by up to around 1.5% (Brunekreef and Holgate 2002, and references therein). Several studies have demonstrated that fires in peat areas are of particular importance for overall fire emission production as fires in peat areas may release up to 50 times (and more) higher emissions per unit area burnt than fires in surface vegetation (Levine 1999, Page et al. 2002). Peat areas have been estimated to account for 3% of the total area burnt in 1994, yet to produce 55% of total soot emissions (Nichol 1997), and to account for 20% of the total area burnt in 1997 while producing 94% of total emissions (Levine 1999). Page et al. (2002) have estimated that 480–2570 Tg of carbon (C) were released during the 1997 peat and forest fires, with the overlying vegetation contributing only 19%. For smoke haze management and mitigation measures it is important to discriminate between fires from surface vegetation and peat soil. To learn more about each type of fire we modeled the atmospheric impacts of emissions from each source separately.

Modeling the atmospheric distribution of fire aerosols from Indonesian fires is particularly important for air quality forecasts and impact assessment because region-covering, continuous, and directly accessible air quality information is lacking. Several numerical models have been applied to investigate the smoke haze in this region. An extensive discussion is provided in Radojevic (2003). For example, Koe et al. (2001) and Roswintiarti and Raman (2003) modeled the transport of emissions from the main fire locations in Indonesia in 1997. These studies did not, however, establish a quantitative emission scenario and therefore did not model absolute concentrations of pollutants. The same applies to the model study on smoke dispersion during 1998 to 2000 by Keywood et al. (2003). All of these studies confirmed the large-scale transport of fire emissions from Indonesia to neighboring countries. Recently, Langmann and Heil (2004) investigated the atmospheric implications of a lower and high emission scenario, which largely followed the estimate of Levine (1999) and Page et al. (2002). In this study, we model the atmospheric impacts of the 1997 Indonesian fires using an intermediate emission scenario and address in detail the influence of the climate factor El Niño on smoke haze distribution.

6.2 Methods

6.2.1 Model Description

REMO (REgional MOdel), a three-dimensional regional scale atmospheric chemistry module (Langmann 2000), is applied to study the atmospheric transport and removal of aerosols emitted from the Indonesian fires in the second half of 1997. In this setup, REMO determines at each model time step the physical and chemical state of the model atmosphere, while the dynamical part of the model uses physical parameterizations from the global ECHAM4 model (Roeckner et al. 1996, Jacob 2001). REMO has three types of convection: penetrative, shallow, and mid-level convection. Only one scheme is allowed in a grid cell. The parameterization of the convective clouds is based on the mass flux concept from Tiedtke (1989) with changes in the deep convection. In the current model setup, atmospheric aerosol is the only prognostic species included, which is represented without further differentiation according to chemical composition and size distribution. Although secondary aerosol formation may play an important role, it is not included in the present study.

The particle transport is determined by horizontal and vertical advection according to the algorithm of Smolarkiewitz (1983), convective up- and downdraft by a modified scheme of Tiedtke (1989), and vertical diffusion after Mellor and Yamada (1974). Because of the elevated sulfur content and hygroscopicity of Indonesian vegetation and peat fire aerosols (Ikegami et al. 2001) particle deposition is calculated as for sulfate. Dry deposition velocities are determined as described by Walcek et al. (1986), dependent on friction velocities and stability of the lowest model layer. Wet deposition is computed according to Walcek and Taylor (1986) by integrating the product of the grid-averaged precipitation rate and the mean cloud water concentration, assuming 100% solubility of the particles. The REMO model was applied with 20 vertical layers of increasing thickness between the Earth's surface and the 10 hPa pressure level using terrain following hybrid pressure-sigma coordinates. In this study, we assume that aerosols emitted by fires are released into the lowest model layer.

The model domain expands over entire Indonesia covering an area from 19°S to 8°N and 91°E to 141°E (around 18 million km^2) with a horizontal resolution of 0.5° (~55 km). A basic model time step of 5 minutes was chosen. In this study, REMO is run in a forecast mode (restart every 30 hours) which is initialized and driven (nudged at the lateral boundary every 6 hours) by the European Centre for Medium-Range Weather Forecasts (ECMWF) analysis while aerosol processes are calculated continuously (cf. Langmann and Heil 2004). By restarting the model every day the internal model variability is suppressed with the purpose of forcing the model to stay close to the observed weather situation (ECMWF analysis) and thereby to model particle transport and removal processes as close to reality as possible.

Previous studies with the REMO atmospheric chemistry model (e.g., Langmann et al. 1998, 2003, Chevillard et al. 2002, Langmann and Heil 2004) give confidence in the ability of the model to reproduce the physicochemical state of the atmosphere. Aldrian et al. (2004) validated REMO performance in simulating the Indonesian rainfall and found good agreement between simulated and observed rainfall variability, particularly over southern Sumatra and Kalimantan. They found that REMO systematically overestimates the amount of rainfall over the ocean surrounding the Indonesian archipelago by up to 70%, but reproduces it well over land with a bias of less than 5% for Kalimantan and Sumatra. Generally, predictability is highest during the normal annual dry season (June–September), notably in regions affected by El Niño – Southern Oscillation (ENSO) events. In view of precipitation directly determining the magnitude of removal of airborne particles by wet deposition (Grantz et al. 2003) and the main fire episode being in the dry season, this is a promising prerequisite for using the model in wide-range smoke haze pollution monitoring and prediction scenarios. However, REMO is likely to overpredict the removal of smoke particles by wet deposition particularly during transport over the ocean and outside the main dry season.

6.2.2 Emission Inventory

The current study builds on previous work described in Langmann and Heil (2004), which has been modified to more realistically represent an intermediate emission scenario by using different parameters for emission calculation such as biomass load and emission factors and an improved map of peat soil distribution.

6.2.2.1 Distribution of Surface and Subsurface Fuels and Emission Factors

Distribution of surface and subsurface fuels and emission factors In this study, the different surface vegetation types from the land cover data set of Loveland et al. (2000) are aggregated into three main surface fuel classes (Figure 6-1 a-c). We use a version of this data set that has been processed for climate modeling into 0.5° × 0.5° fractional vegetation cover data by Hagemann (2002). The fire emission inventory only includes fires occurring in the subarea of the model domain from 10.5°S to 7.0°N, (i.e., including Indonesia and Malaysia but excluding Australia). Within this inventory area, forest makes up 60% of the total area of surface vegetation (2.3 million km^2), while agriculture, grassland, and savannah make up 32%, and fragmented forests and plantations 8%.

We also include emissions from subsurface fires in organic peat soils, which we calculate separately from the surface fire emissions. Estimates of the areas covered by peatland in Indonesia are highly uncertain. The most commonly cited area estimates for Indonesian 'predisturbance peatland' (prior to large-scale drainage for agriculture and forestry) range from 170,000 to 270,000 km^2. The main uncertainty in this estimate is the definition of peatland, as the definition of minimal depth varies greatly from 0.2 m to 0.6 m (Immirzi et al. 1992). Current estimates of peatland in this region are on average 216,000 km^2 (Immirzi et al. 1992, Page et al. 1999).

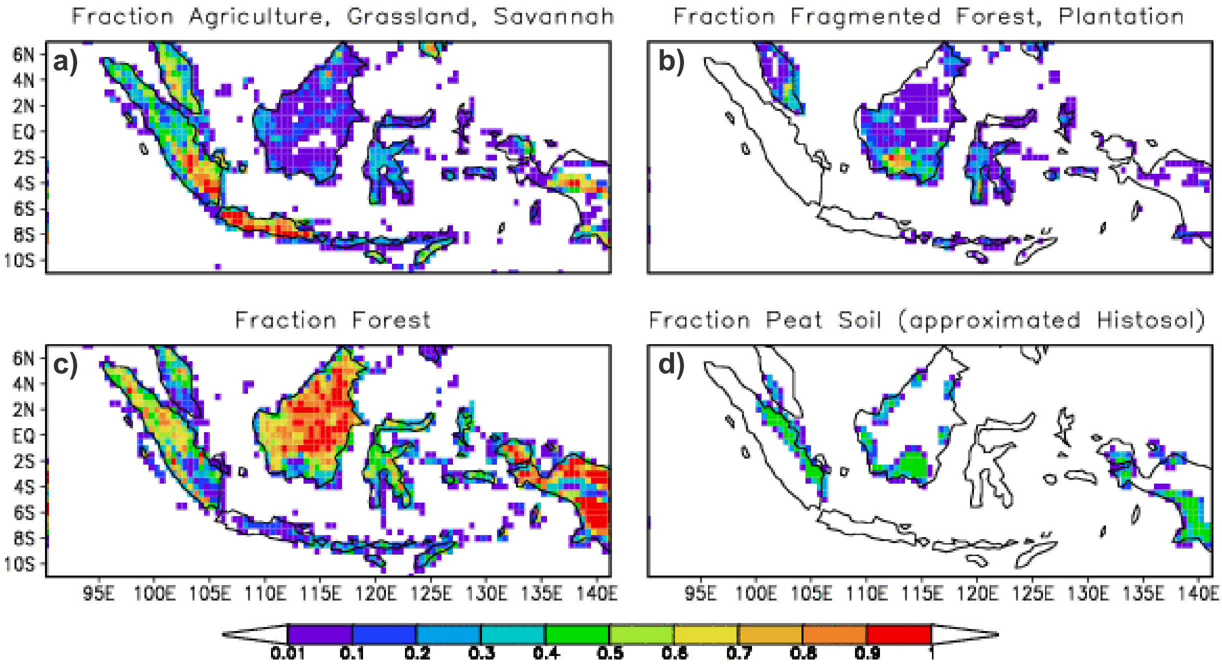

Figure 6-1: Fractional distribution of the aggregated fuel classes used in our study as fraction per grid area based on Hagemann (2002) and FAO (2003): (a) agriculture, grassland, and savannah; (b) fragmented forests, plantations; (c) forest; (d) peat soil.

We derived the distribution of peat soils from areas designated as reference soil group Histosol (HS) in the World Reference Base (WRB) Map of World Soil Resources (FAO 2003). The WRB system defines the soil type histosol as a soil having an organic soil material horizon (histic or folic) of at least 0.1–0.4 m thickness, dependent on the properties of the underlying horizon (FAO 1998). The total area of soils classified as reference soil group HS in the inventory area is 436,000 km^2, twice the cited area estimate of peatland in this region (216,000 km^2) of Immirzi et al. (1992) and Page et al. (1999). Its spatial distribution corresponds well with the drawing of Indonesian peat areas by Rieley et al. (1997). HS mapped in the inventory area using the WRB classification system also includes soil units where histosols are associated with gleysols, which may partly explain the higher value. To account for this overestimation, we assume that 50% of the HS mapped is peat, resulting in a total peat soil area of 218,000 km^2, of which 30% is on Sumatra/Peninsular Malaysia, 34% on Borneo, and 36% on Irian Jaya (Figure 6-1 d).

The above- and belowground biomass densities determine the amount of fuel per unit area that can potentially burn in a fire event. The burning efficiency β (frequently also referred to as combustion factor) describes how much of the biomass available is actually consumed during a fire event, i.e., converted into gases and aerosols. The emission factor (EF_X) determines the mass of compound X emitted per mass of fuel consumed by the fire (gram X /kg dry fuel). The total emissions of X are calculated from the product of area burnt and the corresponding biomass loading, burning efficiency, and emission factor EF_X. Table 6-1 summarizes the parameters used for calculating emissions of PM_{10} for different fuel classes based on a literature study. For later discussion, Table 6-1 also includes other selected trace species. The parameters for surface fuel classes are relatively well documented, but with large ranges. These parameters are, however, poorly investigated for Indonesian or tropical peat in general. Neither the average depth of Indonesian peat soils nor the average depth of peat burnt has been explored in a consistent way that representatively covered the different types of peat areas in this region. For our modeling, we assume a mean peat depth of 2.3 m, which is a reduced estimate for average peat thickness found in Central Kalimantan by Page et al. (2002). The only published study on peat depths burnt in Indonesia found a mean peat depth burnt in Central Kalimantan of 0.51 m in 1997 (range from 0.25 m to 0.85 m) (Page et al. 2002), which we use in this study.

	Agriculture, Grassland, Savannah	Fragmented Forest, Plantation	Forest	Peat soil
Biomass density [t/km^2]	4,035[a]	20,000[b]	50,400[c]	293,825[d]
Burning efficiency [%]	93[e]	54[f]	39[g]	22[h]
Carbon Content [%]	50[i]	50[i]	50[i]	54[j]
Emission factors (EF) in g/kg dry fuel consumed: [k]				
Particulate matter <10 µm (PM_{10})	5.0[l]	8.4[l]	8.4[l]	38.0[m]
Particulate organic carbon (OC)	3.4	5.2	5.2	6.0
Particulate elemental carbon (EC)	0.48	0.66	0.66	0.04
Carbon dioxide (CO_2)	1,613.0	1,580.0	1,580.0	1,703.0
Carbon monoxide (CO)	65.0	104.0	104.0	210.3
Methane (CH_4)	2.3	6.8	6.8	20.8
Benzene (C_6H_6)	0.23	0.40	0.40	0.47

a) Average aboveground biomass of grasslands and annual crops in Indonesia (Lasco 2002).
b) Aboveground biomass of plantantions (Mudiyarso and Wasrin 1995).
c) Average aboveground biomass of undisturbed and logged rainforests (Lasco 2002).
d) Average peat depth (conservative approach) in Kalimantan (Page et al. 2002), biomass load calculated with average bulk density for Indonesian peat of 0.128 g/m^3 (Shimada et al. 2001).
e) Burning efficiency of pasture/grass (Fearnside 2000).
f) Mean burning efficiency of secondary forest (Fearnside 2000).
g) Mean burning efficiency of original forest (Fearnside 2000).
h) Derived from ratio of mean peat depth entirely burned in Central Kalimantan 1997 (0.51 m) and a conservative estimate of mean peat thickness (2.3 m) (Page et al. 2002).
i) C-content of 50% assumed (Fearnside 2000).
j) Mean carbon content of peat cores sampled in Kalimantan (Shimada et al. 2001).
k) Emission factors for agriculture, savannah and grassland taken from emission factors for savanna and grassland (Andreae and Merlet 2001). Emission factors for both, forests and fragmented forests/plantations correspond to emission factors for tropical forest in Andreae and Merlet (2001). Emission factors for Indonesian peat taken from Christian et al. (2003), except for PM_{10}. When emission factors are given as range, average is used.
l) PM_{10}-emission factors derived from $PM_{2.5}$-emission factor given in Andreae and Merlet (2001) using a mean $PM_{2.5}/PM_{10}$ ratio of 0.923 found for burning different forest types by Peterson and Ward (1993).
m) PM_{10}-emission factor of a composite sample of Sumatran peat obtained during the EFEU-campaign (personal communication, 16.04.2004, O. Schmid, Max-Planck-Institute for Chemistry).

Table 6-1: Biomass density, burning efficiency, carbon content, and emission factors used for the four fuel classes used in this study to calculate fire emissions.

An extensive review of emission factors for different biomes by Andreae and Merlet (2001) includes tropical forest and grassland/savannah, but not peat. Christian et al. (2003) provides the first detailed description of emission factors for gaseous compounds and aerosol chemical constituents from Indonesian peat combustion while particulate emission factors (PM_{10}) of Indonesian peat were only recently analyzed within the EFEU (Impact of Vegetation Fires on the Composition and Circulation of the Atmosphere) project (Wurzler et al. 2001) (cf. Table 6-1). Our peat emission inventory rests on the two latter studies, which represent a substantial progress for adequately inventorying aerosol and trace gas emission for peat fires in Indonesia. In the absence of these data, previous studies have estimated the emissions from Indonesian peat fires using emission factors for organic soils in extratropical regions (e.g., Levine 1999), which, however, are generally moss-derived in contrast to woody peat in the tropics.

6.2.2.2 Area Burnt Estimate and Distribution of Surface and Below-ground Fuels

In this study, we use the area burnt estimate of Tacconi (2003) and redistribute this area estimate in space and time using fire count data retrieved from the Along Track Scanning Radiometer (ATSR) satellite instrument (Arino and Rosaz 1999). The area burnt estimate is an update of the area burnt estimate for Indonesia for different vegetation types by ADB/BAPPENAS (1999), which compiled the various data sources available on area burnt based on satellite data, aerial surveillance, and ground assessments. We use this approach because continuous and time-resolved information on the spatial extent of the fire-affected areas in 1997 is not available for entire Indonesia.

So-called ‘hotspot’ or fire count data can provide information on the spatial and temporal occurrence of an active fire event, but not on the area burnt within an individual fire count pixel (Malingreau 1990). We use nighttime data from the ATSR World Fire Atlas (Arino and Rosaz 1999) and aggregate them into 0.5°x0.5° cells on a weekly basis. Only fires occurring in the inventory area are included. A weekly mean is used to smoothen out the three-day acquisition frequency of the ATSR sensor at equatorial latitude to assure that at least two overpasses are included in each time step. The ATSR thermal 3.7µm channel detects active fires through the induced changes in Earth’s radiative temperature using two algorithms: Algorithm 1 identifies a so-called hotspot when the surface temperature is above 312° Kelvin, while the threshold is 308° Kelvin for Algorithm 2. We used Algorithm 2 data in our study because of the resulting enhanced sensitivity to lower-temperature fires (e.g., smoldering peat fires) (Malingreau 1990). Compared with other satellite products, Stolle et al. (2004) found that ATSR data for Indonesia are a fair temporal proxy for area burnt, despite existing commission and omission errors. ATSR data show a high correlation with burn scar area maps (R = 0.82 for Algorithm 2), albeit largely but consistently underrepresenting the number of active fires in Indonesia. Figure 6-2 a) shows the distribution of ATSR Algorithm 2 fire counts as number per model grid cell from July to December 1997. There is widespread occurrence of fires on Sumatra, Kalimantan, and Irian Jaya and an increasing fire intensity towards the southern coastal areas.

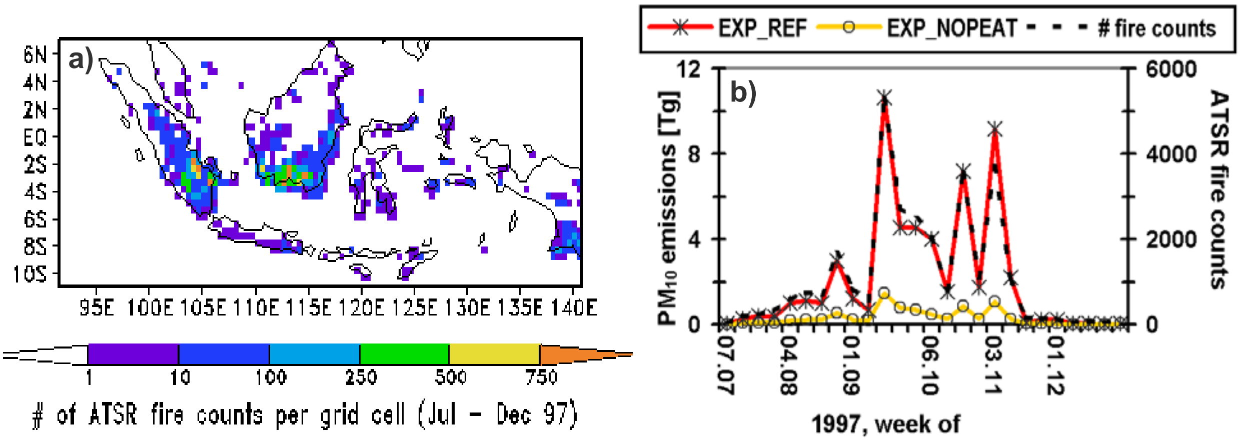

Figure 6-2: 2 (a) Total number of ATSR Algorithm 2 fire counts recorded in the second half of 1997 per 0.5° × 0.5° model grid; (b) weekly total PM_{10} emissions in the second half of 1997 calculated for all fuel classes (EXP REF) and for all fuel classes except peat (EXP NOPEAT). On the secondary axis, the weekly number of ATSR Algorithm 2 fire counts is shown

The total area burnt estimate of Tacconi (2003) for 1997/1998 divided by the total number of ATSR Algorithm 2 fire counts detected over Indonesia from July 1997 to June 1998 (39,240 counts) results in a mean area burnt of 3.0 km^2 per fire count. This ratio, which is around three times the ATSR pixel size, may partly be explained by the ATSR sensor covering Indonesia only every third day. Evaluating TRMM (Tropical Rainfall Measuring Mission)-fire counts, van der Werf et al. (2003) showed that the ratio of area burnt per fire count increases with decreasing percentage of tree cover. We therefore use estimated fuel type dependent ratios to approximate the area burnt estimate of Tacconi (2003). We scaled them to 2.3 km^2, 2.9 km^2, and 4.5 km^2 burnt per fire count for the fuel classes forest and peat soil, fragmented forest/plantation, and agriculture/grassland/savannah, respectively.

	fuel class/ region	Agriculture, Grassland, Savannah	Fragmented Forest, Plantation	Forest	Total surface vegetation	Peat soil
Area burned 1997 approximation (this study)	Total area (km^2)	35,986	15,922	27,922	79,830	19,092
	(% of total area)	*(45)*	*(20)*	*(35)*	*(100)*	*(24)*
Area burned 1997 (Liew et al. 1998)[b]	Total area (km^2)	22,800	11,400	11,400	45,600	9,120
	(% of total area)	*(50)*	*(25)*	*(25)*	*(100)*	*(20)*
Area burned 1997 (Fuller and Fulk 2001)[c]	Total area (km^2)	56,500	20,000	55,300	131,800	-
	(% of total area)	*(43)*	*(15)*	*(42)*	*(100)*	-
Area of peat burned 1997 (Page et al. 2002)	Total area (km^2)	lower estimate				14,500
		intermediate estimate				24,410
		upper estimate				68,047
Area burned 1997/98 approximation (this study)	Total area (km^2)	42,737	18,590	48,605	109,932	23,005
	(% of total area)	*(39)*	*(17)*	*(44)*	*(100)*	*(21)*
Area burned 1997/98 (Tacconi 2003)[a]	Total area (km^2)	49,678	21,105	46,201	116,984	21,240
	(% of total area)	*(42)*	*(18)*	*(39)*	*(100)*	*(18)*

[a] Vegetation type agricultural and plantation areas is aggregated into fuel class agriculture/grassland/ savannah; vegetation type forests and bushes as well as peat swamp forests are distributed equally on the fuel classes fragmented forest/plantation and forest.
[b] Area of unspecified land cover type is aggregated into fuel class fragmented forest/plantation.
[c] Vegetation type agriculture and dry scrub and grass is aggregated into the fuel class agriculture/ grassland/savannah; vegetation type timber plantation and estate crop is aggregated to fragmented forest/plantation, while montane and lowland forest are aggregated to the fuel class forest; vegetation type peat and swamp forest is equally distributed among the three surface fuel classes.

Table 6-2: Estimate of area burnt 1997 and 1997/1998 in this study and estimates of other studies for comparison.

Table 6-2 shows the approximated area burnt for the four fuel classes derived from the scaled ATSR fire counts for 1997. Although we exclusively focus on the 1997 fires in this study, the 1997/1998 area burnt approximation is shown to allow a comparison with the area burnt estimate for 1997/1998 by Tacconi (2003), which was used to scale the area burnt per fire count.

The total area burnt approximation for the different fuel classes for 1997/1998 corresponds well with the estimate of Tacconi (2003). However, there are distinct deviations of the area of surface fuel classes burnt on Sumatra, Kalimantan, and Irian Jaya, resulting in a two times larger area of surface vegetation burnt on Sumatra in our approximation compared with Tacconi (2003), while it is around 30% lower on Kalimantan and Irian Jaya. Compared with 110,000 km^2 approximated area burnt for 1997/1998, 80,000 km^2 (73%) burnt in 1997. Our approximation of 19,000 km^2 of burnt peat soil in 1997 is close to the intermediate estimate of 24,000 km^2 of peat area burnt in 1997 by Page et al. (2002).

6.2.2.3 Calculated Emissions

The emissions of PM_{10} and of other selected species calculated for the Indonesian fires in the second half of 1997 are summarized in Table 6.3 as total amount and as relative contribution of the different fuel classes. We calculate that the 1997 Indonesian fires released 55 Tg of PM_{10} to the atmosphere. Fires in peat soil contribute 86% (47 Tg) to the total PM_{10} emissions, while fires in surface vegetation contribute only 14% although the area of surface vegetation burnt was four times larger than the area of peat soil burnt. Total C released from burning surface vegetation and peat soil in the second half of 1997 is estimated to be 1098 Tg C, most (672 Tg C) of which resulted from peat fires. Total C and PM_{10} emitted from surface fires stem mainly from forest fires (64%–68%). While the other surface vegetation classes contribute 75% to the total area of surface vegetation burnt, their emissions are less because of lower biomass densities (Table 6-1).

Species	Total fire emissions 1997 in Tg	*Contribution of fuel class to total emission [%]* Agriculture, Grassland, Savannah	*Fragmented Forest, Plantation*	*Forest*	*Peat soil*
Particulate matter <10 µm (PM_{10})	54.0	*1.3*	*2.7*	*8.5*	*87.6*
Particulate organic carbon (OC)	12	*3.9*	*7.6*	*24.3*	*64.1*
Particulate elemental carbon (EC)	0.6	*11.1*	*19.2*	*61.3*	*8.5*
Total Carbon (C) released[a]	1,098	*6.2*	*7.8*	*24.9*	*61.2*
Carbon dioxide (CO_2)	3,470	*6.3*	*7.8*	*24.9*	*61.0*
Carbon monoxide (CO)	345	*2.6*	*5.2*	*16.5*	*75.8*
Methane (CH_4)	31	*1.0*	*3.8*	*12.0*	*83.3*
Benzene (C_6H_6)	0.9	*3.4*	*7.6*	*24.2*	*64.8*

[a] Total carbon released is calculated from biomass carbon densities and burning efficiencies. Sum of carbon in the carbon-containing species emitted (derived from emission factors) is larger than calculated total carbon released because of rounding errors and differences in data sources.

Table 6-3: Particulate and gaseous emissions from 1997 Indonesian vegetation and peat fires.

Compared with other estimates of total C released during these fires, our estimate represents an intermediate value: Levine (1999) calculated 245 Tg C, Duncan et al. (2003) reported around 700 Tg C, and Page et al. (2002) provided a range from 480 Tg C to 2570 Tg C for a lower and upper estimate. There are several indications that the upper estimate of Page et al. (2002) is too high (Duncan et al. 2003, Roedenbeck et al. 2003, Langmann and Heil 2004, van der Werf et al. 2004). Via global inversion of atmospheric transport of carbon dioxide (CO_2), for example, Roedenbeck et al. (2003) retraced an estimated flux anomaly of around 1000 Tg C in 1997 from the Indonesian fires, which is in the lower region of the range given by Page et al. (2002), and which is in good agreement with our estimate.

PM_{10} emission fluxes show high variability throughout the main fire episode from August to November 1997 (Figure 2b). PM_{10} emissions peak at 10.6 Tg in the third week of September when both surface and subsurface fires are considered (EXP_REF). The temporal spacing of weekly total PM_{10} emissions is largely congruent with the weekly number of fire counts recorded, indicating a relatively homogenous distribution of fires in the different fuel classes over time. The emissions from surface fires largely follow the temporal development of total emissions from surface and subsurface fires (R = 0.92), but are generally six times smaller.

The presence of a dense, persistent smoke layer over the main fire areas in Kalimantan during the smoke haze period may have strongly impaired the consistent detection of fires by satellite (Siegert and Hoffmann 2000). Compared with Kalimantan, the smoke haze layer over Sumatra was much less pronounced, resulting in a lower underrepresentation of fire counts for the latter region. We therefore consider our ATSR fire count–based approach for establishing the emission inventory (see methods) to result in a potential underestimate for Kalimantan and overestimate for Sumatra.

The ignition probability of peat soils by surface fires increases with decreasing soil moisture (Frandsen 1997), e.g., with persistent dry conditions during the fire season. We used constant factors for the ignition probability of peat soils by surface fires throughout the entire fire season, resulting in a likely overestimation of peat fire emissions in the earlier fire season and a likely underestimation in the later fire season. Further misclassifications of fuel type burnt may also result from shortcomings in the land cover and peat soil distribution information used. Misclassified peat fires in our emission inventory could result in up to 55 times larger emissions than actually produced.

The estimated 55 Tg PM_{10} of fire aerosols released from the 1997 Indonesian fires are equivalent to roughly one third of the annual global anthropogenic emissions of primary particles into the atmosphere in the 1980s (Kiehl and Rodhe 1995). Simultaneously, around 3470 Tg CO_2 and 345 Tg carbon monoxide (CO) were released, about 15% and 130%, respectively, of the global emissions of these species produced in 1990 by fossil fuel combustion (Olivier et al. 1999, Marland et al. 2003). Estimated emissions of particulate organic carbon (OC) of 11.7 Tg and elemental carbon (EC) of 0.6 Tg are equivalent to around 115% and 10% of global emissions of these species in 1984 from fossil fuel combustion, respectively (Cooke et al. 1999).

In contrast to these values, Duncan et al. (2003) estimated lower CO_2 and CO emissions of 2300 Tg and 130 Tg, respectively, and distinctively higher OC and EC emissions of 18.5 Tg and 2.6 Tg, respectively. One reason for this discrepancy is that, in the absence of other information, Duncan et al. (2003) assumed that the biomass burnt during the 1997 Indonesian fires was forest and not peat. We applied specific emission factors for peat combustion, which is characterized by a predominant smoldering, low-efficiency combustion with a higher CO/CO_2 and lower EC/OC ratio than typical for the more flaming combustion processes in surface vegetation (Christian et al. 2003, see also Table 6-1). As a result, we calculate a CO/CO_2 (EC/OC) ratio around two to three times lower (higher) than in the study by Duncan et al. (2003). We think our approach provides a more realistic emission estimate of the absolute and relative abundance of species emitted by the fires.

6.2.3 Scenario Runs

To investigate various influences on smoke dispersion and ambient air quality, we performed three model experiments (Table 6-4). In addition to an experimental scenario using a medium fire emission estimate (EXP_REF), two extreme scenarios were simulated: one neglecting emissions from fires in peat areas (EXP_NOPEAT), the other using 1996 meteorology and still incorporating the 1997 fire emissions (EXP_MET96). The year 1996 was chosen to represent the meteorological conditions of a normal year, i.e., when ENSO-related anomalies from the long-term average are small (McPhaden 1999). Both extreme scenarios are unrealistic, because (a) fires do not affect only surface vegetation, but also the underlying peat soil, rendering this an underestimation of fire emissions and (b) 1996 had much fewer fires than the extreme fire event of 1997, rendering this simulation an overestimation of fire emissions for 1996.

Model run	Description
EXP_REF	Reference run with REMO from July - December 1997 driven by corresponding ECMWF-analysis. A medium estimate of PM_{10}-emissions from fires in surface vegetation and peat is used as model input.
EXP_NOPEAT	Same experimental set up as EXP_REF, with emissions from surface fires only included into the fire emission inventory, peat fire emissions excluded.
EXP_MET96	Same experimental set up as EXP_REF, with the ECMWF meteorological conditions from July - December 1996 (still incorporating the 1997 fire emissions).

Table 6-4: Experimental setup for scenario runs conducted for this study.

6.3 Results and Discussion

6.3.1 Modeled PM_{10} levels for the Different Scenarios in the Near-surface Model Layer

Monthly mean PM_{10} concentration modeled for the three scenario runs in the first vertical model layer above the surface is shown in Figure 6-3. The first vertical model layer (ground to ~50m altitude) can be used as a proxy for near surface or ambient air quality. The PM_{10} air quality standard for Indonesia, Singapore, and Malaysia is 150 µg/m^3 as a daily average (ASEAN 2001).

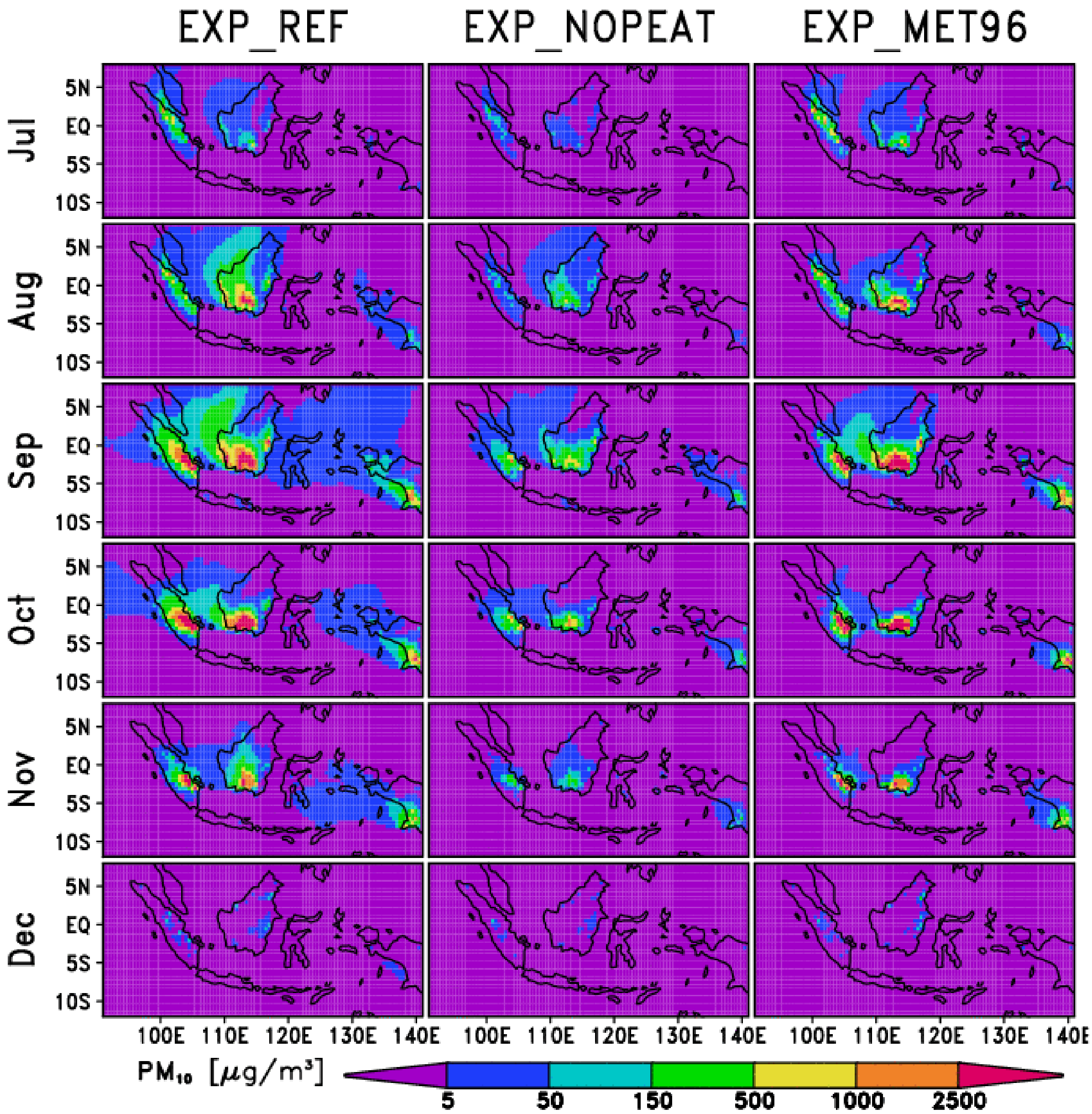

Figure 6-3: Monthly mean PM_{10} concentration modeled for the lowest model layer for the scenario runs EXP_REF (left column), EXP_NOPEAT (middle column) and EXP_MET96 (right column).

All scenario runs show an increase in the extent and intensity of the smoke haze layer from July to October 1997, followed by a subsequent decrease. Maximum PM_{10} concentration is modeled above the main fire areas in southern Sumatra, Kalimantan, and Irian Jaya and the adjacent areas to the northwest (Figure 6-2 a). The spatial extent and PM_{10} concentrations are greatest in the reference run (EXP_REF, Figure 6-3 left column). PM_{10} concentrations in the main fire areas generally range between 3000 µg/m^3 and 9000 µg/m^3 and gradually decrease with the west- and northward expansion of the smoke haze layer. From August to November, monthly mean PM_{10} concentrations above 250 µg/m^3 are modeled for large areas of Sumatra, Kalimantan, and Irian Jaya. Fire-related PM_{10} levels in peninsular Malaysia (including Singapore) are generally in the range of 5 µg/m^3 to 50 µg/m^3, except in September, when they reach 50 µg/m^3 to 150 µg/m^3. An increase in monthly mean PM_{10} concentrations above 5 µg/m^3 is modeled for most of insular Southeast Asia during the fire episode.

The spatial and temporal smoke haze distribution modeled with REMO in 1997 largely reproduces the TOMS (Total Ozone Mapping Spectrometer) Aerosol Index observational data (Herman et al. 1999), as shown in a qualitative comparison by Langmann and Heil (2004). Figure 6-4 shows a quantitative comparison of modeled daily mean PM_{10} concentrations and measurements made at two Malaysian stations, Kuching on Sarawak-Malaysia (1.5°N, 110.3°E) and Petaling Jaya/Kuala Lumpur on peninsular Malaysia (3.1°N, 101.4°E), located around 400–800 km downwind from the main source areas of emissions. Measured particle levels at these stations include the particle background concentration (about 40–60 µg/m^3) and input from Indonesian fires, while the modeled particle levels include only fire emissions. Of the Malaysian stations for which measurements exist, these two stations were the most

severely affected by the 1997 smoke haze (Heil and Goldammer 2001). Kuching was influenced only by emissions from fires in southern Kalimantan, whereas advected emissions from fires in Sumatra, and to a lesser extend Kalimantan, influenced Petaling Jaya (Koe et al. 2001).

Observed daily mean particle concentrations at these stations increase gradually, with large daily fluctuations, from an approximate background level in early July to maximum values in September of around 350 µg/m^3 in Petaling Jaya and 1000 µg/m^3 in Kuching (Figure 6-4). Particle concentrations return to background values by mid-November. The reference model experiment (EXP_REF) reproduces observed particle levels at both stations fairly well, as well as the main temporal characteristics. The predicted duration of the main haze episode during September, however, is shorter than observed, notably at Kuching. The shortfall likely stems from an underestimation of fire emissions from Kalimantan in our emission inventory. There is a distinct overprediction (factor of 2–3) of observed concentrations in late July to early August at Petaling Jaya, possibly because of misclassification of fires on Sumatra.

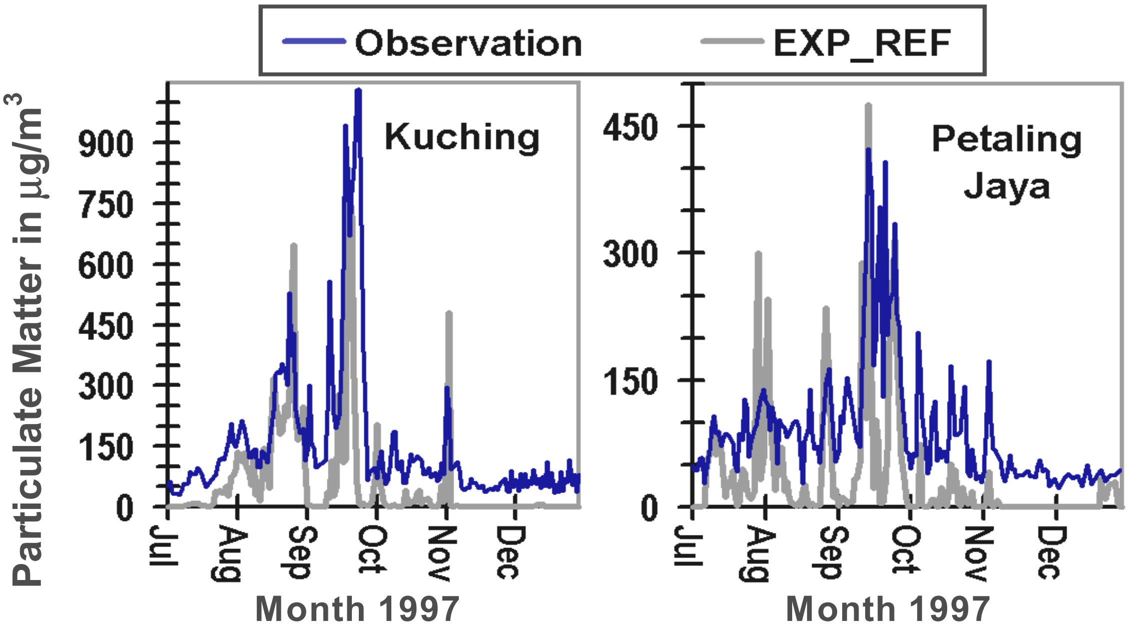

Figure 6-4: Daily mean PM_{10} concentrations modeled in the lowest model layer in EXP_REF and ambient particle measurements at (a) Kuching (total particulate matter TPM) and (b) Petaling Jaya/Kuala Lumpur (PM_{10}) (data source: Malaysian Meteorological Services). Modeled PM_{10} concentrations are directly compared with TPM measurements.

Comparison of the reference run (EXP_REF) and the experiment excluding peat fire emissions (EXP_NOPEAT) (Figure 6-3, middle column) demonstrates the relative importance of surface fires and peat fires in creating smoke haze episodes. Monthly mean PM_{10} concentrations in EXP_NOPEAT show a spatial and temporal pattern largely similar to that of EXP_REF, but with much lower values. Populated areas of northern Sumatra and peninsular Malaysia (including Singapore) are almost entirely spared the exposure to smoke particles in EXP_NOPEAT, whereas distinct increases in particle concentration are predicted for these areas in EXP_REF.

The comparison of EXP_REF and EXP_MET96 (Figure 6-3, right column) demonstrates the influence of meteorological conditions prevailing during an El Niño year (EXP_REF) and a normal year (EXP_MET96) on smoke haze dispersion. Modeled PM_{10} concentrations in the main source areas of emissions in the scenario run EXP_MET96 are largely similar to EXP_REF. The spatial expansion of the smoke haze layer is reduced in EXP_MET96, particularly in October and November, when the monsoon started in 1996. Concentrations are distinctively lower in the northwest regions adjacent to the main fire area in EXP_MET96 than in EXP_REF. Transport of fire emissions to Peninsular Malaysia generally results in monthly mean PM_{10} concentrations of less than 15 μg/m^3. At Kuching and Petaling Jaya, modeled daily mean PM_{10} concentrations in EXP_MET96 (not shown) show a greatly different temporal pattern contrasted with the 1997 meteorology (EXP_REF) (Figure 6-4). Daily mean modeled PM_{10} levels are well below 100 μg/m^3, except for a few days in late August and September at Kuching and in late July and early August at Petaling Jaya. The peak in late July to early August at Petaling Jaya in EXP_MET96 is also demonstrated in EXP_REF and is attributed to the northward expansion of the smoke haze layer originating from fires in southern Sumatra. Compared with EXP_REF, the northward expansion of the smoke haze layer in EXP_MET96 is largely suppressed in the subsequent period (Figure 6-3), resulting in distinctively lower advection of PM_{10} to Petaling Jaya. In summary, the spatial extent in the EXP_MET96 model run is distinctively lower than in the EXP_REF run. The meteorological conditions of a normal year are predicted to result in much smaller increases in particulate air pollution in the highly populated areas of northern Sumatra and peninsular Malaysia (including Singapore).

In our model scenarios, we only predict increases of airborne particles from primary aerosols emitted by the fires. Aged smoke plumes, however, show a significant enrichment in secondary aerosols formed from precursor gases (organic and inorganic gases emitted by the fires) during transport, which may increase total aerosol burden by up to 50% and more (Reid et al. 2004). For this reason, we expect modeled particle levels in smoke plumes downwind of the fires to present a lower boundary. Due to the model's overprediction of wet deposition especially over the ocean, we expect underprediction of particle levels to be most pronounced after a cross-ocean transport, e.g. on peninsular Malaysia.

6.3.2 *Influence of Meteorology on PM_{10} Dispersion*

6.3.2.1 *Meteorological Conditions*

In this section, we compare the meteorological conditions of 1996 and 1997 from model simulations only. Meteorological conditions between 1996 and 1997 are used to explain the discrepancies of model results between EXP_REF and EXP_MET96. Whereas 1996 is considered a normal, non-ENSO year, 1997 is an El Niño year. Figure 6-5 displays monthly total rainfall and mean wind vectors at 925 hPa for model simulations for July to December 1996 (left column) and 1997 (middle column), as well as the wind vector differences between 1997 and 1996 (right column). We chose the 925 hPa level because mean transport of the smoke haze was found to occur at around this mark (Koe et al. 2001).

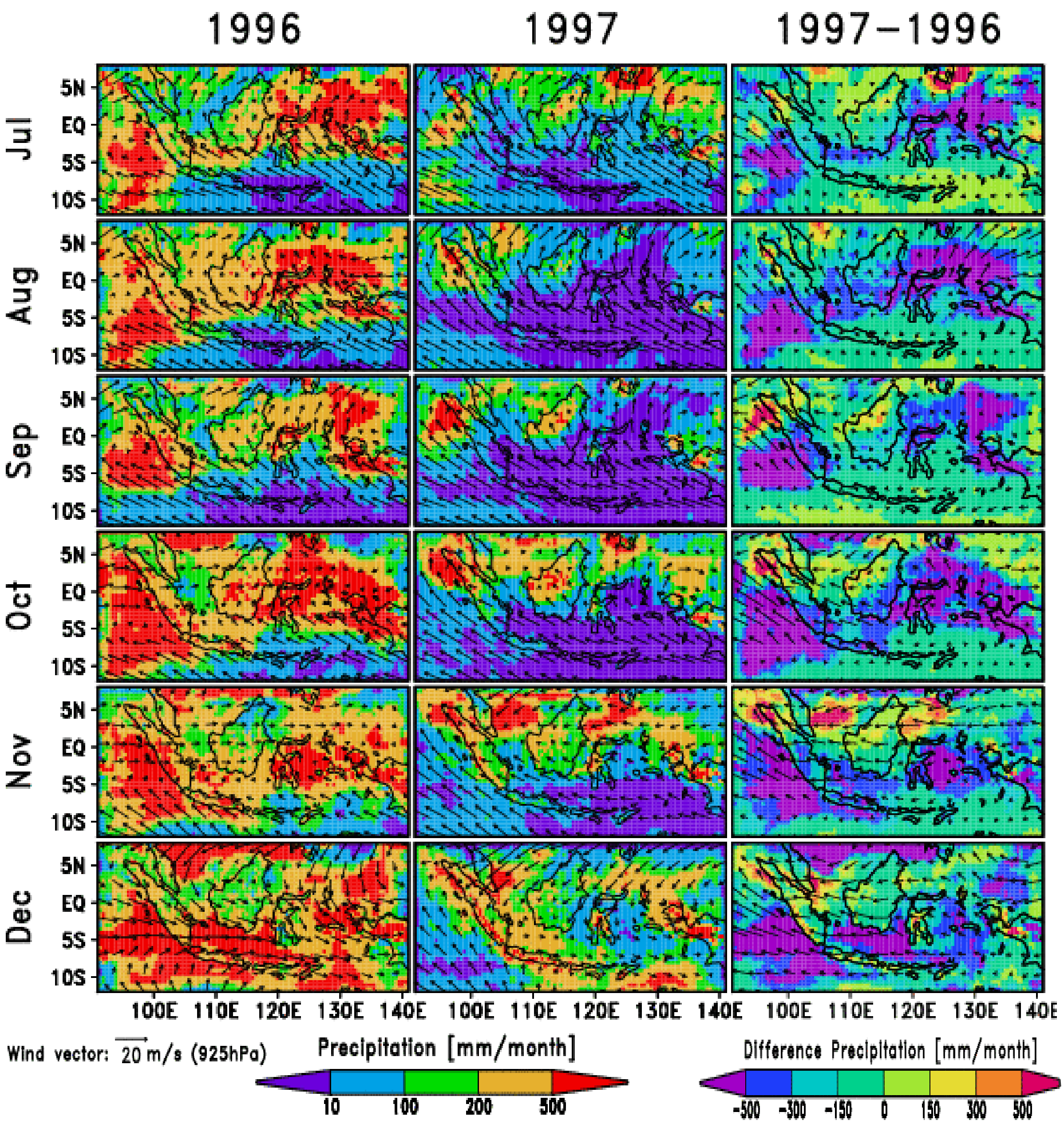

Figure 6-5: Monthly total precipitation and monthly mean wind vectors at 925 hPa for July to December 1996 (left column) and 1997 (middle column). The right column illustrates wind vector differences between 1997 and 1996.

Precipitation patterns are distinctively different in these years because the El Niño phenomenon in 1997 brought strongly reduced precipitation over all Indonesia. Discrepancies occur particularly in regions south of the equator, and the largest differences occur in August and September, when the total dry condition (<10 mm/month) reaches southern Kalimantan and Sumatra. In agreement with Aldrian and Susanto (2003) and references therein indicated, two dominant rainfall climatic regions in the eastern and southern part of Indonesia experience lower amounts of rainfall in El Niño years during the dry period from April to October. During the rainy season, however, the impact of El Niño is unnoticeable. In 1996, the extension of dry area reached out to only the southern Lesser Sunda Islands. The dry season extended until November in 1997 compared with September in 1996. The unusual dryness in 1997 affected three major peat locations in southern Sumatra, southern Kalimantan, and southern Irian Jaya (Figure 6-1 d). In these areas, fire intensity and emission release were highest during the 1997 fire episode (Figure 6-2 a).

Compared with the relatively normal wind conditions in 1996, wind over large parts of Southeast Asia north of around 3◦ south, including the main fire areas on Sumatra and Kalimantan, were more southeasterly in 1997 (Figure 6-5). Especially during July to October 1997 the region exhibited a stronger cross-equatorial flow from southern Sumatra and Kalimantan to peninsular Malaysia and points north. This particular wind pattern during El Niño 1997 provided favorable conditions for an enhanced transport and dispersion of emissions from fires in southern Kalimantan and Sumatra to populated areas in the northwest. Parameswaran et al. (2004) found that strong easterly winds at the equatorial Indian Ocean in 1997 were responsible for the transport of the smoke haze layer to the tropical Indian Ocean (Figure 6-3).

6.3.2.2 Particle Removal by Wet Deposition

In both EXP_REF and EXP_NOPEAT model experiments, modeled maximum wet deposition is shifted around 400 km northwestward from the main source areas of emissions, i.e., the fires cluster in southeastern Sumatra, southern Kalimantan, and southwestern Irian Jaya (Figure 6-6). Wet deposition in the EXP_MET96 model experiment is largely confined over the main source area of emissions and shows higher deposition rates. Maximum wet deposition simulated in EXP_REF of up to 120 g/(m^2 x month) is lower by a factor of 3.5 than the one for EXP_MET96 in October because of rainfall being around five times more intense in 1996 than in 1997 over the main source areas of emissions. With the EXP_NOPEAT scenario, spatial distribution of the wet deposition is similar to EXP_REF, but shows much lower fluxes.

The spatial distribution of the wet deposition differs from the spatial distribution of PM_{10} concentration at the lowest model layer (Figure 6-3) because wet deposition is a function of the entire vertical aerosol column burden and the rainfall. Unfortunately, observational wet deposition data for comparison are unavailable. Figure 6 illustrates the influence of different wind patterns in 1996 and 1997 on wet deposition. As mentioned earlier, more southeasterly winds prevailed in 1997, which contributed to the transport of emissions from main fire areas northwestward. Using meteorological conditions representing a normal year (EXP_MET96), there is less transport of fire emissions away from the main source areas of emissions. Large portions of the fire emissions are then removed from the atmosphere by wet deposition directly over the source regions. Figure 6-6 also illustrates the importance of the quality of rainfall predictions because rainfall determines the amount of wet deposition, which strongly influences the amount of particulate matter remaining in the atmosphere.

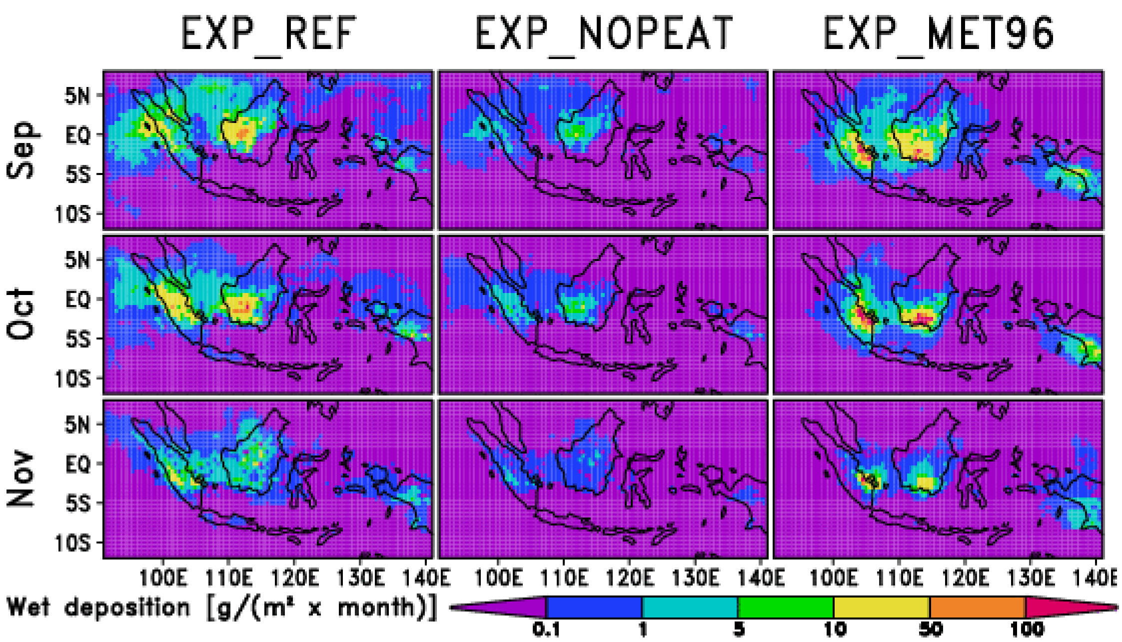

Figure 6-6: Monthly total wet deposition modeled for the scenario runs EXP_REF (left column), EXP_NOPEAT (middle column), and EXP_MET96 (right column).

As noted earlier, we generally expect to overestimate the wet deposition of PM_{10} because of the model's overprediction of precipitation. The effects of fire aerosols on cloud formation, rainfall, and wet deposition, however, are neglected in this study. Several studies have shown that fire aerosols suppress cloud formation and rainfall by a set of complex radiative and cloud microphysical interactions (Graf 2004). Rosenfeld (1999) evidenced that high concentrations of small fire aerosols result in small cloud droplets, which precipitate less efficiently. This microphysical effect strongly depends on particle hygroscopicity, i.e., potential to act as cloud condensation nuclei (CCN) (Reid et al. 2004, and references therein). Because of their high OC/EC ratio and hygroscopicity, Indonesian peat fire aerosols are very efficient CCN (Christian et al. 2003, Reid et al. 2004, see also Table 6-1) and are expected to suppress cloud formation in a significant manner. It is therefore expected that including these interactions into the model's calculations would partially compensate for overprediction of precipitation and particle removal by wet deposition.

6.3.2.3 Vertical Distribution of PM_{10}

The vertical distribution of monthly mean PM_{10} concentration in September for the scenario runs EXP_REF and EXP_MET96 is shown in Figure 6-7 for three locations. Palangkaraya (2.2°S, 113.7°E) is in the vicinity of the main source area of emissions in southern Kalimantan, while Kuching and Petaling Jaya are located around 400 to 800 km north from the fires in southern Kalimantan and Sumatra, respectively.

PM_{10} levels are higher in EXP_REF than EXP_MET96 at all locations and all vertical levels. Fire-related PM_{10} concentration generally decreases with height and reaches very low concentrations at around 4500m at all locations, the strongest decrease occurring below 2000 m. The relative difference in particle concentration between EXP_MET96 and EXP_REF increases with distance of the locations from the main source area of emissions, i.e., 64% at Palangkaraya and around 20% at the other locations. The strong relative reduction of particulate matter concentration up to 1000m height at Palangkaraya is higher in EXP_REF than EXP_MET96. Since emission strengths are similar in both experiments, and rainfall-associated wet deposition is much more reduced in EXP_REF, this result indicates a strong transport away from the source by the enhanced wind in 1997 (see Figure 6-5). Near the source area, EXP_REF shows low vertical mixing, indicating the presence of a strong subsidence. In contrast, the particle concentration reaches higher altitude (2000 m) in locations farther away from the main source area, indicating stronger atmospheric mixing. Koe et al. (2001) found a similar vertical profile of the haze along Singapore with indication of trapping because of inversion at around 1000–1500 m. Parameswaran et al. (2004) also found the smoke haze layer to be generally confined to the lower troposphere (mainly below ~1500 m).

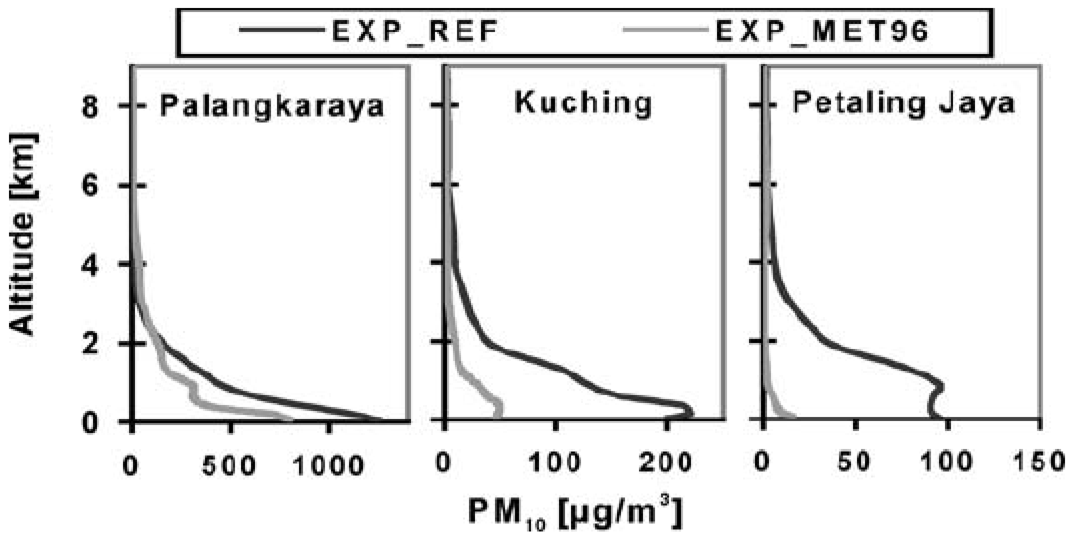

Figure 6-7: Monthly mean vertical distribution of PM_{10} modeled for the scenario runs EXP_REF and EXP_MET96 for September over (a) Palangkaraya, (b) Kuching, and (c) Petaling Jaya/Kuala Lumpur.

6.4 Conclusions and Outlook

The Indonesian fires in 1997 released pyrogenic aerosols in the order of around 55 Tg PM_{10} into the atmosphere, equivalent to around one third of the annual global anthropogenic emissions of primary particles. Using a regional atmospheric chemistry model, we investigated the influence of meteorological conditions and fuel type burnt on large-scale smoke haze pollution.

The particular meteorological conditions prevailing during an El Niño year strongly aggravate smoke distribution to wider areas, including densely populated areas of northern Sumatra and peninsular Malaysia including Singapore. Compared to normal years with similar fire emissions, El Niño conditions strongly reduce removal of particles by wet deposition and favor the cross-equatorial transport of fire emissions. The study also illustrates the dominant role of peat fire emissions in creating severe transboundary air pollution episodes. If peat fires are excluded, ambient air quality standards are exceeded only in areas close to the main fires. Including peat fires, however, air quality standards are exceeded on transboundary scales. During El Niño years, the risk of large-scale, sustained peat fires is much higher because the areas in Sumatra and Kalimantan that experience abnormal dryness contain exceptionally large portions of peat soil. Prevention of fires in peat areas, particularly during El Niño years, is therefore of major importance to the mitigation of adverse health impacts from smoke haze pollution.

The largest uncertainties in model simulation of atmospheric impacts of Indonesian fire emissions stem from missing validated spatio-temporal information on area and depth of peat burnt. Substantial uncertainty also comes from the omission of interactions between fire aerosols and clouds, and of secondary aerosol formation in model studies conducted so far. Further research will address this issue by specifically adapting the regional atmospheric chemistry model REMO to model fire emission dispersion over Indonesia. Such a regional model will be useful for both smoke and fire management and is a promising tool for future impact and mitigation studies.

Acknowledgements

This work was supported by the German Ministry for Education, Science, Research and Technology within Focus Program AFO2000 and by financial assistance of the European Union Project ASIA Pro ECO-ASI/B7-301/2598/20-2004/79071. We thank the meteorological services of Malaysia, Indonesia, and Singapore for providing observational data. We wish to acknowledge valuable comments from M. Pfeffer, P. Weis, and two anonymous reviewers.

7 Public Health Impact of Indonesian Vegetation and Peat Fire Emissions: An Estimate for the Smoke-Haze Event 1997

7.1 Introduction

Over the past decades, forest and peat fires in Indonesia have given rise to several widespread air pollution episodes in the Southeast Asian region. During some of these events, a large number of people were exposed to extreme concentrations of fire aerosols that are comparable to those observed during the famous London smog episode of 1952 (Schwartz 1991, Bell and Davis 2002)[13]. The air pollutants emitted by the Indonesian fires cause a further increase of air pollution levels resulting from urban and industrial sources. This is critical because the background pollution levels are already potentially damaging to health in the Southeast Asian region (Pandey et al. 2006). Air pollution by particulate matter is the most important one with respect to public health in general (Wichmann 2005), and particularly during fire-related air pollution episodes in Southeast Asia (Heil and Goldammer 2001).

Abundant epidemiological studies document a statistically significant exposure-response relationship between increases in particulate air pollution levels and the frequency of adverse acute and chronic health outcomes in various regions of the world (e.g. Ostro 1984, 1987, Pope et al. 1992, Schwartz 1991, 1994, Schwartz and Dockery 1992, Pope 2000, Schwartz 2000, Samet 2000, Ezzati and Kammen 2001, Peters and Pope 2002, Schwartz and Morris 2005). There are indications that exposure to particulate matter may induce inflammatory and coagulation reactions affecting the functioning of the respiratory organs or the immune system. Shortly after an exposure to temporarily increased particle concentrations, acute symptoms such as cough, upper respiratory tract infections, bronchitis and asthmatic attacks may occur. Most susceptible to suffer acute effects from short-term exposure (duration of a day to a few weeks) are people with pre-existing diseases, like elderly people and children. Such short-term exposures also provoke an advancement of death by a few days or weeks among the extremely frails (so-called "harvesting effect") (Künzli et al. 2001). Repeated exposure or continuous long-term exposure to particulate air pollution increases the risk to develop chronic diseases, which increase frailty. Such cumulative health effects include chronic bronchitis, permanent decreases in lung function, and cardiovascular diseases. The effects lead to a reduction in life expectancy (Künzli et al. 2001). If the age distribution of people which die or begin to suffer from pollution induced diseases is known, the cumulative effects of exposure to particulate air pollution within a population are nowadays frequently expressed in years of life lost (YLL) or disability-adjusted life years (DALYs) (Ostro 2004). More generally, they are also expressed in premature mortality cases, which include all deaths of persons whose underlying health condition leads to premature death without being related to the level of pollution shortly before death (Künzli et al. 2001).

The lethal London smog episode of 5-8 December 1952 provoked both, acute and more persistent morbidity and mortality effects (Bell and Davies 2001). The mean concentration of particulate matter smaller than 10 μm (PM_{10}) during the smog episode was 840 $\mu g/m^3$ with maximum concentrations up to 3,000 $\mu g/m^3$. This is around 5.5 times higher than the daily air quality standard of 150 $\mu g/m^3$ PM_{10} established by the US Environmental Protection Agency (USEPA 1999). During the smog episode, mortality rates were more than 300% higher than normally for this period. In total, around 3,000 excess deaths attributable to the smog were observed in Greater London (population 8.3 million) within the 3 weeks following December 5. Bell and Davies (2001) found that elevated death rates persisted more than 3 months after the smog episode. They estimated that at least another 4,000 to 7,000 premature deaths occurred from January to March 1953 as a consequence of the December 1952 smog episode.

[13] see also sections 1.4 and 4.5.2.

Adverse health effects due to exposure to particulate matter including an increased mortality occur even at very low concentrations– with no apparent threshold (Dockery and Pope 1994, Kappos et al. 2004). Adverse health effects related to the exposure to particulate matter are most commonly quantified in terms of relative risks (RR). The RR is the number of incidence of a certain health outcome in a group of persons exposed to increased particulate air pollution divided by the number of incidence of the same health outcome in an unexposed group of the same size. RR estimates in this study refer to an incremental increase in PM_{10} exposure of 10 µg/m^3. According to the review by Dockery and Pope (1994), RR estimates of all-cause daily mortality due to short-term increases in daily PM_{10} exposure range between 1.007 and 1.016. This translates into an average increase in daily mortality risk of 1% per 10 µg/m^3 PM_{10} (weighted mean RR of 1.010).

For long-term (chronic) exposure, the two largest long-term cohort studies conducted so far by Dockery et al. (1993) and Pope et al. (1995) result in a relative increase in premature mortality in adults ($\geq$ 30 years) of 4.3% per 10 µg/m^3 increase in annual mean PM_{10} (weighted mean RR of 1.043, 95% confidence interval (CI_{95}) of 1.026 to 1.061) (Künzli 1999, HEI 2000). The effect of chronic exposure to PM_{10} is higher than for short-term exposure because it incorporates both, the cumulative effects of a life-time or repeated exposure to elevated levels of pollution as well as the effect of short-term exposure (Pope 2000, Künzli et al. 2001). Furthermore, studies have shown that the estimated effect increases with increasing duration of exposure to air pollution, suggesting that the cumulative exposure causes supplementary effects on mortality which cannot only be explained by the day-to-day variations in exposure (Brunekreef and Holgate 2002). According to a recent estimate conducted in the framework of the Clean Air For Europe program of the European Commission (CAFE), permanently increased ambient particulate matter concentrations in Europe cause a reduction in the average life-expectancy by 8.6 months, primarily because of cardiorespiratory diseases and lung cancer, corresponding to a total of 288,000 premature deaths or 3 million of life years lost (Pye and Watkiss 2005).

The magnitude of public health effects due to air pollution episodes caused by Indonesian fires remains largely uncovered and therefore out of the sight of policy-makers. One reason is that epidemiological studies quantifying the effects of these air pollution events by putting together observed increases in air pollution exposure levels and changes in health statistics (number cases of mortality and morbidity) cannot be conducted because of the lack of related information for the affected areas (Sastry 2002). If statistical information is actually available, it is frequently inaccessible in practice. This is the case for Malaysia and Singapore, where first-grade air quality and health related data exist, but are not accessible (compare Masood (1999): “Malaysia backs 'gag' on haze scientists”).

Nevertheless, there are a few studies, which address health impact of the 1997 smoke-haze. However, they are a) either restricted to a relatively small region or b) use satellite-derived exposure levels only or c) assess solely selected acute morbidity effects. A review of these studies is given in the next section (section 7.2).

We apply a widely used approach to assess adverse health effects from particulate air pollution (e.g. Künzli et al. 1999, Künzli et al. 2000, Ostro 2004, Pye and Watkiss 2005) to provide a rough estimate of the magnitude of the public health burden associated with the 1997 extreme smoke-haze event. The approach allows estimating the effects even in the absence of actual health statistics by making use of the exposure-response (ER) relationships between pollution levels and various health outcomes found in epidemiological studies, which are applied to observed or estimated air pollution levels. The ER relationships found for various sites in developed and some developing countries are very similar. Nevertheless, some uncertainty is remaining e.g. to what extent the ER relationships are transferable to the particular exposure situation prevailing during fire-related smoke-haze events in Southeast Asia. So far, there is no sufficient evidence to conclude that fine particles emitted from forest and peat fires are significantly less or more damaging to health than general ambient fine particles (Hinwood and Rodriguez 2005, Naeher et al. 2007). It is therefore reasonable to assume that the ER relationships are probably applicable all over the world.

The aim of this study is to estimate the number of cases of adverse premature mortality attributable to fire-related air pollution using particulate matter (PM) as the single indicator pollutant. PM is chosen because it is considered to represent the relevant aspects of this kind of air pollution best (Sandberg et al. 2002).

7.2 Review of Findings on Morbidity and Mortality Effects of the 1997 Smoke-Haze

Studies quantifying the morbidity and mortality effects of the 1997 smoke-haze based on detailed statistical analysis of patient records from health care units (health care centers, hospitals) have only been conducted for Malaysia, Brunei, Singapore and Thailand so far. For Indonesia, only a few speculative numbers on the health effects exists: according the provincial health offices, acute respiratory infections increased by 180% in South Kalimantan and 380% in South Sumatra during the smoke-haze. In Jambi, Sumatra, there was a 51% increase of respiratory diseases, most of which due to bronchial asthma (Aditama 2000). Of around 600 persons interviewed in Jambi during the smoke-haze, 91% reported haze-related acute respiratory problems and 44% reported shortness of breath when walking (Kunii et al. 2002). Mortality data from the pulmonary ward of Jambi hospital are reported to show an increase in mortality rate by 200% to 400% compared to pre-haze conditions, most of which due to respiratory failure in persons with pre-existing respiratory diseases (Aditama 2000).

Statistical analysis of various observed health outcomes combined with measured air pollution data demonstrate the following health effects of the 1997 smoke-haze in Malaysia, Brunei and Singapore.

Ooyub et al. (2005) investigated the number of daily upper respiratory tract infections (URTI) in adults and asthmatic cases in both, adults and children in the Malaysian province Sarawak (Borneo) during September to mid-October 1997. During this period, smoke-haze conditions were most severe. PM_{10} levels exceeded 210 $\mu g/m^3$ on 13 days during this period (“high-pollution days”), with a maximum of 910 $\mu g/m^3$ PM_{10}. They found that URTI and asthmatic cases were statistically significantly correlated with PM_{10} levels. The coefficient of determination (R^2) for URTI in adults and asthmatic cases in adults and children was 0.56, 0.55 and 0.47 for the entire period, respectively. For high-pollution days, the R^2 values were 0.64, 0.67 and 0.59. During the 13 high-pollution days, at least 7,591 additional cases of URTI in adults, and 4,359 (3,008) asthmatic cases in adults (children) occurred in Sarawak when compared to the average number of cases that have been recorded when PM_{10} levels were below 210 $\mu g/m^3$.

Mott et al. (2005) investigated the cardiorespiratory health effects of the 1997 smoke-haze episode (August to October) among persons who were hospitalized in seven hospitals in Kuching, Malaysia, relative to non-haze conditions during the same period in 1995, 1996 and 1998. They found that there was a distinct, statistically significant smoke-haze related increase in the number of hospitalizations related to cardiorespiratory problems (increase by 18%). Respiratory diseases, which increased by 20%, were the prevalent cause of cardiorespiratory hospitalizations (65%). Among the respiratory diseases, the increase was most pronounced (35%) in hospitalization related to chronic obstructive pulmonary diseases (COPD including asthma). The haze-related enhancement in respiratory hospitalizations increased with increasing age of the patient. Among those aged 40 years and older, the increase was 38% compared to 8% in all younger patients. They also found that elderly persons with previous hospitalization for cardiorespiratory diseases are more likely to be readmitted for the same condition.

Further haze-related medical studies confirm the relevance of the 1997 smoke-haze episode to public health. Emmanuel (2000), for example, investigated changes in outpatient treatments during the 1997 smoke-haze in Singapore. A PM_{10} increase of 100 $\mu g/m^3$ was found to be associated with a 12% and 19% increase in cases of URTI and asthma, respectively. An increase in hospital admissions or mortality was not observed. Brauer and Hisham-Hisham (1998) analyzed outpatient visits in Kuala Lumpur and Kuching during the haze 1997. They found a rise in respiratory-related visits during this period compared to non-haze conditions. Finally, Phonboon et al. (1999)

observed a relative increase in outpatient visits in the moderately haze-affected parts of Southern Thailand in 1997 when compared with unaffected regions in the north of the country. Furthermore, largely similar health effects were found during the smoke-haze episodes that followed the 1997 event in Southeast Asia (e.g. in 1998 and 2002) (Yadav et al. 2003, Mohamed et al. 2004, Ooyub et al. 2005).

In summary, there is sufficient evidence that the 1997 smoke-haze episode resulted in significant increases of adverse health effects among the exposed population. Known effects of enhanced ambient particle concentrations on the human system can causally explain the increases. Generally, smoke-haze particles primarily induced respiratory diseases, most notably URTI and asthma. Persons with pre-existing cardiorespiratory diseases, the elderly and children were most likely to suffer adverse health effects. These characteristic morbidity effects are largely consistent with those observed in various epidemiological studies worldwide. This also applies to RR values found for selected diseases during the smoke-haze. It is therefore reasonable to assume that - similar to epidemiological findings for urban aerosols - the increased exposure to particulate matter during the smoke-haze 1997 resulted not only in additional morbidity cases, but also in additional mortality cases.

The only study known to the author addressing the relationship between smoke-haze related increases in PM_{10} and mortality in 1997 supports this assumption, however, without providing quantitative numbers of additional mortality cases: Sastry (2002) assessed short-term mortality effects of the 1997 smoke-haze episode in Kuala Lumpur by applying statistical models upon daily PM_{10} measurements and daily mortality data contained in the Malaysian vital statistics records. Her analysis showed that non-traumatic mortality rate (excluding accidents etc.) increased by 19% the day after a high-pollution day ($PM_{10} \geq 210\ \mu g/m^3$), corresponding to a RR of 1.007. The mortality effects were highest among the elderly: for persons aged 65 to 74 years, mortality cases increased by 70% following a high-pollution day (RR=1.018). For other age groups the increase was lower and statistically insignificant. Time lag analysis showed that observed increase in mortality was generally due to a short-term displacement of death (in the order of a few days ("harvesting")). The exception is the age group being 65 to 74 years old. In this age group, there were apparently mortality effects also among the nonfrail. The relative increase in mortality risk during the 1997 smoke-haze found by Sastry (2002) falls within the range of RR values for PM_{10}-related short-term mortality commonly reported (Dockery and Pope 1994).

Finally, Jayachandran (2005) indirectly assessed the impact of the 1997 smoke-haze episode on infant and fetal mortality by inferring deaths from "missing children" in the 2000 Census. Information on the spatial and temporal patterns of the air pollution was crudely estimated from daily TOMS (Total Ozone Mapping Spectrometer) Aerosol Index Maps. The results imply that the mortality rate in children younger than 2 years increased by 17% resulting in over 16,400 infant and fetal deaths attributable to fire-related air pollution in Indonesia.

So far, ER-based approaches have only been applied in the study by Ruitenbeek (1999), Shahwahid and Othman (1999) and Hon (1999) to estimate the number of haze-related additional morbidity cases in Indonesia (Kalimantan and Sumatra, only), Malaysia and Singapore in 1997 (Table 7-1). For the assessment, they used an ER function which was obtained by relating daily Air Quality Index (AQI) data for Sarawak-Malaysia with outpatient treatment and hospitalisation (inpatient) figures published by the Sarawak Ministry of Health. The assessment covers only short-term health effects due to haze exposure. The aim of the study is lower bound estimation of the economic costs of the 1997 smoke-haze. Population exposure in Malaysia and Singapore during the 1997 smoke-haze was derived from daily AQI readings combined with population density statistics (Shahwahid and Othman 1999, Hon 1999). In the absence of corresponding air quality information for Indonesia, Ruitenbeck (1999) used a cumulative TOMS (Total Ozone Mapping Spectrometer) Aerosol Index Map for the entire smoke-haze episode 1997 to crudely estimate population exposure to different air pollution levels. The TOMS sensor, which is sensitive to aerosols primarily 1.5 km above ground, provides a value for the atmospheric column burden of UV-absorbing aerosols, which is not necessarily proportional to the aerosol concentration at the ground-level (Herman et al. 1997). As a consequence, the level of confidence of estimated additional morbidity cases for Indonesia is lower than that for the estimates for Malaysia and Singapore.

They estimated that at least 57 Million people were exposed to a higher health risk due to increased fire-related air pollution, most of which in Indonesia (62% or 35.4 Million), followed by Malaysia (31% or 18 Million), and Singapore (7% or 3.8 Million) (Table 7-1). In total, an estimated 11.5 Million additional outpatients and 267,824 hospitalization cases occurred due to short-term effects of the smoke-haze. More than 98.5% of the cases occurred in Indonesia. Correspondingly, the fraction of the population at risk in Indonesia that experiences adverse health impacts is 32% for outpatient cases and 0.8% for hospitalization. These numbers are at least 35 times higher than those estimated for Malaysia and Singapore.

Country KALI=Kalimantan SUMA=Sumatra	**Population at Risk (PaR)** (Million Capita)	**Additional Outpatients** (Outpatient Cases)	**Additional Hospitalization** (Inpatient Cases)	**Monetary Value of Health Costs**[a] (Million US$) *(TDC Total Damage Costs*[b]*)* *{GDP Gross Domestic Product}*
Indonesia (KALI&SUMA) *Ruitenbeek 1999*	35.4	10,403,000 (32% of PaR)	266,695 (0.8% of PaR)	924 (91% of TDC) {0.5% of GDP}
Malaysia *Shahwahid/Othman1999*	18.0	141,112 (0.8% of PaR)	379 (0.002% of PaR)	8.4 (2.7% of TDC) {0.3% of GDP}
Singapore *Hon 1999*	3.8	34,867 (0.9% of PaR)	445 (0.012% of PaR)	4.0 – 13.5 (6.2% of TDC) {< 0.02% of GDP}
Indonesia (KALI&pSUMA)[c] *Aditama 2000*	12.4	36,462 (0.29% of PaR)	15,822 (0.13% of PaR)	n.a. *[2.5 Million working days lost]*

[a] Expenditure due to medical treatment and economical value of health-related workdays or productivity lost.

[b] Total haze-related Damage Costs (TDC): in addition to health-related damage costs, TDC comprise losses in tourism, losses by flight cancellations, productivity loss during the state of emergency, reduction in fishery.

[c] Only parts of Sumatra (pSU), namely the 4 provinces Riau, Jambi, and West and South Sumatra are included into the study.

Table 7-1: Estimated number of additional outpatient and hospitalization cases attributable to the 1997 smoke-haze during September to November in Indonesia, Malaysia and Singapore by Ruitenbeek (1999), Shahwahid and Othman 1999, Hon 1999).

The numbers for Indonesia appear to be unreasonably high, also when related to the number of outpatients and inpatients estimated by the Indonesian Ministry of Health (Aditama 2000) (Table 7-1). It is unclear, however, how the Indonesian Ministry of Health estimated these numbers, making a comparison difficult. Nevertheless, the air pollution levels in Indonesia during the smoke-haze can only partly explain the extremely high fraction of people among those at risk, which in fact experience adverse health outcomes according to Ruitenbeek’s (1999) estimate. Apparently, the usage of TOMS Aerosol Index data combined with the exposure-response function he used led to an overestimation of the actual health effects.

7.3 Methodology

The methodology for assessing the impact of fire-related air pollution on mortality in this study is largely based on Künzli et al. (1999), who quantified the road traffic-related health costs due to air pollution in Austria, France and Switzerland. Similar to Künzli et al. (1999), this study is restricted to the inhalable fraction of airborne PM, generally denoted as PM_{10} (Particulate matter > 10 μm diameter). Although the association between adverse health effects and exposure is statistically more significant for finer particles (Kappos et al. 2004, Wichmann 2005), PM_{10} is chosen because of much less information being available on the emissions of and exposure to finer particles in the study area. We estimate only the longer-term, cumulative mortality effects related to fire-related increases in annual mean PM_{10}-exposure because these they are most important in terms of overall public health impact.

The study area covers a domain ranging from 12.25° South to 8.25° North and 90.75° to 141.25° East covering an area of 12.7 million km^2. The study area covers the regions most affected by the 1997 smoke-haze pollution including Indonesia, Malaysia, Singapore, Brunei, and southern Thailand. The study was restricted to July to December 1997, i.e. the time when the majority all Indonesian fires of the year 1997 occurred.

The impact assessment is subdivided into three major components: 1) modeling the PM_{10} population exposure distribution, 2) derivation of the exposure-response function and demographic baseline statistics, and 3) estimating the number of attributable mortality cases.

7.3.1 Modeling Fire-Related PM_{10} Population Exposure Distribution

As spatially and temporally continuous air quality information covering the entire study area is missing (Heil and Goldammer 2001), fire-related ambient PM_{10} levels were estimated from the model study by Heil et al. (2007)[14]. They used a regional 3-dimensional atmospheric chemistry model (Regional Model REMO) (Langmann 2000) to predict the spatial and temporal dispersion of in total 55 teragram PM_{10} that are estimated to have been emitted by Indonesian vegetation and peat fires during July to December 1997. Fires in Sumatra and Kalimantan caused around 90% of all the fire emissions. The model predicts fire-related PM_{10} concentrations for the study area with 0.5x0.5 degree horizontal resolution ($\approx$ 55km x 55km). PM_{10} from other sources (e.g. traffic, industry) is not considered. The model study represents an intermediate estimate of fire-related air pollution. Detailed information on the fire emission inventory, the model set-up and model validation can be found in Heil et al. (2007). For the assessment of longer-term effects, the increase in the annual mean PM_{10} concentration due to the Indonesian fires was calculated assuming that no PM_{10} was emitted during January to June 1997.

The modeled annual mean fire-related PM_{10} concentrations in 1997 are shown in Figure 7-1. The 1997 Indonesian fires resulted in increases in annual mean PM_{10} levels across entire Southeast Asia (Figure 7-1). Regions south of the fires, however, were only very little affected (increase in annual mean PM_{10} below 1 µg/m^3), including highly populated Java (except some eastern regions) and Nusa Tenggara. Also parts of northern Sumatra, southern Philippines and southern Thailand were only very little affected. In contrast, in areas in the vicinity of the main fires, i.e. southern Kalimantan, southeastern Sumatra and Irian Jaya, annual mean fire-related PM_{10} concentrations are above 250 µg/m^3. The emissions were transported to the northwest by the prevailing southern monsoonal winds (Heil et al. 2007).[15] Around 200 to 600 km downwind to the fires, concentrations are generally above 100 µg/m^3, i.e. far beyond the ambient air quality standard of 50 µg/m^3 PM_{10}. Emissions transported further northward to Singapore, Brunei, and Peninsular Malaysia still result in increases of up to 25 µg/m^3 in the PM_{10} concentration. Considering the prevailing background PM_{10} pollution levels (around 30 to 50 µg/m^3 PM_{10}) in these regions, it becomes clear that the additional contribution from fire emissions caused exceedances of the air quality standard in large areas.

Table 7-2 summarizes the distribution of different fire-related PM_{10} levels among the countries affected by the smoke-haze during 1997. In Indonesia, 69% of all model grid cells over land exhibit an annual mean PM_{10} concentration smaller than 25 µg/m^3. Concentrations above 25 µg/m^3 PM_{10} are almost entirely confined to Sumatra and Kalimantan. 89% of all model grid cells recorded in Indonesia above this threshold can be attributed to these islands (the remainder to Irian Jaya). Compared to Sumatra, larger areas of extremely high concentrations (> 250 µg/m^3 PM_{10}) occur in Kalimantan, reflecting the around 20% higher fire emission production in Kalimantan. In Malaysia, 88% of all model grid cells exhibit an annual mean PM_{10} concentration smaller than 25 µg/m^3.

[14] see also chapter 6.
[15] see also section 6.3.2.

Concentrations above this value occur in Borneo-Malaysia only, demonstrating that Borneo-Malaysia was the most severely affected region in Malaysia. Brunei and southern Thailand experienced an annual mean increase in fire-related PM_{10} concentrations by less than 10 µg/m^3, whereas it increased by 10 to 25 µg/m^3 PM_{10} in Singapore.

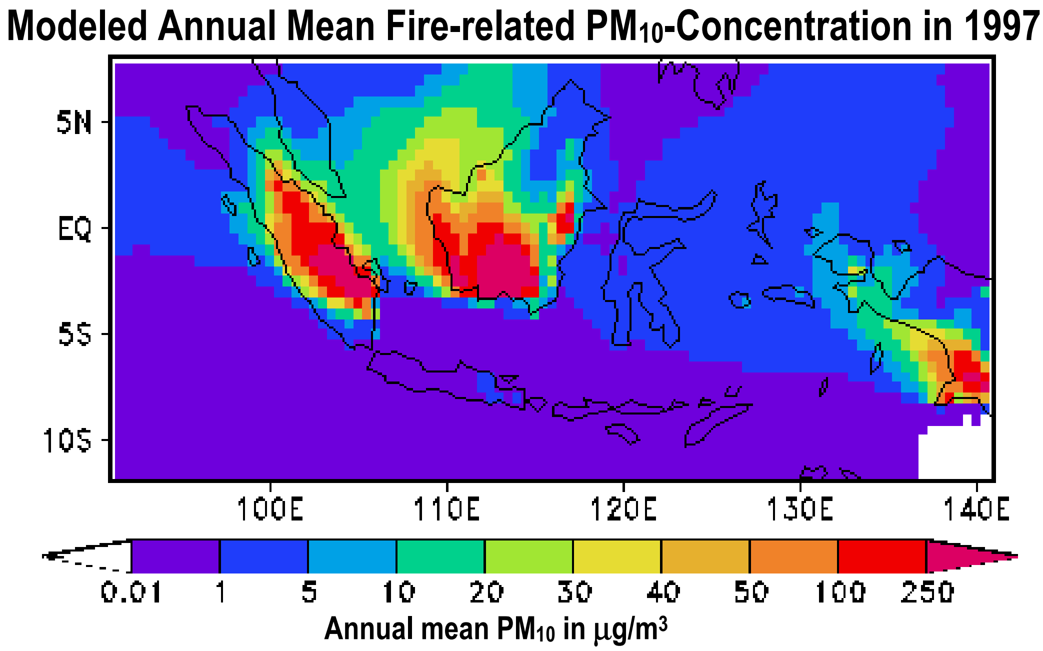

Figure 7-1: Modeled annual mean PM_{10} concentration due to Indonesian fire emissions in 1997.

PM_{10} (µg/m^3)	Indonesia			Malaysia			Bru-nei	Singa-pore	s.Thai-land	*All countries*
	All	SUMA	KALI	All	PI	BO				
1 - 10	514	76	73	94	45	49	3	0	9	**620**
10 - 25	121	43	44	35	17	18	0	1	0	**157**
25 - 50	75	31	31	16	0	16	0	0	0	**91**
50 - 100	70	30	33	1	0	1	0	0	0	**71**
100 - 250	78	32	36	0	0	0	0	0	0	**78**
> 250	56	19	37	0	0	0	0	0	0	**56**
all levels	***914***	***231***	***254***	***146***	***62***	***84***	***3***	***1***	***9***	***1073***
Land Area (10,000 km^2)	*190*	*47*	*54*	*33*	*13*	*20*	*0.6*	*0.1*	*2*	*266*

Table 7-2: Number of model grid cells over land (0.5°x0.5°) within each country, which are in the PM_{10} range given in the first column. The grid area equals 3,061 km^2 to 3,091 km^2 dependent on the latitude. The numbers refer to the annual mean fire-related PM_{10} concentrations (SUMA=Sumatra, KALI=Kalimantan, PI=Peninsular Malaysia, BO=Borneo-Malaysia). Country boundaries are compiled from CIESIN (2005b). Note that the assignment of country or island boundaries due to the coarse resolution of the grid cells leads to some distortion, namely an overrepresentation of land area at coastal boundaries.

In order to estimate fire-related population exposure, i.e. the number of people in each model grid cell exposed to increased PM_{10} levels, fire-related PM_{10} air pollution was related to the number of inhabitants living in each grid. The latter was compiled from population density information for the year 1995 provided by CIESIN (2005a) at a spatial resolution of 2.5 minutes (Figure 7-2).

In total, 197 million people lived in Indonesia 1995, 20 million in Malaysia, 3.8 million in Singapore, 0.3 million in Brunei, and 4.4 million in southern Thailand. Indonesia's population is distributed as follows across the main islands: 117 million in Java (59% of the entire population of Indonesia), 41 million in Sumatra, 14 million in Sulawesi, 11 million in Kalimantan, and the remaining 8% on the other islands (Table 7-3). Correspondingly, Java exhibits a very high population density (generally above 500 persons per km^2. Also Singapore exhibits a very high population density (around 3,800 persons per km^2). High population densities (>150 persons per km^2) also occur in the southern and northern areas of Sumatra and, to a smaller degree, in some coastal areas of Kalimantan. Compared to Sumatra, Kalimantan is sparsely populated. Most inland areas of Kalimantan have a population density below 10 persons per km^2. On average, population density in Sumatra is around 4.3 times higher than in Kalimantan. To the Malaysian population, Peninsular Malaysia contributes 79% (15.8 million). Compared to the Borneo part of Malaysia, Peninsular Malaysia is much more densely populated, notably along its west coast. On average, population density in Peninsular Malaysia is around 5.5 times higher than in Kalimantan (Table 7-3).

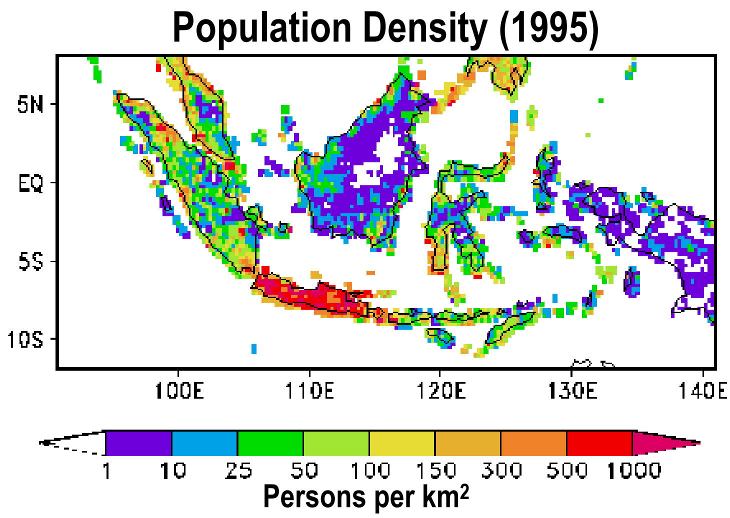

Figure 7-2: Population density in 1995 based on UN adjusted data from CIESIN (2005a).

The multiplicative combination of modeled annual mean PM_{10} concentration with the number of inhabitants in each model grid cell provides an indication of the PM_{10} population exposure resulting from the fires 1997. The population exposure is an estimate of the number of persons exposed to a specific risk level due to enhanced PM_{10} concentrations. For presentability, the calculated population exposure is given for four different PM_{10} ranges in Figure 7-3 and Table 7-3. Regions that were only very little affected by the smoke haze (i.e. PM_{10} < 1 µg/m^3 PM_{10}) are neglected in this study.

PM_{10} (µg/m^3)	Indonesia			Malaysia			Bru-nei	Singa pore	s.Thail and	*All countries*
	All	SUMA	KALI	All	PI	BO				
1 - 10	47.3	14.8	2.7	13.5	11.3	2.2	0.3	0.0	2.5	63.7
10 - 25	6.9	5.5	1.3	4.9	4.5	0.4	0.0	3.8	0.0	15.6
25 - 50	3.7	3.2	0.5	1.1	0.0	1.1	0.0	0.0	0.0	4.8
50 - 100	7.6	5.7	1.9	0.1	0.0	0.1	0.0	0.0	0.0	7.7
100 - 250	7.4	4.2	3.1	0.0	0.0	0.0	0.0	0.0	0.0	7.4
> 250	5.6	4.3	1.3	0.0	0.0	0.0	0.0	0.0	0.0	5.6
all levels	***78.5***	***37.6***	***10.8***	***19.7***	***15.8***	***3.9***	***0.3***	***3.8***	***2.5***	***104.7***
Population (Mio.)	**197.0**	**40.7**	**10.8**	**19.7**	**15.8**	**3.9**	**0.3**	**3.8**	**4.4**	**225.2**
Population Density (persons/km^2)	104	87	20	61	120	22	50	3800	220	85

Table 7-3: Estimated number of people exposed (in million people) to different levels of fire-related PM_{10} exposure in the study area in 1997 (SUMA=Sumatra, KALI=Kalimantan, PI=Peninsular Malaysia, BO=Borneo-Malaysia). The total number of inhabitants in each region is given in the last row.

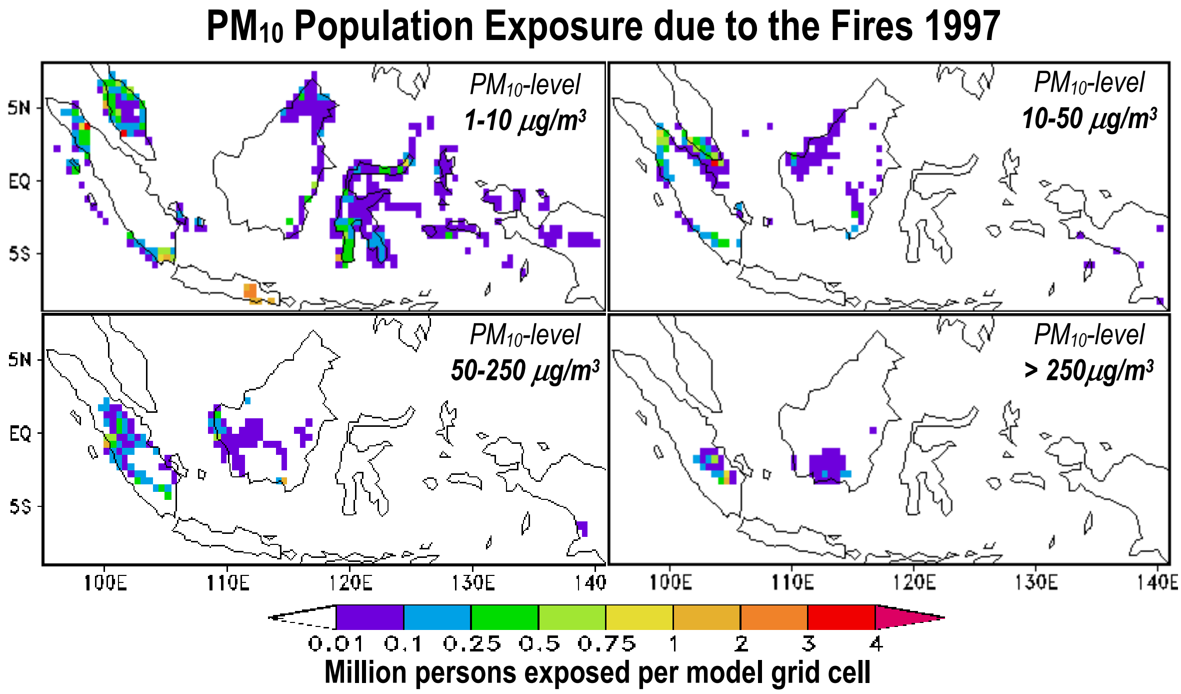

Figure 7-3: Population exposure in 1997 calculated for four different ranges of fire-related annual mean PM_{10} concentrations.

In total, an estimated 105 million people were exposed to increased fire-related PM_{10} levels in 1997 in Southeast Asia (Table 7-3), corresponding to 46% of all people living in this area. 75% (79 million) of all the affected people live in Indonesia, 19% (20 million) in Malaysia, 4% (4 million) in Singapore, 2% in southern Thailand and 0.3% in Brunei. The majority of these people (61% or 64 million) were exposed to annual mean concentrations between 1 to 10 µg/m^3 PM_{10}, most of which live in Sulawesi (including Maluku islands) (16 million), southern and northern Sumatra (15 million), Java (12 million), and Peninsular Malaysia (11 million) (Figure 7-3). Note that the high number of people exposed in Java results from very localized fire-related air pollution in a highly populated region while the high number in Sulawesi results from long-range transport of fire-emissions from Irian Jaya (Figure 7-2 and Figure 7-1). In all the other areas, population exposure is almost exclusively attributed to fire emissions in Kalimantan and Sumatra[16].

Another 20.4 million people were exposed to annual mean PM_{10} concentrations between 10 and 50 µg/m^3 (Table 7-3). Half of them (10.6) lived in Indonesia, either in Sumatra (8.6) or in Kalimantan (1.8 million). The other half lived in southern Malaysia (4.5 million) and Borneo-Malaysia (1.5 million) or in highly populated Singapore (3.8 million) (Figure 7-3). 20.7 million people in Southeast Asia were exposed to fire-related increases in annual mean PM_{10} above 50 µg/m^3. 20.5 million (99%) live in Sumatra and Kalimantan. 5.6 million of these people are exposed to concentrations even above 250 µg/m^3 PM_{10}.

Due to the much higher population density in Sumatra going along with these severely increased PM_{10} levels, population exposure is 3.5 times higher in Sumatra than in Kalimantan (4.3 million versus 1.3 million). This is noteworthy since the area with concentrations above 250 µg/m^3 PM_{10} in Kalimantan is about 2 times larger than in Sumatra. Because of the prevailing southeasterly monsoonal winds over the main fire areas in southern Kalimantan some relatively densely populated areas east of the fires are spared from these high pollution levels.

[16] see also section 4.5.2.

7.3.2 Epidemiology

There is broad evidence that the slope of the ER relationship of particle-related mortality and morbidity effects is generally (near-)linear within concentration ranges typically observed in urban areas in developed countries (generally below 200 µg/m³ and 50 µg/m³ daily and annual mean PM_{10}, respectively) (Dockery et al. 1993, Pope et al. 1995, Daniels et al. 2000, Panyacosit 2000, Pope 2000, Dominici et al. 2002, Roberts 2004, Samoli et al. 2005). This implies that the RR value for a given health outcome is approximately constant in this range.

How the slope of the ER function evolves at higher concentrations – such as those occurring during episodic fire-related air pollution episodes in Southeast Asia – is much more uncertain, but there are indications of a gradual flattening of the curve at higher concentrations (Schwartz and Markus 1990, Spix et al. 1993, Verhoeff et al. 1996, Pope 2000, Samet et al. 2000, Ezzati and Kammen 2001). The World Health Organization (WHO 2001) emphasizes that extrapolating the ER function beyond the range of the pollutant concentrations reported in evidentiary studies has to be considered with caution. For a very conservative effect estimate, the WHO recommends to assume that the slope above this range is zero, i.e. that the health risks remain constant with any incremental particulate matter exposure ("WHO-Model", Wichmann 2004).

In agreement with the near-linear relationship found between chronic PM_{10} exposure and premature mortality for annual mean concentrations up to 50 µg/m³ PM_{10} by Dockery et al. (1993) and Pope et al. (1995), the ER-function is considered to be linear up to this value. Up to an annual mean PM_{10} concentration of 50 µg/m³, the slope of the ER-function for premature mortality in adults is 4.3% per 10 µg/m³, corresponding to the RR estimate of 1.043 used by Künzli et al. (1999). In analogy to Künzli et al. (1999), an additive risk function is used throughout this study because the widely used multiplicative model tends to yield unrealistic high numbers of attributable cases at higher PM_{10} levels. Accordingly, an increase in annual mean PM_{10} exposure of 50 µg/m³ enhances the premature mortality risk by 21.5%.

For PM_{10} exposures above 50 µg/m³, the slope of the ER-function was roughly extrapolated using the observed premature mortality risks associated with cigarette smoking (Formula 7.1). Iwasaki et al. (2006) found that, on average, regular cigarette smokers exhibit a 48 to 83% higher risk in all-cause mortality than non-smokers. Regular smokers were consuming around 25 cigarettes per day, which corresponds to an estimated annual mean exposure of around 20,000 µg/m^3 PM_{10} when assuming that smoking one cigarette per day is related to an annual mean personal exposure of around 800 µg/m^3 PM_{10} (Gamble 1998). Dockery et al. (1993) and Pope et al. (1995) found total mortality rates that were increased by 200% and 207%, respectively, for people smoking on average 20 cigarettes per day. These values translate into an enhancement of premature mortality risk by 0.02% to 0.12% per 10 µg/m^3 PM_{10} annual mean exposure, when a) conservatively assuming a linear ER-function over the entire exposure range above 50 µg/m³ PM_{10} and b) accounting for an 21.5% increase in mortality risk due to the exposure above 50 µg/m³ PM_{10}. In this study, a mean value of 0.06% was chosen for the calculation of additional health effects above. To avoid a possible overprediction of mortality effects notably in highly smoke-haze affected areas, the incremental increase of fire-related PM_{10} exposure above an annual mean of 50 µg/m³ PM_{10} is thus considered to cause only very small additional mortality effects compared to exposures below 50 µg/m³ PM_{10}.

The exposure-response function (ERF) for premature mortality risk in adults (≥ 30 years) for an estimated change point exposure ($cpEX_{PM10}$) of 50 µg/m^3 PM_{10} is defined as follows:

(Formula 7-1)

$$ERF(EX_{PM10}) := \begin{cases} ((RR_{below} - 1)/10) * EX_{PM10} & \text{if } EX_{PM10} < cpEX_{PM10} \\ ((RR_{above} - 1)/10) * cpEX_{PM10} + ((RR_b - 1)/10) * (EX_{PM10} - cpEX_{PM10}) & \text{if } EX_{PM10} \geq cpEX_{PM10} \end{cases}$$

RR_{below} = 1.043 (1.026 - 1.061 95%-Confidence Interval) (Künzli et al. 1999)
RR_{above} = 1.0006 (1.0002 – 1.0012 estimated range) (see text)

with EX_{PM10} is the modeled annual mean PM_{10} exposure (in µg/m^3 PM_{10}), and RR_{below} and RR_{above}, respectively, are the relative risk estimate for a 10 µg/m^3 increment in PM_{10} exposure below and above $cpEX_{PM10}$.

The number (N) of cases of premature death attributable to each modeled fire-related annual mean PM_{10} exposure level (EX_{M10}) and each country or region (c) can be calculated as follows:

(Formula 7-2)

$$N(EX_{PM10},c) := NPop(EX_{PM10},c) * fA(c) * Base(c) * 10^{-3} * ERF(EX_{PM10})$$

with $NPop(EX_{PM10},c)$ is the number of people in each country (c) modeled to be exposed to EX_{PM10},
fA(c) is the country-dependent fraction of adults (≥ 30 years) within Npop, and
Base(c) is the country-dependent baseline mortality rate in adults per year and 1,000 persons.
The latter were derived from the demographic statistics contained in SEAMIC (2001) (Table 7-4).

Demographic Parameter		Indonesia	Malaysia	Brunei	Singapore	s.Thailand
Fraction of Adults (≥30 years) in the Population	*fA*	0.41	0.38	0.41	0.56	0.46
Baseline Mortality Rate in Adults (deaths per 1,000 persons and year)	*Base*	12.3	9.9	5.8	7.7	10.6
Baseline Mortality Cases among the Adult Population (in 1,000 persons per year)		*993.5*	*75.2*	*0.7*	*16.4*	*21.5*

Table 7-4: Country-specific demographic data calculated from SEAMIC (2001). The baseline mortality rate refers to the year 1999, when smoke-haze related effects on mortality are considered as negligible.

The overall number of premature mortality cases in 1997 in each country is calculated from the sum of $N(EX_{PM10},c)$ over the entire range of fire-related increases in PM_{10} exposure (Table 7-5). To provide an estimate of the uncertainty range resulting from the uncertainty in the RR values alone, the 95%-confidence interval (CI_{95}) of the RR_{below} value (estimated range for RR_{above}) was used in the calculation.

7.4 Estimated Additional Premature Mortality Cases

Using the method described in section 7.3, the total population burden of premature mortality (age ≥ 30 years) in Southeast Asia caused by PM_{10} air pollution due to the 1997 fires in Indonesia is estimated to reached 35,487 additional cases (CI_{95} 22,248-53,687) (Table 7-5). Indonesia as the source region of emissions exhibits the highest total population burden with about 31,093 additional premature mortality cases (CI_{95} 19,894-48,165). Transboundary transport of fire emissions to the neighboring countries results in another 4,063 additional mortality cases in the Southeast Asian region (CI_{95} 2,457-5,764), most of which (74%) in Malaysia (3,007 cases, CI_{95} 1,708-4,007), followed by Singapore (936 cases, CI_{95} 566-1,328), southern Thailand (99 cases, CI_{95} 67-157) and Brunei (21 cases, CI_{95} 12-29).

PM_{10} ($\mu g/m^3$)	Indonesia All	Indonesia SUMA	Indonesia KALI	Malaysia All	Malaysia PI	Malaysia BO	Brunei	Singapore	s.Thailand	*All countries*
1 - 10	3,114 *1,883-4,418*	1,543 *933-2,188*	349 *211-495*	1,258 *760-1,784*	1,134 *685-1,608*	124 *75-176*	21 *12-29*	0 *0-0*	99 *60-140*	4,491 *2,716-6,371*
10 - 25	2,380 *1,439-3,376*	1,916 *1,159-2,719*	414 *250-587*	1,073 *649-1,522*	958 *579-1,359*	115 *70-163*	0 *0-0*	936 *566-1,328*	0 *0-0*	4,388 *2,653-6,225*
25 - 50	2,986 *1,805-4,236*	2,328 *1,407-3,302*	614 *371-871*	563 *340-799*	0 *0-0*	563 *340-799*	0 *0-0*	0 *0-0*	0 *0-0*	3,549 *2,146-5,035*
50 – 100	8,252 *4,991-11,756*	6,203 *3,752-8,838*	2,027 *1226-2888*	114 *69-162*	0 *0-0*	114 *69-162*	0 *0-0*	0 *0-0*	0 *0-0*	8,365 *5,059-11,918*
100 – 250	8,073 *4,889-11,730*	4,640 *2,810-6,743*	3,367 *2039-4890*	0 *0-0*	0 *0-0*	0 *0-0*	0 *0-0*	0 *0-0*	0 *0-0*	8,073 *4,889-11,730*
> 250	6,619 *4,037-10,657*	5,127 *3,128-8,266*	1,474 *899-2364*	0 *0-0*	0 *0-0*	0 *0-0*	0 *0-0*	0 *0-0*	0 *0-0*	6,619 *4,037-10,657*
all levels	***31,424*** *19,894-48,165*	***21,756*** *13,365-32,470*	***8,245*** *4,897-11,861*	***3,007*** *1,708-4007*	***2,091*** *1,175-2,756*	***916*** *533-1,251*	***21*** *12-29*	***936*** *566-1,328*	***99*** *67-157*	***35,487*** *22,248-53,687*

Table 7-5: Estimated number of premature mortality cases in adults due to different levels of fire-related PM_{10} exposure in the study area in 1997 (SUMA=Sumatra, KALI=Kalimantan, PI=Peninsular Malaysia, BO=Borneo-Malaysia). The italic numbers represent the estimated lower and upper bound of the confidence (CI_{95}) (see text).

Most of the smoke-haze related Indonesian mortality cases (69%) are predicted to occur in Sumatra (21,756 cases as central estimate). Kalimantan covers 26% of the Indonesian mortality burden (8,245 cases). The remaining 5% are distributed among the other islands (Figure 7-4). Sumatra thus exhibits 2.6 times more mortality cases than Kalimantan, although PM_{10}-emission production and the related expansion and severity of fire-related PM_{10} air pollution in Sumatra was lower (Table 7-2). As discussed in Section 7.3.1, this discrepancy can be explained by the much higher population density in the areas in Sumatra that were affected by distinctively elevated PM_{10} levels (Figure 7-3). Peninsular Malaysia even exhibits a 5.5 times higher fire-related mortality burden (2,091 cases) compared to Borneo-Malaysia (916 cases). Also here, the much higher population density in Peninsular Malaysia – notably along its west coast, which was most affected by smoke-haze (Figure 7-1) – is responsible for the higher mortality burden. The clustering of additional mortality cases along the west coast from Singapore to Kuala Lumpur is clearly visible in Figure 7-4. The mortality burden in these regions mainly emanates from PM_{10} that was advected from fires in Sumatra (see also Section 6.3.2).

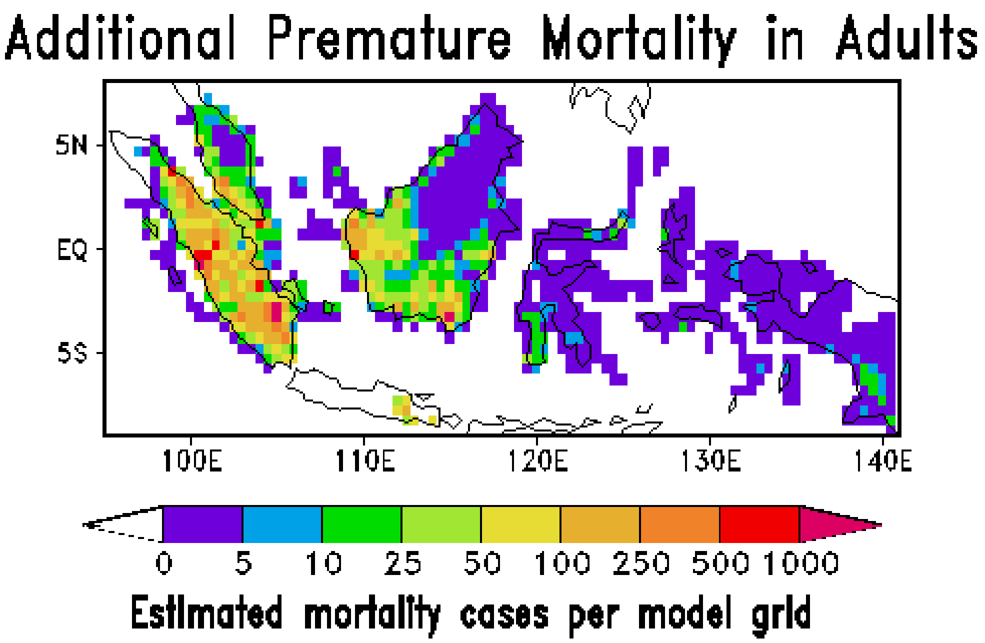

Figure 7-4: Estimated additional premature mortality cases in adults related to increases in PM_{10} exposure due to the 1997 Indonesian fires.

7.5 Discussion

According to this estimate, the number of additional premature mortality cases in the Southeast Asian region related to the 1997 smoke-haze event were within the range of 22,000 to 54,000 cases. The bulk of the cases (around 90%) occurred in Indonesia, notably on Sumatra, while the remaining 10% of additional mortality cases occurred due to long-range transport of Indonesian fire emissions to the neighboring countries. Most affected by the transboundary fire-related air pollution effects was Peninsular Malaysia, where the additional mortality burden is estimated to range between 1,700 to 4,000 cases. PM_{10} emissions from the 1997 fires in Indonesia are estimated to have increased total mortality among the adult population by around 3% in the affected regions, provided that all estimated additional haze-related mortality cases had occurred within a single year ("baseline mortality cases", Table 7-4).

So far, there are no estimates available on additional premature mortality cases in adults connected to the 1997 smoke-haze episode that could be used for comparison. The only mortality estimate available on the 1997 smoke-haze episode by Jayachandran (2005) refers to infant and fetal mortality. Jayachandran (2005) estimated over 16,400 attributable cases in Indonesia, which is about half the number of premature mortality cases in adults estimated in our study.

In a recent estimate of the global burden of disease (GBD), outdoor air pollution in urban areas was found to account for 0.8 million cases of premature deaths in the year 2000, which is approximately 1.4% of total mortality (Ezzati et al. 2002, Ostro 2004, Cohen et al. 2005). Approximately 32,000 cases occur per year in Indonesia alone (Ezatti et al. 2002), of which at least around 4,500 cases in Jakarta (Gronskei et al 1996). This study indicates that the additional public health burden of the severe air pollution episode caused by the 1997 fires was in the same order of magnitude than the permanently elevated air pollution levels in urban areas of Indonesia.

Although fire emission production was higher in Kalimantan than in Sumatra, the impact of the fires in Kalimantan on mortality was lesser because of the much lower population density near or downwind to the Kalimantan fires. Furthermore, the outflow of the smoke-plumes from fires in Sumatra resulted in high local additional mortality in highly populated Singapore, western Peninsular Malaysia, and southern Thailand. It therefore appears that due to the demographic distribution in the region and the prevalent pattern of fire emission dispersion, PM_{10} emissions from fires in Sumatra exert the highest public health burden on mortality.

This study has been restricted to the longer-term effects of particulate air pollution caused by the 1997 Indonesian fires on premature mortality. In addition to mortality impacts, which primarily occur among the elderly, the fire aerosols emitted will cause acute and chronic diseases, such as respiratory tract infections, asthma, impaired lung function and cardiovascular dysfunctions. Respiratory tract infections, for example, are the leading cause of the burden of disease globally especially among children and in developing countries (Ezzati and Kammen 2001). Morbidity effects induced by fire related air pollution are potentially large and would need to be included into further studies in order to quantify the total public health burden associated with the fires.

Despite the large uncertainties involved in the assessment, the results indicate that public health burden from Indonesian fire emissions is considerable and that activities are urgently required to reduce this health risk.

8 Conclusion and Outlook

8.1 Conclusion

The overall objective of this study was to assess the impact of emissions caused by Indonesian surface vegetation and peat fires on air quality and human health in the Southeast Asian region and to investigate the influence of the El Niño Southern Oscillation (ENSO) on fire emission production and smoke plume dispersion. These research questions, outlined in detail in Chapter 1.6, have been scientifically addressed using a broad spectrum of methods and data sources, which include statistical analysis of various observational datasets (ground-based and satellite measurements) and numerical simulations of the atmospheric transport of fire aerosols and their impacts on air quality and human health.

The relationship between ENSO conditions, precipitation anomalies and temporal and spatial relationships of fire activity in Indonesia has been investigated separately for surface vegetation and peat fires using monthly time series analysis. The statistical analysis takes advantage of recently available satellite-derived precipitation and fire activity data that provide a complete spatial and temporal coverage of the entire Southeast Asian region over the period 1998 to 2006. Interannual variations in precipitation anomalies during the traditional land clearing fire season in Indonesia from July to November (JASON) show to be clearly connected to the state of the ENSO, with abnormally dry (wet) conditions prevailing during El Niño (La Niña). Linear correlation of the mean Ocean Niño Index (ONI) and precipitation yields a coefficient of determination (R^2) of 0.86 for Indonesia. Within Indonesia, the correlation is more pronounced for Kalimantan (R^2 of 0.74) than for Sumatra (R^2 of 0.58). The proportion of the land area in Kalimantan that experiences severe drought (< 50 mm per month) during El Niño is much higher than in Sumatra, and affects around 48% of Kalimantan's peat areas and only 25% of the non-peat areas. Such severe drought conditions strongly increase flammability of fuels. Kalimantan's peat areas have therefore a particularly high susceptibility for sustained burning during these periods, if ignited. Accordingly, the strongest correlation between JASON total peat fire activity during 1996 to 2006 and the mean ONI index was found for Kalimantan (R^2 of 0.69), while the connection is weaker for Sumatra (R^2 of 0.48). In summary, the results indicate that fire activity in Indonesia, and notably peat fire activity in Kalimantan, can be realistically predicted by ENSO indices.

The Indonesian fire emission inventory established for the period 1960 to 2006 represents the first attempt to individually quantify emissions from surface vegetation fires and peat fires. Peat fires contribute 22% to the total area burned in Indonesia, but 58%, 78% and 88% to the total carbon (C), carbon monoxide (CO) and particulate matter (PM) emitted by all fires. More than 95% of these emissions resulted from fires on the islands Sumatra and Borneo-Kalimantan. The interannual variability of fire emission production is large. In the 1990ies, annual total C emissions varied by a factor of 22, i.e. from 0.05 GtC in 1996 to 1.1 GtC in 1997. The emissions produced by the 1997 El Niño fires in Indonesia were the highest throughout 1960 to 2006, contributing roughly 30% to the global annual emissions of CO and PM produced by anthropogenic sources and fires. Fires in Indonesia may thus considerably influence the interannual variability of the global budget of atmospheric trace species.

The aerosols released by the 1997 fires resulted in a severe air pollution episode in Southeast Asia. Daily mean PM levels reached 2000 $\mu g/m^3$ and more in Indonesian locations close to the most extensive fires during July to November, exceeding the ambient air quality standard by at least a factor of 7. Also downwind to the fires in Malaysia and Singapore, air quality standards were frequently exceeded.

The evaluation of the regional atmospheric climate model REMO with observations for the period 1997/98 showed a sufficiently accurate prediction of the dispersion of Indonesian fire aerosols throughout the Southeast Asian region for our purposes. However, the model tends to overpredict the precipitation rate and may therefore yield too low particle concentrations downwind from the fires. Modeled concentrations are most realistic when prescribed fire emissions are in the order of about 1 GtC. It has been demonstrated that fires in peat areas play the prominent role in regional air pollution episodes. Furthermore, strongly reduced rainfall and the generally stronger southeasterly winds prevailing during El Niño years aggravate the severity of these episodes.

A first assessment of the health impact associated with fire-related increase in PM concentrations during the 1997 smoke-haze episode has been done. In total 105 million people in Southeast Asia were exposed to fire-related air pollution, 75% of which live in Indonesia and 20% in Malaysia. Virtually all (99%) of the 20.7 million people, which were exposed to fire-related increase in annual mean PM levels above 50 µg/m^3 live in Sumatra and Kalimantan. The number of additional premature mortality cases in adults related to this exposure is estimated to be between 22,200 to 53,700. This would imply that total mortality among the adult population increased by around 3%. Regionally, the largest public health burden was observed in Sumatra (13,400 to 32,500 premature mortality cases), followed by Kalimantan (4,900 to 11,900). Malaysia, and notably Peninsular Malaysia, suffers the highest public health burden from the transboundary transport of fire emissions. An estimated 1,200 to 2,800 additional mortality cases occurred in Malaysia. Due to the population distribution in the region and with the prevalent pattern of fire emission dispersion, PM emissions from fires in Sumatra, although lower than from Kalimantan, exert the highest public health burden.

8.2 Outlook

This study provided a first step forward towards a comprehensive understanding of the complex linkages between fires in Indonesia, climate variability, atmospheric transport of fire aerosols, air quality and human health. Several aspects, however, still need to be analyzed in more detail. This detailed analysis would strongly benefit from advanced satellite fire monitoring systems and improvements in the regional atmospheric chemistry model REMO that are currently in development.

The level of confidence in the modeled concentrations of fire aerosols is still largely constrained by *i)* uncertainties in the emission data and *ii)* inaccuracies in the simulated transport and removal processes. Both aspects currently represent a major limitation for in-depth atmospheric impact studies and would need to be addressed with priority. Most promising activities are:

i) Improvements of Emission Data

- Use of satellite-derived fire radiative energy (FRE) measurements for emission estimation.

  The FRE refers to the emitted radiant energy released per time by a fire, which is related to the rate at which fuel is being consumed. Recently, Ichoku and Kaufman (2005) published an approach to quantitatively estimate the emission rate of fire aerosols and other trace species directly and exclusively from FRE MODIS data which are available since the year 2000. To a large extent, it circumvents the large uncertainties in the parameterization of area burned, fuel density and combustion efficiency of the ‘classical’ emission estimation approach used in this study. Its successful application to Indonesia is thus likely to greatly reduce the uncertainties of estimated fire emissions. In contrast to most available fire satellite products, the FRE data allows for the calculation of the buoyant plume rise induced by the fire, which, when used in atmospheric chemistry modeling, is important to realistically parameterize the effective height at which the emissions are released.
- Establishment of land cover type-dependent scaling factors to convert active fire count data to area burned using high-resolution burn scar scenes.

  Area burned data which were derived from the relatively coarsely resolved active fire pixels suffer from large uncertainties because too simplistic assumptions are used of what fraction of the 1 km^2 pixel actually burned. An approach to reduce and statistically quantify these uncertainties is to make use of a large set of post-fire ERS-Synthetic Aperture Radar (SAR) scenes, which contain precise and spatially highly resolved area burned (burn scar) information for the restricted area covered by each scene. The scenes can therefore be used to derive a probabilistic description of the actual average area burned per detected fire count, discriminated by vegetation type and preferentially other variables that may strongly influence the relation between fire counts and actual area burned (e.g. preceding rainfall).

- Development of mechanistic modeling approach to calculate peat fire emissions.

  In current studies, a fixed peat depth burned is assumed. More realistic results are expected from a more mechanistic approach that predicts the probability of ignition and the subsequent vertical propagation of the combustion zone within a vertical peat soil column as function of the actual moisture. Peat soil moisture can be calculated using a hydrological model that takes into account the amount of prior rainfall.

ii) Improvements of the atmospheric transport model

- Implementation of size-resolved aerosol microphysics module into REMO.

  The bulk aerosol approach used in REMO for this study does not calculate a size-resolved concentration of the aerosol load. Similarly, only average chemical properties of the aerosol particles are taken into account. This leads to considerable inaccuracies in the prediction of the aerosol concentration. Furthermore, the bulk approach does not provide direct predictions of the particle size fractions (PM_{10}, $PM_{2.5}$) relevant to ambient air quality and public health. A promising alternative is the microphysical aerosol module M7 (Vignati et al. 2004), which explicitly simulates the chemical composition and size distribution of airborne particulate matter.
- Implementation of a new convection scheme into the regional model REMO.

  With its current parameterization, REMO tends to strongly overpredict precipitation over Indonesia and the neighboring regions, most notably over the sea. Consequentially it also over predicts the atmospheric removal of fire aerosols by wet deposition. Recently, Graf and Yang (2007) implemented a new Convective Cloud Field Model (CCFM) into REMO, which clearly improves the simulated precipitation patterns and total rainfall. The use of this advanced model will not only be beneficial for more realistic regional predictions of fire-related air pollution levels. Longer-term predictions of rainfall obtained by such a model could also provide a solid basis to gain a better understanding of the interaction of fire, rainfall and climate in the Indonesian region.

These improvements will provide a promising basis to advance public health-related impact studies of air pollution episodes caused by Indonesian fires aiming at quantifying both, the attributable short-term and long-term morbidity effects over the last decades.

In a more applied direction, the development of a combined fire emission-atmospheric transport model using near-real time atmospheric boundary and fire data would provide a system that can be used for early warning of fire-related air pollution. Such predictions can support the management of fires (controlled burning) aiming at the reduction of smoke-related health impacts.

REFERENCES

(Scientific Journals, Monographies and Grey-Literature)

Abbey DE, Ostro BE, Frase G, Vancuren T, and Burchette RJ (1995) Estimating fine particulates less than 2.5 microns in aerodynamic diameter ($PM_{2.5}$) from airport visibility in California. Journal of Exposure Analysis and Environmental Epidemiology 5: 161-180.

ADB (Asian Development Bank)/BAPPENAS (National Development Planning Agency) (1999) Causes, Extent, Impact and Costs of 1997/98 Fires and Drought. Final Report, Annex 1 and 2, Planning for Fire Prevention and Drought Management Project, Asian Development Bank TA 2999-INO Fortech, Pusat Pengembangan Agribisnis, Margueles Pöyry, Jakarta, Indonesia. Available online at http://www.adb.org/Documents/Reports/Fire_Prevention_Drought_Mgt/default.asp (25 November 2003).

Aditama TY (2000) Impact of haze from forest fire to respiratory heath: Indonesian experience. Respirology 5: 169-174.

Ahmad-Zainal MI (2001) Forest Fire in Malaysia: Its Management and Impact on Biodiversity. Asean Biodiversity 1(3): 31-35.

Aidid SB (1985) Multi-element studies of air particulates collected during the hazy periods in Kuala Lumpur, Malaysia. Malaysian Journal of Physics 6(71): 71-80.

Aldhous P (2004) Land remediation: Borneo is burning. Nature 432: 144-146, doi:10.1038/432144a.

Aldrian E (2003) Simulations of Indonesian Rainfall with a Hierarchy of Climate Models. Dissertation at the University of Hamburg, Faculty Geosciences, Examination Report No. 92, Max-Planck-Institute for Meteorology, Hamburg, Germany.

Aldrian E and Susanto RD (2003) Identification of three dominant rainfall regions within Indonesia and their relationship to sea surface temperature. International Journal of Climatology, 23(12): 1,435-1,452.

Aldrian E, Dümelich-Gates L, Jacob D, Podzun R, and Gunawan D (2004) Long term simulation of the Indonesian rainfall with the MPI Regional Model. Climate Dynamics 22: 795-814.

Aldrian E, Dümenil-Gates L and Widodo FH (2007) Seasonal variability of Indonesian rainfall in ECHAM4 simulations and in the reanalyzes: The role of ENSO. Theoretical and Applied Climatology 87 (1-4), doi: 10.1007/s00704-006-0218-8.

Anaman KA and Ibrahim (2003) Statistical Estimation of Dose-response Functions of Respiratory Diseases and Societal Costs of Haze-related Air Pollution in Brunei Darussalam. Pure and Applied Geophysics 160(1): 279-293.

Anderson IP (2001) NOAA/GIS Training Expert, Final Report of Forest Fire Prevention and Control Project; Palembang, Indonesia, in cooperation with the European Union and the Ministry of Forestry. Forest Fire Prevention and Control Project; Palembang, Indonesia. Available online at http://www.dephut.go.id/INFORMASI/PHPA/FFPCP/PDF/NOAA_GIS_Training_Expert_final_report.PDF (25 December 2002).

Andreae MO (1991) Biomass burning: Its history, use, and distribution and its impact on environmental quality and global climate. In: Levine JS (ed) Global biomass burning. Atmospheric, climatic, and biospheric implications. MIT Press, Cambridge, Massachusetts (pp 3-21).

Andreae MO (1998) The IGAC Biomass Burning Experiment (BIBEX): rationale and evolution. International Global Atmospheric Chemistry (IGAC) Project Newsletter IGACtivities No. 15: 2-3.

Andreae MO and Merlet P (2001) Emission of trace gases and aerosols from biomass burning. Global Biogeochemical Cycles 15 (4): 955-966.

Andreae MO, Atlas A, Cachier H, Cofer III WR, Geoffrey WH, Helas G, Koppmann R, Lacaux J-P, and Ward DE (1996) Trace gas and aerosol emissions from savanna fires. In: Levine JS (ed) Biomass burning and global change. MIT Press, Cambridge, Massachusetts (pp 278-295).

Andreae MO, Rosenfeld D, Artaxo P, Costa AA, Frank GP, Longo KM, and Silva-Dias MAF (2004) Smoking Rain Clouds over the Amazon. Science 303 (5662), 1337, doi 10.1126/science.1092779.

Andriesse JP (1988) Nature and Management of Tropical Peat Soils. FAO Soils Bulletin 59. Soil Resources, Management and Conservation Service, FAO Land and Water Development Division, FAO - Food and Agriculture Organization of the United Nations, Rome. Available online at http://www.fao.org/docrep/x5872e/x5872e00.htm (12 January 2003).

Arino O and Rosaz J-M (1999) 1997 to 1999 ATSR World Fire Atlas. Proceeding of the Joint Fire Science Conference, Boise, 15-17 June 1999, University of Idaho.

Arndt RL, Carmichael GR, Streets DG, and Bhatti N (1997) Sulfur dioxide emissions and sectoral contributions to sulfur deposition in Asia. Atmospheric Environment 31(10): 1,553-1,572.

ASEAN (Association of South East Asian Nations) (2001) Second ASEAN State of the Environment Report 2000. Technical Report, ASEAN Secretariat, Jakarta, Indonesia.

Awang M (1998) Environmental studies to control the atmospheric environment in East Asia. Department of Environmental Sciences, Universiti Putra Malaysia, 43400 UPM, Serdang, Selangor, Malaysia.

Awang M, Hisham J, Benedict I, Sahani M, and Kumarjothy J (1998) Country report Malaysia. Report prepared for the biregional workshop on health impacts of haze-related air pollution, Kuala Lumpur, Malaysia, 1 -4 June 1998. Kuala Lumpur: World Health Organization, WPR/EHH/EHE(O)(1)/98/INF./3.

Awang MB, Jaafar AB, Abdullah AM, Ismail MB, Hassan MN, Abdullah R, Johan S, and Noor H (2000) Air quality in Malaysia: Impacts, management issues and future challenges. Respirology 5 (2): 183-196, doi:10.1046/j.1440-1843.2000.00248.x.

Balasubramanian R, Qian W-B, Decesari S, Facchini MC, and Fuzzi S (2003) Comprehensive characterization of $PM_{2.5}$ aerosols in Singapore. Journal of Geophysical Resarch 108(D169) 4523, doi:10.1029/2002JD002517.

Balasubramanian R, Victor T and Begum R (1999) Impact of biomass burning on rainwater acidity and composition in Singapore. Journal of Geophysical Research 104 (D21): 26,881-26,890.

Bartholome E and Belward A (2005) GLC2000: a new approach to global land cover mapping from Earth observation data. International Journal of Remote Sensing 26(9): 1,959-1,977.

Bell ML and Davis DL (2001) Reassessment of the Lethal London Fog of 1952: Novel Indicators of Acute and Chronic Consequences of Acute Exposure to Air Pollution. Environmental Health Perspectives 109 (3): 389-394.

Berlage HP (1927) East-monsoon forecasting in Java. Verhandelingen 20, Koninklijk Magnetisch en Meteorologisch Observatorium te Batavia, Magnetic Meteorology Observation, Batavia, Indonesia.

Bertschi IT and Jaffe DA (2005) Long-range transport of ozone, carbon monoxide, and aerosols to the NE Pacific troposphere during the summer of 2003: Observations of smoke plumes from Asian boreal fires. Journal of Geophysical Research 110, D05303, doi:10.1029/2004JD005135.

Board AS, Fuelberg HE, Gregory GL, Heikes BG, Schultz MG, Blake DR, Dibb JE, Sandholm ST, and Talbot RW (1999) Chemical characteristics of air from different source regions during the Pacific Exploratory Mission-Tropics A (PEM-Tropics A). Journal of Geophysical Research 104 (D13): 16,181-16,196.

Boehm H-DV and Siegert F (2001) Ecological impact of the one million hectare rice project in Central Kalimantan, Indonesia, using remote sensing and GIS. Proc. ACRS 2001 - 22nd Asian Conference on Remote Sensing, 5-9 November 2001, Singapore, Vol. 1 (pp 439-444).

BPS (Badan Pusat Statistik) (2001) Results of the 2000 Population Census, Series L2.2. Badan Pusat Statistik, Jakarta, Indonesia: BPSStatistics Indonesia.

Braak C (1919) Atmospheric variations of short and long duration in the Malay Archipelago. Verhandelingen 5, Koninklijk Magnetisch en Meteorologisch Observatorium te Batavia, Magnetic Meteorology Observation, Batavia, Indonesia.

Brauer M (1997) Assessment of health implications of haze in Malaysia. Mission Report RS/97/0441 Rev.1, November 1997. WHO Regional Office for the Western Pacific, Manila.

Brauer M (1998) Health impacts of biomass air pollution. Report prepared for the biregional workshop on health impacts of haze-related air pollution, Kuala Lumpur, Malaysia, 1-4 June 1998. Kuala Lumpur: World Health Organization, WPR/EHH/EHE(O)(1)98.2.

Brookfield H, Potter L and Byron Y (1995) In Place of the Forest. Environmental and Socio-economic Transformation in Borneo and the Eastern Malay Peninsula. In: Kasperson JX, Kasperson RE, and Turner II BL (eds) UNU Studies on Critical Environmental Regions. United Nations University Press, Tokyo, Japan.

Bruenig EF (1977) The tropical rain forest: A wasted asset or an essential biospheric resource?. Ambio: (4): 187-191.

Brunekreef B (1997) Air pollution and life expectancy: is there a relation? Occupational and Environmental Medicine 54: 781-784.

Brunekreef B and Holgate ST (2002) Air pollution and health. Lancet 360: 1,233-1,242.

Cahoon Jr. DR, Stocks BJ, Levine JS, Cofer III WR, and O'Neill KP (1992) Seasonal distribution of African savanna fires. Nature 359: 812-815.

Carmona-Moreno C, Belward A, Malingreau JP, Hartley A, Garcia-Alegre M, Antonovskiy M, Buchshtaber V, and Pivovarov V (2005) Characterizing interannual variations in global fire calendar using data from Earth observing satellites. Global Change Biology 11(9): 1,537-1,555.

CGIF (Consultative Group on Indonesian Forestry) (1998) Fifth meeting of ASOEN haze technical task force. CGIF Meeting on Forest Fires, 27th January 1998, Jakarta. Bureau of International Cooperation and Investment, Ministry of Forestry, Jakarta, Indonesia.

Chandra S, Ziemke JR, Min W, and Read WG (1998) Effects of 1997-1998 El Niño on tropospheric ozone and water vapor. Geophysical Research Letters 25(20): 3,867-3,870.

Chang CP, Wang Z, Ju JH, and Li T (2004) On the relationship between western maritime continent monsoon rainfall and ENSO during northern winter. Journal of Climate 17 (3): 665-672.

Chang CP, Wang Z, McBride J and Liu CH (2005) Annual cycle of Southeast Asia - Maritime Continent rainfall and the asymmetric monsoon transition. Journal of Climate18: 287-301.

Charlson RJ and Lelieveld J (1994) Multiphase atmospheric chemistry. Implications for Climate. In: Prinn R (ed) Global Atmospheric-Biospheric Chemistry. Plenum Press, New York (pp 57-69).

Charlson RJ, Horvath H, and Pueschel RF (1967) The direct measurement of atmospheric light scattering coefficient for studies of visibility and pollution. Atmospheric Environment 1: 469-478.

Chevillard A, Ciais P, Karstens U, Heimann M, Schmidt M, Levin I, Jacob D, Podzun R, Kazan V, Sartorius H, and Weingartner E (2002a) Transport of Rn-222 using the regional model REMO: a detailed comparison with measurements over Europe. Tellus B 54: 50-871.

Chevillard A, Karstens U, Ciais P, Lafon S, and Heimann M (2002b) Simulation of atmospheric CO_2 over Europe and western Siberia using the regional scale model REMO, Tellus B 54: 872-894,

Chew FT, Goh DY, Ooi BC, Saharom R, Hui JK, and Lee BW (1999) Association of ambient air-pollution levels with acute asthma exacerbation among children in Singapore. Allergy 54(4): 320-329.

Chew FT, Ooi BC, Hui JK, Saharom R, Goh DY, and Lee BW (1995) Singapore's haze and acute asthma in children. Lancet 346: 1427.

Chia LS (1979) Weather and climate. In: Hill RD (ed) South-east Asia: A systematic geography, Oxford University Press (pp 16-30).

Chokkalingam U, Kurniawan I and Ruchiat Y (2005) Fire, livelihoods, and environmental change in the middle Mahakam peatlands, East Kalimantan. Ecology and Society 10(1): 26.

Chokkalingam U, Suyanto S, Permana RP, Kurniawan I, Mannes J, Darmawan A, Khususiyah N, and Robiyanto HSto (2006) Community fire use, resource change, and livelihood impacts: the downward spiral in the wetlands of southern Sumatra. Mitigation and Adaptation Strategies for Global Change 12 (1): 75 -100.

Christian TJ, Kleiss B, Yokelson RJ, Holzinger R, Crutzen PJ, Hao WM, Saharjo BH, and Ward DE (2003) Comprehensive laboratory measurements of biomass-burning emissions: 1. Emissions from Indonesian, African, and other fuels. Journal of Geophysical Research 108(D23):4719, doi:10.1029/2003JD003704.

Chuvieco E, Aguado I, and Dimitrakopoulos AP (2004) Conversion of fuel moisture content values to ignition potential for integrated fire danger assessment. Canadian Journal of Forest Research 34(11): 2,284-2,293.

Cicerone RJ (1994) Fires, Atmospheric Chemistry, and the Ozone Layer. Science 263: 1,243-1,244.

CIESIN (Center for International Earth Science Information Network) Columbia University and Centro Internacional de Agricultura Tropical (CIAT) (2005a) Gridded Population of the World Version 3 (GPWv3): Population Grids. Palisades, NY: Socioeconomic Data and Applications Center (SEDAC), Columbia University. Available online at http://sedac.ciesin.columbia.edu/gpw (8 March 2006).

CIESIN (Center for International Earth Science Information Network) Columbia University and Centro Internacional de Agricultura Tropical (CIAT) (2005b) Gridded Population of the World Version 3 (GPWv3): National Boundaries. Palisades, NY: Socioeconomic Data and Applications Center (SEDAC), Columbia University. Available online at http://sedac.ciesin.columbia.edu/gpw (8 March 2006).

Cochrane MA (2003) Fire Science for Rainforests. Nature 421: 913-919.

Cochrane MA, Alencar A, Schulze MD, Souza CM Jr, Nepstad DC, Lefebvre P, and Davidson EA (1999) Positive feedbacks in the fire dynamic of closed canopy tropical forests. Science 284(5421): 1,832-1,835.

Cohen AJ, Anderson HR, Ostro B, Pandey KD, Krzyzanowski M, Kunzli N, Gutschmidt K, Pope A, Romieu I., Samet JM, and Smith K (2005) The global burden of disease due to outdoor air pollution. Journal of Toxicology and Environmental Health 68 (13/14) : 1,301-1,307.

Cooke WF, Liousse C, Cachier H, and Feichter J (1999) Construction of a 1°×1° fossil fuel emission data set for carbonaceous aerosol and implementation and radiative impact in the ECHAM4 model. Journal of Geophysical Research 104(D18): 22,137-22,162.

Coulter JK (1957) Development of the peat soils of Malaya. Malayan Agricultural Journal 60: 188-199.

Crutzen PJ and Andreae MO (1990) Biomass Burning in the Tropics: Impact on Atmospheric Chemistry and Biogeochemical Cycles. Science 250 (4988) 1,669-1,678.

Crutzen PJ and Carmichael GR (1993) Modeling the Influence of Fires on Atmospheric Chemistry. Emissions from the Combustion Process in Vegetation. In: Crutzen PJ and Goldammer JG (eds) Fire in the environment: the ecological, atmospheric and climatic importance of vegetation fires. Dahlem Workshop Reports, Environmental Sciences Research Report 13. John Wiley & Sons, Chichester (pp 89-105).

Crutzen PJ and Lelieveld J (2001) Human Impacts on Atmospheric Chemistry. Annual Review of Earth and Planetary Sciences 29: 17-45, doi:10.1146/annurev.earth.29.1.17.

Crutzen PJ, Heidt LE, Krasnec JP, Pollock WH, and Seiler W (1979) Biomass burning as a source of atmospheric CO, H_2, N_2O, CH_3Cl, and COS. Nature 282: 253-256.

Daniels MJ, Dominici F, Samet JM, and Zeger SL (2000) Estimating Particulate Matter-Mortality Dose-Response Curves and Threshold Levels: An Analysis of Daily Time-Series for the 20 Largest US Cities. American Journal of Epidemiology 152: 397-406.

Davies SJ and Unam L (1999) Smoke-haze from the 1997 Indonesian forest fires: effects on pollution levels, local climate, atmospheric CO_2 concentrations, and tree photosynthesis. Forest Ecology and Management 124: 137-144.

de Groot WJ, Wardati and Wang Y (2005) Calibrating the Fine Fuel Moisture Code for grass ignition potential in Sumatra, Indonesia. International Journal of Wildland Fire(14): 161-168.

Defries RS, Hansen MC, Townshend JRG, Janetos AC, and Loveland TR (2000) A new global 1-km dataset of percentage tree cover derived from remote sensing. Global Change Biology 6(2): 247-254, doi:10.1046/j.1365-2486.2000.00296.x.

Dennis R (1998) A review of fire projects in Indonesia 1982-1998. Center for International Forestry research (CIFOR), Bogor, Indonesia.

Dennis RA (1999) A review of fire projects in Indonesia 1982-1998. Center for International Forestry Research, Bogor, Indonesia.

Dentener F, Kinne S, Bond T, Boucher O, Cofala J, Generoso S, Ginoux P, Gong S, Hoelzemann JJ, Ito A, Marelli L, Penner JE, Putaud J-P, Textor C, Schulz M, van der Werf GR, and Wilson J (2006) Emissions of primary aerosol and precursor gases in the years 2000 and 1750 prescribed data-sets for AeroCom. Atmospheric Chemistry and Physic 6: 4321-4344, 2006

Depperman CE (1941) On the occurrence of dry stable maritime air in equatorial regions. Bulletin of the American Meteorological Society 22: 143-149.

Dickinson RE (1993) Effect of fires on global radiation budget through aerosol and cloud properties. In: Crutzen PJ and Goldammer JG (eds) Fire in the environment: the ecological, atmospheric and climatic importance of vegetation fires. Dahlem Workshop Reports, Environmental Sciences Research Report 13. John Wiley & Sons, Chichester (pp 107-122).

Dierke Weltatlas (1980) Georg Westermann Verlag, Braunschweig, Germany (pp 140-141).

DIN (Deutsches Institut für Normung) (1996) ISO 7708. Luftbeschaffenheit - Festlegung von Partikelgrößenverteilungen für die gesundheitsbezogene Schwebstaubprobenahme. Beuth Verlag, Berlin.

Dockery DW and Pope III CA (1994) Acute respiratory effects of particulate air pollution. Annual Reviews in Public Health 15: 107-132.

Dockery DW, Pope CA III, Xu X, Spengler JD, Ware JH, Fay ME, Ferris BG Jr, and Speizer FE (1993) An association between air pollution and mortality in six U.S. cities. The New England Journal of Medicine 329: 1,753-1,759.

DOE (Department of Environment)(1996) Malaysia environmental quality report 1995. Department of Environment, Ministry of Science, Technology and Environment, Kuala Lumpur, Malaysia.

DOE (Department of Environment) (1995) Malaysia environmental quality report 1994. Department of Environment, Ministry of Science, Technology and Environment, Kuala Lumpur, Malaysia.

DOE (Department of Environment) (1998) Malaysia environmental quality report 1997. Department of Environment, Ministry of Science, Technology and Environment, Kuala Lumpur, Malaysia.

DOE (Department of Environment) (2005) Malaysia Environmental Quality Report 2004, Department of Environment, Kuala Lumpur, Malaysia. Available online at http://www.doe.gov.my/dmdocuments/publications/yearlyReport/2004/DOE-AR2004part1.pdf (7 September 2006).

Dominici F, Daniels M, Zeger SL, and Samet JM (2002) Air pollution and mortality: estimating regional and national dose-response relationships. Journal of the American Statistical Association 97(457): 100-111.

Duncan BN, Bey I, Chin M, Mickley LJ, Fairlie TD, Martin RV, and Matsueda H (2003a) Indonesian wildfires of 1997: Impact on tropospheric chemistry. Journal of Geophysical Research 108(D15):4458, doi:10.1029/2002JD003195.

Duncan BN, Martin RV, Staudt AC, Yevich R, and Logan JA (2003b) Interannual and seasonal variability of biomass burning emissions constrained by satellite observations, Journal of Geophysical Research 108(D2), 4100, doi:10.1029/2002JD002378.

Dwyer E, Gregoire J-M, and Pereira JMC (2000) Climate and vegetation as driving factors in global fire activity In: Innes JL, Beniston M and Verstraete MM (eds) Biomass Burning and Its Inter-Relationships with the Climate System, Kluwer Academic Publishers, Dordrecht, Boston, London (pp 171-192).

EEPSEA/WWF (Economy and Environment Program for South East Asia/World Wide Found for Nature) (1998) The Indonesian fires and haze of 1997: the economic toll. International Development Research Centre, Ottawa, Canada.

Einfield W, Ward DE and Hardy C (1991) Effects of fire behaviour on prescribed fire smoke characteristics: a case study. In: Levine JS (ed) Global biomass burning. Atmospheric, climatic, and biospheric implications. MIT Press, Cambridge, Massachusetts (pp 412-419).

Emmanuel SC (2000) Impact to lung health of haze from forest fires: The Singapore experience. Respirology 5: 175-182.

Emmanuel SC and Lim OP (1998) Singapore country report on the 1997 smoke-haze. Report prepared for the biregional workshop on health impacts of haze-related air pollution, Kuala Lumpur, Malaysia, 1-4 June 1998. Kuala Lumpur: World Health Organization, WHR/EHH/EHE (O)(1)/98/INF./6.

Ezzati M and Kammen DM (2001) Quantifying the Effects of Exposure to Indoor Air Pollution from Biomass Combustion on Acute Respiratory Infections in Developing Countries. Environmental Health Perspectives 109(5):481-488.

Ezzati M, Lopez AD, Rodgers A, Vander Hoorn S and Murray CJ (2002) Selected major risk factors and global and regional burden of disease. Lancet. 360(2) : 1,347-1,360.

Fang M and Huang W (1998) Tracking the Indonesian forest fire using NOAA/AVHRR images. International Journal of Remote Sensing 19(3): 387-390.

Fang M, Zheng M, Wang F, To KL, Jaafar AB, and Tong SL (1999) The solvent-extractable organic compounds in the Indonesia biomass burning aerosols - characterization studies. Atmospheric Environment 33: 783-795.

FAO (Food and Agriculture Organization) (1988) FAO/Unesco Soil Map of the World, Revised legend, with corrections and updates. World Soil Resources Report 60, FAO, Rome, Italy.

FAO (Food and Agriculture Organization) (1998) FAO/WFP Crop and food supply assessment mission to Indonesia, Special report, 17th April 1998, Food and Agriculture Organization of the United Nations, Rome, Italy.

FAO (Food and Agriculture Organization) (2000) Forest cover mapping and monitoring with NOAA-AVHRR and other coarse spatial resolution sensors. FAO Forest Resources Assessment Programme (FRAP) Working Paper 29, FAO, Rome, Italy. Available online at ftp://ftp.fao.org/docrep/fao/007/ae161e (15 March 2006).

FAO (Food and Agriculture Organization) (2003) WRB (World Reference Base) Map of World Soil Resources. Land and Water Development Division AGL, Food and Agriculture Organization of the United Nations, Rome, Italy. Available online at http://www.fao.org/ag/agl/agll/wrb/soilres.stm (2 January 2004).

FAO (Food and Agriculture Organization) (2006) Global Forest Resources Assessment 2005. Progress towards sustainable forest management. FAO Forestry Paper 147, FAO, Rome, Italy.

FAO (Food and Agriculture Organization) (in cooperation with International Society of Soil Science ISSS and International Soil Reference and Information Centre ISRIC) (1998) World Reference Base for Soil Resources. World Soil Resources Reports 84, FAO, Rome, Italy,. Available online at ftp://ftp.fao.org/agl/agll/docs/wsrr84e.pdf (22 March 2003).

FAO/UNESCO (Food and Agriculture Organization/United Nations Educational, Scientific and Cultural Organization) (2003) Digital Soil Map of the World (DSMW) and Derived Soil Properties (Version 3.6). CD-ROM, UNESCO Publishing/FAO, Rome, Italy.

Fearnside PM (2000) Global warming and tropical land use change: greenhouse gas emissions from biomass burning, decomposition and soils in forest conversion, shifting cultivation and secondary vegetation. Climate Change 46: 115-158.

Ferrari L (1997) Haze disaster assignment. WHO Indonesia, report of the short-term consultancy allotment SE/INO/DGB/011/RB/96, earmarking SE/97/912526, 3rd November 1997, Jakarta.

Field RD, Wang Y, Roswintiarti O, Guswanto (2004) A drought-based predictor of recent haze events in western Indonesia. Atmospheric Environment 38: 1,869-1,878.

Fosberg MA, Stocks BJ and Lynham TJ (1996) Risk analysis and strategic planning: Fire and climate change in the boreal forest. In: Goldammer JG and Furyaev VV (eds) Fire in ecosystems of boreal Eurasia. Kluwer Academic Publ., Dordrecht (pp 495-504).

Frandsen WH (1997) Ignition probability of organic soils. Canadian Journal of Forest Research 9: 1,471-1,477.

Fujiwara M, Kita K, Kawakami S, Ogawa T, Komala N, Saraspriya S, and Suripto A (1999) Tropospheric ozone enhancements during the Indonesian forest fire events in 1994 and 1997 as revealed by ground-based observations. Geophysical Research Letters 26: 2,417-2,420.

Fuller DO and Fulk M (2001) Burned area in Kalimantan, Indonesia mapped with NOAA-AVHRR and Landsat TM imagery. International Journal of Remote Sensing 22:691-697.

Fuller DO and Murphy K (2006) The ENSO-fire dynamic in Insular Southeast Asia. Climatic Change 74: 435-455.

FWI/GFW (Forest Watch Indonesia/Global Forest Watch) (2002) The State of the Forest: Indonesia. Forest Watch Indonesia, Bogor, Indonesia and and Global Forest Watch, Washington DC. Available online at http://www.wri.org/biodiv/pubs_description.cfm?pid=3147 (19 August 2003).

Gamble JF (1998) PM2.5 and mortality in long-term prospective cohort studies: cause-effect or statistical association? Environmental Health Perspectives 106: 535-549.

Garstang M, Tyson PD, Cachier H, and Radke L (1997) Atmospheric transport of particulate and gaseous products by fires. In: Clark JS, Cachier H, Goldammer JG, Stocks B (eds) Sediment records of biomass burning and global change. NATO ASI Series No I, Global environmental change Vol. 51, Springer Verlag, Berlin, Heidelberg, New York (pp 207-252).

Geophysical Research Letters (1999) Highlights of this issue: Volume 26: 16.

Gergis J, Braganza K, Fowler A, Mooney S, and Risbey J (2006) Reconstructing El Niño Southern Oscillation (ENSO) from high-resolution palaeoarchives. Journal of Quaternary Science 21(7): 707.

Gergis JL and Fowler AM (2005) Classification of synchronous oceanic and atmospheric El Niño Southern Oscillation (ENSO) events for paleoclimatic reconstruction. International Journal of Climatology 25: 1,541-1,565.

Giglio L, van der Werf GR, Randerson JT, Collatz GJ, and Kasibhatla PS (2006) Global estimation of burned area using MODIS active fire observations. Atmospheric Chemistry and Physics 6: 957-974.

Giri C, Zhu Z and Reed B (2005) A comparative analysis of the Global Land Cover 2000 and MODIS land cover data sets. Remote Sensing of Environment 94(1): 123-132.

Glover D and Jessup T (1999) (eds) Indonesia's Fires and Haze: The Cost of Catastrophe. Institute of Southeast Asian Studies, Singapore. Available online at http://idrinfo.idrc.ca/archive/corpdocs/113538/332-1.htm#page_113 (24 November 2006).

Goh KT, Schwela DH, Goldammer JG, and Simpson O (1999) Health Guidelines for Vegetation Fire Events. Background Papers. Published on behalf of UNEP, WHO, and WMO. Institute of Environmental Epidemiology, Ministry of the Environment Singapore, Namic Printers, Singapore.

Goldammer JG (1993) Feuer in Waldökosystemen der Tropen und Subtropen. Birkhäuser-Verlag, Basel-Boston.

Goldammer JG (1997) The ASEAN Fire Forum: Initial thoughts towards cooperation in fire and smoke research and management in the ASEAN region. In: Abu Hassan H, Taha D, Puat Dahalan M, and Mahmud A (eds) Transboundary Pollution and the Sustainability of Tropical Forests: Towards Wise Forest Fire Management- The

Proceedings of the AIFM International Conference, ASEAN Institute for Forest Management, Ampang Press, Kuala Lumpur (pp 137-165).

Goldammer JG (1999) Environmental problems arising from land use, climate variability, fire and smog in Indonesia: Development of policies and strategies for land use and fire management. In: Carmichael GR (comp) WMO Workshop on Regional Transboundary Smoke and Haze in Southeast Asia, Singapore, 2-5 June 1998, Vol. 2. World Meteorological Organization, Global Atmosphere Watch Report Ser. No. 131, WMO TD No. 948, Geneva (pp 13-88).

Goldammer JG and Crutzen PJ (1993) Fire in the environment. Scientific rationale and summary of results of the Dahlem workshop. In: Crutzen PJ and Goldammer JG (eds) Fire in the environment: the ecological, atmospheric and climatic importance of vegetation fires. Dahlem Workshop Reports, Environmental Sciences Research Report 13. John Wiley &Sons, Chichester (pp 1-14).

Goldammer JG and Hoffmann AA (2001) Fire situation in Indonesia. In: FAO (Food and Agriculture Organization) FRA Global Forest Fire Assessment 1990-2000. Forest Resources Assessment Programme, Working Paper 55. FAO, Rome, Italy (pp 132-144).

Goldammer JG and Hoffmann AA (2001) Fire situation in Indonesia. In: FAO (Food and Agriculture Organization) FRA Global Forest Fire Assessment 1990-2000. Forest Resources Assessment Programme, Working Paper 55. FAO, Rome, Italy (pp 132-144).

Goldammer JG and Peñafiel SR (1990) Fire in the pine-grassland biomes of tropical and subtropical Asia. In: Goldammer JG (ed) Fire in the tropical biota. Ecosystem processes and global challenges. Ecological Studies 84, Springer-Verlag, Berlin-Heidelberg-New York (pp 45-62).

Goldammer JG and Price C (1998) Potential impacts of climate change in fire regimes in the tropics based on MAGICC and a GISS GCM-derived lightning model. Climate Change 39: 273-296.

Goldammer JG and Seibert B (1990) The impact of droughts and forest fires on tropical lowland rain forest of Eastern Borneo. In: Goldammer JG (ed) Fire in the tropical biota. Ecosystem processes and global challenges. Ecological Studies 84, Springer-Verlag, Berlin-Heidelberg-New York (pp 11-31).

Goldammer JG, Hogan Rufelds C, Malingreau JP, Yokelson R, Abberger H, and Manila A (1997) The ASEAN Fire Forum: Results of the Working Group Discussions. In: Abu Hassan H, Taha D, Puat Dahalan M, Mahmud A (eds) Transboundary Pollution and the Sustainability of Tropical Forests: Towards Wise Forest Fire Management - The Proceedings of the AIFM International Conference, ASEAN Institute for Forest Management, Ampang Press, Kuala Lumpur (Annex II) (pp 420-437).

Goldammer JG, Seibert B and Schindele W (1996) Fire in dipterocarp forests. In: Schulte A and Schöne D (eds) Dipterocarp forest ecosystems: Towards sustainable management. World Scientific Publ., Singapore-New Jersey-London-Hongkong (pp 155-185).

Gorham E (1991) Northern peatlands: Role in the carbon cycle and probable responses to climate warming. Ecological Applications 52: 182-195.

Graf HF (2004) The complex interaction of aerosols and clouds. Science 203:1,309-1,311.

Graf HF and Yang J (2007) Evaluation of a new convective cloud field model: precipitation over the maritime continent . Atmospheric Physics and Chemistry 7: 409–421.

Graf HF, Yang J and Wagner TM (2007) Effects of smoke from peat burning in Indonesia on precipitation over the warm pool area. Geophysical Research Abstracts 9: 01148, SRef-ID: 1607-7962/gra/EGU2007-A-01148.

Granier C, Müller JF, and Brasseur G (2000) The Impact of Biomass Burning on the Global Budget of Ozone and Ozone Precursors. In: Innes JL, Beniston M and Verstraete MM (eds) Biomass Burning and Its Inter-Relationships with the Climate System, Kluwer Academic Publishers, Dordrecht, Boston, London (pp 69-85).

Grantz DA, Garner JHB and Johnson DW (2003) Ecological effects of particulate matter. Environment International 29:213-239.

Gras JL and Cohen DD (1997) Particles and haze in Jakarta, Indonesia. In: Cohen DD, Gras JL, Garton D, Firestone T, Johnson G, Bailey G, Ayers G (eds) Study of fine atmospheric particles and gases in the Jakarta region. Final project report No. 38, consultants (ANSTO/CSIRO) report No. 3. BAPEDAL and the East Java Pollution Control Implementation Project, Jakarta.

Gras JL, Jensen JB, Okada K, Ikegami M, Zaizen Y, and Makino Y (1999) Some optical properties of smoke aerosol in Indonesia and tropical Australia. Geophysical Research Letters 26(10): 1,393-1,396.

Gronskei KE, Gram F, Hagen LO, Larssen S, Jansen HMA, Olsthoorn AA, Soedomo M, and Achmadi UF (1997) Urban Air Quality Managmenet Strategy in Asia URBAIR. Jakarta Report. Report number IVM-E97/05. World Bank, Washington, USA.

Hagemann S (2002) An Improved Land Surface Parameter Dataset for Global and Regional Climate Models. Max-Planck-Institute for Meteorology Report 336, Hamburg, Germany, Max-Planck-Institute for Meteorology. Available online at http://www.mpimet.mpg.de/en/web/science/a_reports_archive.php?actual$=$2002 (8 June 2003).

Hairiah K, Sitompul SM, van Noordwijk M and Palm C (2001) Carbon stocks of tropical land use systems as part of the global C balance: effects of forest conversion and options for ‘clean development’ activities. ASB Lecture Note 4B, International Center for Research in Agroforestry, Bogor, Indonesia. Available online at http://www.worldagroforestry.org/sea/Products/Training/Materials/lecture%20notes/ASB-LecNotes/ASBLecNote%204A.pdf (2 February 2003).

Hamada J-I, Yamanaka MD, Matsumoto J, Fukao S, Winarso PA and Sribimawati T (2002) Spatial and temporal variations of the rainy season over Indonesia and their link to ENSO. Journal of the Meteorological Society of Japan 80: 285-310.

Hansen M, DeFries R, Townshend JRC, and Sohlberg R (2000) Global land cover classification at 1km resolution using a decision tree classifier. International Journal of Remote Sensing 21: 1,331-1,365.

Hao WM and Liu MH (1994) Spatial and temporal distribution of tropical biomass burning. Global Biogeochemical Cycles 8: 495-503.

Hao WM, Liu M-H, and Crutzen PJ (1990) Estimates of annual and regional releases of CO_2 and other trace gases to the atmosphere from fires in the tropics, based on FAO statistics for the period 1975-1980. In: Goldammer JG (ed) Fire in the tropical biota. Ecosystem processes and global challenges. Ecological Studies 84, Springer-Verlag, Berlin-Heidelberg-New York (pp 440-462).

Hassan MN, Awang M, Abdullah R, Othman MSH, Alias MA, Dzulkifly K, Abdullah AM, Muda A, and Chong TL (1998) The damage costs of haze episodes in Malaysia. Concepts, empirical studies and improvement policies. Department of Environmental Sciences, Universiti Putra Malaysia, 43400 UPM, Serdang, Selangor, Malaysia.

Haylock M (2002) BMG BMRC seasonal rainfall forecasting scheme for Indonesia. Australian Bureau of Meteorology Research Centre BMRC. Available online at http://www.bom.gov.au/bmrc/clfor/cfstaff/jmb/Seasonal_Forecast_CD/Forecasting_Report.pdf (2 June 2003).

HEI (Health Effects Institute) (2000) Reanalysis of the Harvard Six Cities Stud and the American Cancer Society Study of Particulate Air Pollution and Mortality. Special Report. Health Effects Institute, Cambridge, MA.

Heil A and Goldammer JG (2001) Smoke-haze pollution: a review of the 1997 episode in South-east Asia. Regional Environmental Change 2: 24-37.

Heil A, Langmann B and Aldrian E (2007) Indonesian peat and vegetation fire emissions: Factors influencing large-scale smoke-haze dispersion. Mitigation and Adaptation Strategies for Global Change 12: 113-133.

Hendon HH (2003) Indonesian Rainfall Variability: Impacts of ENSO and local air-sea interaction. Journal of Climate 16 (11): 1,775-1,790.

Herman JR, Bhartia PK, Torres O, Hsu C, Seftor C, and Celarier E (1997) Global distribution of UV-absorbing aerosols from Nimbus 7/TOMS data. Journal of Geophysical Research 102: 16,911-16,922.

Herman JR, Krotkov N, Celarier E, Larko D, and Labow G (1999) Distribution of UV radiation at the Earth's surface from TOMS-measured UV-backscattered radiances. Journal of Geophysical Research 104(D10): 12,059-12,076.

Hinwood AL and Rodriguez C (2005) The potential health impacts associated with peat smoke: a review. Journal of the Royal Society of Western Australia 88: 133-138.

Hoelzemann JJ, Schultz MG, Brasseur GP, Granier C, and Simon M (2004) Global Wildland Fire Emission Model (GWEM): Evaluating the use of global area burnt satellite data Journal of Geophysical Research 109, D14S04, doi:10.1029/2003JD003666.

Hoffa EA, Ward DE, Hao WM, Susott RA, Wakimoto RH (1999) Seasonality of carbon emissions from biomass burning in a Zambian savanna. Journal of Geophysical Research 104 (D11): 13,841-13,853.

Hoffmann WA, Schroeder W and Jackson RB (2003) Regional feedbacks among fire, climate, and tropical deforestation. Journal of Geophysical Research 108(D23), 4721, doi:10.1029/2003JD003494.

Holmes D (2002) Indonesia: Wherehaveall the forests gone?. World Bank Discussion Paper. Environmental and Social Development, South Asia and the Pacific Region. The World Bank, Washington, D.C..

Hon PML J (1999) Malaysia. In: Glover D and Jessup T (eds) Indonesia's Fires and Haze: The Cost of Catastrophe. Institute of Southeast Asian Studies, Singapore (pp 51-85). Available online at http://idrinfo.idrc.ca/archive/corpdocs/113538/332-1.htm#page_113 (24 November 2006).

Hope G, Chokkalingam U and Anwar S (2005) The stratigraphy and fire history of the Kutai Peatlands, Kalimantan, Indonesia. Quaternary Research 64: 407-417.

Huffman GJ, Adler RF, Arkin P, Chang A, Ferraro R, Gruber A, Janowiak J, McNab A, Rudolf B, and Schneider U (1997) The Global Precipitation Climatology Project (GPCP) combined precipitation data set Bulletin of the American Meteorological Society 78: 5-20.

Huffman GJ, Adler RF, Bolvin DT, Gu G, Nelkin EJ, Bowman KP, Hong Y, Stocker EF, Wolff DB (2007) The TRMM Multi-satellite Precipitation Analysis: Quasi-global, multi-year, combined-sensor precipitation estimates at fine scale, Journal of Hydrometeorology 8: 38-55, doi:10.1175/JHM560.1.

Husar RB, Husar JD, and Martin L (2000), Distribution of continental surface aerosol extinction based on visual range data. Atmospheric Environment 34: 5,067- 5,078.

Ichoku C and Kaufman YJ (2005) A Method to Derive Smoke Emission Rates From MODIS Fire Radiative Energy Measurements. IEEE Transactions on Geoscience and Remote Sensing 43(11): 2,636- 2,649.

IGAC (Int. Global Atmospheric Chemistry) (1998) Science feature: The IGAC Biomass Burning Experiment. Special issue, Int. Global Atmospheric Chemistry (IGBP) Project Newsletter IGACtivities No. 15: 2-19.

Ikegami M, Okada K, Zaizen Y, Makino Y, Jensen YB, Gras JL and Harjanto H (2001) Very high weight ratios of S/K in individual haze particles over Kalimantan during the 1997 Indonesian forest fires. Atmospheric Environment 35: 4,237-4,243.

Ilyas M, Pandy A, Hassan SIS (1999) UV-B radiation at Penang. Atmospheric Research 51: 141-152.

Immirzi P, Maltby E, Clymo RS (1992) The Global Status of Peatlands and Their Role in Carbon Cycling. Report No. 11, Exeter, U.K., The Wetland Ecosystems Research Group, University of Exeter.

Inoue M (1999) Indonesian Forest Policy and the Role of NGO. In IGES (The Institute for Global Environmental Strategies) A Step Toward Forest Conservation Strategy: Research on a desirable forest management system." Interim Report 1999: Forest Conservation Project, The Institute for Global Environmental Strategies (IGES), Japan. Available online at http://www.iges.or.jp/en/fc/phase1/ir99/4-2-Inoue.pdf (5 March 2003).

Inoue T (2000) Rural Development of Peat Swamp Area of Central Kalimantan from Hydrological Aspect. Proceedings of the International Symposium on Tropical Peatlands, Bogor, Indonesia, 22-23 November 1999, Hokkaido University & Indonesian Institute of Sciences (pp 145-149). Available online at http://www.ees.hokudai.ac.jp/coe21/E/indonesia/trpt99_3.pdf (30 December 2002).

IPCC (Intergovernmental Panel on Climate Change) (2001) Climate Change 2001: The Scientific Basis. Cambridge University Press, Cambridge, UK.

IPCC (Intergovernmental Panel on Climate Change) (2007) Climate Change 2007: The Physical Science Basis - Summary for Policymakers Geneva (Approved version of February 2007). IPCC Secretariat, Geneva. Available online at http://www.ipcc.ch/SPM2feb07.pdf (20 April 2007).

Ito A and Penner JE (2005) Historical emissions of carbonaceous aerosols from biomass and fossil fuel burning for the period 1870-2000, Global Biogeochemical Cycles, 19, GB2028,doi:10.1029/2004GB002374.

Iwasaki M, Yamamoto S, Otani T, Inoue M, Hanaoka T, Sobue T, and Tsugane S (2006) Generalizability of relative risk estimates from a well-defined population to a general population. European Journal of Epidemiology 21(4): 253-262.

Jacob D (2001) Investigation of the annual and interannual variability of the water budget over the Baltic Sea Drainage Basin using the regional climate model REMO. Meteorology and Atmospheric Physics 77: 61-73.

Jänicke R (1993) Tropospheric aerosols. In: Hobbs PV (ed) Aerosol-cloud-climate interactions. International Geophysics Series 54. Academic Press, San Diego, London.

Jayachandran S (2005) Air Quality and Infant Mortality During Indonesia's Massive Wildfires in 1997. California Center for Population Research, On-Line Working Paper Series CCPR-023-05. Available online at http://www.ccpr.ucla.edu/ccprwpseries/ccpr_023_05.pdf (9 September 2005).

Journal of Geophysical Research Special Issue (1996) Southern Tropical Atlantic Regional Experiment (STARE): TRACE-A and SAFARI. Journal of Geophysical Research 101(D19): 23,519-24,330.

Justice CO, Smith R, Gill AM, and Csiszar I (2003) A review of current space-based fire monitoring in Australia and the GOFC/GOLD program for international coordination. International Journal of Wildland Fire 12(4): 247-258.

Kandun IN (1998) Role of the health sector in preventing adverse health impacts from forest fire haze in Indonesia. Proceedings of the International Cross Sectoral Forum on Forest Fire Management in South-East Asia, 7-8 December 1998, ITTO/Bapenas/Jica, Jakarta.

Kappos AD, Bruckmann P, Eikmann T, Englert N, Heinrich U, Hoppe P, Koch E, Krause GH, Kreyling WG, Rauchfuss K, Rombout P, Schulz-Klemp V, Thiel WR, and Wichmann HE (2004) Health effects of particles in ambient air. International Journal of Hygiene and Environmental Health 207(4): 399-407.

Kasischke E S, Hyer EJ, Novelli PC, Bruhwiler LP, French NHF, Sukhinin AI, Hewson JH, and Stocks BJ (2005) Influences of boreal fire emissions on Northern Hemisphere atmospheric carbon and carbon monoxide. Global Biogeochemical Cycles, 19, GB1012, doi:10.1029/2004GB002300.

Kaufman YJ and Fraser RS (1997) The effect of smoke particles on clouds and climate forcing. Science 277: 1,636-1,639,

Kaufman YJ and Nakajima T (1993) Effect of Amazon Smoke on Cloud Microphysics and Albedo-Analysis from Satellite Imagery. Journal of Applied Meteorology 32(4): 729-744.

Keywood MD, Ayers GP, Gras JL, Boer R and Leong CP (2003) Haze in the Klang Valley of Malaysia. Atmospheric Chemistry and Physics 3: 591-605.

Kiehl JT and Rodhe H (1995) Modeling Geographical and Seasonal Forcing Due to Aerosols. In: Charlson RJ, Heintzenberg J (eds) Aerosol Forcing of Climate. Chichester, John Wiley & Sons (pp 281-296).

Kim YJ, Kim KW, and Oh SJ (2001) Seasonal characteristics of haze observed by continuous visibility monitoring in the urban atmosphere of Kwangju, Korea. Environmental Monitoring and Assessment 70(1-2): 35-46.

Kirono DGC, Tapper NJ and McBride J (1999) Documenting Indonesian rainfall in the 1997-1998 El Niño event. Physical Geography 20: 422-435.

Kita K, Fujiwara M and Kawakami S (2000) Total ozone increase associated with forest fires over the Indonesian region and its relation to the El Niño-Southern oscillation. Atmospheric Environment 34(17): 2681-2690.

KLH (Kementerian Negara Lingkungan Hidup) (2003) Status Lingkungan Hidup Indonesia 2002. Kementrian Lingkungan Hidup, Asdep Urusan Informasi, Jakarta, Indonesia. Available online at http://www.menlh.go.id/archive.php?action=info&id=25 (30 March 2004).

Koe LCC, Arellano AF and McGregor JL (2001) Investigating the haze transport from 1997 biomass burning in Southeast Asia: its impact upon Singapore. Atmospheric Environment 35: 2,723-2,734.

Kunii O, Kanagawa S, Yajima I, Hisamatsu Y, Yamamura S, Amagai T, Ismail IT (2002) The 1997 haze disaster in Indonesia: its air quality and health effects. Archives in Environmental Health 57(1):16-22.

Künzli N, Kaiser R, Medina S, Studnicka M, Chanel O, Filliger P, Herry M, Horak Jr F, Puybonnieux-Texier V, Quenel P, Schneider J, Seethaler R, Vegnaud JC, and Sommer H (2000) Public-health impact of outdoor and traffic-related air pollution: a European assessment. The Lancet 356: 795– 801.

Künzli N, Kaiser R, Medina S, Studnicka M, Oberfeld G, and Horak F (1999) Air Pollution due to Road Traffic-related Air Pollution. An impact assessment project of Austria, France, and Switzerland. Technical Report on Epidemiology prepared for the Third Ministerial Conference for Environment and Health, London, 1999. Available online at http://www.airimpacts.org/documents/local/cases.pdf (10 April 2002).

Künzli N, Medina S, Kaiser R, Quénel P, Horak Jr F, and Studnicka M (2001) Assessment of Deaths Attributable to Air Pollution: Should We Use Risk Estimates based on Time Series or on Cohort Studies? American Journal of Epidemiology 153(11): 1050-1055.

Langmann B (2000) Numerical modeling of regional scale transport and photochemistry directly together with meteorological processes. Atmospheric Environment 34: 3,585-3,598.

Langmann B (2006) Rauchpartikel in der Atmosphäre: Modellstudien am Beispiel indonesischer Brände. Habilitationsschrift an dem Fachbereich Geowissenschaften der Universität Hamburg. Berichte zur Erdsystemforschung, 18, Max-Planck-Institute for Meteorology, Hamburg, Germany.

Langmann B and Graf H-F (2003) Indonesian smoke aerosols from peat fires and the contribution from volcanic sulfur emissions. Geophysical Reseach Letters 30 (11), 1547, doi:10.1029/2002GL016646.

Langmann B and Heil A (2004) Release and dispersion of vegetation and peat fire emissions in the atmosphere over Indonesia 1997/1998. Atmospheric Chemistry and Physics 4: 2,145-2,160.

Langmann B, Bauer SE and Bey I (2003) The influence of the global photochemical composition of the troposphere on European summer smog, Part I: application of a global to mesoscale model chain. Journal of Geophysical Research 108(D4), 4146, doi:10.1029/2002JD002072.

Langmann B, Herzog M and Graf HF (1998) Radiative forcing of climate by sulfate aerosols as determined by a regional circulation chemistry transport model. Atmospheric Environment 32: 2,757-2,768.

Lasco RD (2002) Forest carbon budgets in Southeast Asia following harvesting and land cover change. Science in China (Series C) 45: 55-64.

Legg CA and Laumonier Y (1999) Fires in Indonesia, 1997: A remote sensing perspective. Ambio 28(6): 479-485.

Levine JS (1996) Introduction. In: Levine JS (ed) Biomass burning and global change. MIT Press, Cambridge, Massachusetts.

Levine JS (1999a) The 1997 fires in Kalimantan and Sumatra, Indonesia: Gaseous and particulate emissions. Geophysical Research Letters 26(7): 815-818.

Levine JS (1999b) Correction to 'The 1997 fires in Kalimantan and Sumatra, Indonesia: Gaseous and particulate emissions'. Geophysical Research Letters 26(15): 2,407.

Levy JI, Hammitt JK, Spengler JD (2000) Estimating the mortality impacts of particulate matter: what can be learned from between-study variability? Environmental Health Perspectives 108(2):109-117.

Li R and Fu Y (2005) Tropical Precipitation Estimated by GPCP and TRMM PR Observations. Advances in atmospheric Sciences 22 (6): 852–864.

Liew SC, Lim OK, Kwoh LK, and Lim H (1998) Study of the 1997 forest fires in South East Asia using SPOT quicklook mosaics, Proceedings of the 1998 International Geoscience and Remote Sensing Symposium, Seattle, Washington. USA, 6-10 July 1998, Volume 2 (pp 879-881).

Limin HS, Saman TN and Alim S (2004) Developing public awareness and responsibility of local community through direct involvement in action for suppressing the forest fire. In : Osaki M, Iwakuma T, Kohyama T, Hatano R, Yonebayashi K, Tachibana H, Takahashi H, Shinano T, Higashi S, Simbolon H, Limin SH, Wijaya H, Tuah SJ, Usup A, Jaya A (eds.) Proceedings of the international workshop on the human dimension on the management of peatlands in Southeast Asia, Palangka Raya, Central Kalimantan, Indonesia, December 1-2, 2003. Hokkaido University, Japan and Research Center for Biology, the Indonesian Institute of Science, Bogor, Palangka Raya University, Indonesia. Available online at http://wwwgeo.ees.hokudai.ac.jp/core-univ/english/proceeding/WS2003PalangkaR.pdf (06 January 2007).

Limin SH, Layuniati, and Jamal YM (2000) Utilisation of inland peat for food crop commodity development requires high input and is detrimental to peat swamp forest ecosystem. Proceedings of the International Symposium on tropical peatlands, Bogor, Indonesia 33-23 November 1999. Hokkaido University and Indonesian Institute of Sciences (pp 135-143).

Lindesay JA, Andreae MO, Goldammer JG, Harris G, Annegarn HJ, Garstang M, Scholes RJ, and van Wilgen BW (1996) International Geosphere-Biosphere Programme/International Global Atmospheric Chemistry SAFARI-92 field experiment: Background and overview. Journal of Geophysical Research 101(D19): 23,521-23,530.

Liousse C, Andreae MO, Artaxo P, Barbosa P, Cachier H, Grégoire JM, Hobbs P, Lavoué D, Mouillot F, Penner J, Scholes M, and Schultz MG (2004) Deriving global quantitative estimates for spatial and temporal distributions of biomass burning emissions. In: Granier C, Artaxo P and Reeves CE (eds) Emissions of atmospheric trace compounds – Advances in global change research. Kluwer Academic Publishers, Dordrecht (pp 71-113).

Lobert JM and Warnatz J (1993) Emissions from the combustion process in vegetation. In: Crutzen PJ and Goldammer JG (eds) Fire in the environment. The ecological, atmospheric and climatic importance of vegetation fires. Dahlem Workshop Reports, Environmental Sciences Research Report 13. John Wiley & Sons, Chichester (pp 15-37).

Loveland TR, Reed BC, Brown JF, Ohlen DO, Zhu J, Yang L, Merchant JW (2000) Development of a global land cover characteristics database and IGBP DISCover from 1-km AVHRR data. International Journal of Remote Sensing 21: 1,303-1,330.

Majewski D (1991) The Europa Modell of the Deutscher Wetterdienst. Seminar proceedings ECMWF 2: 147-191.

Makarim N, Arba'i YA, Deddy A, and Brady M (1998) Assessment of 1997 Land and Forest Fires in Indonesia: National Coordination. International Forest Fire News 18: 4-12.

Malingreau JP (1990) The contribution of remote sensing to the global monitoring of fires in tropical and subtropical ecosystems. In: Goldammer JG (ed) Fires in the Tropical Biota, Ecological Studies 84, Berlin, Springer-Verlag (pp 337-370).

Malingreau JP, Stephens G, and Fellows L (1985) Remote sensing of forest fires: Kalimantan and North Borneo in 1982-83. Ambio 14(6): 314-321.

Manö S and Andreae MO (1994) Emission of methyl bromide from biomass burning. Science 263: 1,255-1,257.

Marland G, Boden TA and Andres RJ (2003) Global, regional, and national CO_2 emissions, in Trends, A Compendium of Data on Global Change. Oak Ridge, Tennessee, USA, Carbon Dioxide Information Analysis Center, Oak Ridge National Laboratory, U.S. Department of Energy.

Martuzzi M, Galassi C, Ostro B, Forastiere F, and Bertollini R (2002). Health impact assessment of air pollution in the eight major Italian cities. Report EURO/02/5040650WHO Regional Office for Europe, Copenhagen, Denmark. Available online at http://www.euro.who.int/document/E75492.pdf (27 February 2007).

Masood E(1999) Malaysia backs 'gag' on haze scientists. Nature 390 (6,656): 107.

Matsueda H and Inoue HY (1999) Aircraft measurements of trace gases between Japan and Singapore in October of 1993, 1996, and 1997. Geophysical Research Letters 26(16): 2,413-2,416.

Matsueda H, Inoue HY, Ishii M, and Tsutsumi Y (1999) Large injections of carbon monoxide into the upper troposphere due to intense biomass burning in 1997. Journal of Geophysical Research 104(D21): 26,867-26,879.

Matsueda H, Taguchi T, Inoue HY, and Ishii M (2002) A large impact of tropical biomass burning on CO and CO_2 in the upper troposphere. Science in China (Series C) 45: 116-125.

Mayaux P, Eva H, Gallego J, Strahler AH, Herold M, Agrawal S, Naumov S, De Miranda EE, Di Bella CM, Ordoyne C, Kopin Y, and Roy PS (2006) Validation of the global land cover 2000 map. IEEE Transactions on Geoscience and Remote Sensing 44(7/1): 1,728- 1,739, doi 10.1109/TGRS.2006.864370.

McPhaden MJ (1999) Climate oscillations: genesis and evolution of the 1997-98 El Niño. Science 283: 950-954.

McPhaden MJ, Zebiak SE, and Glantz MH (2006) ENSO as an Integrating Concept in Earth Science. Science 314 (5806), 1740, doi 10.1126/science.1132588.

Mellor B and Yamada T (1974) A hierarchy of turbulence closure models for planetary boundary layers. Journal of Atmospheric Science 31: 1,791-1,806.

Mesinger F and Arakawa A (1976) Numerical methods used in atmospheric models. GARP Publication Series 17: 1-64.

Mestayer P, Almbauer R, and Tchepel O (2003) Urban Field Campaigns. In: Moussiopoulos N (ed) Air Quality in Cities, Springer, Berlin (pp 51-87).

Michel C, Liousse C, Grégoire J-M, Tansey K, Carmichael GR, and Woo J-H (2005) Biomass burning emission inventory from burnt area data given by the SPOT-VEGETATION system in the frame of TRACE-P and ACE-Asia campaigns. Journal of Geophysical Research 110, D09304, doi:10.1029/2004JD005461.

Miettinen J, Langner A, and Florian S (2007) Burnt area estimation for the year 2005 in Borneo using multi-resolution satellite imagery. International Journal of Wildland Fire 16: 45-53.

MoF (Ministry of Forestry) (2003) Statistik Kehutanan Indonesia 2003. Departemen Kehutanan, Sekretariat Jenderatö and Biro Perencanaan, Jakarta, Indonesia.

Mohamed N, Ishak R, Rahmat R, Aziz A, Kasri AR, Ebenezer C, and Naing L (2004) The Relationship Between PM_{10} and Daily Upper Respiratory Tract Infection: Epidemiological Surveillance Data Analysis. The Bulletin of Epidemiology and Public Health on Noncommunicable Diseases in Malaysia 3(3): 3-7.

Mota BW, Pereira JMC, Oom D, Vasconcelos MJP, and Schultz M (2006) Screening the ESA ATSR-2 World Fire Atlas (1997-2002). Atmospheric Chemistry and Physics 6: 1,409-1,424.

Mott JA, Mannino DM, Alverson CJ, Kiyu A, Hashim J, Lee T, Falter K, and Redd SC (2005) Cardiorespiratory hospitalizations associated with smoke exposure during the 1997, Southeast Asian forest fires. International Journal of Hygiene and Environmental Health 208(1-2): 75-85.

Mouillot F and Field CB (2005) Fire history and the global carbon budget: a 1°x1° fire history reconstruction for the 20th century. Global Change Biology 11: 398-420.

Mudiyarso D and Wasrin UR (1995) Estimating land use change and carbon release from tropical forests conversion using remote sensing technique. Journal of Biogeography 22: 715-721.

Naeher LP, Brauer M, Lipsett M, Zelikoff JT, Simpson CD, Koenig JQ, and Smith KR (2007) Woodsmoke Health Effects: A Review. Inhalation Toxicology 19: 67-106.

Nakajima T, Higurashi A, Takeuchi N, and Herman JR (1999) Satellite and ground-based study of optical properties of 1997 Indonesian forest fire aerosols. Geophysical Research Letters 26(16): 2,421-2,424.

Narukawa M, Kawamura K, Takeuchi N, and Nakajima T (1999) Distribution of dicarboxylic acids and carbon isotopic composition in aerosols from 1997 Indonesian forest fires. Geophysical Research Letters 26 (20): 3,101-3,104.

Neale RB and Slingo JM (2003) The Maritime Continent and its role in the global circulation: A GCM study. Journal of Climate 16(5): 834-848.

Nichol J (1997) Bioclimatic impacts of the 1994 smoke haze event in Southeast Asia. Atmospheric Environment 31(8): 1,209-1,219.

Nichol J (1998) Smoke haze event in Southeast Asia: A predictable recurrence. Atmospheric Environment 32(14/15): 2,715-2,716.

Novakov T, Cachier H, Clark JS, Macko S, Masclet P (1997) Characterisation of particle products of biomass burning combustion. In: Clark JS, Cachier H, Goldammer JG, Stocks B (eds) Sediment records of biomass burning and global change. NATO ASI Series No I, Global environmental change Vol. 51, Springer Verlag, Berlin, Heidelberg, New York (pp 117-144).

Odihi JO (2001) Haze and Health in Brunei Darussalam: The Case of the 1997-98 Episodes. Singapore Journal of Tropical Geography 22(1): 38-51.

Okada K, Ikegami M, Zaizen Y, Makino Y, Jensen JJ, and Gras JL (2001) The mixture of individual aerosol particles in the 1997 Indonesian haze episode. Journal of Aerosol Science 32: 1,269-1,729.

Olivier JGJ, Bloos JPJ, Berdowski JJM, Visschedijk AJH, Bouwman AF (1999) A 1990 global emission inventory of anthropogenic sources of carbon monoxide on 1° × 1° developed in the framework of EDGAR/GEIA. Chemosphere 1: 1-17.

Olson JR, Baum BA, Cahoon DR, Crawford JH (1999) Frequency and distribution of forest, savanna, and crop fires over tropical regions during PEM-Tropics A. Journal of Geophysical Research 104 (D5): 5,865-5,876.

Omar A, Winker D, and Won J (2004). Aerosol models for the CALIPSO lidar inversion algorithms. Laser Radar Technology for Remote Sensing Proceedings SPIE 5240: 153-164.

Ooyub S, Ishak R and Krishnan J (2005) The Monitoring of The Impact of Forest Fire on Public Health in Malaysia. NCD Malaysia 4(2): 13-20.

Orlic I, Wen X, Ng TH, Tang SM (1999) Two years of aerosol monitoring in Singapore: a review. Nuclear Instruments and Methods in Physical Research B150: 457-464.

Ostro B (1984) A search for a threshold in the relationship of air pollution to mortality: a reanalysis of data on London winters. Environmental Health Perspectives 58: 397-399.

Ostro B (1993) The association of air pollution and mortality: examining the case for inference. Archives of Environmental Health 48: 336-342.

Ostro B (2004) Outdoor air pollution: assessing the environmental burden of disease at national and local levels. WHO Environmental Burden of Disease Series 5, World Health Organization, Geneva, Switzerland.

Ostro BD (1987) Air pollution and morbidity revisited: a specification test. Journal of Environmental Economy and Management 14: 87-98.

Page SE, Rieley JO, Shotyk W, Weiss D (1999) Interdependence of peat and vegetation in a tropical peat swamp forest. Philosophical Transactions of the Royal Society of London. Series B 354: 1,885- 1,897.

Page SE, Siegert F, Rieley JO, Boehm H-DV, Jaya A, Limin S (2002) The amount of carbon release from peat and forest fires in Indonesia during 1997. Nature 420: 61-65.

Page SE, Wuest R, Weiss D, Rieley J, Shotyk W, and Limin SH (2004) A record of Late Pleistocene and Holocene carbon accumulation and climate change from an equatorial peat bog (Kalimantan, Indonesia): implications for past, present and future carbon dynamics. Journal of Quaternary Science 19(7): 625-635.

Pandey KD, Wheeler D, Ostro B, Deichmann U, Hamilton K, Bolt K (2006) Ambient Particulate Matter Concentrations in Residential and Pollution Hotspot areas of World Cities: New Estimates based on the Global Model of Ambient Particulates (GMAPS), The World Bank Development Economics Research Group and the Environment Department Working Paper. The World Bank, Washington DC, USA.

Panyacosit L (2000) A Review of Particulate Matter and Health: Focus on Developing Countries. Working Papers of the International Institute for Applied Systems Analysis IR-00-005. Available online at http://ideas.repec.org/p/wop/iasawp/ir00005.html (21 April 2006).

Parameswaran K, Sandhya K, Nair M and Rajeev K (2004) Impact of Indonesian forest fires during the 1997 El Niño on the aerosol distribution over the Indian Ocean. Advance in Space Research 33: 1,098-1,103.

Park RJ, Jacob DJ, Kumar N, and Yantosca RM (2006) Regional visibility statistics in the United States: Natural and transboundary pollution influences, and implications for the Regional Haze Rule. Atmospheric Environment 40: 5,405-5,423.

Pentamwa P (2006) Air Quality in Southern Thailand during The 2005 Haze Episode. Yogyakarta, Indonesia. Proceedings of the Better Air Quality (BAQ-2006) Conference, 12 December 2006, Yogyakarta, Indonesia. Available online at http://www.cleanairnet.org/caiasia/1412/article-71359.html (5 May 2007).

Peters A and Pope CA III (2002) Cardiopulmonary mortality and air pollution. The Lancet 360(9341): 1184-1185.

Peterson J and Ward D (1993) An Inventory of Particulate Matter and Air Toxic Emissions from Prescribed Fires in the United States for 1989. Report IAG # DW12934736-01-0-1989, Fort Collins, Colorado, USA, Rocky Mountain Research Station, USDA Forest Service.

Philander SGH (1990) El Niño, La Niña, and the Southern Oscillation. International geophysics series 46, Academic Press, San Diego, New York (pp 35-38).

Phonboon K (1998) (ed) Health and environmental impacts from the 1997 Asian haze in southern Thailand. Health Systems Research Institute, Bangkok.

Pope CA III, Schwartz J and Ransom M (1992) Daily mortality and PM_{10} pollution in the Utah Valley. Archives of Environmental Health 47: 118-24.

Pope CA, Thun MJ, Namboodiri MM, Dockery DW, Evans JS, Speizer FE, and Heath CW Jr (1995) Particulate air pollution as a predictor of mortality in a prospective study of U.S. adults. American Journal of Respiratory and Critical Care Medicine 151: 669-674.

Pope III CA (2000) Invited Commentary: Particulate Matter-Mortality Exposure-Response Relations and Thresholds. American Journal of Epidemiology 152(5): 407-412.

Poulter B, Christensen Jr NL, and Halpin PN (2006), Carbon emissions from a temperate peat fire and its relevance to interannual variability of trace atmospheric greenhouse gases. Journal of Geophysical Research 111, D06301, doi:10.1029/2005JD006455.

Prasetyo LB, Saito G and Tsuruta H (2000) Development for data base for eco-system changes and emission changes of GHG using remote sensing and GIS in Sumatra Island, Indonesia, in Proceedings of the 21st Asian Conference on Remote Sensing, Taipei, 591-596. Available online at http://www.gisdevelopment.net/aars/acrs/1999/ts13/ts13079pf.htm (24 October 2001).

Pye S and Watkiss P(2005) CAFE (Clean Air For Europe) programme CBA: baseline analysis 2000 to 2020 (AEAT/ED51014/Baseline Scenarios). International Institute for Applied Systems Analysis, Vienna, Austria. Available online at http://www.iiasa.ac.at/docs/HOTP/Mar05/cafe-cba-baseline-results.pdf (8 April 2005).

Qadri ST (ed) (2001) Fire, Smoke, and Haze The ASEAN Response Strategy. Asian Development Bank, Manila, Philippines. ISBN No. 971-561-338-1. Available online at http://www.adb.org/Documents/Reports/Fire_Smoke_Haze/Executive_Summary/default.asp (2 August 2003).

Quinn WH, Zopf D, Short K, and Yang R (1978) Historical trends and statistics of the Southern Oscillation, El Niño and Indonesian droughts. Fishery Bulletin 76(3): 663-678.

Radojevic M (1998) Burning issues. Chemistry in Britain 34(12): 38-42.

Radojevic M (2003) Chemistry of forest fires and regional haze with emphasis on Southeast Asia. Pure and Applied Geophysics 160: 157-187.

Radojevic M and Hassan H (1999) Air quality in Brunei Darussalam during the 1998 haze episode. Atmospheric Environment 33: 3,651-3,658.

Ramage CS (1971) Monsoon meteorology. International geophysics series 15, Academic Press, New York.

Rasmusson EM and Carpenter TH (1982) Variations in tropical sea surface temperature and surface wind fields associated with the Southern Oscillation/El Niño. Monthly Weather Reviews 110: 354-384.

Reid JS, Koppmann R, Eck TF and Eleuterio DP (2005[17]) A review of biomass burning emissions, part II: intensive physical properties of biomass burning particles. Atmospheric Chemistry and Physics 5: 799-825.

Rieley JO and Page SE (eds) (2005) Wise Use Guidelines for Tropical Peatlands. Alterra, Wageningen, The Netherlands, ISBN 90327-0347-1.

Rieley JO, Ahmad-Shah AA and M.A. Brady (1997) extent and nature of tropical peat swamps. In: Maltby E and Immirzi CP and Safford RJ (eds) Tropical Lowland Peatlands of Southeast Asia. Proceedings of a Workshop on Integrated Planning and Management of Tropical Lowland Peatlands, International Union for the Conservation of Nature and Natural Resources (IUCN), Gland, Switzerland (pp 17-53).

Rieley JO, Page S and Sieffermann G (1995) Tropical peat swamp forests of Southeast Asia: Ecology and environmental Importance. Malaysian Journal of Tropical Geography 26(2): 131-141.

Rieley JO, Page SE and Shepherd PA (1997) Tropical bog forests of South East Asia. In: Parkyn L, Stoneman RE, Ingram HAP (eds) Conserving Peatlands, Wallingford. CAB International (pp 35-41).

Roberts S (2004) Biologically Plausible Particulate Air Pollution Mortality Concentration–Response Functions. Environmental Health Perspectives 112(3):309-313

Robinson JM (1989) On uncertainty in the computation of global emission from biomass burning. Climatic Change 14: 243-262.

Roeckner E, Arpe K, Bengtsson L, Christoph M, Claussen M, Dümenil L, Esch M, Giorgetta M, Schlese U, and Schulzweida U (1996) The Atmospheric General Circulation Model ECHAM4: Model Description and Simulation of Present-Day Climate. Max-Planck-Institute for Meteorology Report 218, Max Planck Institute for Meteorology, Hamburg, Germany.

Roedenbeck C, Houweling S, Gloor M, and Heimann M (2003) CO_2 flux history 1982-2001 inferred from atmospheric data using a global inversion of atmospheric transport. Atmospheric Chemistry and Physics 3: 1,919-1 964.

[17] Also referred to as Reid et al. (2004) in the text, which is the Atmospheric Physics and Chemistry Discussions version in the paper.

Ropelewski C and Halpert M (1987) Global and regional scale precipitation patterns associated with the El Niño/Southern Oscillation. Monthly Weather Review 115: 1606–1626.

Ropelewski C and M Halpert (1987) Global and Regional Scale Precipitation Patterns Associated with the El Niño/Southern Oscillation. Monthly Weather Reviews 115: 1606-1626.

Rosenfeld D (1999) TRMM observed first direct evidence of smoke from forest fires inhibiting rainfall. Geophysical Research Letters 26: 3,105-3,108.

Roswintiarti O and Raman S (2003) Three-dimensional simulations of the mean air transport during the 1997 forest fires in Kalimantan, Indonesia using a mesoscale numerical model. Pure and Applied Geophysics 160: 429-438.

Ruitenbeck J (1999) Indonesia. In: Glover D and Jessup T (eds) Indonesia's Fires and Haze: The Cost of Catastrophe. Institute of Southeast Asian Studies, Singapore (pp 86-129). Available online at http://idrinfo.idrc.ca/archive/corpdocs/113538/332-1.htm#page_113 (24 November 2006).

Saharjo BH and Munoz CP (2005) Controlled burning in peat lands owned by small farmers: a case study inland preparation. Wetland Ecology and Management 13: 105-110.

Samet JM, Zeger SL, Dominici F, Curriero F, Coursac I, Dockery DW, Schwartz J, and Zanobetti A (2000) The national morbidity, mortality, and air pollution study. Part II: Morbidity, mortality, and air pollution in the United States. HEI Research Report 94 (Part II). Health Effects Institute, Cambridge, MA (pp 1-84).

Samoli E, Analitis A, Touloumi G, Schwartz J, Anderson HR, Sunyer J, Bisanti L, Zmirou D, Vonk JM, Pekkanen J, Goodman P, Paldy A, Schindler C, and Katsouyanni K (2005) Estimating the exposure-response relationships between particulate matter and mortality within the APHEA multicity project. Environmental Health Perspectives 113(5): 88-95.

Sandberg DV, Ottmar RD, Peterson JL, and Core J (2002) Wildland fire on ecosystems: effects of fire on air. General Technical Report RMRS-GTR-42-vol.5, Rocky Mountain Research Station, U.S. Department of Agriculture, Forest Service, Ogden, UT, USA. Available online at http://www.fs.fed.us/rm/pubs/rmrs_gtr042_5.pdf (3 January 2003).

Sastry N (2002) Forest fires, air pollution and mortality in Southeast Asia. Demography 39(1): 1-23.

Sawa Y, Matsueda H, Tsutsumi Y, Jensen JB, Inoue HY, and Makino Y (1999) Tropospheric carbon monoxide and hydrogen measurements over Kalimantan in Indonesia and northern Australia during October 1997. Geophysical Research Letters 26(10): 1,389-1,392.

Schell II (1947) Dynamic persistence and its applications to long-range forecasting. vol. 8, Harvard Meteorological studies, blue hill observatory, Milton, MA.

Scholze M (2003) Model studies on the response of the terrestrial carbon cycle to climate change and variability. Ph.D. thesis, Examination Report No.90, Max-Planck-Institute for Meteorology,Hamburg, Germany. Available online at http://www.sub.uni-hamburg.de/disse/1007/dissertation.pdf (15 February 2004).

Schönwiese C-D (2006) Praktische Statistik für Meteorologen und Geowissenschaftler. Gebrüder Borntraeger Verlagsbuchhandlung, Stuttgart, Germany.

Schultz MG, Heil A, Hoelzemann JJ, Spessa A, Thonicke K, Goldammer JG, Held AC, Pereira JM, and van het Bolscher M (submitted to Global Biogeochemical Cycles 2007) Global Emissions from Wildland Fires from 1960 to 2000.

Schultz MG, Pulles T, Brand R, van het Bolscher M, and Dalsoren SB (in preparation) Global data set of anthropogenic CO, NOx, and NMVOC emissions for 1960-2000.

Schwartz J (1991) Particulate air pollution and daily mortality: a synthesis. Public Health Reviews 19: 39-60.

Schwartz J (1993) Particulate air pollution and chronic respiratory disease. Environmental Research 62: 7-13.

Schwartz J (1994) Air pollution and daily mortality: a review and metaanalysis. Environmental Research 64: 36-52.

Schwartz J (2000) The Distributed Lag between Air Pollution and Daily Deaths. Epidemiology 11(3): 320-326.

Schwartz J and Dockery DW (1992) Particulate air pollution and daily mortality in Steubenville, Ohio. American Journal of Epidemiology 135: 12-19.

Schwartz J and Markus A (1990) Mortality and air pollution in London: a time-series analysis. American Journal of Epidemiology 131: 185–94.

Schwartz J and Morris R (1995) Air pollution and hospital admissions for cardiovascular disease in Detroit, Michigan. American Journal of Epidemiology 142: 23-35.

Schwartz J, Dockery DW and Neas LM (1996) Is daily mortality associated specifically with fine particles? Journal of the Air and Waste Management Association 46: 927.

Schwela DH, Goldammer JG, Morawska LH, and Simpson O (1999) Health Guidelines for Vegetation Fire Events. Guideline document. Published on behalf of UNEP, WHO, and WMO. Institute of Environmental Epidemiology, Ministry of the Environment Singapore.

SEAMIC (Southeast Asian Medical Information Center International Medical Foundation of Japan) (2001) SEAMIC Health Statistics 2000. SEAMIC Publication No. 84, Tokyo, Japan. Available online at http://www.shobix.co.jp/gu/seamic/2000.pdf (9 April 2004).

Seiler W and Crutze PJ (1980) Estimates of gross and net fluxes of carbon between the biosphere and the atmosphere from biomass burning. Climatic Change 2: 207-247.

Seinfeld JH and Pandis SN (1998) Atmospheric chemistry and physics: from air pollution to climate change. Wiley-Interscience, New York, NY.

Seinfeld JH and Pandis SN (2006) Atmospheric Chemistry and Physics, From Air Pollution to Climate Change Seinfeld. Wiley and Sons, Inc., New York.

Semmler T, Jacob D, Schlünzen KH, and Podzun R (2004) Influence of sea ice treatment in a regional climate model on boundary layer values in the Fram Strait region. Monthly Weather Review 132: 985-999.

Shahwahid MHO and Othman J (1999) Malaysia. In: Glover D and Jessup T (eds) Indonesia's Fires and Haze: The Cost of Catastrophe. Institute of Southeast Asian Studies, Singapore (pp 22-50). Available online at http://idrinfo.idrc.ca/archive/corpdocs/113538/332-1.htm#page_113 (24 November 2006).

Sharkey B (1997) (ed) Health hazards of smoke: recommendations of the April 1997 Consensus Conference. Tech. Rep. 9751-2836-MTDC. Missoula, MT: U. S. Department of Agriculture, Forest Service, Missoula Technology and Development Center.

Shimada S, Takahashi H, Haraguchi A, and Kaneko M (2001) Carbon content characteristics of tropical peats in Central Kalimantan, Indonesia: Estimating their spatial variability in density. Biogeochemistry 53: 249-267.

Siegert F and Hoffmann AA (2000) The 1998 forest fires in East Kalimantan (Indonesia): a quantitative evaluation using high resolution, multitemporal ERS-2 SAR images and NOAA-AVHRR hotspot data. Remote Sensing Environment 72: 64-77.

Siegert F, Rücker G and Hoffmann A (1999) Evaluation of the 1998 Forest Fires in East-Kalimantan (Indonesia) Using NOAA-AVHRR hotspot Data and Multitemporal ERS-2 SAR images. Proceedings of the International Geoscience and Remote Sensing Symposium Hamburg, 28.6.-2.7.1999 (IGARSS), IEEE Geoscience and Remote Sensing Society, Spring, TX 77379 USA.

Siegert F, Zhukov B, Oertel D, Limin S, Page SE, Rieley JO (2004) Peat fires detected by the BIRD satellite. International Journal of Remote Sensing 25: 3,221-3,230.

Simons LM (1998) Indonesia's plague of fire. National Geographic 194 (2): 100-118.

Smolarkiewitz PK (1983) A simple positive definite advection scheme with small implicit diffusion. Monthly Weather Review 111: 479-486.

SMS (Singapore Meteorological Service) (1995) Smoke haze over Singapore, Malaysia and Indonesia. WMO Bulletin 24: 147-150.

Soleiman A, Othman M, Shamah AA, Sulaiman NM, and Radojevic M (2003) The occurrence of haze in Malaysia: a case study in an urban industrial area. Pure and Applied Geophysics 160: 221-238.

Sorensen KW (1993) Indonesian peat swamp forests and their role as a. carbon sink. Chemosphere 27: 1065-1082.

Spix C, Heinrich J, Dockery D, Schwartz J, Volksch G, Schwinkowski K, Collen C, and Wichmann HE (1993) Air pollution and daily mortality in Erfurt, east Germany, 1980-1989. Environmental Health Perspectives 101 (6): 518-26.

Stibig H-J and Malingreau JP (2003) Forest cover of insular southeast Asia mapped from recent satellite images of coarse spatial resolution. Ambio 32(7): 469-475.

Stocks BJ and Kaufman JB (1997) Biomass consumption and behaviour of wildland fires in boreal, temperate, and tropical ecosystems: parameters necessary to interpret historic fire regimes and future fire scenarios. In: Clark JS, Cachier H, Goldammer JG, Stocks B (eds) Sediment records of biomass burning and global change. NATO ASI Series No I, Global environmental change Vol. 51, Springer Verlag, Berlin, Heidelberg, New York (pp 169-188).

Stolbovoi V (2002) Carbon in Russian Soils. Climatic Change 55(1-2): 131-156.

Stolle F, Dennis RA, Kurniawan I, and Lambin EF (2004) Evaluation of remote sensing-based active fire datasets in Indonesia. International Journal of Remote Sensing 25: 471-479.

Stolle F, Tomich TP and Dennis R (undated) Fire Review of Sumatran Islands in 1997. Global Fire Monitoring Center GFMC homepage. General Analyses and Overviews, Available online at http://www.uni-freiburg.de/fireglobe/other_rep/analyzes/ri/ri_an_1.htm (6 May 1999).

Stott P (2000) Combustion in tropical biomass fires: a critical review. Progress in Physical Geography 24 (3): 355-377.

Stott PA, Goldammer JG and Werner WW (1990) The role of fire in the tropical lowland deciduous forests of Asia. In: Goldammer JG (ed) Fire in the tropical biota. Ecosystem processes and global challenges. Ecological Studies 84, Springer-Verlag, Berlin-Heidelberg-New York (pp 32-44).

Sumawijaya N (2006) Hydrology and peat-land development in Indonesia. Tropics 15(3): 279-284.

Sunderlin WD and Resosudarmo IAP (1999) Rate and Causes of Deforestation in Indonesia: Towards a Resolution of the Ambiguities. CIFOR Occasional Paper No. 9, Center for International Forestry Research (CIFOR), Bogor, Indonesia.

Supardi A, Subekty D and Neuzil SG (1993) General geology and peat resources of the Siak Kanan and Bengkalis Island peat deposits, Sumatra, Indonesia. In: Cobb JC and Cecil CB (eds) Modern and Ancient Coal Forming Environments. Geological Society of America Special Paper 86: 45-61.

Suyanto S, Applegate G, Permana RP, Khususiyah N, and Kurniawan I (2004) The role of fire in changing land use and livelihoods in Riau-Sumatra. Ecology and Society 9(1): 15.

Tacconi L (2003) Fires in Indonesia: causes, costs and policy implications. CIFOR Occasional Papers 38, Bogor, Indonesia, Center for International Forestry Research. Available online at http://www.cifor.cgiar.org/publications/pdf_files/OccPapers/OP-038.pdf (3 October 2003).

Takahashi H, Shimada S., Ibie BF, Usup A, Yudha, and Limin SH (2001) Annual change of water balance and drought index in a tropical peat swamp forest of Central Kalimantan, Indonesia. In: Rieley JO and Page SE with Setiadi B (eds) Peatlands for people: Natural Resource and Functions and Sustainable Management. Proceeding of the

International Symposium on Tropical Peatland, 22-23 August 2001. Jakarta Indonesia. BPPT and Indonesia Peat Association (pp 63-67).

Tan WC, Qiu D, Liam BL, Ng TP, Lee SH, van Eeden SF, D'Yachkova Y, and Hogg JC (2000) The human bone marrow response to acute air pollution caused by forest fires. American Journal of Respiratory and Critical Care Medicine 161(4): 1,213-1,217.

Tang SM and Orlic I (unpublished) The particulate matter in Singapore atmosphere: Its elemental composition and size fraction before and during the haze period 1997. Department of Physics, National University Singapore. Unpublished draft of a paper submitted to the South-East Asian land/forest fires: science and policy workshop organised by the Centre for Remote Imaging, Sensing and Processing (CRISP), 30 April - 2 May 1998, Singapore.

Tapper N (2002) Climate, climatic variability and atmospheric circulation patterns in the Maritime Continent region. In: Kershaw DAB, Tapper N, Penny D and Brown J (eds) Bridging Wallace's Line: Environmental and Human History and Dynamics of the Southeast Asian-Australian Region, Advances in Geoecology 34, Catena-Verlag, Germany (pp 5-28).

Taylor D, Saksena P, Sanderson PG, and Kucera K (1999) Environmental change and rain forests on the Sunda shelf of Southeast Asia: drought, fire and the biological cooling of biodiversity hotspots. Biodiversity and Conservation 8(9): 1,159-1,177.

Thevenon F, Bard E, Williamson D, and Beaufort L (2004) A biomass burning record from the West Equatorial Pacific over the last 360 ky: methodological, climatic and anthropic implications. Paleogeography, Paleoclimatology, Paleoecology 213: 83-99.

Tiedtke M (1989) A comprehensive mass flux scheme for cumulus parameterization in large-scale models. Monthly Weather Reviews 117: 1,778-1,800.

Timmermann A, Oberhuber J, Bacher A, Esch M, Latif M, and Roeckner E (1999) Increased El Niño Frequency in a Climate Model Forced by Future Greenhouse Warming. Nature 398: 694-696.

Tsutsumi Y, Sawa Y, Makino Y, Jensen JB, Gras JL, Ryan BF, Diharto S, and Harjanto H (1999) Aircraft measurements of ozone, NOx, CO, and aerosol concentrations in biomass burning smoke over Indonesia and Australia in October 1997: Depleted ozone layer at low latitude over Indonesia. Geophysical Research Letters 26(5): 595-598.

Turetsky MR, Harden JW, Friedli HR, Flannigan M, Payne N, and Radke L 2006. Wildfires threaten mercury stocks in northern soils. Geophysical Research Letters 33, L16403, doi:10.1029/2005GL025595. 33, L16403.

UNDAC (United Nations Disaster Assessment and Coordination Team) (1998) Mission on Forest Fires, Indonesia, Sept.-Nov. 1997. International Forest Fire News No. 18.

UNEP (United Nations Environmental Programme) (1999) (Levine JS, Bobbe T, Ray N, Singh A, Witt RG) Wildland fires and the environment: a global synthesis. UNEP/DEIAEW/TR.99-1.

UN-OCHA (United Nations Office for the Coordination of Humanitarian Affairs) (2006) Indonesia: Fires and haze OCHA Situation Report No. 2 Issued 10 Oct 2006. Ref: OCHA/GVA - 2006/0212. Available online at http://www.reliefweb.int/rw/RWB.NSF/db900SID/KKEE-6UFPHX?OpenDocument (19 November 2006).

USEPA (United States Environmental Protection Agency) (1994) Measuring air quality. The Pollutant Standards Index. Office of Air Quality, Planning and Standards. Research Triangle Park, NC. EPA-451/K94001.

USEPA (United States Environmental Protection Agency) (1999) Air Quality Index Reporting. 40 CFR Part 58. Office of Air Quality, Planning and Standards. Research Triangle Park, NC. RIN 2060-AH92.

USEPA (United States Environmental Protection Agency) (2004) Air Quality Criteria for Particulate Matter. EPA/600/P-99/002aF. National Center for Environmental Assessment, U.S. Environmental Protection Agency, Research Triangle Park, NC. Available online at http://cfpub.epa.gov/ncea/cfm/partmatt.cfm (13 June 2005).

USEPA (United States Environmental Protection Agency) (2006a) National Ambient Air Quality Standards for Particulate Matter; Final Rule, 40 CFR Part 50, Part II, Federal Register 71 (200). U.S. Environmental Protection Agency, Research Triangle Park, NC.

USEPA (United States Environmental Protection Agency) (2006b) Guidelines for the reporting of daily air quality-the air quality index (AQI). United States Environmental Protection Agency, Office of Air Quality Planning and Standards, Research Triangle Park, N.C.. Available online at http://www.epa.gov/ttncaaa1/t1/memoranda/rg701.pdf (8 September 2006).

Usup A, Takahashi H and Limin SH (2000) Aspect and mechanism of peat fire in tropical peat land: a case study in Central Kalimantan 1997, Proceedings of the International Symposium on Tropical Peatlands. Bogor, Indonesia, Hokkaido University and Indonesian Institute of Science (pp 79-88).

van Ardenne JA, Carmichael GR, Levy II H, Streets D, and Hordijk L (1999) Anthropogenic NOx emissions in Asia in the period 1990-2020. Atmospheric Environment 33: 633-646.

van der Werf GR, Randerson JT, Collattz GJ, and Giglio L (2003) Carbon emissions from fires in tropical and subtropical ecosystems. Global Change Biology 9: 547-562.

van der Werf GR, Randerson JT, Collatz GJ, GiglioL, Kasibhatla PS, Arellano AF, Olsen SC, and Kasichke ES (2004) Continental-scale partitioning of fire emissions during the 1997 to 2001 El Niño/La Niña period. Science 303: 73-76.

Van der Werf GR, Randerson JT, Giglio L, Collatz GJ, Kasibhatla PS, and Arellano Jr AF (2006) Interannual variability in global biomass burning emissions from 1997 to 2004. Atmospheric Chemistry and Physics 6: 3,423-3,441.

Van Noije TCP, Eskes HJ, Dentener FJ, Stevenson DS, Ellingsen K, Schultz MG, Wild O, Amann M, Butler T, Cofala J, Drevet J, Fiore AM, Gauss M, Hauglustaine DA, Horowitz LW, Isaksen ISA, Krol MC, Lamarque J-F, Lawrence MG, Martin RV, Montanaro V, Mueller JF, Pitari G, Prather MJ, Pyle JA, Richter A, Rodriguez JM, Savage NH, Strahan SE, Sudo K, Szopa S, and van Roozendaal M (2006) Multi-model ensemble simulations of tropospheric NO2 compared with GOME retrievals for the year 2000. Atmospheric Chemistry and Physics 6: 2,943-2,979.

Verhoeff AP, Hoek G, Schwartz J and van Wijnen JH (1996) Air pollution and daily mortality in Amsterdam. Epidemiology 7: 225-230.

Vignati E, Wilson J and Stier P (2004) M7: An efficient size-resolved aerosol microphysics module for large-scale aerosol transport models. Journal of Geophysical Research 109, D22202, doi:10.1029/2003JD004485.

von Hoyningen-Huene W, Schmidt T, Schienbein S, Kee CA, and Tick LJ (1999) Climate-relevant aerosol parameters of South-East-Asian forest fire haze. Atmospheric Environment 33: 3,183-3,190.

Von Storch HV and Zwiers FW (1998) Statistical analysis in climate research. Cambridge University Press, Cambridge, UK.

Wahyanto, Ritung S and Subagjo H (2003) Peta sebaran Gambut, Luas dan Kandungan Karbon di Pulau Sumatera/ Maps of area of peatland Distribution and Carbon Content in Sumatra, 1990-2002. Wetland International - Indonesia Programme & Wildlife Habitat Canada, Bogor, Jakarta.

Wahyunto, Ritung S, Suparto, and Subagio H (2004) Peta sebaran Gambut, Luas dan Kandungan Karbon di Kalimantan/ Map of Peatland Distribution Area and Carbon Content in Kalimantan, 2000-2002. Wetland International - Indonesia Programme & Wildlife Habitat Canada, Bogor, Jakarta, ISBN: 979 - 95899 - 9 -1.

Walcek CJ and Taylor GR (1986) A theoretical method for computing vertical distributions of acidity and sulfate production within cumulus clouds. Journal of Atmospheric Sciences 43: 339-355.

Walcek CJ, Brost RA, Chang JS, and Wesley ML (1986) SO_2, sulfate and HNO_3 deposition velocities computed using regional landuse and meteorological data. Atmospheric Environment 20: 949-964.

Wang Y, Field RD and Roswintiarti O (2004) Trends in atmospheric haze induced by peat fires in Sumatra Island, Indonesia and El Niño phenomenon from 1973 to 2003. Geophysical Research Letters 31, L04103, doi:10.1029/2003GL018853.

Ward DE (1990) Factors influencing the emissions of gases and particulate matter from biomass burning. In: Goldammer JG (ed) Fire in the tropical biota. Ecosystem processes and global challenges. Ecological Studies 84, Springer-Verlag, Berlin-Heidelberg-New York (pp 418-436).

Ward DE, Hao WM, Susott RA, Babbitt RE, Shea RW, Kauffman JB, Justice CO (1996) Effect of fuel composition on combustion efficiency and emission factors for African savanna ecosystems. Journal of Geophysical Research 101(D19): 23,569-23,576.

Weiss D, Shotyk W, Rieley J, Page S, Gloor M, Reese S, Martinez-Cortizas A (2002) The geochemistry of major and selected trace elements in a forested peat bog, Kalimantan, SE Asia, and its implications for past atmospheric dust deposition. Geochimica et Cosmochimica Acta 66: 2,307-2,323.

WHO (World Health Organization) (1997) WHO is deeply concerned by the health effects of the forest fires in South-East Asia. Press Release 26th September 1997. World Health Organization, Geneva.

WHO (World Health Organization) (1998) Report on the biregional workshop on health impacts of haze-related air pollution, Kuala Lumpur, Malaysia, 1-4 June 1998. World Health Organization, Kuala Lumpur, (WP)EHE(O)/ICP/EHH/004-E.

WHO (World Health Organization) (2001) Quantification of the Health Effects of Exposure to Air Pollution. Report of a WHO Working Group, Bilthoven, Netherlands, 20-22 November 2000. European Center for Environment and Health. WHO Regional Office for Europe, Copenhagen.

WHO/UNEP (World Health Organization / United Nation Environmental Programme) (1992) Urban air pollution in megacities of the world. Blackwell, Oxford (pp 107-113).

Wichmann H-E (2004) Positive gesundheitliche Auswirkungen des Einsatzes von Partikelfiltern bei Dieselfahrzeugen – Risikoabschätzung für die Mortalität in Deutschland. Umweltmedizin in Forschung und Praxis 9(2): 85 - 99.

Wichmann H-E (2005) Feinstaub: Lufthygienisches Problem Nr. 1 - eine aktuelle Übersicht. Umweltmedizin in Forschung und Praxis 10(3): 157 - 162.

WMO (World Meteorological Organization) (1992) International meteorological vocabulary. World Meteorological Organization, Geneva, WMO/OMM/BMO- No. 182.

WMO (World Meteorological Organization) (1998) Report of the WMO Workshop on Regional Transboundary Smoke and Haze in Southeast Asia, Singapore, 2-5 June 1998. World Meteorological Organization, Geneva, SG/59.

Woesten JHM, Van Den Berg J, Van Eijk P, Gevers GJM, Giesen WBJT, Hooijer A, Idris A, Leenman PH, Rais DS, Siderius C, Silvius MJ, Suryadiputra N, and Wibisono IT (2006) Interrelationships between Hydrology and Ecology in Fire Degraded Tropical Peat Swamp Forests. International Journal of Water Resources Development 22 (1): 157-174.

Wolter K and Timlin MS (1998) Measuring the strength of ENSO events - how does 1997/98 rank? Weather 53: 315-324.

Wooster MJ, Roberts G, Perry GLW, and Kaufman YJ (2005) Retrieval of biomass combustion rates and totals from fire radiative power observations: FRP derivation and calibration relationships between biomass consumption and fire radiative energy release, Journal of Geophysical Research 110, D24311, doi:10.1029/2005JD006318.

Wurzler S, Hermann H, Neusüß,C, Wiedensohler A, Stratmann F, Wilck M, Trautmann T, Andreae MO, Helas G, Trentmann J, Langmann B, Graf H, and Textor C (2001) Impact of vegetation fires on the composition and circulation of the atmosphere: introduction of the research project EFEU. Journal of Aerosol Science 32: 199-200.

Yadav AK, Kumar K, Kasim AMBHA, Singh MP, Parida SK, and Sharan M (2003) Visibility and incidence of respiratory diseases during the 1998 haze episode in Brunei Darussalam. Pure and Applied Geophysics 160: 265-277.

Yokelson RJ, Susott RA, Babbitt RE, Hao WM, and Ward DE (1999) Trace Gas Emissions from Specific Biomass Fire-types. In: Moya TB (e.d) Proceedings of a Synthesis Workshop on Greenhouse Gas Emission, Aerosols and Land Use and Cover Change in Southeast Asia. Sponsored by SARCS, IGAC, LUCC, IGBP China-Taipei, National Central University, Chungli, China-Taipei, 15-18 November 1997 (pp 60-68).

Yokelson RJ, Ward DE, Susott RA, Reardon J, and Griffith DWT (1997) Emissions from smoldering combustion of biomass measured by open-path Fourier transform infrared spectroscopy. Journal of Geophysical Research 102: 18,865-18,877.

Yuan C-S, Lee C-G, Liu S-H, Chang J-C, Yuan C, and Yang H-Y (2006) Correlation of atmospheric visibility with chemical composition of Kaohsiung aerosols. Atmospheric Research 82(3-4): 663-679.

Zhong A, Alves O, Hendon H, and Rikus L (2006). On aspects of the mean climatology and tropical interannual variability in the BMRC Atmospheric Model (BAM 3.0). Bureau of Meteorology Research Centre Research Report No. 121, Bureau Meteorological Australia.

Ziemke JP and Chandra S (1999) Seasonal and interannual variabilities in tropical tropospheric ozone. Journal of Geophysical Research 104 (D21): 21,425-26,442.

Zoltai SC, Morrissey LA, Livingston GP, and de Groot WJ (1998) Effects of fires on carbon cycling in North American boreal peatlands. Environmental Reviews 6: 13-24.

Zoumas A, Wooster M and Perry G (2004) Fire and El Niño in Borneo, Se Asia. International Archives of Photogrammetry and Remote Sensing 35 (7): 596-600.

Electronic Literature or Data Sources:

Web-Reference 1: ATSR World Fire Atlas, available from the Data User Element of the European Space Agency. http://dup.esrin.esa.it/ionia/wfa/index.asp (2 February 2007).

Web-Reference 2: Cold and Warm Episodes by season, ONI Oceanic Niño Index (ONI) data from 1951 to present, available from the Climate Prediction Center (CPC) of the NOAA/ National Weather. http://www.cpc.ncep.noaa.gov/products/analysis_monitoring/ensostuff/ensoyears.shtml (17 April 2007).

Web-Reference 3: http://www.rhc.at/kalteng/gallery.php (31 May 2004).

Web-Reference 4: http://www.orangutan.or.id/office/modules/image/uploads/orangutan998220060913115923.jpg (31 May 2004).

Web-Reference 5: BBC News, 11 August 2005, Malaysia haze triggers emergency http://news.bbc.co.uk/2/hi/asia-pacific/4140660.stm (13 August 2005).

Web-Reference 6: NASA Earth Observatory News, 9 July 2001, Haze over Malaysia, http://earthobservatory.nasa.gov/ Newsroom/NewImages/images.php3?img_id=5026 (22 February 2006).

Web-Reference 7: National Environmental Agency Singapore, Haze Update, http://app.nea.gov.sg/ (1 September 2003).

Web-Reference 8: Department of Environment Malaysia, API Daily Readings-2006. http://www.doe.gov.my/index.php?option=com_content&task=view&id=818&Itemid=370&lang=en (15 August 2007).

Web-Reference 9: http://www.epa.gov/air/particlepollution/pdfs/20060929_factsheet.pdf (2 August 2007).

Web-Reference 10: http://trmm.gsfc.nasa.gov/3b43.html (13 July 2007).

Web-Reference 11: ftp://disc2.nasacom.nasa.gov/data/TRMM/Gridded/3B43_V6/ (7 July 2007).

Web-Reference 12: http://www.cpc.ncep.noaa.gov/products/analysis_monitoring/ensostuff/ensoyears.shtml (21 March 2007).

Web-Reference 13: http://www.cdc.noaa.gov/people/klaus.wolter/MEI/mei.html#discussion (31 January 2007).

Web-Reference 14: http://dup.esrin.esa.it/ionia/wfa/index.asp (8 September 2007).

Abbreviations

β	Burning efficiency
a.r.t.	and references therein
AATSR	Advanced Along Track Scanning Radiometer
API	Air Pollution Index
AQI	Air Quality Index
ASEAN	Association of Southeast Asian Nations
ATSR	Along Track Scanning Radiometer
AVHRR	Advanced Very High Resolution Radiometer
BMG	Indonesian Meteorological and Geophysical Agency
C	Carbon
CI_{95}	95% Confidence Interval
CO	Carbon Monoxide
CO_2	Carbon Dioxide
COPD	Chronic Obstructive Pulmonary Diseases
EC	Elemental (or ‘Black’) Carbon
ECMWF	European Center for Medium-Range Weather Forecasts
EF_x	Emission Factor of compound *x*
ENSO	El Niño Southern Oscillation
EQAS	Equatorial Asia
ER	Exposure-Response (Chapter 7) or Emission Ratio (Chapter 5)
ERF	Exposure-Response Function
EXP_MET96	Model experiment with REMO (using 1996 meteorology)
EXP_NOPEAT	Model experiment with REMO (excluding peat fires)
EXP_REF	Model experiment with REMO (Reference run)
FAO	Food and Agriculture Organization
GFED	Global Fire Emissions Database
GLC2000	Global Land Cover Database for the year 2000
HS	Histosol (Soil Group)
HTE	High-Temperature Event
KA	Kalimantan
MEI	Multivariate El Niño Index
MMS	Malaysian Meteorological Services
MODIS	Moderate Resolution Imaging Spectroradiometer
MOE	Ministry of Environment Singapore
MoH	Indonesian Ministry of Health
N	Sample size
OC	Organic Carbon
ONI	Ocean Niño Index
PM	Particulate Matter
PM_{10}	Particulate Matter smaller than 10 μm diameter
$PM_{2.5}$	Particulate Matter smaller than 2.5 μm diameter
PSI	Pollution Standard Index
REMO	Regional Climate Model
RETRO	REanalysis of the TROpospheric chemical composition over the past 41 years. Research project funded under the 5th EC framework programme.
RoI	Remaining parts of Indonesia except Sumatra and Kalimantan
RR	Relative Risk
SD	Standard Deviation
SPOT	Satellite Pour l’ Observation de la Terre (or "Earth-Observing Satellite")
SST	Sea Surface Temperature
SU	Sumatra
TOMS	Total Ozone Mapping Spectrometer
TPM	Total Particulate Matter (here synonymously used with
TRMM	Tropical Rainfall Measuring Mission
TSP	Total Suspended Particulate Matter (here synonymously used with TPM)
URTI	Upper Respiratory Tract Infection
USEPA	US Environmental Protection Agency
VIRS	Visible and Infrared Spectrometer

Acknowledgements

First of all, I would like to express my sincere thanks to my supervisor Dr. Bärbel Langmann for her guidance into modeling, for the helpful discussions and the sympathy. Likewise, I'm very grateful to my supervisor Dr. Sebastian Rast for his wise, dedicated and understanding guidance during the final period of my PhD. Furthermore, I also greatly thank my doctoral advisor Prof. Dr. Hans Graf as well as Prof. Dr. Hartmut Graßl for their support and expertise.

I thank the Max Planck Institute for Meteorology in Hamburg for granting my PhD studies and for giving me the opportunity to work within such an excellent infrastructure. I would like to thank the International Max Planck Research School on Earth System Modeling (IMPRS-ESM) for the many-sided scientific training, and, very noteworthy, to Dr. Antje Weitz for her far-reaching guidance.

Furthermore, I would like to thank my colleagues for their support and inspiration on all levels of work and life. Just to name a few of them: Melissa Pfeffer, Elina Marmer, Gabriela Santos, Claas Teichmann, Irene Fischer-Bruns, Traute Krueger, and Martin Schultz.

It was the greatest pleasure to share my office with you, Steven (Xuefeng Cui) and Irene Stemmler: your humor is unbeatable and the best antidote against displeasure and weak-spiritedness.

Finally, I owe many thanks to my family, especially for their support during my surgeries and the recovery. Many thanks to all my friends, to Rosa, Birgit, Katja, Kalle, Gerhard and Carsten, and, of course, to the entire family Hoppe for all the encouragement, distraction, sympathy, reflection, inspiration and fun. Very special thanks to Michael for your good-natureness, understanding and support.

Publikationsreihe des MPI-M
„Berichte zur Erdsystemforschung“ , „*Reports on Earth System Science*“, ISSN 1614-1199
Sie enthält wissenschaftliche und technische Beiträge, inklusive Dissertationen.

Berichte zur Erdsystemforschung Nr.1 Juli 2004	**Simulation of Low-Frequency Climate Variability in the North Atlantic Ocean and the Arctic** Helmuth Haak
Berichte zur Erdsystemforschung Nr.2 Juli 2004	**Satellitenfernerkundung des Emissionsvermögens von Landoberflächen im Mikrowellenbereich** Claudia Wunram
Berichte zur Erdsystemforschung Nr.3 Juli 2004	**A Multi-Actor Dynamic Integrated Assessment Model (MADIAM)** Michael Weber
Berichte zur Erdsystemforschung Nr.4 November 2004	**The Impact of International Greenhouse Gas Emissions Reduction on Indonesia** Armi Susandi
Berichte zur Erdsystemforschung Nr.5 Januar 2005	**Proceedings of the first HyCARE meeting, Hamburg, 16-17 December 2004** Edited by Martin G. Schultz
Berichte zur Erdsystemforschung Nr.6 Januar 2005	**Mechanisms and Predictability of North Atlantic - European Climate** Holger Pohlmann
Berichte zur Erdsystemforschung Nr.7 November 2004	**Interannual and Decadal Variability in the Air-Sea Exchange of CO2 - a Model Study** Patrick Wetzel
Berichte zur Erdsystemforschung Nr.8 Dezember 2004	**Interannual Climate Variability in the Tropical Indian Ocean: A Study with a Hierarchy of Coupled General Circulation Models** Astrid Baquero Bernal
Berichte zur Erdsystemforschung Nr9 Februar 2005	**Towards the Assessment of the Aerosol Radiative Effects, A Global Modelling Approach** Philip Stier
Berichte zur Erdsystemforschung Nr.10 März 2005	**Validation of the hydrological cycle of ERA40** Stefan Hagemann, Klaus Arpe and Lennart Bengtsson
Berichte zur Erdsystemforschung Nr.11 Februar 2005	**Tropical Pacific/Atlantic Climate Variability and the Subtropical-Tropical Cells** Katja Lohmann
Berichte zur Erdsystemforschung Nr.12 Juli 2005	**Sea Ice Export through Fram Strait: Variability and Interactions with Climate**- Torben Königk
Berichte zur Erdsystemforschung Nr.13 August 2005	**Global oceanic heat and fresh water forcing datasets based on ERA-40 and ERA-15** Frank Röske
Berichte zur Erdsystemforschung Nr.14 August 2005	**The** HAM**burg** O**cean** C**arbon** C**ycle Model HAMOCC5.1 - Technical Description Release 1.1** Ernst Maier-Reimer, Iris Kriest, Joachim Segschneider, Patrick Wetzel
Berichte zur Erdsystemforschung Nr.15 Juli 2005	**Long-range Atmospheric Transport and Total Environmental Fate of Persistent Organic Pollutants - A Study using a General Circulation Model** Semeena Valiyaveetil Shamsudheen

Publikationsreihe des MPI-M
„Berichte zur Erdsystemforschung“ , „*Reports on Earth System Science*“, ISSN 1614-1199
Sie enthält wissenschaftliche und technische Beiträge, inklusive Dissertationen.

Berichte zur Erdsystemforschung Nr.16 Oktober 2005	**Aerosol Indirect Effect in the Thermal Spectral Range as Seen from Satellites** Abhay Devasthale
Berichte zur Erdsystemforschung Nr.17 Dezember 2005	**Interactions between Climate and Land Cover Changes** Xuefeng Cui
Berichte zur Erdsystemforschung Nr.18 Januar 2006	**Rauchpartikel in der Atmosphäre: Modellstudien am Beispiel indonesischer Brände** Bärbel Langmann
Berichte zur Erdsystemforschung Nr.19 Februar 2006	**DMS cycle in the ocean-atmosphere system and its response to anthropogenic perturbations** Silvia Kloster
Berichte zur Erdsystemforschung Nr.20 Februar 2006	**Held-Suarez Test with ECHAM5** Hui Wan, Marco A. Giorgetta, Luca Bonaventura
Berichte zur Erdsystemforschung Nr.21 Februar 2006	**Assessing the Agricultural System and the Carbon Cycle under Climate Change in Europe using a Dynamic Global Vegetation Model** Luca Criscuolo
Berichte zur Erdsystemforschung Nr.22 März 2006	**More accurate areal preciption over land and sea, APOLAS Abschlussbericht** K. Bumke, M. Clemens, H. Graßl, S. Pang, G. Peters, J.E.E. Seltmann, T. Siebenborn, A. Wagner
Berichte zur Erdsystemforschung Nr.23 März 2006	**Modeling cold cloud processes with the regional climate model REMO** Susanne Pfeifer
Berichte zur Erdsystemforschung Nr.24 Mai 2006	**Regional Modeling of Inorganic and Organic Aerosol Distribution and Climate Impact over Europe** Elina Marmer
Berichte zur Erdsystemforschung Nr.25 Mai 2006	**Proceedings of the 2nd HyCARE meeting, Laxenburg, Austria, 19-20 Dec 2005** Edited by Martin G. Schultz and Malte Schwoon
Berichte zur Erdsystemforschung Nr.26 Juni 2006	**The global agricultural land-use model KLUM – A coupling tool for integrated assessment** Kerstin Ellen Ronneberger
Berichte zur Erdsystemforschung Nr.27 Juli 2006	**Long-term interactions between vegetation and climate -- Model simulations for past and future** Guillaume Schurgers
Berichte zur Erdsystemforschung Nr.28 Juli 2006	**Global Wildland Fire Emission Modeling for Atmospheric Chemistry Studies** Judith Johanna Hoelzemann
Berichte zur Erdsystemforschung Nr.29 November 2006	**CO_2 fluxes and concentration patterns over Eurosiberia: A study using terrestrial biosphere models and the regional atmosphere model REMO** Caroline Narayan

Publikationsreihe des MPI-M
„Berichte zur Erdsystemforschung“ , „*Reports on Earth System Science*“, ISSN 1614-1199
Sie enthält wissenschaftliche und technische Beiträge, inklusive Dissertationen.

Berichte zur Erdsystemforschung Nr.30 November 2006	**Long-term interactions between ice sheets and climate under anthropogenic greenhouse forcing Simulations with two complex Earth System Models** Miren Vizcaino
Berichte zur Erdsystemforschung Nr.31 November 2006	**Effect of Daily Surface Flux Anomalies on the Time-Mean Oceanic Circulation** Balan Sarojini Beena
Berichte zur Erdsystemforschung Nr.32 November 2006	**Managing the Transition to Hydrogen and Fuel Cell Vehicles – Insights from Agent-based and Evolutionary Models –** Malte Schwoon
Berichte zur Erdsystemforschung Nr.33 November 2006	**Modeling the economic impacts of changes in thermohaline circulation with an emphasis on the Barents Sea fisheries** Peter Michael Link
Berichte zur Erdsystemforschung Nr.34 November 2006	**Indirect Aerosol Effects Observed from Space** Olaf Krüger
Berichte zur Erdsystemforschung Nr.35 Dezember 2006	**Climatological analysis of planetary wave propagation in Northern Hemisphere winter** Qian Li
Berichte zur Erdsystemforschung Nr.36 Dezember 2006	**Ocean Tides and the Earth’s Rotation - Results of a High-Resolving Ocean Model forced by the Lunisolar Tidal Potential** Philipp Weis
Berichte zur Erdsystemforschung Nr.37 Dezember 2006	**Modelling the Global Dynamics of Rain-fed and Irrigated Croplands** Maik Heistermann
Berichte zur Erdsystemforschung Nr.38 Dezember 2006	**Monitoring and detecting changes in the meridional overturning circulation at 26°N in the Atlantic Ocean- The simulation of an observing array in numerical models** Johanna Baehr
Berichte zur Erdsystemforschung Nr.39 Februar 2007	**Low Frequency Variability of the Meridional Overturning Circulation** Xiuhua Zhu
Berichte zur Erdsystemforschung Nr.40 März 2007	**Aggregated Carbon Cycle, Atmospheric Chemistry, and Climate Model (ACC2) – Description of the forward and inverse modes –** Katsumasa Tanaka, Elmar Kriegler
Berichte zur Erdsystemforschung Nr.41 März 2007	**Climate Change and Global Land-Use Patterns — Quantifying the Human Impact on the Terrestrial Biosphere** Christoph Müller
Berichte zur Erdsystemforschung Nr.42 April 2007	**A Subgrid Glacier Parameterisation for Use in Regional Climate Modelling** Sven Kotlarski

Publikationsreihe des MPI-M
„Berichte zur Erdsystemforschung" , „*Reports on Earth System Science*", ISSN 1614-1199
Sie enthält wissenschaftliche und technische Beiträge, inklusive Dissertationen.

Berichte zur Erdsystemforschung Nr.43 April 2007	**Glacial and interglacial climate during the late Quaternary: global circulation model simulations and comparison with proxy data** Stephan J. Lorenz
Berichte zur Erdsystemforschung Nr.44 April 2007	**Pacific Decadal Variability: Internal Variability and Sensitivity to Subtropics** Daniela Mihaela Matei
Berichte zur Erdsystemforschung Nr.45 Mai 2007	**The impact of african air pollution: A global chemistry climate model study** Adetutu Mary Aghedo
Berichte zur Erdsystemforschung Nr.46 Juni 2007	**The Relative Influences of Volcanic and Anthropogenic Emissions on Air Pollution in Indonesia as Studied With a Regional Atmospheric Chemistry and Climate Model** Melissa Anne Pfeffer
Berichte zur Erdsystemforschung Nr.47 Juli 2007	**Sea Level and Hydrological Mass Redistribution in the Earth System: Variability and Anthropogenic Change** Felix Landerer
Berichte zur Erdsystemforschung Nr.48 September 2007	**REanalysis of the TROpospheric chemical composition over the past 40 years, Final Report** Edited by Martin G. Schultz
Berichte zur Erdsystemforschung Nr.49 Oktober 2007	**Sensitivity of ENSO dynamics to wind stress formulation as simulated by a hybrid coupled GCM** Heiko Hansen

ISSN 1614-1199